

# **Effect of Netrin-1 on the mature enteric nervous system and colorectal cancer**

---

**Suh Youn Ko**

This thesis is submitted in total fulfilment of the requirements for  
the degree of Doctor of Philosophy  
November 2017

Principal Supervisor: Professor Greg Blatch  
Co-supervisors: Associate Professor Kulmira Nurgali and  
Associate Professor John Price

College of Health and Biomedicine  
Victoria University, Melbourne, Australia

# Abstract

The enteric nervous system (ENS) plays a pivotal role in regulating gastrointestinal functions including intestinal wall movement, water/electrolyte absorption and secretion. Clinical studies have alerted that enteric neuropathy is induced by colorectal cancer (CRC), and this deficit may be a primary reason for CRC patients experiencing clinical symptoms such as constipation and diarrhoea. Manifested clinical symptoms are likely to be seen in CRC patients undergoing chemotherapy, as chemotherapeutic agents are known to be associated with neurotoxicity as a side-effect. Despite this, no efficient treatment for enteric neuropathy is currently available. This heightens the importance of developing neuroprotective treatment.

This thesis hypothesised that Netrin-1 could be an ideal candidate as a neuroprotective agent, as it is a well-known axonal guidance cue in the developing central nervous system, and its expression in the adult nervous system is shown to be involved in nerve regeneration after injury. It is recently found that Netrin-1 plays a guidance role in the developing ENS for establishing vagal afferent innervations to the gut. However, the role of Netrin-1 in the mature ENS is yet to be elucidated.

In addition to the nervous system, Netrin-1 is found to play a regulatory role in tumourigenesis. This therefore makes the use of Netrin-1 complicated, and thus far it is unclear whether Netrin-1 can be used therapeutically.

This thesis aims to investigate the effect of Netrin-1 on adult enteric neurons and colorectal cancer cells at a cellular level, and uncover the impact of Netrin-1 treatment on the ENS under cancer condition in an *in vivo* model.

The results of *in vitro* studies, shown in this thesis, demonstrate that Netrin-1 exerts neurotrophic guidance for post-natal enteric neuronal precursor cells by an increase in migration and neurite outgrowth, whilst no apparent effect of Netrin-1 was noted on differentiated neurons. Furthermore, Netrin-1 treatment inhibited caspase-3 activation, which was induced by CRC secretion, in precursor cells.

In addition, the effect of Netrin-1 on murine CRC cells indicated that Netrin-1 plays a role in tumourigenesis. Netrin-1 activated pFAK/pMEK/pERK signalling pathway in colorectal cancer cells via UNC5H2 and Neogenin receptors, resulting in increased proliferation, adhesion and migration.

In contrast to these effects of Netrin-1 shown in *in vitro* models, the *in vivo* study of this thesis demonstrated that a high concentration of Netrin-1 treatment in CRC mice inhibited tumour growth. Furthermore, Netrin-1 treatment did not affect any obvious changes in the ENS component of the CRC mice.

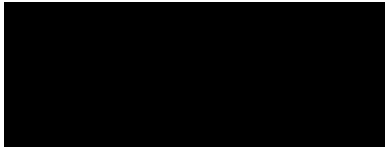
A potential reason why the ENS was unaffected by Netrin-1 treatment could be due to the following new findings shown in this thesis. Namely, that Netrin-1 is intrinsically expressed in the mature myenteric plexus of the colons in mice. Specifically, Netrin-1 and DCC receptors are present and co-localised in almost all ganglia and processes of the mature myenteric plexus of the colon in healthy and CRC conditions. Furthermore, Netrin-1 expression was found to correlate with ChAT and nNOS phenotypes in healthy and CRC conditions. Differential expression of Netrin-1 and changes in the distribution of Netrin-1 expression in relation to ChAT were found to be evident in CRC condition.

Collectively, this thesis provides groundwork for a potential therapeutic use of Netrin-1 as a neurotrophic factor for the adult enteric neurogenesis, and exhibited a potential safe use of Netrin-1 treatment for the ENS in the context of cancer.

# Student Declaration

## Doctor of Philosophy Declaration

“I, Suh Youn Ko, declare that the PhD thesis entitled [title of thesis] is no more than 100,000 words in length including quotes and exclusive of tables, figures, appendices, bibliography, references and footnotes. This thesis contains no material that has been submitted previously, in whole or in part, for the award of any other academic degree or diploma. Except where otherwise indicated, this thesis is my own work”.



Suh Youn Ko

Date: 22<sup>nd</sup> November 2017

# Table of Contents

Abstract .....	ii
Student Declaration .....	iv
Table of Contents .....	v
List of Figures .....	xiii
List of Tables .....	xvii
List of Abbreviations .....	xviii
Acknowledgements .....	xxii
<b>Chapter 1 General introduction</b> .....	<b>1</b>
<b>1.1 Importance of the enteric nervous system</b> .....	<b>2</b>
1.1.1 Organisation of the enteric nervous system .....	2
1.1.2 Diversity of enteric neurons .....	6
<b>1.2 Enteric nervous system development and neurogenesis</b> .....	<b>7</b>
1.2.1 Overview of enteric nervous system development .....	7
1.2.2 Neurogenesis in the enteric nervous system development .....	11
1.2.3 Neurogenesis in the adult enteric nervous system .....	12
<b>1.3 Cross-talk between nerves and cancer</b> .....	<b>14</b>
<b>1.4 Colorectal cancer progression and metastasis</b> .....	<b>15</b>
1.4.1 Tumour microenvironment .....	19
1.4.2 Tumour angiogenesis .....	20
<b>1.5 Netrin family and their receptors</b> .....	<b>25</b>
1.5.1 Netrin-1 structure .....	26
1.5.2 Netrin-1 receptor DCC structure .....	27
1.5.3 Netrin-1 receptor Neogenin structure .....	27
1.5.4 Netrin-1 receptor UNC5H structure .....	28

<b>1.6</b>	<b>Netrin-1 chemotropic receptors in neuronal tissues: chemoattraction versus chemorepulsion.....</b>	<b>32</b>
<b>1.7</b>	<b>Netrin-1 dependence receptors in non-neuronal tissues: tumour suppressor versus tumour promoter.....</b>	<b>35</b>
<b>1.8</b>	<b>Netrin-1 chemotropic signalling pathways.....</b>	<b>36</b>
1.8.1	Chemoattraction.....	36
1.8.2	Chemorepulsion.....	40
<b>1.9</b>	<b>Netrin-1 dependence receptor signalling pathways.....</b>	<b>40</b>
1.9.1	Pro-apoptosis.....	40
1.9.2	Anti-apoptosis.....	44
<b>1.10</b>	<b>The roles of Netrin-1 in the developing enteric nervous system.....</b>	<b>44</b>
<b>1.11</b>	<b>The role of Netrin-1 in nerve injury.....</b>	<b>50</b>
<b>1.12</b>	<b>The roles of Netrin-1 in colorectal cancer.....</b>	<b>52</b>
1.12.1	Netrin-1 intrinsic to colorectal cancer cells.....	57
1.12.2	The roles of Netrin-1 in angiogenesis.....	59
1.12.3	The roles of Netrin-1 in the tumour microenvironment and metastasis.....	65
<b>1.13</b>	<b>Summary.....</b>	<b>70</b>
<b>1.14</b>	<b>Research rationale, aims and hypotheses.....</b>	<b>71</b>
	<b>Chapter 2 Investigating the effect of Netrin-1 on post-natal enteric neuronal cell line.....</b>	<b>73</b>
<b>2.1</b>	<b>Introduction.....</b>	<b>74</b>
<b>2.2</b>	<b>Materials and methods.....</b>	<b>77</b>
2.2.1	Cell culture.....	77
2.2.2	Cell viability assay.....	77
2.2.3	Wound-healing assay.....	78
2.2.4	Immunofluorescence.....	78

2.2.5	Western blot and densitometric analysis .....	80
2.2.6	Quantitative RT-PCR.....	82
2.2.7	Flow cytometry (cell staining and data analysis) .....	84
2.2.8	Neurite measurement.....	85
2.2.9	Statistical analysis .....	85
<b>2.3</b>	<b>Results.....</b>	<b>85</b>
2.3.1	Optimisation of the <i>in vitro</i> IM-PEN culture for differentiation.....	85
2.3.2	IM-PEN cells present neuronal markers.....	94
2.3.3	Characterisation of IM-PEN cell differentiation by flow cytometric analysis .....	99
2.3.4	Determining the expression of Netrin-1 and its receptors in IM-PEN cells .....	111
2.3.5	Netrin-1 does not affect IM-PEN precursor cell proliferation .....	114
2.3.6	Netrin-1 effects on IM-PEN cell migration .....	118
2.3.7	Increased neurite outgrowth of IM-PEN precursor cells in the presence of Netrin-1 .....	123
2.3.8	Flow cytometric analysis of Netrin-1-treated IM-PEN precursor cells.....	133
<b>2.4</b>	<b>Discussion.....</b>	<b>136</b>
2.4.1	Differentiation of IM-PEN cells .....	136
2.4.2	Expression of CD surface markers in IM-PEN cells cultured at 33°C and 40.5°C.....	137
2.4.3	The effect of Netrin-1 on IM-PEN precursor cell proliferation .....	139
2.4.4	The effect of Netrin-1 on wound-healing cell migration .....	140
2.4.5	The effect of Netrin-1 on a neurite extension of precursor cells and differentiated cells .....	142
<b>2.5</b>	<b>Summary .....</b>	<b>143</b>

Chapter 3 The effect of Netrin-1 on colorectal cancer cells: in vitro study .....	145
<b>3.1 Introduction.....</b>	<b>146</b>
<b>3.2 Materials and methods .....</b>	<b>148</b>
3.2.1 Cell culture .....	148
3.2.2 Quantitative RT-PCR.....	148
3.2.3 Western blot .....	149
3.2.4 Cell viability .....	150
3.2.5 Adhesion assay.....	151
3.2.6 Wound-healing migration assay .....	152
3.2.7 Statistical analysis .....	152
<b>3.3 Results.....</b>	<b>153</b>
3.3.1 CT26 cells express Neogenin and UNC5H2 receptors .....	153
3.3.2 Netrin-1 increases CT26 cell proliferation .....	156
3.3.3 Netrin-1 contributes to CT26 cell adhesiveness .....	162
3.3.4 High concentration of Netrin-1 promotes CT26 cell migration .....	165
3.3.5 Netrin-1 treatment activates pFAK/pMEK/pERK signalling pathway in CT26 cells .....	178
<b>3.4 Discussion.....</b>	<b>183</b>
3.4.1 The effect of Netrin-1 on CT26 cell proliferation and adhesion.....	183
3.4.2 The effect of Netrin-1 on migration of CT26 cells .....	185
3.4.3 The effect of Netrin-1 on CT26 cells via activation of pFAK/pMEK/pERK pathway.....	186
<b>3.5 Summary .....</b>	<b>188</b>

Chapter 4	The effect of colorectal cancer conditioned media on neuronal cells in in vitro system .....	190
<b>4.1</b>	<b>Introduction</b> .....	<b>191</b>
<b>4.2</b>	<b>Materials and methods</b> .....	<b>192</b>
4.2.1	IM-PEN cell culture.....	192
4.2.2	CT26 cells conditioned media .....	192
4.2.3	Cell viability .....	193
4.2.4	Immunofluorescence .....	193
4.2.5	Imaging .....	194
4.2.6	Statistical analysis .....	194
<b>4.3</b>	<b>Results</b> .....	<b>194</b>
4.3.1	The effect of colorectal cancer conditioned media on post-natal enteric neuron precursors.....	194
4.3.2	The effect of colorectal cancer conditioned media on post-natal differentiated enteric neurons .....	202
<b>4.4</b>	<b>Discussion</b> .....	<b>206</b>
4.4.1	The effect of colorectal cancer conditioned media and Netrin-1 on caspase-3 activation in enteric neuronal precursors .....	206
4.4.2	The effect of colorectal cancer conditioned media on caspase-3 activation in differentiated enteric neurons.....	208
<b>4.5</b>	<b>Summary</b> .....	<b>212</b>
Chapter 5	Netrin-1 treatment in an orthotopic colorectal cancer mouse model: pilot study .....	214
<b>5.1</b>	<b>Introduction</b> .....	<b>215</b>
<b>5.2</b>	<b>Materials and methods</b> .....	<b>217</b>
5.2.1	Animals .....	217
5.2.2	Cell culture .....	217

5.2.3	Orthotopic colorectal cancer mouse model .....	218
5.2.4	Netrin-1 administration .....	218
5.2.5	Enzyme-linked immunosorbent assay .....	218
5.2.6	Hematoxylin and eosin staining.....	219
5.2.7	3,3'-diaminobenzidine immunohistochemistry .....	219
5.2.8	Wholemount immunofluorescence .....	220
5.2.9	Imaging .....	221
5.2.10	Neural cell counting and quantitative analysis.....	222
5.2.11	Statistical analysis .....	222
<b>5.3</b>	<b>Results.....</b>	<b>223</b>
5.3.1	Netrin-1 treated colorectal cancer orthotopic mouse model .....	223
5.3.2	Recombinant mouse Netrin-1 protein in plasma .....	227
5.3.3	Primary tumour growth in the caecum with or without Netrin-1 treatment .....	232
5.3.4	Defining the expression of Netrin-1 and its receptor, DCC, in the myenteric plexus of the colon from healthy adult mice.....	240
5.3.5	Identifying the co-expression of Netrin-1 with ChAT and nNOS in the myenteric plexus of the colon from healthy adult mice.....	248
5.3.6	The expression of DCC and Netrin-1 in the colonic myenteric plexus of colorectal cancer mice with or without Netrin-1 treatment .....	254
5.3.7	The co-expression of Netrin-1 and nNOS in the colonic myenteric plexus of colorectal cancer mice with or without Netrin-1 treatment .....	259
5.3.8	The co-expression of Netrin-1 and ChAT in the colonic myenteric plexus of colorectal cancer mice with or without Netrin-1 treatment .....	264

<b>5.4 Discussion</b> .....	<b>269</b>
5.4.1 The effect of Netrin-1 treatment on primary tumour growth and progression .....	269
5.4.2 Intrinsic expression of Netrin-1 and DCC in the colonic myenteric plexus of healthy and CRC mice.....	271
5.4.3 Correlation between Netrin-1 expression and the phenotypes of nNOS- and ChAT-positive neurons in the myenteric plexus .....	274
<b>5.5 Summary</b> .....	<b>281</b>
<b>Chapter 6 General discussion and future directions</b> .....	<b>283</b>
<b>6.1 General comments</b> .....	<b>284</b>
<b>6.2 The effect of Netrin-1 treatment on the post-natal enteric precursors and differentiated neurons</b> .....	<b>284</b>
<b>6.3 Intrinsic Netrin-1 expression in the myenteric plexus of healthy young adult mice</b> .....	<b>286</b>
<b>6.4 The effect of Netrin-1 treatment on the ENS in the context of colorectal cancer</b> .....	<b>288</b>
<b>6.5 The effect of Netrin-1 treatment on colorectal cancer cells and in <i>in vivo</i> model of colorectal cancer</b> .....	<b>291</b>
<b>6.6 Limitations and future directions</b> .....	<b>294</b>
6.6.1 Primary enteric neuronal cell culture .....	294
6.6.2 The ENS of CRC mice with Netrin-1 treatment .....	296
6.6.3 The effect of Netrin-1 in CRC immune response.....	297
<b>6.7 Conclusions</b> .....	<b>298</b>
<b>References</b> .....	<b>300</b>

Appendices .....	322
Appendix A .....	323
Appendix B .....	324
Publications .....	325

## List of Figures

Figure 1.1	A schematic diagram illustrating the organisation of the ENS.....	4
Figure 1.2	A schematic diagram showing colonisation of neural crest cells in developing gut and generation of mature enteric neurons and glia.....	9
Figure 1.3	A cascade of events in cancer progression and metastasis.....	17
Figure 1.4	Key molecules involved in colorectal cancer progression .....	23
Figure 1.5	The structure of netrins and major Netrin-1 receptors.....	30
Figure 1.6	Chemoattraction or chemorepulsion mediated by Netrin-1 receptors .....	33
Figure 1.7	Netrin-1 chemotropic signalling pathways .....	38
Figure 1.8	Netrin-1 dependence receptor signalling.....	42
Figure 1.9	The effect of Netrin-1 and its dependence receptors on normal colonic epithelial cells.....	55
Figure 1.10	Netrin-1 is produced by malignant cells.....	68
Figure 2.1	Viability of IM-PEN cells under permissive and non-permissive conditions.....	88
Figure 2.2	Morphological changes in IM-PEN cells under permissive and non-permissive conditions.....	90
Figure 2.3	The proliferative marker Ki67 and neuronal-specific marker $\beta$ -Tubulin III expression in IM-PEN cells under permissive and non-permissive conditions.....	92
Figure 2.4	Expression of neuronal marker PGP9.5 and glial cell marker GFAP on IM-PEN cells under permissive and non-permissive conditions.....	95
Figure 2.5	Expression of neuronal markers NeuN and Synaptophysin expression on IM-PEN cells under permissive and non-permissive conditions.....	97
Figure 2.6	Flow cytometry analysis of IM-PEN cells cultured at 33°C expressing surface and internal markers.....	103
Figure 2.7	Flow cytometric analysis of CD24-positive IM-PEN cells cultured at 33°C versus 40.5°C.....	106

Figure 2.8	Flow cytometric analysis comparing CD90 and CD24-positive IM-PEN cells cultured at 33°C versus 40.5°C .....	109
Figure 2.9	The expression of Netrin-1 receptors in IM-PEN cells cultured at 33°C and 40.5°C.....	112
Figure 2.10	The effect of Netrin-1 on IM-PEN progenitor cell viability.....	116
Figure 2.11	The effect of Netrin-1 on IM-PEN progenitor cell migration .....	119
Figure 2.12	Morphological changes in IM-PEN cells cultured at 33°C and 40.5°C in the presence of Netrin-1 .....	125
Figure 2.13	Immunofluorescent images of IM-PEN cells cultured at 33°C in the presence of Netrin-1 .....	127
Figure 2.14	Immunofluorescent images of IM-PEN cells cultured at 40.5°C in the presence of Netrin-1 at early time-point.....	129
Figure 2.15	Immunofluorescent images of IM-PEN cells cultured at 40.5°C in the presence of Netrin-1 at late time-point.....	131
Figure 2.16	Flow cytometric analysis of IM-PEN cells cultured at 33°C in the presence of Netrin-1 .....	134
Figure 3.1	CT26 cells express UNC5H2 and Neogenin receptors .....	154
Figure 3.2	The effect of Netrin-1 on CT26 cell proliferation.....	159
Figure 3.3	The effect of Netrin-1 on CT26 cell adhesion.....	163
Figure 3.4	The effect of Netrin-1 on CT26 cell migration.....	167
Figure 3.5	The effect of CT26 cell migration in the presence of Netrin-1 after blocking Netrin-1 receptors .....	172
Figure 3.6	Netrin-1 induces the activation of pFAK/pMEK/pERK signalling pathway in CT26 cells .....	181
Figure 4.1	Cell viability test and imaging of IM-PEN precursors cultured in CRC conditioned media with or without Netrin-1 .....	198
Figure 4.2	Cleaved caspase-3 expression in IM-PEN precursors after incubation in conditioned media with or without Netrin-1.....	200
Figure 4.3	Cleaved caspase-3 expression in IM-PEN differentiated cells after incubation in conditioned media with or without Netrin-1 .....	204
Figure 5.1	Surgical procedures for orthotopic mouse model of colorectal cancer .....	225

Figure 5.2	The levels of His-tagged Netrin-1 in plasma from Netrin-1-treated mice.....	228
Figure 5.3	3,3'-diaminobenzidine immunohistochemistry of liver tissues from the CRC mice treated with Netrin-1 .....	230
Figure 5.4	Caeca from the CRC mice in the absence or presence of Netrin-1 treatment .....	234
Figure 5.5	Hematoxylin and eosin staining of caecum and colon tissues from Netrin-1 or vehicle-treated CRC mice .....	236
Figure 5.6	3,3'-diaminobenzidine immunohistochemistry of caecum and colon tissues from Netrin-1 or vehicle-treated CRC mice.....	238
Figure 5.7	Localisation of DCC receptors in the myenteric plexus of the colon from healthy young adult mice.....	242
Figure 5.8	Localisation of Netrin-1 in the myenteric plexus of the colon from healthy young adult mice.....	244
Figure 5.9	Co-localisation of DCC-IR and Netrin-1-IR in the myenteric plexus of the colon from healthy young adult mice.....	246
Figure 5.10	Co-localisation of Netrin-1-IR and ChAT-IR in the myenteric plexus of the colon from healthy young adult mice.....	250
Figure 5.11	Co-localisation of Netrin-1-IR and nNOS-IR in the myenteric plexus of the colon from healthy young adult mice.....	252
Figure 5.12	DCC-IR in the myenteric plexus of the colon from Netrin-1 or vehicle-treated CRC mice .....	255
Figure 5.13	Netrin-1-IR in the myenteric plexus of the colon from Netrin-1 or vehicle-treated CRC mice.....	257
Figure 5.14	Co-localisation of Netrin-1-IR and nNOS-IR in the myenteric plexus of the colon from Netrin-1 or vehicle-treated CRC mice.....	260
Figure 5.15	Netrin-1-IR and nNOS-IR in the myenteric plexus of the colon tissues from Netrin-1 or vehicle-treated CRC mice.....	262

Figure 5.16	Co-localisation of Netrin-1-IR and ChAT-IR in the myenteric plexus of the colon from Netrin-1 or vehicle-treated CRC mice.....	265
Figure 5.17	Quantitative analysis of Netrin-1-IR and ChAT-IR co-localisation in the myenteric plexus of the colon tissues from Netrin-1 or vehicle-treated CRC mice .....	267
Figure 5.18	A schematic diagram indicating changes in relationship between Netrin-1-IR, nNOS-IR, and ChAT-IR in CRC mice with or without Netrin-1 treatment .....	279

## List of Tables

Table 1.1	Major Netrin-1 functions in the developing nervous system .....	47
Table 1.2	The effect of Netrin-1 in angiogenesis.....	62
Table 2.1	List of primary antibodies used in immunofluorescence assays .....	79
Table 2.2	List of secondary antibodies used in immunofluorescence assays .....	80
Table 2.3	List of primary antibodies used in western blot assays.....	81
Table 2.4	List of secondary antibodies used in western blot assays .....	82
Table 2.5	Oligonucleotide sequences used in RT-PCR analysis .....	83
Table 2.6	List of antibodies used in flow cytometry assays .....	84
Table 3.1	List of primary antibodies used in western blot assays.....	150
Table 3.2	List of secondary antibodies used in western blot assays .....	150
Table 5.1	List of primary antibodies used in immunofluorescence assays .....	221
Table 5.2	List of secondary antibodies used in immunofluorescence assays .....	221

## List of Abbreviations

5-HT	5-hydroxytryptamine
ACh	Acetylcholine
AKT	Serine/threonine kinase
APC	Adenomatous polyposis coli
B-FABP	Brain fatty acid-binding protein
BM	Basement membrane
BSA	Bovine serum albumin
CCL9	Chemokine ligand 9
CD	Cluster of differentiation
Cdc42	Cell division cycle 42
CDK	Cyclin dependent kinases
CGRP	Calcitonin gene-related peptide
ChAT	Choline acetyltransferase
CM	Conditioned media
CNS	Central nervous system
COX-2	Cyclooxygenase-2
CRC	Colorectal cancer
DAB	3,3'-diaminobenzidine
DAPI	4',6-diamidino-2-phenylindole
DAPK	Serine/threonine death-associated protein kinase
DB	DCC-binding domain
DCC	Deleted in colorectal cancer
DD	Death domain
DMEM	Dulbecco's modified eagle medium
DMSO	Dimethyl sulfoxide
DSCAM	Down syndrome cell adhesion molecule
ECM	Extracellular matrix
EGF	Epidermal growth factor
ELC	Enhanced chemiluminescence
ENS	Enteric nervous system
EP <sub>2</sub>	Extracellular protein 2
EP <sub>4</sub>	Extracellular protein 4

ERK	Extracellular-signal-regulated kinase
FACS	Fluorescence-activated cell sorting
FAK	Focal adhesion kinase
FBS	Fetal bovine serum
FITC	Fluorescein isothiocyanate
FN-III	Fibronectin type III
FSC-A	Forward scatter-area
GDNF	Glial cell line-derived neurotrophic factor
GFAP	Glial fibrillary acidic protein
GIT	Gastrointestinal tract
Grb2	Growth factor receptor-bound protein 2
HIF-1 $\alpha$	Hypoxia inducible factor-1 $\alpha$
IAP	Inhibitor of apoptosis protein
IF	Immunofluorescence
Ig	Immunoglobulin
IHC	Immunohistochemistry
iMCs	Immature myeloid cells
IM-PEN	Immortalised post-natal enteric neuron
IP3	Inositol triphosphate
IPANs	Intrinsic primary afferent neurons
IR	Immunoreactivity
JNK	c-Jun N-terminal kinase
LOH	Loss of heterozygosity
MAPK	Mitogen-activated protein kinase
MEK	Mitogen-activated protein kinase kinase
MES	2-(N-morpholino)ethanesulfonic acid
MMP-9	Matrix metalloproteinase 9
MOPS	3-(N-morpholino)propanesulfonic acid
NCCs	Neural crest-derived cells
NCSCs	Neural crest stem cells
NeuN	Neuronal-specific nuclear protein
NF-H	Neurofilament-heavy chain
NF- $\kappa$ B	Nuclear factor $\kappa$ B
nNOS	Neuronal nitric oxide synthase

NO	Nitric oxide
NRAGE	Neurotrophin receptor-interacting melanoma-associated antigen homologue
NRT	No reverse transcriptase
NTC	No template control
PACAP	Pituitary adenylate cyclise-activating polypeptide
PBS	Phosphate-buffered saline
PGE <sub>2</sub>	Prostaglandin E <sub>2</sub>
PGP9.5	Protein gene product 9.5
PI	Propidium iodide
PI3K	Phosphoinositide 3-kinase
PIP2	Phosphatidylinositol (4,5) bisphosphate
PKB	Protein kinase B
PLC $\gamma$	Phospholipase C $\gamma$
PNS	Peripheral nervous system
PTEN	Phosphatase and tensin homologue
PTK2	Protein tyrosine kinase 2
PVDF	Polyvinylidene difluoride
Rac1	Ras-related C3 botulinum toxin substrate 1
RET	Rearranged during transfection
RGM	Repulsive guidance molecule
RhoA	Ras homologous member A
RT	Room temperature
RT-PCR	Reverse transcription-polymerase chain reaction
SFKs	Src-family kinases
SMAD4	Mothers against decapentaplegic homologue 4
SOX-10	Sex-determining region Y (SRY)-related high mobility group (HMG) box gene
SP	Substance P
SSC-A	Side scatter-area
Thbs1	Thrombospondin type 1
TNFRSF1B,	Tumour necrosis factor receptor superfamily member 1B
TNF- $\alpha$	Tumour necrosis factor- $\alpha$
UNC5H	Uncoordinated-5 homologue

VACht	Vesicular acetylcholine transporter
VEGF	Vascular endothelial growth factor
VIP	Vasoactive intestinal polypeptide
ZU5	Zona occludens 5

## Acknowledgements

This PhD would not have been possible without the support, patience and encouragement of my supervisors, Greg Blatch, Kulmira Nurgali and John Price. Thank you all for giving me an opportunity to grow as an independent scientist. This PhD course has been a true learning journey.

Also, I would like to thank Alan, Varsha, Valentina and Faye for setting up the new lab and new facility for us to work properly. Thanks to the VU technician team, Nikola, Lillian, Min, Jing and Senani for their assistance in reagents deliveries.

A big thanks to Valentina and Monica for animal training that you provided to me. Thanks to Sami for FACS training and thanks to Vasso for her mentoring. Thanks to Crispin who used to be my supervisor who help me at the beginning of the PhD course. Thanks to my old lab members, Mina and Natasha. Their endurance is inspirational. Also, thanks to Kulmira and John's lab members, Elif, Ainsley, Rhian, Ahmed, Chau and Charlett for their stimulating conversation and good company.

I would like to thank Rob, Gulay, Min, Kim, Elif, Ainsley and Valentina for being wonderful friends and always being supportive in my PhD journey.

Finally I would like to thank my husband Aaron and my family for their incredible support and patience. Looking forward to sharing the next chapter of life together.

# Chapter 1

---

## General introduction

The majority of sections presented in this chapter are published and have been reproduced here with the permission of the publishers with minor alterations:

**Ko, S.Y.**, Dass, C.R., and Nurgali, K. (2012) Netrin-1 in the developing enteric nervous system and colorectal cancer. *Trends in Molecular Medicine* 18, 544-554.

**Ko, S.Y.**, Blatch, G.L., and Dass, C.R. (2013) Netrin-1 as a potential target for metastatic cancer: focus on colorectal cancer. *Cancer and Metastasis Reviews*, 1-13.

## 1.1 Importance of the enteric nervous system

The enteric nervous system (ENS) is the largest subdivision of the autonomic nervous system and provides innervation to the gastrointestinal tract (GIT) [1]. The ENS sends an intrinsic signal to the GIT, while the sympathetic and parasympathetic nervous systems send extrinsic signals to the GIT. The significance of the ENS lies in the fact that it can directly control the autonomous functions of the GIT in the absence of signals from the brain and spinal cord [2]. In addition to this autonomy, the network of the ENS resembles the structure of the central nervous system (CNS). Clusters of enteric neurons, ganglia, are formed in the absence of collagen. The enteric neurons are supported by astrocyte-like enteric glia, instead of Schwann cells in the peripheral nervous system (PNS) [3, 4]. Neurochemically, many neurotransmitters and neuromodulators, that are involved in the CNS, are also found to be associated with the ENS [5]. Hence, the ENS is known as the “second brain” [6]. Many functions of the GIT, that are controlled by the ENS, are essential for host survival. The major functions include digestion and absorption of nutrients, intestinal motility and secretion of water/mucus, transport of food and elimination of waste, blood flow, and intestinal protection from ingested toxins and pathogens [7, 8]. The critical role played by the ENS in the fundamental activities of the GIT is illustrated by the fact that mice lacking a portion of the ENS along the GIT die within 24 hours of birth [9]. Similarly, human infants lacking the ENS associated with the large intestine will not survive if the condition is left untreated [10].

Following sections outline an intricate network of the ENS organisation in mammalian gut and the presence of diverse enteric neuronal types in the ENS.

### 1.1.1 Organisation of the enteric nervous system

The ENS is generated by clusters of enteric neurons and glial cells that combine to form multiple ganglia. These ganglia are interconnected by internodal strands containing axons, and they are organised into two concentric ganglionated plexuses that form networks within the gut wall (**Figure 1.1**) [11]. The plexus that is located between the longitudinal and circular muscle layers is called the myenteric (also known as Auerbach’s) plexus. This plexus runs from

the oesophagus to the rectum and regulates the motility of the gut [12]. The other plexus that lies within the connective tissue of the submucosa except for the oesophagus is named as the submucosal plexus. In large mammals, there are the inner submucosal (Meissner's) plexus and the outer submucosal (Schabadasch's or Henle's) plexus [13]. Meissner's plexus is positioned at the serosal side of the muscularis mucosae, while Schabadasch's plexus is located next to the luminal side of the circular muscle layer. In humans, there is a third plexus, intermediate plexus, that lies in between the outer and inner submucosal plexuses [14]. The submucosal plexus regulates mostly secretion and vascular tone of the gut [15]. In addition to the ganglionated plexuses, there are a few non-ganglionated plexus containing axons that innervate target tissues in the GIT [16].

The human ENS contains just as many neurons (approximately  $10^6$  -  $10^9$  nerve cells) as in the spinal cord [16, 17]. Various subtypes of enteric neurons are grouped into ganglia and form neuronal circuitry for the GIT. The density of neurons in the myenteric plexus is found to be greater than in the submucosal plexus. The size of ganglia between myenteric and submucosal plexuses can vary depending on the regions of the gut within an individual, as well as between species [2].

**Figure 1.1 A schematic diagram illustrating the organisation of the ENS**

This is representative of ENS organisation in human and medium to large size mammals. Two major ganglionated plexuses include the myenteric plexus and the submucosal plexus (SMP). The myenteric plexus lies in between the longitudinal and circular muscle, and it controls the gut motility. The SMP is located in the submucosa. There are outer and inner SMP, and they sense the contents of the lumen and regulate secretion and blood flow of the gut. (adapted from Furness *et al.*, 2014 [11]).

**Abbreviation:** SMP, submucosal plexus.

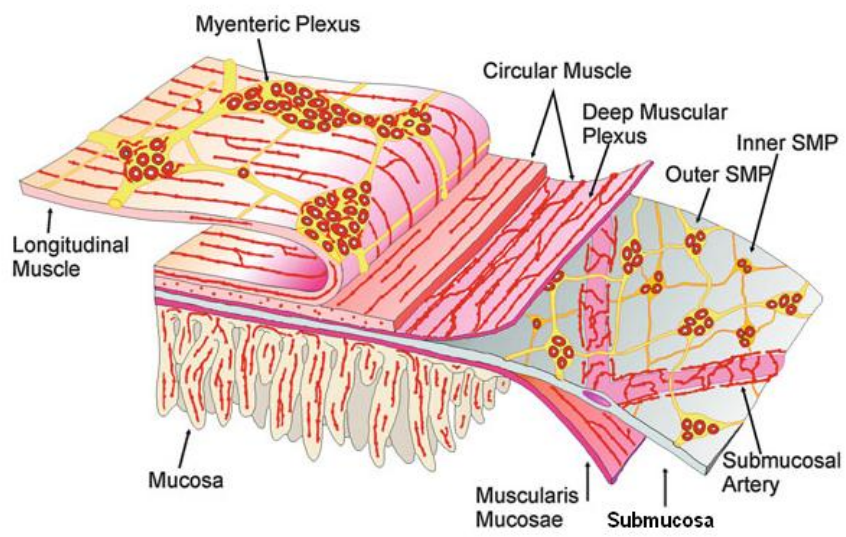


Figure 1.1

### 1.1.2 Diversity of enteric neurons

The intrinsic nerve circuits of the ENS contain 14-20 types of enteric neurons depending on species and the region of the gut [18]. The most extensive studies on enteric neurons have been carried out in guinea-pigs, with smaller scale studies being undertaken on humans, mice, rats and pigs. The neurons are classified based upon results obtained using a combination of morphology, neurochemistry and functional properties by employing various techniques including immunohistochemistry (IHC) and electrophysiology [19].

Broadly, 3 classes of enteric neurons have been identified in the plexuses. These include intrinsic primary afferent neurons (IPANs, also called intrinsic sensory neurons), interneurons and motor neurons [2, 8]. IPANs receive signals from sensory receptors present in the mucosa and muscle. They respond to chemical and mechanical stimuli by sending signals to interneurons and/or directly to motor neurons. Ascending and descending interneurons integrate signals from sensory neurons to motor neurons. Motor neurons control the gut mobility and secretion by directly acting on effector cells such as smooth muscle cells and secretory cells. Motor neurons include excitatory and inhibitory motor neurons, secretomotor neurons, and vasodilator neurons [2, 20].

A vast number of neurotransmitters and neuropeptides have been identified in enteric neurons at different stages of the development [21]. The neurochemical coding of the enteric neurons has revealed a useful distinction between the enteric neurons in relation to their functional types [18]. As consequence, diverse subtypes of enteric neurons have been generated based on neurochemical phenotypes.

In the guinea-pig ileum, 10-15 subtypes of neurons in the myenteric plexus and 4-5 subtypes of neurons in the submucosal plexus have been identified [21]. Certain neurochemical codes have been highly conserved between species. The conserved chemical codes are mostly for excitatory and inhibitory muscle motor neurons that are essential for gut motility. These include choline acetyltransferase (ChAT, an enzyme synthesizing acetylcholine) and tachykinins for excitatory muscle motor neurons. The chemical codes for inhibitory muscle motor neurons include nitric oxide synthase (NOS, an enzyme

synthesising nitric oxide), vasoactive intestinal polypeptide (VIP) and pituitary adenylate cyclase-activating polypeptide (PACAP). Secretomotor neurons are found to contain VIP in all species. The neurochemical codes for IPANs include calcium-binding proteins such as calbindin and calretinin. IPANs also express more than one coding and the other coding includes substance P (SP) and calcitonin gene-related peptide (CGRP). The neurochemical codes for interneurons include calretinin, 5-hydroxytryptamine (5-HT) and somatostatin.

It is well-established that many different subtypes of enteric neurons are present in the ENS, and they are all derived from neural crest cells. However, it is yet to be determined what factors might cause this diversity of enteric neurons generated from the single source.

The generation of new neurons, known as neurogenesis, in the ENS is thought to occur by neural crest stem cells maintaining the reserve pool of enteric neuron numbers in the ENS throughout the life of the organism [22, 23].

## **1.2 Enteric nervous system development and neurogenesis**

### **1.2.1 Overview of enteric nervous system development**

During embryogenesis, cells from the vagal and sacral regions of the neural crest give rise to the enteric neurons and glial cells which form the ENS [24]. The majority of the ENS is composed of the cells that are derived from the vagal origin of the neural crest, with a minor contribution being made by sacral neural crest cells [25]. Enteric neural crest-derived cells (NCCs) are a heterogeneous population which includes progenitors and neural crest stem cells (NCSCs) [26].

It has been found in mice that vagal neural crest progenitors delaminate from the dorsal neural tube at the embryonic (E) days around E8.5-E9 [27]. After delamination, they then migrate in a rostral to caudal direction and enter the foregut around E9.5 (**Figure 1.2**). The foregut refers to the anterior portion of the alimentary canal, from the esophagus to stomach [28]. These vagal neural crest progenitors populate within the gut mesenchyme, and then further migrate via midgut and to colonise the hindgut by E12.5. The midgut gives rise to the

small intestine and the hindgut forms the large intestine [28]. Following on the arrival of vagal progenitors at the hindgut, sacral progenitors migrate ventrally to colonise the pelvic mesenchyme and enter the hindgut at E13.5. Sacral progenitors then mix with vagal progenitors and continuously migrate caudorally and complete the colonisation of the entire hindgut by around E14.5 in mice [24, 29]. The complete colonisation of the gut by enteric NCCs takes approximately 7 weeks gestation in humans [23]. Once this colonisation is completed, a complex neuronal network is generated by interconnecting multiple ganglia containing enteric neurons and glial cells.

In the following sections, enteric neurogenesis in the ENS development is described. Also, evidence supporting the presence of enteric neurogenesis in the adult ENS is discussed to explore a potential therapy for treating neurodegenerative conditions.

**Figure 1.2 A schematic diagram showing colonisation of neural crest cells in developing gut and generation of mature enteric neurons and glia**

**(A)** Vagal neural crest cells invade foregut (FG) and colonise the entire gut by migrating towards hindgut (HG). Sacral neural crest cells also contribute to the ENS by colonising HG. **(B)** A formation of the neural network in the postnatal gut. **(C)** The neural network is composed of multiple ganglia. Each ganglion contains mature neurons and glial cells that are derived from neural crest cells (adapted from Goldstein *et al.*, 2013 [30]).

**Abbreviations:** FG, foregut; MG, midgut; HG, hindgut; MYP, myenteric plexus; SMP, submucosal plexus.

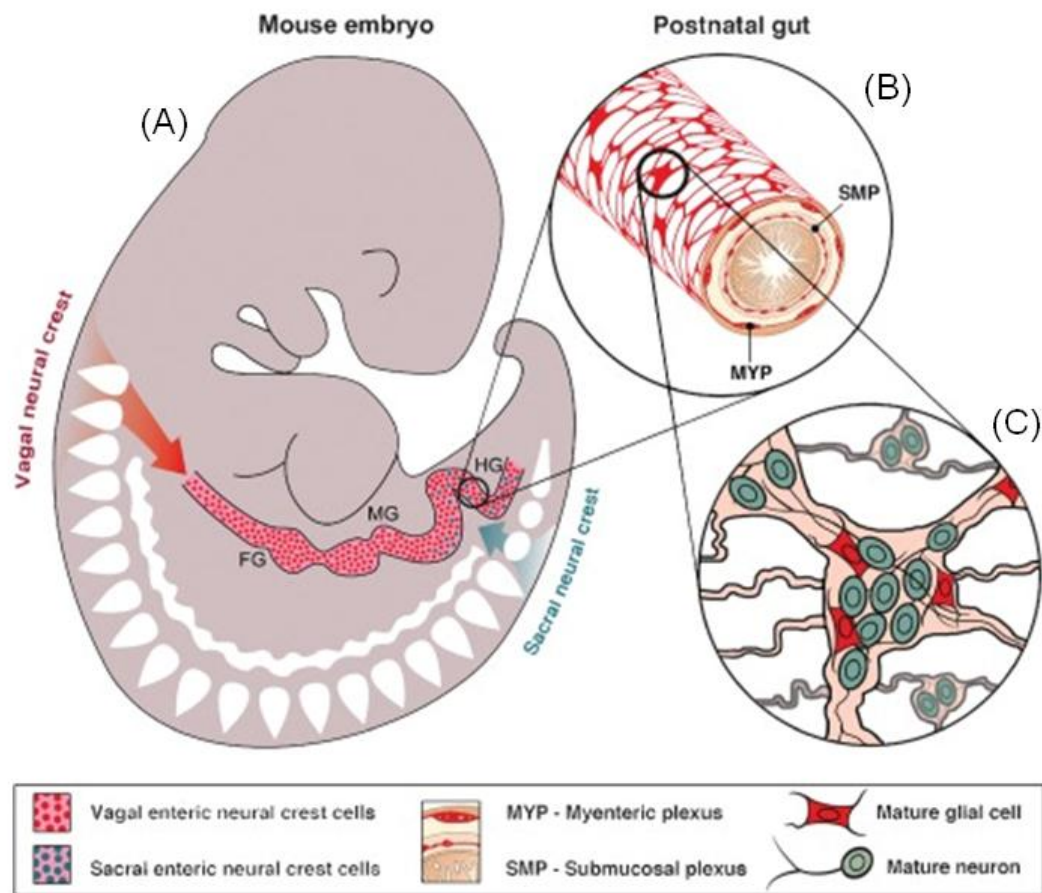


Figure 1.2

### 1.2.2 Neurogenesis in the enteric nervous system development

Neurogenesis is a critical process that occurs during ENS development. It increases cell density so that enteric neurons colonise the entire gut [23]. Multipotent NCSCs that have migrated to the embryo foregut initially express a high level of SRY-related HMG-box gene (Sox10) [31]. During colonisation, NCSCs increase their numbers and also up-regulate a panel of progenitor genes. The progenitors are characterised by markers labelling the expression of Ret, p75, nestin, Mash1 and Phox2b [32, 33]. Subsequently, the neuronal markers such as  $\beta$ -Tubulin III, PGP9.5 and HuC/C are up-regulated when NCSCs become more committed to produce unipotent neuronal precursors [23].

Once NCCs reach their final destination in the process of gut colonisation, Sox10 is highly expressed by glial cells but not by enteric neurons [34]. The NCSCs can also differentiate into glial cells which are recognised by the markers such as brain fatty acid-binding protein (B-FABP), calcium-binding protein B (S100) and Sox10 [35]. A subpopulation of enteric glial cells is found to be able to undergo proliferation in order to maintain plasticity under pathological conditions [36]. Accordingly, some markers, such as nestin and Sox10 that are used for characterising NCSCs are also shown to label the glial cells [33].

The birth period for each particular enteric subtype is relatively long. Different subtypes can be born simultaneously or born at different periods of time [37]. For example, the myenteric neurons that express 5-HT are born between E8 and E14. Similarly, neurons expressing ChAT are born between E8 and E15. However, neurons expressing VIP are born from E10 till postnatal (P) day 5 [21, 37, 38]. The appearance of post-mitotic neurons expressing 5-HT and ChAT (E8) is earlier than the day (E8.5-E9) on which NCCs begin to colonise the gut. On the other hand, the appearance of post-mitotic neurons expressing VIP is continued after the gut is fully developed. It was suggested that dividing neuronal precursors and post-mitotic enteric neurons coexist during ENS development and during maturation of the ENS. It is further believed that this coexistence continues after birth [23, 33].

### 1.2.3 Neurogenesis in the adult enteric nervous system

The age at which precursors end mitosis and exit the cell cycle is referred to as the birth-date of enteric neurons [21]. Enteric neurons are detected by pan-neuronal markers, soon after NCSCs enter the foregut mesenchyme. The birth-dates of different enteric neuron subtypes appear at different stages of the ENS development, but also some enteric neuron subtypes such as VIP and CGRP expressing neurons are found to appear continuously even after birth [37]. Furthermore, an increase in murine enteric neurons has been detected at the postnatal stage [39, 40].

It has been found that neurogenesis occurs not only during embryonic development but also throughout adulthood [41]. A number of studies have demonstrated that self-renewing neural crest progenitor cells were isolated from the adult gut. Those isolated progenitors were shown to give rise to neurons and glial cells in an *in vitro* system [42-44]. Also, studies using *in vivo* models have shown that the neural stem cells are retained in postnatal murine gut [42, 45]. However, several studies reported that detecting active enteric neurogenesis in the adult mammalian gut under physiological condition has been difficult [37, 46-48]. Interestingly, when injury was introduced to the murine gut, the presence of enteric neurogenesis has been readily detected using *in vivo* models [22, 49].

For example, recovery of the ENS was investigated in guinea-pigs after transection and reanastomosis of the ileum was performed [49]. It was found that an increase in the number of enteric neurons was shown near the operated lesion and they formed small clusters. However, it was yet to be determined whether the extraganglionic neurons that appeared in the area adjacent to the lesion were due to *de novo* neurons or neurons migrated from adjacent ganglia.

Another *in vivo* study conducted by Hanani *et al.* demonstrated a recovery of morphological changes in the colonic myenteric plexus after introducing benzalkonium chloride (BAC) into mice [22]. BAC is a cationic detergent that is capable of destroying myenteric plexus and generating aganglionosis in animal models [50, 51]. The authors observed that regenerating nerve fibers in the ablated myenteric plexus region by day 7, and from day 14 onwards,

undifferentiated cells and differentiating neurons in ganglia were found in the denervated region. New neural plasticity was exhibited by day 30. The authors suggested that quiescent NCSCs are contained in the adult ENS, and can be stimulated to undergo proliferation and differentiation in response to injury.

Further evidence for enteric neurogenesis in the adult ENS has been demonstrated by Liu *et al.* [47]. The authors showed that the number of enteric neurons was increased in wild-type mice during a 4-month period after birth. However, the number of enteric neurons was shown to subsequently decline with age in the adult ENS. This phenomenon was found to be dependent upon the presence of 5-HT<sub>4</sub> receptor, since a greater reduction in the number of enteric neurons was observed in 5-HT<sub>4</sub> knock-out mice after 4-months of age. The authors indicated that application of 5-HT<sub>4</sub> agonists in mice was able to stimulate neurogenesis, hence detection of adult neurogenesis was possible, otherwise difficult due to its slow rate under physiological condition.

Recently, enteric neurogenesis in the adult mice has been also confirmed by Kulkarni *et al.* The authors have found that neurogenesis is required to maintain a healthy adult ENS, since there is ongoing apoptosis of the enteric neurons in the gut [52]. It was also suggested that adult neurogenesis *in vivo* may be regulated by the phosphatase and tensin homologue (PTEN) signalling pathway.

These studies raise a possibility that enteric NCSCs and progenitors can be stimulated by intrinsic changes or extrinsic factors that are provided in the neuronal microenvironment. Identifying factors that are involved in the regulation of the enteric NCCs proliferation and differentiation would be a useful target for treating various pathological conditions involving neuropathy.

However, recent studies have highlighted the central role of cross-talk between the nervous system and the cancer microenvironment that has an influence on cancer progression [53, 54]. In order to determine a therapeutic factor that could assist in the ENS regeneration without enhancing cancer progression, the interplay between nerves and cancer cells is discussed in the next section.

### 1.3 Cross-talk between nerves and cancer

It has been found that nerves can stimulate cancer cell growth and enhance cancer cell dissemination by releasing neurotransmitters such as catecholamine and acetylcholine into the cancer region [55, 56]. The released neurotransmitters then bind to their corresponding receptors, such as  $\beta$ -adrenergic receptors and muscarinic receptors, which are present on the membranes of cancer stromal cells. Upon binding, the stromal cells become activated to interact with tumour cells, and that in turn promote cancer development [57]. Reciprocally, cancer cells release neurotrophic growth factors, which support outgrowth of nerves into the tumours. This leads to creating a positive feedback loop of the interplay between nerves and cancer cells, resulting in cancer progression, ultimately metastasis [58].

Perineural invasion (PNI) is a pathologic process that cancer cells migrate along the nerve structure, and this process has been first reported in head and neck cancers in mid-1800 [59]. Its clinical significance has emerged in recent years, since several malignant cancers, including prostate [60] and pancreatic cancer [61] have shown PNI as a key pathological feature.

In addition, parasympathetic neurogenesis and cancer-related axonogenesis describe pathologic processes that the number of neurons in ganglia and nerve density are increased in cancers. These processes are shown to be associated with aggressive nature of cancers, thereby correlated to poor prognosis [62, 63]. In prostate cancer, the density of nerves became a parameter for grading the Gleason prostate cancer score [58]. On the other hand, with gastric cancers, surgically removed nerve fibers were found to suppress gastric tumorigenesis [64]. *In vivo* studies of transplanting human colorectal and gastric cancer stem cells into nude mice demonstrated that some cancer stem cells were able to give rise to neurons and that generation of neurons in the tumour region promoted tumorigenesis. However, when the process of differentiating cancer stem cells into neurons was blocked by using knock-down strategies, the tumourigenesis was suppressed [53].

Recently, Rademakers *et al.* [65] extensively reviewed on a topic concerning a direct and indirect impact of the ENS on cancer progression and highlighted the

factors released from the ENS should be taken into account for a potential anti-cancer therapy.

The following sections of this thesis summarise a cascade of events involved in colorectal cancer metastasis to understand cellular processes and tumour microenvironmental factors that attribute to colorectal cancer progression.

## **1.4 Colorectal cancer progression and metastasis**

Worldwide, colorectal cancer (CRC) has been marked as one of the leading causes of cancer deaths affecting both men and women [66, 67]. The vast majority of cancer-associated deaths are caused by metastasis [68, 69]. Metastasis is a complex pathological process by which a subpopulation of cancer cells from the primary tumour site is able to disseminate and form a secondary tumour at anatomically different site(s) [70, 71]. Metastasis results from a cascade of events that involve multiple cellular processes, such as detachment, migration, invasion, adhesion, and proliferation. Further to these cellular processes, tumour angiogenesis and microenvironment play instrumental roles in enabling the tumour cells to successfully colonise sites within selectively favourable secondary target organs [72].

Not all cancer cells have a capacity to metastasise [73, 74]. Cancer cells containing several genetic alterations can progress toward malignant cells. These cells exhibit a diminished cell-cell adhesive interaction compared to normal epithelial cells, and that allows the disaggregation of cancer cells within the primary tumour mass [72]. Some detached malignant cells can then invade and migrate through both epithelial basement membrane (BM) and the extracellular matrix (ECM), and enter the bloodstream [70, 71, 75]. When malignant cells are detached from the matrix, they are resistant to anoikis [69]. Within the circulatory system, these resistant malignant cells can adhere to microvascular beds, and the extravasation of malignant cells may be achieved by various mechanisms [76]; (i) paracellular migration of malignant cells through the intercellular junctions between adjacent endothelial cells [77], (ii) paracellular migration through between adjacent retracted endothelial cells, induced by malignant cell secretions [78], and/or (iii) vessel compression by the expansion of an adherent malignant cell mass [79]. Once malignant cells are

able to invade underlying secondary tissue parenchyma, they interact with both stromal cells and the microenvironment [80]. This interaction enhances the growth of malignant cells. Accordingly, the establishment of malignant cells in new sites requires a blood supply that is adequate to meet their metabolic demands [81]. Hence malignant cells up-regulate proangiogenic factors to form new vascularisation, angiogenesis, which arises from adjacent microvascular endothelial cells. Formation of angiogenesis in the secondary tumour site allows malignant cells to repeat the entire sequence of events necessary for further metastasis [71, 82] (**Figure 1.3**).

The importance of tumour microenvironment and tumour angiogenesis has long been recognised in the process of metastasis [71]. Two proposals pinpointed a major phenomenon associated with metastasis and advanced our understanding in the field of cancer metastasis research. The first proposal was “the seed and the soil” concept, a metaphor first used by the English surgeon, Stephen Paget [82, 83]. This means a particular tumour cell type (the seed) has a predilection toward its favoured organ microenvironment (the soil), and highlighting the phenomenon of organ-specific metastasis. The second proposal was made by the American pathologist, James Ewing, who stated that organ specificity in metastasis can be explained by “circulatory patterns between a primary tumour and specific secondary organs” [82, 84]. Recent metastasis research has been revisiting these proposals in order to further understand the complexity of the interactions between a tumour, its microenvironment and angiogenesis.

In the next section, key molecules that are associated with tumour microenvironment and tumour angiogenesis, in relation to colorectal cancer progression and metastasis are reviewed.

**Figure 1.3 A cascade of events in cancer progression and metastasis**

**(A)** Weakly adherent malignant cells are detached from the tumour mass at the primary site. The malignant cells are able to migrate and invade through surrounding stroma and then enter the local circulation either directly via blood vessels or indirectly via the lymphatics (intravasation). The tumour cells can be arrested at capillary beds in the distant target organ. Thereafter, tumour cells can invade from the capillaries to the surrounding tissue (extravasation) through migration **(B)** between epithelial cell intercellular junctions, **(C)** between retracted epithelial cells that were induced by tumour cell secretions, and/or **(D)** between compressed epithelial cells that were generated by an accumulating adherent tumour cell mass. **(E)** Once colonising tumour cells establish at the distant target organ, tumour cells secrete factors to promote angiogenesis toward the colonised tumour mass [82].

**Abbreviation:** VEGF, vascular endothelial growth factor.

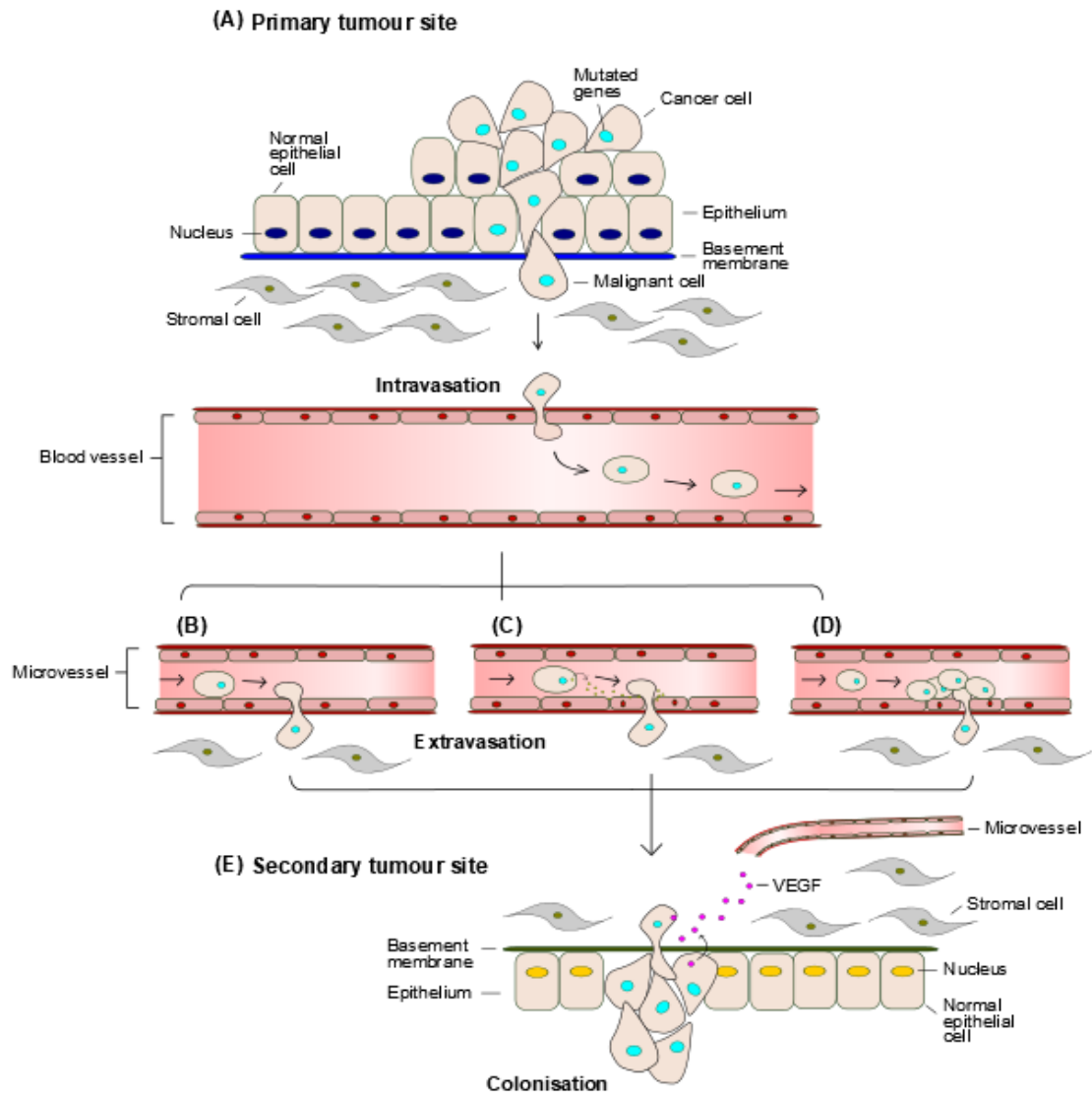


Figure 1.3

### 1.4.1 Tumour microenvironment

It is now widely-recognised that the tumour microenvironment, which provides a metastatic niche for cancer cells, plays a critical role in cancer progression and metastasis [85]. The tumour microenvironment is generated by various factors produced from the transformed tumour cells and stromal cells [86]. The profound impact of microenvironment upon tumours was clearly demonstrated when fully malignant breast cancer cells were treated to restore their normal phenotype by providing them with the non-permissive contents of stroma. The non-permissive stromal content was generated by blocking  $\beta$ 1-integrin and the downstream effector molecules of the epidermal growth factor receptor pathway. The inhibitions allowed the malignant cells to re-enter growth arrest, rearrangement of the actin cytoskeleton and formation of normal adhesion junctions in response to the ECM [87, 88]. Conversely, tumour progression was induced by the permissive stromal environment, such as that procured by overexpression of chemokines [89, 90]. The proof for a tumour-specific microenvironment conditioning its pre-metastatic niche was obtained using B16 melanoma and Lewis lung carcinomas [72, 91]; the lung-specific pre-metastatic niche was conditioned by forming clusters of haematopoietic bone marrow progenitors into the lungs, and hosting the arrival of the lung cancer cells. Meanwhile, melanoma induced the clusters of bone marrow-derived progenitor cells into the melanoma-specific metastatic organs. Below, major molecules, identified in the CRC cells-associated microenvironment, conditioning the liver as a pre-metastatic niche, are discussed.

#### ***Tumour microenvironment related to colorectal cancer***

In human CRC, the *adenomatous polyposis coli (APC)* gene is frequently mutated at the earlier stage of colorectal cancer, and the human homologue of the *Drosophila mad gene (SMAD4)* gene is often deleted by a loss of chromosome 18q at the later stage of colorectal cancer [92, 93]. The mouse model with inactivation of these two genes indicated that their tumour epithelial cells produce an elevated level of the chemokine, chemokine (C-C motif) ligand 9 (CCL9, also known as CCL15 in humans) [94, 95]. CCL9 is released from the tumour epithelial cells and attracts bone marrow-derived immature myeloid cells (iMCs) that are expressing chemokine (C-C motif) receptor 1 (CCR1, receptor for CCL9) to the stroma underneath the tumour epithelium [95]. These recruited

iMCs then produce matrix metalloproteinases, matrix metalloproteinase (MMP)-9 and MMP-2, which in turn assist the tumour cells to migrate and invade the stroma [96]. This mechanism is not only evident in the earlier events of metastasis, but also in later events, in particular, where metastatic colorectal cancer cells colonised the liver after dissemination [94]. An *in vivo* study demonstrated that syngeneic C57BL/6 mice which were injected with CMT93 CRC cells in their spleen for dissemination of the cells to the liver, were surrounded by up to 10 times greater infiltrations of iMCs than the number of the tumour cells [51]. The molecular targeting therapy strategies involving either using anti-CCL9 antibodies or using *Ccr1* knockout mice showed a lack of expansion of the disseminated CRC cells [94]. Furthermore, using a CCR1 antagonist in the mouse model indicated that inhibiting CCR1 can diminish the size and number of metastatic CRC colony lesions in liver [97]. Similarly, MMP-9 or MMP-2 mutant mice showed no expansion of the disseminated metastatic CRC cells, although iMC cells were recruited. However, clinical trials attempting to block MMP-9 and MMP-2 activity with metalloproteinase inhibitors have been unsuccessful due to severe side-effects [98-101]. Most matrix metalloproteinases are involved in normal physiological processes of many tissues and organs, making systemic inhibition approaches prone to side-effects.

#### **1.4.2 Tumour angiogenesis**

It has been shown that rapid tumour growth is accompanied by an enriched vascular supply, whereas inhibiting vascularisation prevents tumour development [102-104]. This is because as tumour progression occurs, neovascularisation is vital for supplying nutrients and overcoming hypoxia, caused by the uncontrolled growth of tumour cells [70]. Under hypoxic conditions, hypoxia inducible factor-1 $\alpha$  (HIF-1 $\alpha$ ) is stabilised in tumour cells and it activates genes that are involved in enhancing angiogenesis [105]. Accordingly, tumour cells produce diffusible factors which can stimulate the growth of blood vessels located close to the tumours, and this ultimately contributes to tumour progression [103, 106]. Hence, strategies revolving around anti-angiogenic factors were developed to block tumour angiogenesis as an anticancer treatment [102]. There exist a diverse range of factors and signalling molecules that are involved in tumour angiogenesis [106, 107]. The

key molecules associated with angiogenesis during colorectal cancer progression are highlighted in the next section.

### ***Tumour angiogenesis related to colorectal cancer***

In human CRC biopsies, a high level of HIF-1 $\alpha$  protein expression is observed, and this protein in turn induces a major angiogenic factor, vascular endothelial growth factor (VEGF) [106, 107]. VEGF interacts with pre-existing blood vessel endothelial cells and promotes vessel growth, thereby promoting tumour angiogenesis [102]. Patients with malignant colorectal cancer show a high level of expression of VEGF [108, 109]. In particular, VEGF189 mRNA isoform has been reported to be a poor prognosis for patients with CRC metastasising to the liver [110]. In addition to VEGF, many other cytokines and chemokines that are derived from the inflammatory response during cancer progression, and oncogene dysregulation are also associated with tumour angiogenesis [111]. Overexpression of prostaglandin E<sub>2</sub> (PGE<sub>2</sub>) has been observed in colorectal adenocarcinoma when compared to adjacent normal tissue [112]. This increased level of PGE<sub>2</sub> synthesis has been shown to promote endothelial cell migration and tube formation in a coculture consisting of endothelial cells and CRC cells overexpressing cyclooxygenase-2 (COX-2) [113]. The production of PGE<sub>2</sub> is induced by COX-2, which is generated by stromal fibroblasts in the early stage of tumorigenesis, and by tumour cells at a later stage of human colorectal cancer [94]. Overexpression of COX-2 in malignant cells is found to be associated with cell survival signals, such as nuclear factor- $\kappa$ B (NF- $\kappa$ B) and signal transducer and activator of transcription 3 (Stat3). Hence the COX-2-dependent pathway is shown to play a pivotal role in colonic polyp expansion [111, 114].

Subsequent findings have described the mechanism that activates colon tumour angiogenesis and this is shown to be via COX-2-induced PGE<sub>2</sub>, which in turn generates HIF-1 $\alpha$  protein and VEGF mRNA in colorectal cancer [111, 112]. The induction of VEGF is mediated by Mitogen-activated protein kinase kinase (MEK) – Extracellular signal regulated kinase (ERK) pathways and Phosphoinositide 3-kinase/Phosphatase and tensin homologue (PI3K/PTEN) – Protein kinase B (PKB, also known as AKT) pathways (**Figure 1.4**). Transfecting CRC cells with an expression vector encoding constitutively active MEK leads to expression of both HIF-1 $\alpha$  protein and VEGF mRNA. Conversely,

MEK inhibitors were able to block the induction of both HIF-1 $\alpha$  protein and VEGF mRNA transcription in PGE<sub>2</sub>-treated cells [115]. Blocking HIF-1 $\alpha$  with siRNA prevented the synthesis of VEGF mRNA, confirming that VEGF expression is mediated by HIF-1 $\alpha$  [112]. Based on an understanding of these hierarchical pathways, a COX-2 inhibitor could then be applied to suppress polyp expansion. The role of this inhibitor was also investigated in clinical trials [94, 116]. However, COX-2 inhibitors for senior sporadic colonic polyposis patients were unsuccessful because the side-effects of the inhibitor posed a high risk factor for patients with a cardiovascular history [117].

On the other hand, in conjunction with chemotherapy drugs, the use of human monoclonal antibodies which block VEGF is now accepted as a first-line treatment for CRC progression [118]. However, hypertension is a common side-effect of this treatment. Also, unwanted side-effects are observed when this treatment is used with other anti-angiogenic drugs. Drugs targeting different checkpoints of the signalling pathways have been developed and the investigation of their anti-angiogenic effects is underway for cancer treatment [111, 119, 120].

In the following sections, diffusible laminin-related protein called Netrin-1 is reviewed. Netrin-1 is a well-known chemoattractant involved in neuronal guidance in the developing ENS, but it is also found to be a key regulator of tumourigenesis. In order to allow better utilisation of Netrin-1 as a therapeutic target for enteric nerve regeneration in the context of colorectal cancer, the effects of Netrin-1 in the developing ENS and colorectal cancer progression are summarised.

#### **Figure 1.4 Key molecules involved in colorectal cancer progression**

**(A)** The expression of COX-2 in both stromal fibroblasts and tumour cells can catalyse PGE<sub>2</sub>, which binds to EP2 or EP4 receptors present on tumour cells in an autocrine and paracrine manner [121]. This leads to activation of the PI3K signalling pathway downstream effector molecule NF-κB, which in turn promotes transcription of genes that are required for tumour cell invasion [122].

**(B)** COX-2-induced PGE<sub>2</sub> produces HIF-1α protein and VEGF via MEK-ERK and PI3K-AKT pathways. The HIF-1α protein heterodimerises with HIF-1β protein and activates target genes such as VEGF and promotes angiogenesis.

**Abbreviations:** COX-2, cyclooxygenase-2; PGE<sub>2</sub>, prostaglandin E<sub>2</sub>; EP<sub>2</sub>, extracellular protein 2; EP<sub>4</sub>, extracellular protein 4; PI3K, phosphoinositide 3-kinase; NF-κB, nuclear factor κB; MMP-9, Matrix metalloproteinase 9; MEK, mitogen-activated kinase kinase; AKT, serine/threonine kinase; HIF-1α, Hypoxia inducible factor-1 α; HIF-1β, Hypoxia inducible factor-1 β; VEGF, Vascular endothelial growth factor.



## 1.5 Netrin family and their receptors

Netrins are a family of secreted proteins that function as a chemotropic directional cue for axonal growth and cell migration during nervous system development [123, 124]. The first member of the Netrin family, UNC-6, was identified in the nematode worm *Caenorhabditis elegans* (*C. Elegans*) by examining mutants with loss of the *unc-6* gene [125]. In the wild type, the UNC-6/Netrin protein is secreted by floor plate cells at the ventral midline, and orients the commissural axons to grow from the dorsal part of the spinal cord to the ventral midline. However, as a consequence of this mutation, the directional cue for the correct trajectory of the spinal commissural axons was absent in this organism. Hence, the mutant exhibited an uncoordinated phenotype as a result of defects in nervous system development [125, 126].

The function of the Netrin family is known to be highly conserved in various animal species [124]. In mammals, there are three secreted Netrin members (Netrin-1, either Netrin-2 in chick or Netrin-3 in mice and Netrin-4, also called  $\beta$ -Netrin) and two membrane-anchored glycosylphosphatidylinositol (GPI) linked Netrin members (Netrin-G1 and Netrin-G2) [123, 124, 127]. The membrane-anchored Netrin-Gs are reported to have evolved independently of the secreted Netrins [128], and are found only in vertebrates [123].

Although all Netrin members are structurally related to the extracellular matrix (ECM) protein, laminin, which is a major glycoprotein in the ECM, a diverse range of Netrin receptors have been identified [123, 124, 129]. The secreted Netrins interact with single-pass transmembrane receptors including deleted in colorectal cancer (DCC), the uncoordinated-5 homolog family (UNC5H1-4, also known as UNC5A-D in human), Neogenin and the Down's syndrome cell adhesion molecule (DSCAM),  $\alpha 6\beta 4$  and  $\alpha 3\beta 1$  integrins [130]. The membrane-anchored Netrin-G1 and Netrin-G2 interact with other transmembrane receptors, Netrin-G ligand-1 and Netrin-G ligand-2, respectively [123, 124]. The adenosine A2b receptor (Adora2b) has also been reported to be a Netrin-1 receptor; however this is still debatable since it binds to another ligand, with higher affinity [127, 131].

Among the members of the Netrin family, Netrin-1 has been best characterized for function and expression [132]. The chemotropic function of Netrin-1 is shown as either chemoattractant [133] or chemorepellant [134] in the developing CNS. Which of these two antagonistic effects of Netrin-1 is observed depends on the particular receptor that Netrin-1 interacts with [135]. In this thesis, DCC, Neogenin and UNC5H2/UNC5B receptors will be focused. This is because they are known to mediate two antagonistic functional effects upon Netrin-1 binding, in terms of chemotropic guidance in neuronal tissues [126, 136]. But also, these receptors have been linked to tumourigenesis depending on the availability of Netrin-1 in non-neuronal tissues [137].

In the following sections, the structure and binding sites of Netrin-1 and its receptors, specifically DCC, Neogenin and UNC5-H are discussed.

### **1.5.1 Netrin-1 structure**

Netrin-1 is a laminin-related extracellular matrix protein. It is approximately 600-amino acid residues long and has a head-to-stalk feature [138, 139]. Netrin-1 is composed of three domains, namely VI, V, and C (**Figure 1.5 A**) [140]. The globular shape of the VI domain located at amino-(N)-terminus represents the head feature. This domain is structurally identical to the N-terminal gamma-chain of a laminin protein. Next to the VI domain, three rod-like structure of the V domain forms the stalk. The V domain consists of laminin-type, three cysteine-rich epidermal growth factor (EGF) repeats, called EGF-1, EGF-2 and EGF-3. The EGF-2 motif is longer than the other two EGF motifs as it has an extra helix-strand. This motif is conserved among the Netrin family. The C domain is positioned at the carboxyl-(C)-terminus of Netrin-1, and is positively charged [141, 142]. This domain is not required for receptor binding, but it binds to heparin sulfate ions, which assist in receptor binding affinities [142].

Studies using crystallography have revealed that one molecule of Netrin-1 interacts with two receptors in the form of either homo-dimers or hetero-dimers. Two receptor-binding sites are found in the V domain of Netrin-1. The structure of the binding site 1 is identified to be evolutionarily conserved from *C.elegans* to *Homo sapiens*, whereas the binding site 2 is shown to be evolutionarily

divergent. Receptor binding site 1 is located at the tip of the EGF-3 region. This binding site is found to be a specific site for DCC binding. The binding of DCC is facilitated by a sulfate ion, located at the periphery of the binding site on Netrin-1, providing a bridge between residues of Netrin-1 and DCC. The binding site 2 is identified in a region between EGF-1 and EGF-2, and this site has been shown to be a generic site for binding receptors [141]. Binding to site 2 is assisted by sulfate and chloride ions that are embedded on the Netrin-1 surface. These negatively charged ions reside on Netrin-1 and are essential for neutralizing the positively charged interface in the binding sites. Furthermore, heparin sulfate ions and environmental factors are thought to play an important role in selecting receptors for the binding site 2 of Netrin-1. As a consequence, binding site 2 determines a chemotropic response that is either chemoattractive or chemorepulsive.

### **1.5.2 Netrin-1 receptor DCC structure**

DCC is a 1,447-amino acid long, single-pass transmembrane receptor that is a member of immunoglobulin (Ig) superfamily [140] (**Figure 1.5 B**). In the extracellular region, the DCC protein contains four Ig-like domains at the N-terminus followed by six fibronectin (FN) type III repeats. It is found that FN4, FN5 FN6 domains are the locations where Netrin-1 interacts. Biolayer interferometry binding studies conducted by Xu *et al.* indicated that the FN4 and FN5 domains of DCC are involved in the binding site 1 of Netrin-1 [142]. Crystal structure studies from Finci *et al.* [141] demonstrated that the FN5 domain of DCC is involved with both binding sites 1 and 2 of Netrin-1. The FN5 domain is exclusively associated with binding site 1, while the FN6 domain is essential for binding site 2 of Netrin-1. The intracellular region of the DCC protein contains three highly conserved sequence motifs namely P1, P2 and P3. When Netrin-1 binds to the extracellular region of two DCC receptors, it leads to homodimerisation of P3 motifs in the intracellular region of DCC receptors. This results in recruitment of intracellular signalling molecules, and that in turn induces chemoattractive activity [141].

### **1.5.3 Netrin-1 receptor Neogenin structure**

Neogenin is known to be a DCC paralogue that shares approximately 50% amino acid identity in vertebrates [143, 144]. Like DCC, Neogenin is a 1,461

amino acids long, single-transmembrane protein that is a member of the Ig superfamily [145] (**Figure 1.5 B**). It is composed of four Ig domains and 6 FN type III repeats in the extracellular portion. Neogenin receptors have two Netrin-1 binding sites at the FN4 and FN5 domains. The FN4 domain of Neogenin is found to interact with the VI domain of Netrin-1, while the FN5 domain of Neogenin is found to engage with the EGF-3 motif of Netrin-1. A key feature that distinguishes Neogenin from DCC is that Neogenin has a slightly longer alpha-helix linker in between FN4 and FN5 domains. Because of this linker, the Netrin-1 and Neogenin complex forms a distinct architecture during its assembly on the cell membrane, and that complex structure is a 2:2 heterotetramer. This means that two Netrin-1 molecules link to two Neogenin receptors sitting side by side by forming a 'head to head'-shaped dimerisation of Netrin-1 molecules [142].

Similar to DCC, Neogenin contains three intracellular motifs namely P1, P2 and P3, and they show about 37% amino acid identity to the cytoplasmic sequence of DCC [144]. These motifs are known to play a key role in cytosolic signalling transduction upon ligand binding [146].

In addition to Netrin-1 binding, repulsive guidance molecule family members (RGMs) bind to Neogenin. The binding sites for RGMs are located at the FN5 and FN6 domains of Neogenin [145]. It was found that Neogenin has a binding site which has a higher affinity for RGMs than Netrin-1 [147]. Upon binding of RGMs, Neogenin induces axonal repulsion and neurite growth inhibitory effects [148]. On the other hand, Neogenin mediates axonal attraction towards Netrin-1 gradient. Neogenin is found to transduce two opposing effects based on context-dependent signals during axonal pathfinding in the embryonic vertebrate brain [149].

#### **1.5.4 Netrin-1 receptor UNC5H structure**

The UNC5 homologue family is a group of single-pass transmembrane receptors that range from 919- to 963-amino acids long [140, 150] (**Figure 1.5 B**). The UNC5 family also belongs to the Ig superfamily. They contain two Ig domains at the N-terminus followed by two thrombospondin (TSP) type I domains in the extracellular region. In the intracellular region, there are three conserved domains including a ZU5 domain (named after the mouse tight

junction protein called zonula occludens-1, ZO-1, and *C.elegans* Unc5), a DCC-binding (DB) domain and a death domain (DD).

The studies using truncated versions of UNC5H2 have demonstrated that extracellular Ig-1 and Ig-2 domains of UNC5H are the regions that have a high affinity for Netrin-1 binding. The Ig-1 domain is found to be primarily responsible for interacting with the EGF-2 motif of Netrin-1 [138].

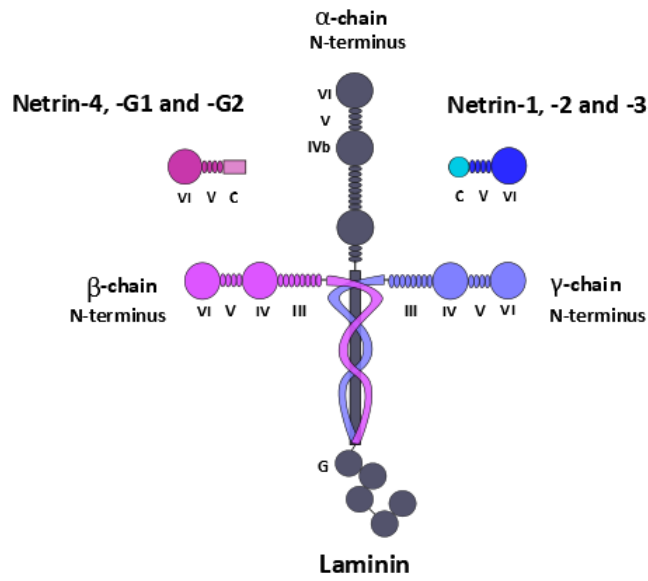
When Netrin-1 binds to the extracellular region of DCC and UNC5 receptors, it leads to hetero-dimerisation between the P1 motif of the DCC receptor and the DB motif of the UNC5 in the intracellular region [151]. This results in recruitment of different sets of signalling molecules to DCC homo-dimerisation and that mediates chemorepulsive activity [141].

Radar plots from repulsion/attraction assays have indicated that occupying the DCC-specific binding site 1 by DCC is required for inducing UNC5A-dependent chemorepulsion. Also it was found that UNC5A must outcompete DCC to preferentially gain access binding to site 2 of Netrin-1 in order to mediate chemorepulsive activity [141].

### **Figure 1.5 The structure of netrins and major Netrin-1 receptors**

**(A)** Netrins consist of three domains, namely, domain V, VI and C. All netrin members belong to the laminin superfamily [124]. Domains V and VI of Netrin-1,-2 and -3 are homologous to the N-terminus of domains V and VI of the laminin  $\gamma$  chain, whereas those of netrin-4, netrin G1 and netrin G2 are homologous to the laminin  $\beta$  chain. However, domain C is homologous to a number of different molecules other than laminin. In the case of Netrin-1, the N-terminal of domain VI is globular, and domain V comprises three epidermal growth factor repeats. Both domains interact with netrin receptors such as DCC and UNC5H [132]. **(B)** The Netrin-1 receptor, DCC is a single-pass transmembrane receptor. The extracellular domain of DCC is composed of four immunoglobulin-like domains and six fibronectin type III-like motifs. The 4<sup>th</sup> and 5<sup>th</sup> of fibronectin type III domains interact with Netrin-1. The intracellular domain of DCC consists of three regions, known as P1, P2 and P3. These regions are found to be conserved among orthologs and are associated with a functional role of DCC. Neogenin has a similar structure to DCC. A key difference between Neogenin and DCC is that there is a longer linker in between 4<sup>th</sup> and 5<sup>th</sup> of fibronectin type III domains. Another Netrin-1 receptor, UNC5H is a type I transmembrane receptor. It consists of two immunoglobulin-like domains and two thrombospondin type I domains in the extracellular portion. The immunoglobulin repeats interact with Netrin-1. The intracellular portion of UNC5H contains a ZU-5 domain, a DCC-binding domain and a death domain. These domains are known to elicit the functional effects of Netrin-1 [125, 126]. **Abbreviations:** Ig, immunoglobulin; FN-III, fibronectin type III; Thbs1, thrombospondin type 1; ZU5, zona occludens 5; DB, DCC-binding domain; DD, death domain.

(A)



(B)

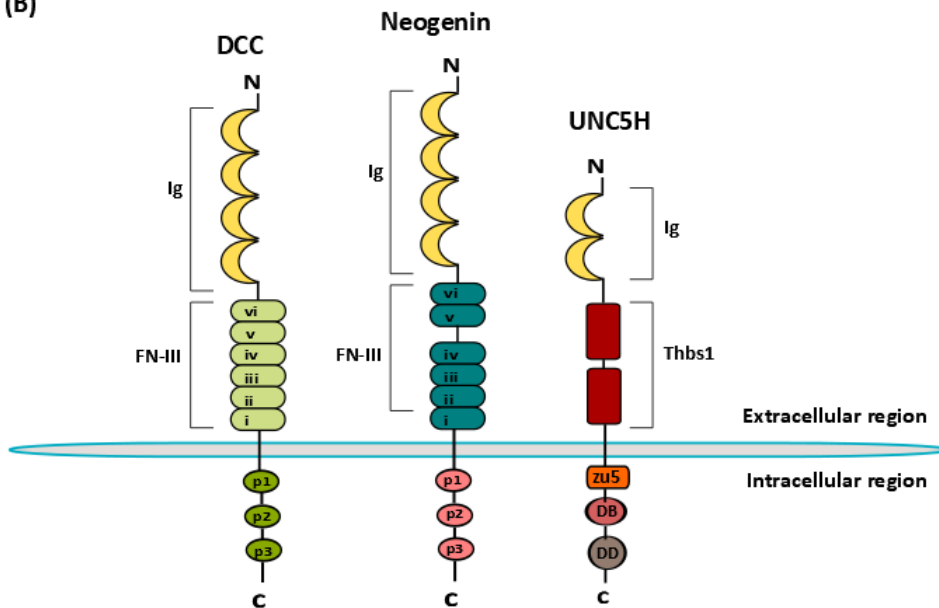


Figure 1.5

## 1.6 Netrin-1 chemotropic receptors in neuronal tissues: chemoattraction versus chemorepulsion

It is now well-established that upon Netrin-1 binding, a homo-dimerised DCC receptors mediate chemoattractive activity, while a hetero-dimerised UNC5H and DCC receptors elicit chemorepulsive activity in neuronal tissues [124] (**Figure 1.6**). The extracellular domains of these receptors bind to Netrin-1, and the intracellular domains of receptors are responsible for modulating the chemotropic effect in the migratory properties of neurons [132]. This was clearly demonstrated in cultured *Xenopus* spinal neuron studies using chimeric receptors [135]. The chimeric receptor was made by fusing the extracellular domain of DCC to the intracellular domain of UNC5H, and this was sufficient to mediate axonal chemorepulsion in response to Netrin-1. In contrast, when the chimeric receptors containing the extracellular domain of UNC5H fused to the intracellular domain of DCC was introduced, chemoattraction was observed in response to Netrin-1. Furthermore, when UNC5H receptors are co-expressed with DCC receptors in migrating growth cones, UNC5H receptors are able to switch chemoattractive effect of DCC receptors to chemorepulsive. Consistent with previous finding in *C. elegans* [125], this leads to axonal growth cones being repelled by the source of Netrin-1 [135].

In addition to the antagonistic migratory function, DCC and UNC5H receptors are found to initiate either anti-apoptosis or pro-apoptosis intracellular signalling pathways depending on the presence or absence of Netrin-1 binding, respectively [152]. The following section describes another two antagonistic activities of these receptors in dictating the fate of cells, and discusses their function in relation to cancer in non-neuronal tissues.

**Figure 1.6 Chemoattraction or chemorepulsion mediated by Netrin-1 receptors**

**(A)** In the presence of Netrin-1, homo-dimerisation of DCC receptors mediates the axonal growth cone to move towards a Netrin-1 source. In contrast, **(B)** either UNC5H receptor alone or hetero-dimerisation of DCC and UNC5H receptors induces the axonal growth cone to move away from a Netrin-1 source.

**Abbreviations:** DCC, deleted in colorectal cancer; UNC5H, uncoordinated-5 homologue.

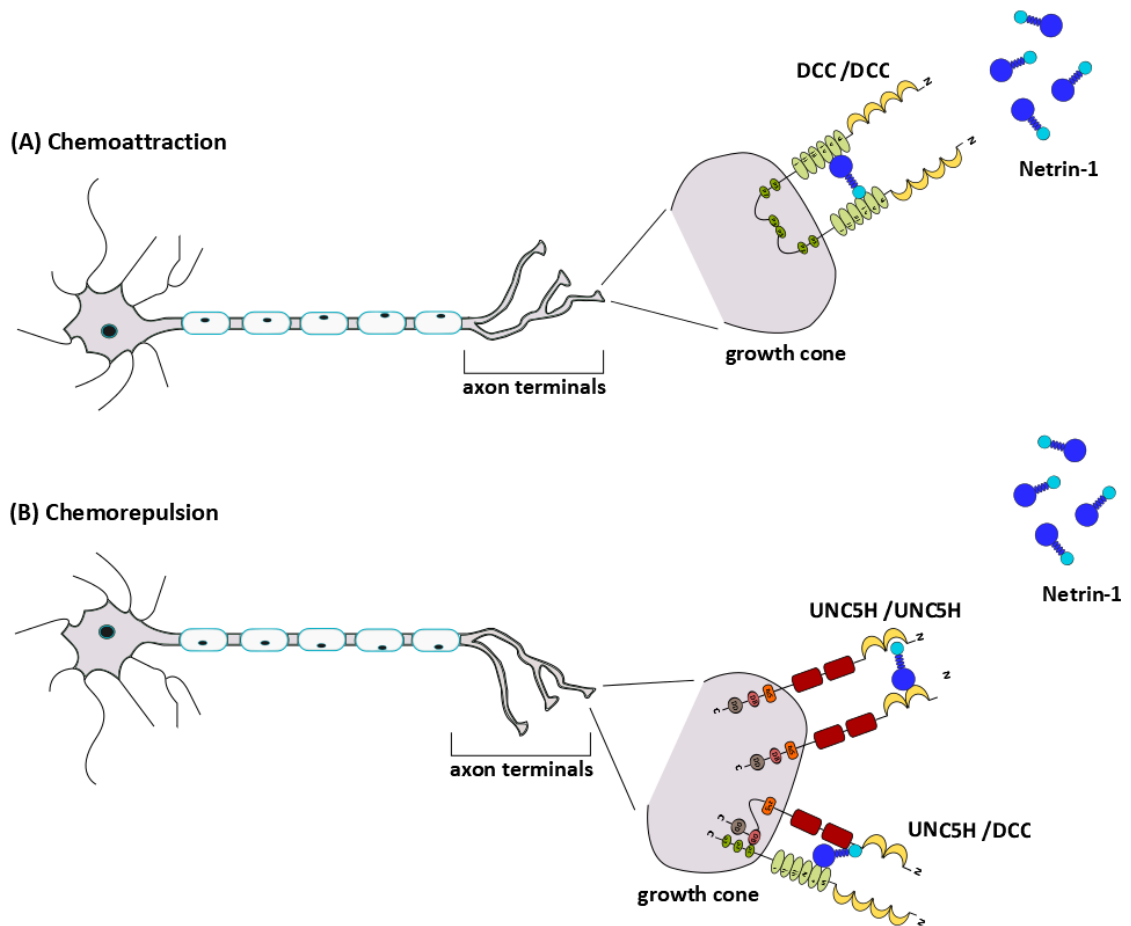


Figure 1.6

## 1.7 Netrin-1 dependence receptors in non-neuronal tissues: tumour suppressor versus tumour promoter

As the name suggests, *DCC* gene is known to be frequently deleted in human colorectal cancer [126]. The *DCC* gene is located in chromosome 18q21, a common locus for tumour suppressor genes. However, this region is often subject to a loss of heterozygosity (LOH) event among various cancers, particularly in colorectal cancer [93, 153]. The LOH results in decreased expression of tumour suppressor proteins such as DCC, leading to tumour growth [126]. Suppression of tumour growth was demonstrated when an intact copy of chromosome 18 was introduced to a colorectal cancer cell line, which lacked endogenous DCC expression [154]. Also, an inhibition of tumour growth was observed in nude mice when DCC expression was restored [155]. Given this, DCC was originally thought to play a tumour suppressor role [126].

However, the tumour suppressor role of DCC has been questioned since point mutations of the DCC coding sequence are rarely observed [156]. Also, heterozygous mice with an inactivating mutation of the *DCC* gene did not show any increase in frequency of tumour formation [157]. Accordingly, the putative tumour suppressor role of DCC was revised.

Further studies concerning the mechanism of action underlying the Netrin-1 receptors brought new insight into the role of DCC [158] and UNC5H [152]. These receptors are found to be functionally related to the dependence receptor family, such as the nerve growth factor receptor, p75<sup>NTR</sup>, the rearranged during transfection (RET) and  $\alpha\beta3$  integrin [159, 160]. Dependence receptors are membrane receptors, which can mediate or inhibit cellular apoptosis depending on the absence or presence of their corresponding ligand binding, respectively [161]. *In vitro* assays showed that in the absence of Netrin-1, the intracellular portion of DCC and UNC5H is cleaved by caspase activity, and subsequent cellular apoptosis is induced. In contrast, caspase-dependent cellular apoptosis is inhibited when Netrin-1 binds to its receptors [152, 158]. In support of this, Netrin-1 knock-out mice demonstrated an increase in death of DCC- or UNC5H-

expressing neurons in the brainstem [152]. Collectively, these results indicated that Netrin-1 can act as a cell survival factor.

Given that, this dependence receptor notion was further investigated with respect to cancer [126]. DCC and UNC5H receptors are able to block tumour growth via triggering apoptosis in the absence of Netrin-1. In contrast, they can enhance tumour growth via blocking apoptosis of DCC and UNC5H receptors in the presence of Netrin-1, leading to ultimate cell proliferation.

Importantly, it has been found that the expression of DCC and UNC5H receptors is either lost or decreased in many cancers. This means that cancer cells lack the capacity to undergo apoptosis that is mediated by these receptors. As a consequence, this can lead to a selective advantage for cancer cells to develop further and enhance progression [162].

Collectively, these receptors are proposed to be conditional tumour suppressors instead of putative tumour suppressors [137]. It would be important to understand the receptor dependency in the context of various cancer conditions.

## **1.8 Netrin-1 chemotropic signalling pathways**

### **1.8.1 Chemoattraction**

Netrin-1 signalling activates multiple intracellular signalling transduction pathways, that are associated with altering the architecture of the cytoskeleton network [123]. When Netrin-1 binds to the extracellular domain of the DCC receptor it triggers homo-dimerisation of DCC receptors via interacting with intracellular P3 domains [163] (**Figure 1.7 A**). This leads to the activation of a number of kinases, including protein tyrosine kinase 2 (PTK2), Src-family kinases (SFKs) and Fyn [164, 165]. The intracellular domain of DCC is constitutively bound by PTK2, which serves as a scaffold. Upon Netrin-1 stimulation, Src is recruited to the DCC and phosphorylates PTK2 to create a binding site for the adaptor protein such as growth factor receptor-bound protein 2 (Grb2) [166]. Association between PTK2 and Grb2 results in activation of the extracellular-signal-regulated kinase (ERK)-2 and mitogen-activated protein

kinase (MAPK) cascade [167]. These pathways are required for synthesizing local proteins, which contribute to neuronal outgrowth [124].

In addition to Src, Fyn is also recruited to DCC. Activated Fyn is thought to regulate the activity of Rho GTPases [168] via activating Ras-related C3 Botulinum toxin substrate 1 (Rac1) and cell division cycle 42 (Cdc42), but inhibiting Ras homologous member A (RhoA) in mammalian neurons. This pathway is shown to modulate actin polymerization, hence contributing to a directional cell migration [169].

Moreover, Netrin-1 binding activates PI3K and phospholipase C $\gamma$  (PLC $\gamma$ ) [166]. The activated PI3K stimulates the activity of MIG10, the homolog of mammalian lamellipodin. Blocking PI3K resulted in preventing lamellipodial outgrowth, suggesting that PI3K is important for axonal guidance. Upon activation of PLC $\gamma$ , protein kinase C (PKC) becomes activated, which in turn stimulates the cells to release calcium from intracellular stores. This calcium influx promotes neurite outgrowth [170, 171].

Further evidence has shown that cytosolic cAMP and calcium levels play a crucial part in determining the chemotropic activity of commissural neurons in *Xenopus*. The chemoattractive activity is found to be associated with a high level of cAMP, while the chemorepulsive activity is related to a low level of cAMP [126]. Subsequent findings have demonstrated that Netrin-1 stimulation induces an increase in cAMP level and a transient release of calcium in the growth cones of retinal axons in *Xenopus* [172]. This correlation between Netrin-1 stimulation and increased cAMP level is also thought to be mediated by A2b receptors [173].

### **Figure 1.7 Netrin-1 chemotropic signalling pathways**

**(A)** In response to Netrin-1, homo-dimerisation of DCC receptors occurs via P3 domain interaction. P3 domain is constitutively bound by PTK2, also known as FAK. Upon Netrin-1 binding, Src is recruited to DCC and phosphorylates PTK2. This allows Grb2 to bind PTK2, which in turn activates ERK and MAPK cascade. In addition, PI3K and PLC $\gamma$  are activated in response to Netrin-1 binding. Activated PI3K stimulates the activity of MIG10, and activated PLC $\gamma$  hydrolyses PIP2 into IP3 and DAG. IP3 stimulates the release of intracellular calcium, and DAG activates PKC, which in turn stimulates the downstream effect on cytoskeleton remodeling. Collectively, these pathways contribute to a neuronal outgrowth. Furthermore, recruited Fyn activates Rac1 and Cdc42 whilst it inhibits RhoA. N-WASP, a downstream effector is activated and this pathway regulates actin polymerization, which provides a direction of the cell migration [124, 166]. **(B)** The hetero-dimerisation of UNC5H and DCC occurs via interaction between DB domain of UNC5-H and P1 domain of DCC. The phosphorylation of UNC5H occurs via PTK2 and Src. This leads to tyrosine phosphatase Shp2. However, the mechanism of action is yet to be unraveled [124].

**Abbreviations:** PTK2, protein tyrosine kinase 2; FAK, focal adhesion kinase; Src, tyrosine kinase sarcoma; Grb2, growth factor receptor-bound protein 2; ERK, extracellular-signal-regulated kinase; MAPK, mitogen-activated protein kinase; PLC $\gamma$ , phospholipase C $\gamma$ ; PI3K, phosphatidylinositol 3-kinase; PIP2, phosphatidylinositol (4,5) bisphosphate; IP3, inositol triphosphate; Rac1, ras-related C3 Botulinum toxin substrate 1; Cdc42, cell division cycle 42; RhoA, ras homologous member A; N-WASP, neuronal Wiskott-Aldrich syndrome protein; Shp2, Src homology region 2 domain-containing phosphatase 2.

(A) Chemoattraction

(B) Chemorepulsion

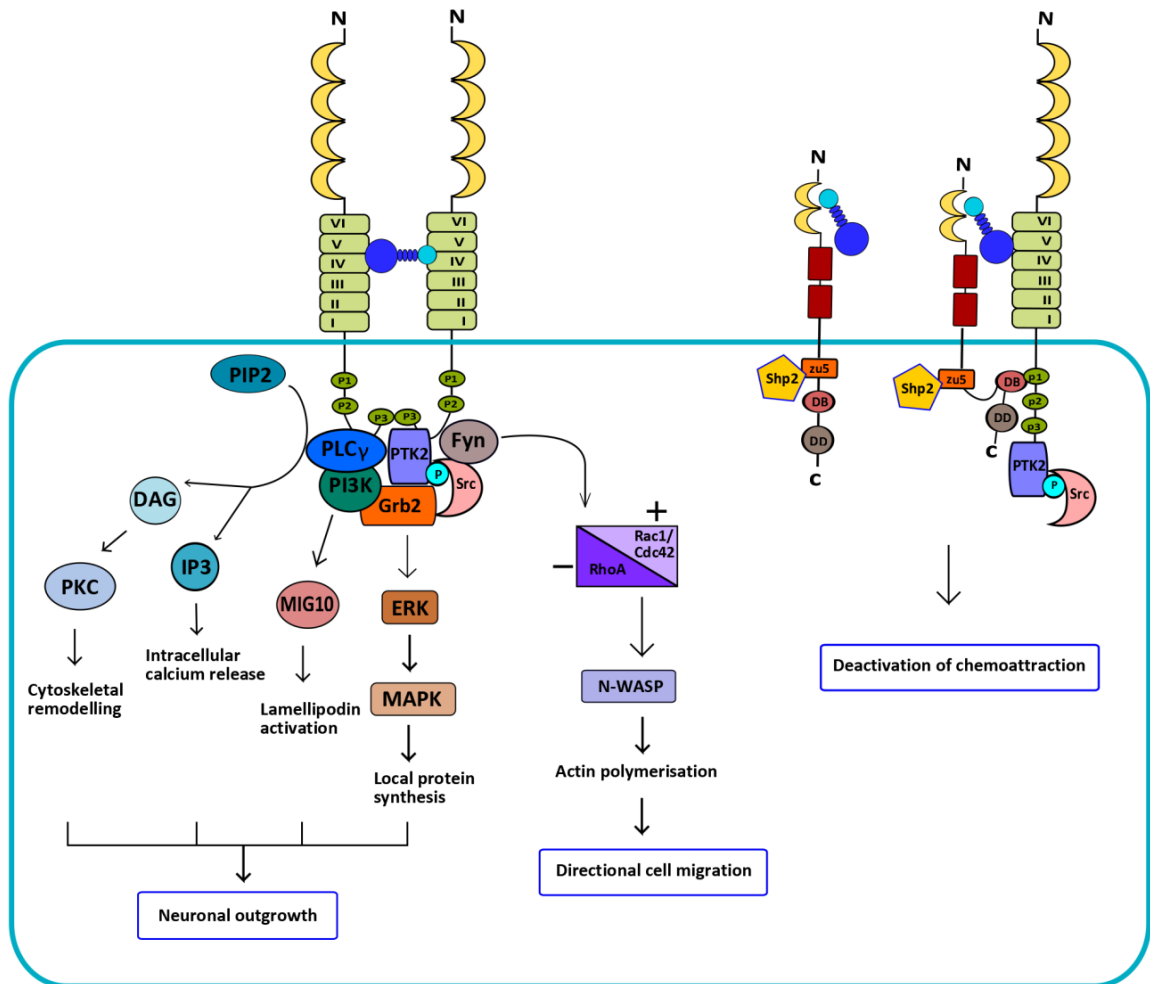


Figure 1.7

### 1.8.2 Chemorepulsion

The chemorepulsive activity is mediated by either UNC5H receptor alone or hetero-dimerised UNC5H and DCC receptors [135]. Both *in vitro* and *Drosophila* studies demonstrated that UNC5H alone induces short-range repulsion, whereas hetero-dimerised receptors mediate long-range repulsion in response to Netrin-1 [174]. Netrin-1 stimulates tyrosine phosphorylation of UNC5H receptors via Src and PTK2, and also stimulates tyrosine phosphatase, Shp2 (**Figure 1.7 B**). Activated Shp2 is proposed to regulate the phosphorylation of the receptor by inducing dephosphorylation, which results in the receptor to be re-activated upon Netrin-1 stimulation [175]. Further understanding of this Netrin-1 dependence pathway is required in relation to chemorepulsive activity.

## 1.9 Netrin-1 dependence receptor signalling pathways

### 1.9.1 Pro-apoptosis

In the absence of Netrin-1, DCC remains as a monomer, which reveals the caspase-3 cleavage site, Asp1290, at the intracellular portion of the receptor [176, 177]. Accessibility to the cleavage site is essential for DCC to induce apoptosis since the pro-apoptotic effect of DCC can be inhibited when a point mutation in this site is introduced [153].

DCC is cleaved by caspase-3 *in vitro* [158]. However, DCC is cleaved by caspase-3 or other unknown proteases *in vivo* (**Figure 1.8 A**) [153]. This cleavage allows the addition dependence domain (ADD) to be exposed upstream to the caspase-3 cleavage site. The ADD domain acts as a scaffold to recruit adaptor proteins, such as DCC-interacting protein 13- $\alpha$  (DIP13 $\alpha$ ). Caspase-9 is recruited and binds indirectly to the ADD domain. This leads to activation of caspase-9, which in turn activates more caspase-3 [160, 177, 178].

UNC5H receptors are also cleaved by caspase-3 (**Figure 1.8 B**). The classic cleavage site for caspase-3 is located within the death domain of the UNC5H receptors [152]. Apoptosis is induced by the death domain of the cleaved UNC5H2 receptor, interacting with the serine/threonine death-associated protein kinase (DAPK) [179]. The activated DAPK is found to initiate the

apoptotic pathway through caspase-9 followed by caspase-3 activation. However, exact mechanisms underlying DAPK-induced apoptosis is still unclear. Furthermore, ZU-5 domain of UNC5H1-3 receptors is shown to interact with the activated protein kinase, neurotrophin receptor-interacting melanoma-associated antigen homologue (NRAGE) [180]. NRAGE is reported to mediate UNC5H-induced apoptosis via two pathways; 1) degrading the caspase inhibitor of apoptosis protein (IAP), and 2) activating the pro-apoptotic c-Jun N-terminal kinase (JNK) signalling pathway [180].

Still, many gaps to be unravel in the Netrin-1-independent apoptotic signalling. However, both DCC and UNC5H-induced apoptosis is shown to take a different pathway to commonly known apoptotic pathways, such as the mitochondrial apoptosis pathways and the death receptor caspase-8 pathways. Hence, there is no involvement of cytochrome *c* released from mitochondria and a subsequent apoptosome complex formation containing cytochrome *c*, apaf-1 and caspase-9 [153, 181].

Furthermore, it is worth noting that the pro-apoptotic pathway is already initiated by activated caspase-3 before cleaving the receptors [153]. The current view favors a model proposing that the conformation of the receptors in the presence or absence of Netrin-1 triggers the recruitment and/or activation of caspase to the cleavage site [177]. Following cleavage, both DCC and UNC5H receptors are proposed to serve as a local amplifier of caspase activation, since the downstream activation of caspase-3 provides a feed-back loop and amplifies further caspase activation at the receptor [153].

### **Figure 1.8 Netrin-1 dependence receptor signalling**

**(A)** In the absence of Netrin-1, monomeric DCC is cleaved by caspase-3 at the cleavage site, D 1290. After cleavage, DIP13 $\alpha$ , also known as APPL is recruited to the cleaved DCC revealing ADD domain. Caspase-9 is also recruited to the ADD domain by unknown mechanism. This leads to the activation of caspase-9, which in turn activates caspase-3. This activated caspase-3 then stimulates a positive feed-back on the receptor that is unbound to Netrin-1. **(B)** In the absence of Netrin-1, UNC5-H receptor is cleaved by caspase-3 at the D412 site in the DD. This leads to activation of DAPK pathway which then stimulates caspase-9 followed by caspase-3 activation. In addition, NRAGE interacts with ZU-5 domain of UNC5H and induce apoptosis via degrading IAP and activating JNK signalling pathway [153]. **(C)** In the presence of Netrin-1, the caspase-3 cleavage site of DCC is masked as DCC receptors form homo-dimerisation. DIP13 $\alpha$ , also known as APPL is dissociated from the DCC and activates the AKT signalling pathway. This leads to inhibition of mitochondrial pro-apoptotic proteins, cytochrome *c* release, and promotion of anti-apoptotic genes via activating NF- $\kappa$ B transcription. Also, activation of MAPK pathway blocks caspase-9 activity.

**Abbreviations:** DIP13 $\alpha$ , DCC-interacting protein 13- $\alpha$ ; APPL, adaptor protein that containing pleckstrin homology domain, phosphotyrosine binding domain and leucine zipper motif; DAPK, serine/threonine death-associated protein kinase; NRAGE, neurotrophin receptor-interacting melanoma-associated antigen homologue; IAP, inhibitor of apoptosis protein; JNK, c-Jun N-terminal kinase.

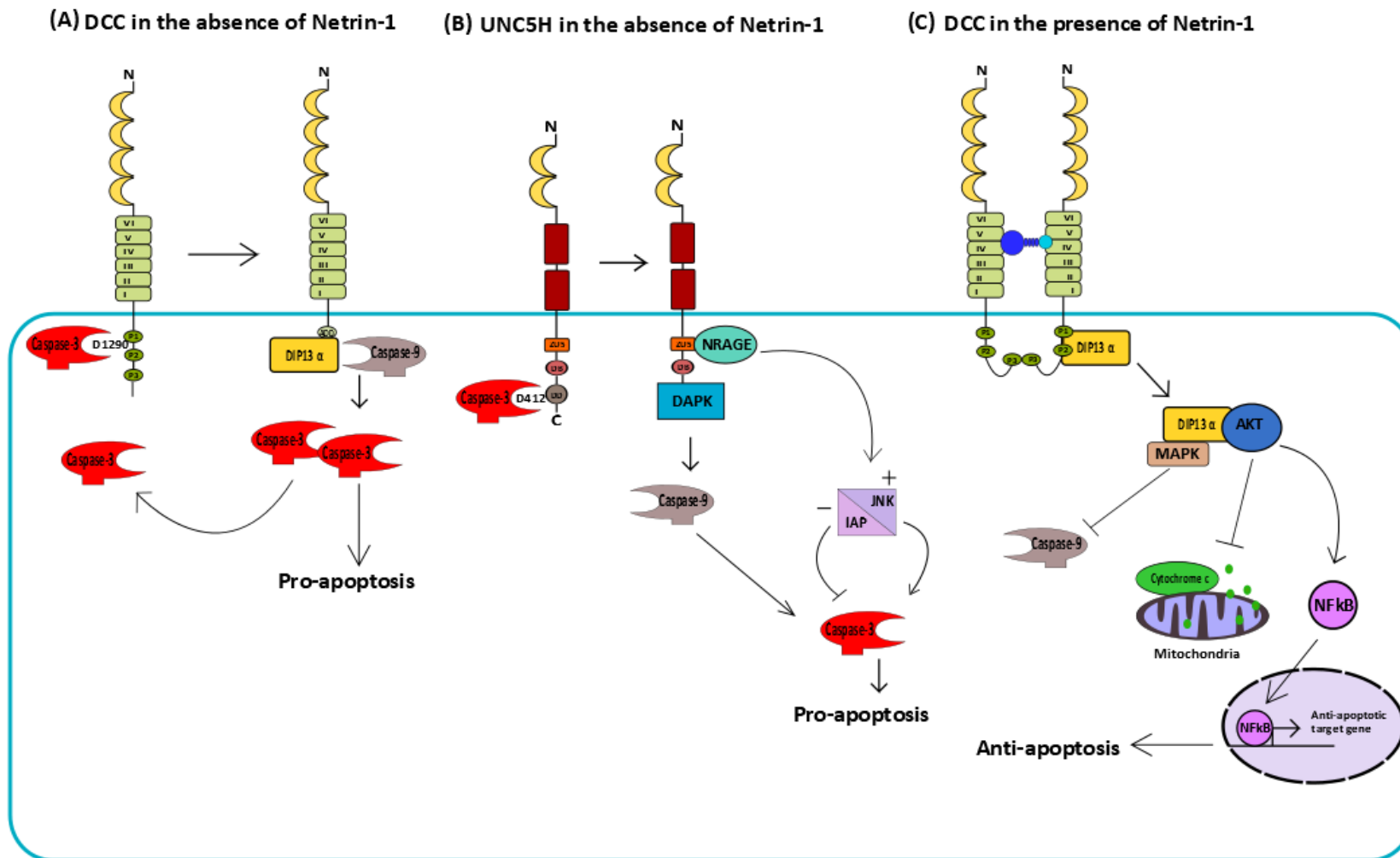


Figure 1.8

### 1.9.2 Anti-apoptosis

The inhibition of apoptotic signalling is induced by the receptor dimerisation upon Netrin-1 binding [135, 153]. The dimerised receptors change their conformation, which prevents the exposure of the caspase-3 cleavage site (**Figure 1.8 C**). Also, dissociation of DIP13 $\alpha$  from the receptor enables the activation of the AKT signalling pathway. This event is thought to block release of pro-apoptotic proteins from the mitochondria and activate NF- $\kappa$ B-mediated transcription, inducing anti-apoptotic genes [153]. Moreover, activation of the MAPK signalling pathway, involved in chemoattraction, is also thought to block apoptosis via regulating caspase inhibitors, resulting in inhibition of caspase-9 and pro-caspase-3 activities [182]. The details of this mechanism are yet to be elucidated.

## 1.10 The roles of Netrin-1 in the developing enteric nervous system

It is now well-established that Netrin-1 plays a crucial role for axonal guidance and cell migration in the developing CNS. The expression and function of Netrin-1 in the developing CNS have been extensively reviewed in previous research (summarized in **Table 1.1**).

In the early 2000s, interest of Netrin-1 function has been investigated beyond the CNS, and the expression of Netrin-1 receptor, DCC, is found in the developing ENS [183]. The ENS is the largest division of the autonomic nervous system that innervates the wall of the gastrointestinal tract (GIT), and is essential for controlling the GIT functions [184]. The ENS is composed of enteric neurons and glial cells, derived from neural crest cells [185]. These neural crest cells undergo two stages of migration to establish the ENS during development. First, they migrate toward the gut via guidance molecules expressed by the gut mesenchyme, and become differentiated into myenteric ganglia [127, 186]. Second, a subset of these neural crest cells migrates toward the mucosa and into the pancreas and form submucosal and pancreatic ganglia, respectively. The immunohistochemical analysis of embryonic mouse gut at E13 showed that Netrin-1 is localized in cells within the outer layer of mesenchyme, at the base of the mucosal epithelium and in the basolateral

borders of acinar cells in pancreas [127]. Consistent with earlier finding [183], DCC-immunoreactivity is localized in the presumptive myenteric plexi of the stomach and small intestine, and the region close to the islets of Langerhans [127]. These DCC-immunoreactive cells are also labeled with neuronal marker, indicating that developing enteric neurons contain DCC receptors.

Furthermore, the explant assay using quail small intestine showed that neural crest-derived cells are able to migrate toward co-cultured Netrin-1 expressing cells. This migration of the neural crest-derived cells is inhibited by using anti-DCC antibody, which blocks the Netrin-1 binding site of the DCC, suggesting that the migration of neural crest cells is DCC-dependent attraction in response to Netrin-1 [127, 187]. Together with this *in vitro* assay, the lack of formation of submucosal and pancreatic ganglia shown in DCC knock-out mice indicates that the secondary migration of neural crest-derived cells are mediated by Netrin-1 and DCC attraction [127].

In addition to DCC-expressing neural crest cell migration, innervation of DCC-expressing vagal sensory axons to the fetal mouse gut has been revealed [188]. The establishment of the vagal sensory innervation to the gut is important for coordination between GIT and the CNS. Vagal sensory axons descending from nodose ganglia are also found to be DCC-immunoreactive, and they are extended to outer gut mesenchyme where the first source of Netrin-1 is localised. Subsequently, these DCC expressing sensory axons are found to branch out toward the mucosal epithelium, where the second source of Netrin-1 is detected [186]. In a study using Ret knock-out mice, which lack enteric neurons, it is demonstrated that innervation of vagal sensory axons to the gut requires the presence of enteric neurons, suggesting the enteric neurons as a possible Netrin-1 source [189]. This was further investigated by co-culture assay using embryonic rat neural crest-derived cells and 293-EBNA cells, transfected with c-Myc-tagged Netrin-1. In this study, the enteric neurons were only Netrin-1-immunoreactive, not c-Myc-immunoreactive, which confirms that the enteric neurons synthesize Netrin-1, instead of acquiring Netrin-1 [189].

In the adult mice GIT, mRNA encoding Netrin-1 is detected in the stomach and small intestine, while mRNA encoding DCC is found in the adult nodose ganglia

[188]. However, the role of Netrin-1 and DCC in the adult ENS has not been elucidated either *in vitro* or *in vivo*. Furthermore, the expression of UNC5H in response to Netrin-1 in the developing and adult GIT is yet to be investigated.

**Table 1.1 Major Netrin-1 functions in the developing nervous system**

Netrin-1 origin	Netrin-1-expressing cells	Receptor type	Receptor-expressing cells	Receptor-expressing cell origin	Receptor role	Biological function	Assay(s)	Refs
Forebrain	Mitral cells in olfactory bulb	DCC	Precursors of the olfactory interneurons	Subventricular zone of the brain	Attraction	Guidance for cell migration - migrate to the olfactory bulb and become differentiated into periglomerular and granule cells	Embryonic rats and mice	[190, 191]
Ventral midbrain	Striatum	DCC	Axons of dopaminergic (DA) neurons	Substantia nigra pars	Attraction	Guidance for axons – DA axonal outgrowth to form the nigrostriatal pathway	Explant culture from embryonic rat ventral midbrain	[192]
Spinal cord	Floor plate cells at the ventral midline	DCC	Commissural axons	Dorsal part of spinal cord	Attraction	Guidance for axons - spinal commissural axons to project towards ventral midline	Embryonic rat spinal cord, embryonic dorsal spinal cord explants culture and <i>DCC</i> knock-out mice	[136] [157]
Spinal cord	Floor plate cells at the ventral midline	UNC-5H3	Axons of the trochlear motor neurons	Caudal midbrain	Repulsion	Guidance for axons - spinal motor axons to project ventrally away from the midline	<i>Unc5h3</i> knock-out mice	[193]
Spinal cord	Floor plate cells and ventral neuroepithelium	DCC and UNC-5H1	Oligodendrocyte precursor cells (OPs)	Ventricular zone	Repulsion	Guidance for cell migration – migrate OPs away from the ventral midline and contribute to later OPs differentiation	Embryonic mouse spinal cord and microchemotaxis assay of OPs	[194]

Spinal cord	Floor plate cells	DCC	Precerebellar neurons	Dorsal hindbrain	Attraction	Guidance for cell migration - form the pontine nuclei in the hindbrain	Embryonic rat and cells from DRN explants culture	[133]
Spinal cord	Dorsal spinal cord cells	UNC-5H3	Axons of dorsal root ganglion neurons	Dorsal part of the spinal cord	Repulsion	Guidance for axons – DRG axons to grow into the dorsolateral margin of the spinal cord and form the dorsal funiculus	<i>netrin-1</i> knock-out embryonic mice	[195]
Optic disc and fissure	Neuroepithelial cells at the disk	DCC	Axons of the retinal ganglion (RGC) cells	Dorsal central retina near the optic fissure	Attraction	Guidance for axons – extend RGC axons toward the optic disc and exit from the retina and grow into the optic nerve	Embryonic mice retinal explants and <i>netrin-1</i> and <i>DCC</i> knock-out embryonic mice	[196]
Gut and pancreas	Mesenchyme cells, mucosal epithelium and acinar cells of pancreas	DCC	Vagal-neural crest cells	Neural plate border	Attraction	Guidance for cell migration – migrate neural crest cells into GIT and form myenteric ganalia, largely submucosal and pancreatic ganglia	Embryonic chick explants, embryonic <i>DCC</i> knock-out mice and <i>Ret</i> <sup>TGM/+</sup> mice	[127]
ENS	Enteric neurons	DCC	Vagal sensory axons	Nodose and jugular ganglia	Attraction	Guidance for axons – vagal sensory innervation to the gut	<i>In vitro</i> Embryonic mice <i>Ret</i> knock-out mice	[189]

**Abbreviations:**

- a DCC, deleted in colorectal cancer
- b DA, dopaminergic
- c DRN, dorsal rhombencephalic neuroepithelium
- d UNC5H3, uncoordinated-5 homolog 3
- e UNC5H1, uncoordinated-5 homolog 1
- f Ops, oligodendrocyte precursor cells (OPs)
- g DRG, dorsal root ganglion
- h RGC, retinal ganglion cells
- i GIT, gastrointestinal tract
- j ENCDs, enteric neural crest derived cells

## 1.11 The role of Netrin-1 in nerve injury

In the developing CNS, Netrin-1 serves as a long-range guidance cue to make correct axonal trajectories [197]. Netrin-1 expression is found to persist in motor neurons and dorsal interneurons of the rodent spinal cord in the adult. Particularly, Netrin-1 expression is mostly enriched in periaxonal myelin membranes, and Netrin-1 is thought to serve as a short-range cue to maintain the appropriately formed network structure in the adult mammalian CNS [198]

In the case of rat spinal cord injury, the levels of Netrin-1 mRNA and protein are found to be significantly reduced in neurons and oligodendrocytes at the lesional site, whilst Netrin-1 expression is shown to persist in those cells near and outside the injury site [199]. It was reported that the reduced level of Netrin-1 expression at the lesion remained for several months following the injury [199].

In addition to Netrin-1, its receptors such as DCC, Neogenin and UNC5A-D are also expressed in the rat spinal cord throughout the embryo till adulthood [200]. During maturation, down-regulation of DCC and Neogenin, which elicit chemo-attractive response, was noted. Conversely, up-regulation of UNC5A-D, which mediates chemo-repulsive response, was evident [200].

Following rat spinal cord injury, the levels of Netrin-1 receptors are found to be reduced in the lesion as well as the adjacent area to the injury site. It was indicated that a further reduction in the level of DCC remained for several months after injury, whereas the reduced levels of UNC5A-C lasted for 1 month after injury. However, 40 days subsequent to injury, no significant difference in the levels of UNC5A-C was found in the injured spinal cord in comparison to the intact spinal cord [199].

It was demonstrated that Netrin-1 inhibits axonal regeneration in the adult rat CNS after spinal cord injury [199, 201], since dominant expression of UNC5A-C over DCC and Neogenin was present at the spinal cord lesion 40 days following injury, as well as continuous expression of Netrin-1 in oligodendrocytes surrounding the lesion [199].

In addition to CNS, Netrin-1 expression is also found at a low level in the rat adult PNS, namely sciatic nerve and Schwann cells [202]. It was indicated that upon sciatic nerve crush injury, a significant increase (approximately 40-fold) in the level of Netrin-1 mRNA was produced predominantly in Schwann cells during anastomosis 2 weeks after sciatic nerve transaction [202, 203]. Furthermore, an increase in the level of Netrin-1 in the distal nerve stump was reported a few days after sciatic nerve transaction in rats [202]. Up-regulation of Netrin-1 mRNA level was indicated a few weeks after mouse median nerve transaction. A subsequent elevation of Netrin-1 expression in the median nerve segment distal to the injury site was reported [204]. Collectively, expression of Netrin-1 is up-regulated in Schwann cells upon peripheral nerve transaction injury.

Peripheral nerve injury causes damages to axons of two major types of neurons, such as motor and sensory [150]. The cell bodies of motor neurons are located in the ventral horn of the spinal cord [198]. The cell bodies of sensory neurons are located in the dorsal root ganglia (DRG) [205]. The motor neurons express Netrin-1 receptors such as DCC, Neogenin, and UNC5A-D in the adult rodent spinal cord. Following sciatic nerve injury, DCC expression was markedly increased whereas expression of UNC5B-C was down-regulated in the motor neurons in DRG, a few days after the injury.

In the rat PNS, nerve regeneration is promoted by activated Schwann cells releasing neurotrophic molecules at the distal nerve segment, therefore outgrowth of Schwann cells at the nerve injury site is recognised as an important strategy for nerve regeneration [206]. Expression of both DCC and UNC5H2 is noted in the intact Schwann cells. However, following an axotomy, activated Schwann cells at the regenerating nerve front are found to exhibit a dominant DCC expression and a low level of UNC5H2 [206]. In addition, migration of Schwann cells into a nerve gap to form a nerve bridge after injury is important for axon navigation, and Netrin-1 is found to promote proliferation and migration of rat Schwann cells [206].

Moreover, knock-down of DCC or UNC5B expression using siRNA was continuously introduced into the injury site to see whether or not Netrin-1 signalling affects the nerve regeneration in the adult rat PNS [206]. It was found that block of DCC receptors results in fewer axons extending into the injury site. Conversely, blocked of UNC5B receptors induced extension of axons at the nerve front and distal extension of activated Schwann cells [206].

As Netrin-1 receptors contribute to defining the role of Netrin-1 as a repellent or attractant for nerve regeneration. These results underscore the importance of Netrin-1 receptor type expressed in cells following nerve injury, in addition to Netrin-1 expression in the lesion.

Furthermore, as Netrin-1 knock-out mice are not viable after birth [207], Netrin-1 heterozygous mice were used to compare the peripheral nerve regeneration with wild-type control mice. It was found that no significant difference in the axon and fiber diameter, total number of myelinated fibers and myelinated thickness between those two types of mice. However, it was noted that Netrin-1 heterozygous mice exhibited a slower functional recovery during anastomosis after median nerve transaction [208].

Collectively, Netrin-1 has been suggested to play a regulatory role in peripheral nerve regeneration. However, Netrin-1 has a numerous receptors and it is difficult to apply Netrin-1 in these circumstances when opposing types of Netrin-1 receptors are present in the same type of cells. Also, expression of those opposing function of the receptors fluctuates depending on the circumstances. Despite this limitation, Netrin-1 has been recognised as a potent chemoattractant and it is believed to guide axons to the targets with high accuracy. Many studies are underway finding a therapeutic use of Netrin-1 with regards to peripheral nerve regeneration.

### **1.12 The roles of Netrin-1 in colorectal cancer**

In the intestines, DCC receptors are present all along the epithelium, while Netrin-1 is preferentially expressed and forms a gradient [209]. A high concentration of Netrin-1 is present at the crypt base where stem cells/transient

amplifying cells reside. In contrast, a low concentration of Netrin-1 is present at the tip of the villi, where many cells are undergoing apoptosis and are sloughed off (**Figure 1.9**). This Netrin-1 gradient was further examined by using transgenic mice to determine if Netrin-1 is responsible for regulating DCC-induced apoptosis in the intestinal epithelium [137]. The results of this study indicated that overexpression of Netrin-1 caused a decrease in intestinal epithelial cell death, while no increase in proliferation and differentiation of cells was observed. On the contrary, Netrin-1 mutant newborn mice show increased cell death. Collectively, these data support the theory that Netrin-1 regulates apoptosis through DCC dependence receptor in the intestine. However, Netrin-1 is unlikely to be a direct regulator of intestinal homeostasis, since the normal epithelial organization is not disrupted by Netrin-1 overexpression [137].

Similar to DCC expression, mentioned above, a reduction in expression of UNC5A, UNC5B and UNC5C has also been reported in the human colorectal cancer cases [160]. Especially, a significant downregulation of UNC5C expression has been observed in more than 70% of the cases, and this is found to be associated with epigenetic gene inactivation, such as promoter methylation [210]. A high methylation of the UNC5C promoter is detected in the colorectal tumours, whereas methylation is absent in the normal tissues adjacent to the tumours [211]. This methylation is inhibited by applying the methylation inhibitor 5-aza2'-deoxycytidine (5aza2dC) to colorectal cancer cell lines. Investigation of UNC5C<sup>rcm</sup> mutant mice indicated that UNC5C inactivation alone is insufficient to trigger tumour formation. However, the genetically backcrossed mutants, UNC5C<sup>rcm</sup> with APC<sup>+1638N</sup>, indicated that UNC5C inactivation was linked to tumour progression. Interestingly, this tumour progression was found to occur as a result of a significant reduction in the number of apoptotic cells in the intestines in the backcrossed mutant mice, rather than involving cell proliferation and differentiation [211].

It is noteworthy that, overexpression of Netrin-1 in the mouse gut is associated with both tumour formation and progression [137], while loss of UNC5C receptor in the intestinal epithelium is only associated with tumour progression. Importantly, these phenomena are induced by apoptosis rather than the

proliferation and differentiation events [211]. In reality, the loss of DCC and UNC5H receptors is likely to mimic human colorectal cancer, instead of overexpression of Netrin-1. Hence, the current view supports the notion that Netrin-1 dependence receptors play a tumour suppressor role in the regulation of sporadic colorectal cancer [211].

However, another view was proposed that the DCC intracellular domain (DCC-ICD), which is produced by  $\gamma$ -secretase cleavage, may function as a transcriptional coactivator, thereby mediating cell cycle regulation in neoplasia [212]. However, the factors that regulate the translocation and transcriptional activities of DCC-ICD remain to be demonstrated.

**Figure 1.9 The effect of Netrin-1 and its dependence receptors on normal colonic epithelial cells**

**(A)** In the normal colon, Netrin-1 receptors are evenly distributed throughout the single layer of epithelium. A high expression of Netrin-1 is found in the bottom of crypt where stem cells and progenitor cells reside. On the other hand, a low expression of Netrin-1 is localised at the tip of the crypt from where fully differentiated cells are shed. **(B)** When Netrin-1 binds to its receptors, the receptors send signals to initiate cell survival, ultimately promoting cell proliferation. When Netrin-1 is unbound, the receptors mediate apoptosis.

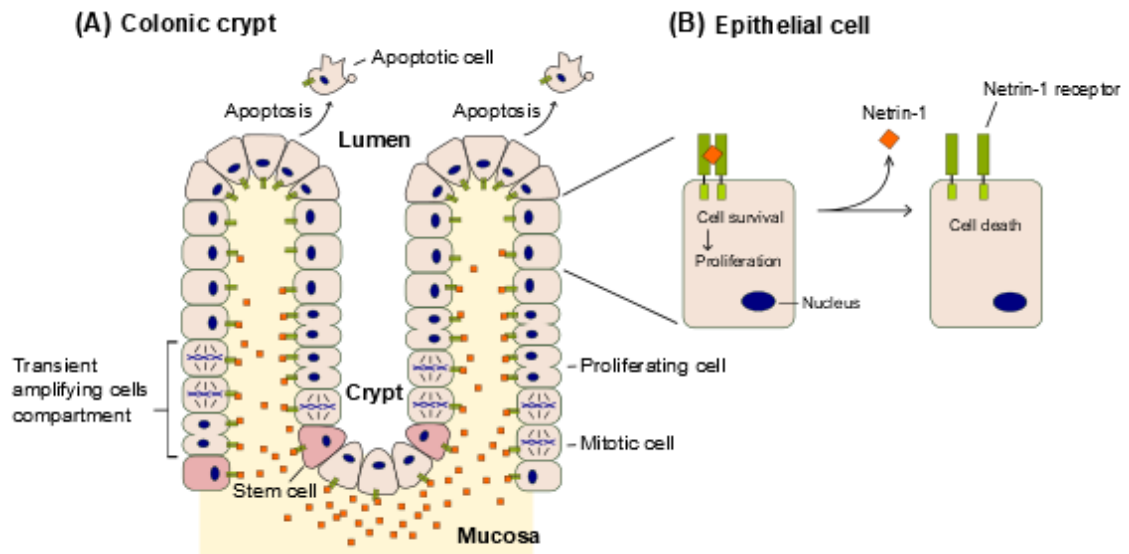


Figure 1.9

### 1.12.1 Netrin-1 intrinsic to colorectal cancer cells

The processes of migration and invasion are essential steps for metastasis as these processes allow malignant cancer cells to be motile and penetrate into blood and/or lymph vessels, thereby allowing dissemination of cancer cells from the primary lesion site [213]. It is known that the mechanisms by which malignant cancer cells migrate and invade are similar to that seen in normal cells undergoing embryonic morphogenesis, and immune cells trafficking in response to inflammatory stimuli [214]. Often, these processes are mediated by the gradient of chemoattractants [70]. One well-known chemotropic guidance molecule for cell migration in both developmental and tumour biology is Netrin-1. In particular, the proinvasive activity of Netrin-1 was investigated in two different stages of colorectal cancer cell lines, namely premalignant colon adenoma cells (PCAA/C1) and adenocarcinoma cells (HCT8/S11) [215]. Both cell types exhibited transcription of *Netrin-1* and *UNC5A-C*, but lacked DCC receptors. Upon addition of Netrin-1, proinvasive activity was induced in both cell types. The signalling pathways involved in proinvasive activity by Netrin-1 have been determined to be cAMP/PKA-dependent Rho GTPase/Rho-kinase ROK pathways. These pathways mediate actin cytoskeletal activity for epithelial cell movement [216]. In particular, RhoA, Rac1, Cdc42 and PI3K are intimately involved in proinvasive activity induced by Netrin-1 [215].

This proinvasive activity was further investigated in DCC-deficient HCT8/S11 cells by transfecting the cells with vectors encoding Netrin-1 (HCT8/S11-Netrin-1 cells) and DCC (HCT8/S11-wt-DCC cells) [215]. HCT8/S11-Netrin-1 cells exhibited proinvasive activity in a manner similar to when Netrin-1 was added externally. However, introduction of wild-type (wt)-DCC expressing vectors into DCC-deficient HCT8/S11 cells suppressed proinvasive activity of Netrin-1. This suppression was thought to be related to the level of RhoA-GTP expression, which is normally elevated in response to Netrin-1, and yet was unaffected in the HCT8/S11-wt-DCC cells. Furthermore, it was found that wt-DCC can exert suppression on the promoter of genes inducing invasion, such as transforming growth factor- $\alpha$  (TGF- $\alpha$ ) and trefoil factors (TFFs). The intracellular domain of DCC plays a key suppressor role in Netrin-1-induced invasion, since the cells that were transfected with mutated DCC at the caspase-3 cleavage site were

unable to facilitate Netrin-1-induced proinvasive activity as shown in the wild type.

Given that the ectopic expression of Netrin-1 induces invasion while wt-DCC suppresses invasion, the impact of either Netrin-1 or wt-DCC on primary tumour growth and metastasis was investigated using a nude mice model [215]. Specifically, the onset of tumour formation was examined after injecting HCT8/S11-wt-DCC cells or HCT8/S11-Netrin-1 cells into the subcutaneous flanks of nude mice. The results showed that the onset of tumour formation and growth that occurred in HCT8/S11-wt-DCC cells was similar to that seen in the control (HCT8/S11-pcDNA3 cells), whereas a two fold increase in tumorigenicity was observed in HCT8/S11-Netrin-1 cells. Moreover, a study with expression of wt-DCC in metastatic kidney cancer cell xenografts indicated that wt-DCC expression reduced cancer cell invasion to the regional lymph nodes and/or lungs when compared to the control pcDNA3 xenografts. In addition to invasion, wt-DCC expression reduced the tumour size. This brought up the question of whether ectopic expression of wt-DCC results in apoptosis of cancer cells that were implanted into the nude mice. This hypothesis was tested by using wt-DCC-transfected and control plasmid-transfected metastatic kidney cancer cells under serum-deprived and hypoxic conditions, both of which resemble the tumour microenvironment. The results indicated that serum deprivation did not impact on apoptosis of either type of cancer cell construct. However, under hypoxic conditions, wt-DCC expression exhibited a higher incidence of apoptosis in response to serum withdrawal when compared to the control. Notably, the incidence of apoptosis was not reversed by the addition of Netrin-1. The apoptotic processes observed here exhibited elements of the classic extrinsic apoptotic pathway, such as cleaved caspase-8, caspase-3, caspase-6, and cleaved PARP. This is inconsistent to the previous finding of Netrin-1-independent apoptotic signalling, which involves no death receptor caspase-8 pathway [153, 217]. However, the authors assumed this dominance of apoptosis over cell survival in the presence of Netrin-1 was because the normal survival mechanisms of the DCC construct was diverted and abolished during hypoxic conditions [215]. One might speculate that there may be other biomolecules produced in hypoxia which may interfere with the Netrin-1 cell

survival signalling pathway. Nonetheless, the opposing roles played by Netrin-1 and its receptor, DCC, need to be clarified further.

### 1.12.2 The roles of Netrin-1 in angiogenesis

It is now well-known that the molecular cues which regulate nerve networks can also guide vessel networks [218]. Involvement of the axonal guidance molecule, Netrin-1, in angiogenesis has been reported for almost a decade. In this period, contradictory observations of the role of Netrin-1, where it acts either as a pro- or anti-angiogenic factor, have been reported, although current data largely suggests that Netrin-1 functions in pro-angiogenesis. Current views of Netrin-1 in angiogenesis are summarised in **Table 1.2**.

Initially, the role of Netrin-1 was thought to be an anti-angiogenic factor [219]. Both *in vivo* and *in vitro* assays showed that Netrin-1 binds to a repulsive netrin receptor, UNC5B, in the developing vascular system, and inhibits the branching of the endothelial tip cells. When *Unc5b* is genetically disrupted in mouse embryos, aberrant endothelial tip extensions and excessive vessel branching are observed. Also, knockdown of either *Unc5b* or *Netrin-1a* (Netrin-1 orthologue) in zebrafish embryos exhibited aberrant vessel branching as observed in *Unc5b* mutant mice embryos.

In contrast to this, the role of Netrin-1 has also been reported as a pro-angiogenic factor. In one study [220], Netrin-1 acted as a potent mitogen as well as a directional chemoattractant for endothelial cells via unidentified receptors. The pro-angiogenic effect of Netrin-1 was mediated by neogenin receptors (a homologue of DCC) in vascular smooth muscle cells (VSMCs). Blocking neogenin prevented migration and adhesion of VSMCs, otherwise promoted in the presence of Netrin-1. Furthermore, exposure to Netrin-1 resulted in vessel sprouting in the chick-chorioallantoic membrane (CAM) assay, and blood vessel growth in the murine corneal neovascularisation assay. When a combination of equimolar amounts of VEGF and Netrin-1 was used in murine corneal and *in vitro* endothelial migration assays, synergistic increase in blood vessel growth and migration was observed [220].

In another study [221], UNC5B was found to be expressed in vessels undergoing active angiogenesis. Hence, upregulation of UNC5B expression in the vascular system of embryos and postnatal mice was observed. However, the expression of UNC5B was downregulated once the vasculature was fully established in the adult [221]. Notably, re-expression of UNC5B is evident when active angiogenic sprouting arises under conditions such as oxygen-induced ischaemic retinopathy (OIR) and tumours [222]. In the case of Netrin-1 however, inconsistent with previous findings [219], suppression of *netrin1a* messenger RNA showed inhibition of vascular sprouting in zebrafish embryos. Also, inactivation of *Netrin-1a* led to loss of vessels in zebrafish development [223]. The loss of vessels in this case has been partially explained by applying the dependence receptor theory, mentioned earlier. This property was tested on human umbilical vein endothelial cell (HUVEC) and human umbilical artery endothelial cell (HUAEC), which express UNC5B receptors but not Netrin-1 [224]. Accordingly, either treating these cells with Netrin-1 or silencing UNC5B receptors led to a decrease in caspase-3 activity of UNC5B receptors, thereby reducing the incidence of cell death. However, a combination of treatments introducing Netrin-1 and silencing UNC5B receptors showed no additive reduction in caspase-3 activity when compared to individual treatments. Therefore, it is thought that the survival effect of Netrin-1 on endothelial cells will only apply when sufficient expression of UNC5B receptors is present to inhibit UNC5B-mediated apoptosis. This highlights the point that the functional dependence receptor expression in cells is equally as important as the corresponding ligand availability [224].

Accordingly, a correlation between pro-angiogenic and cell survival activities of Netrin-1 was examined in *ex vivo* assays including a mouse aortic ring assay and a CAM assay [224]. The results showed; (i) enhanced capillary sprouting by Netrin-1 treatment, (ii) promotion of neovessel branching by silencing UNC5B receptors, and (iii) induction of neocapillary tube formation by caspase inhibitors such as z-VADfmk and boc-aspartyl-(OMe)-fluoromethyl-ketone (BAF). Collectively, these data demonstrate that Netrin-1 and UNC5B function antagonistically in the process of angiogenesis.

Under hypoxic conditions, it was shown that the level of HIF-1 $\alpha$  affects the expression level of UNC5B, but not Netrin-1 [222]. When the knockdown of HIF-1 $\alpha$  was achieved with siRNA, UNC5B expression was increased. Also, accumulating evidence supports the view that Netrin-1 promotes neovascularisation in both mouse and rat models of ischaemia [225-227]. Undoubtedly, the role of Netrin-1 in angiogenesis associated with pathological conditions is more complex, and it needs to be dealt with on an individual case-by-case basis. For instance, administration of Netrin-1 to ischaemic and diabetic mice promoted neovascularisation [223]. Both neuropathy and vasculopathy conditions exhibited in diabetic mice were ameliorated by introduction of Netrin-1. This is because Netrin-1 is capable of stimulating the proliferation and migration of both endothelial and nerve cells. Hence, Netrin-1 is proposed to be a unique potential therapeutic agent for neurovascular diseases. However, a *caveat* is that in some cancers like pancreatic cancer and glioblastoma, Netrin-1 can facilitate tumour progression via enhancing neoangiogenesis and tumour cell invasion [228, 229]. Therefore, Netrin-1 may be a potential molecular target for cancer treatment. The role of Netrin-1 influencing colon tumour invasion is specifically discussed in the next section.

**Table 1.2 The effect of Netrin-1 in angiogenesis**

<b>In vitro cell lines/ In vivo model</b>	<b>Ligand/Receptor treatment</b>	<b>Assays</b>	<b>Outcome</b>	<b>Pro- or Anti-angiogenesis</b>	<b>Ref</b>
Ischemic hindlimb rat	Implantation of netrin-1	Angiography; IHC for vascular endothelial cells	Extensive collateral artery formation; High capillary density	Pro-angiogenesis	[226]
Human placental microvascular endothelial cells HPMECs	Addition of netrin-1	In vitro rat aortic ring assay; In vivo mouse Matrigel plug assay	Increased microvessel sprouting and outgrowth of aortic rings; Increased vessel number	Pro-angiogenesis	[230]
Rat placenta	Addition of netrin-1	Migration assay; tube formation assay; and Microvessel density IHC for CD34-positive endothelial cells	Increased number of migrating cells; Increased branching points of dendritic and tube-like structures ; Increased microvessel number	Pro-angiogenesis	[231]
Mouse brain	Adeno-associated viral vectors carrying <i>netrin-1</i> gene injected into mouse brain (AAV-NT-1-treated mice	Microvessel counting	Increased number of microvessels in per-infarct area	Pro-angiogenesis	[232]
Mouse brain endothelial cells	Addition of netrin-1	Sprouting assay; tube formation; and <i>in vivo</i> matrigel plug assay	Increased total sprout length and sprout number; Increased HUVEC formation; Increased infiltration of endothelial cells	Pro-angiogenesis	[229]
HUVEC	Addition of netrin-1	Tube formation	Increased tube formation	Pro-angiogenesis	[223]
Mouse	Addition of netrin-1	Corneal micro-pocket assay	Increased blood vessels growth	Pro-angiogenesis	[220]
Chicken	Addition of netrin-1	CAM assay	Increased vascular sprouting	Pro-angiogenesis	[220]

Rat and human VSMC	Addition of netrin-1	Adhesion	Increased adhesion	Pro-angiogenesis	[220]
HAEC, HMEC/HMVEC, rat and human VSMC, HUVEC, HUAEC, HCAEC, and MSI	Addition of netrin-1	Transwell migration	Increased migration	Pro-angiogenesis	[220] [223]
HAEC, HMEC/HMVEC, rat and human VSMC, HUVEC, HUAEC, HCAEC, and MSI	Addition of netrin-1	Proliferation	Increased cell proliferation	Pro-angiogenesis	[220] [223]
HUAEC	Addition of netrin-1	Wound healing migration	Dose dependent inhibition of migration	Anti-angiogenesis	[219]
HUVEC	Addition of netrin-1	Aortic ring sprouting assay with a time lapse video microscopy	Retraction or backward movement of the tip cell filopodia	Anti-angiogenesis	[219]
Zebrafish embryos	<i>Netrin-1a</i> knock down	<i>Netrin-1a</i> knock down zebrafish embryos	Aberrant vessels	Anti-angiogenesis	[219]
Mouse embryos	<i>Unc5b</i> mutant	<i>Unc5b</i> Knock-out mice embryos	Increased capillary branching and filopodia extension	Anti-angiogenesis	[219]
<i>unc5b LacZ-plap</i> mice	Addition of netrin-1	Aortic ring assay and Whole mount X-gal staining of Matrigel plug	Decreased <i>unc5b</i> -expressing endothelial tip sprouting	Anti-angiogenesis	[221]
Chick and quail embryos	Human embryonic kidney (HEK) 293 cells stably transfected with chick netrin-1 (cNetrin-1)	CAM assay	Reduced sprouting of <i>unc5b</i> expressing blood vessels	Anti-angiogenesis	[233]
Human umbilical vein endothelial cells HUVECs	Addition of netrin-1	Cell death assay	Reduced apoptosis of endothelial cell exposed to metabolic stress	Anti-apoptosis	[228]

**Abbreviations:**

HUVEC<sup>a</sup>, human umbilical vein endothelial cell

AAV-NT-1<sup>b</sup>, adeno-associated viral vectors carrying *Netrin-1* gene

HPMECs<sup>c</sup>, human placental microvascular endothelial cells

IHC<sup>d</sup>, immunohistochemistry

HEK<sup>e</sup>-293 cells, human embryonic kidney-293 cells

CAM<sup>f</sup>, chick chorioallantoic membrane

*unc5b*<sup>g</sup>, uncoordinated 5 homolog b

HAEC<sup>h</sup>, human aortic endothelial cell

HMVEC<sup>i</sup>, human microvascular endothelial cell

VSMC<sup>j</sup>, vascular smooth muscle cell

HUAEC<sup>k</sup>, human umbilical artery endothelial cell

### 1.12.3 The roles of Netrin-1 in the tumour microenvironment and metastasis

In many cases of human sporadic colorectal cancer, decreased expression of Netrin-1 receptors, as opposed to the increase in Netrin-1 expression, is commonly observed [234]. However, in a small fraction of colorectal cancers, upregulation of Netrin-1 expression is found. This is often seen in the case of patients with inflammatory bowel disease (IBD), such as Crohn's disease and ulcerative colitis, who have developed colorectal cancer.

During the intestinal inflammation response, nuclear factor-kappaB (NF- $\kappa$ B) is activated in epithelial cells as well as immune cells in mucosa, such as dendritic cells and macrophages [235]. The activation of NF- $\kappa$ B in immune cells upregulates the genes involved in proinflammatory cytokines, such as tumour necrosis factor-alpha (TNF- $\alpha$ ), interleukin-1 beta (IL-1 $\beta$ ), and cyclooxygenase-2 (COX-2). The production of these cytokines can then interact with corresponding cytokine receptors present on the intestinal epithelial cells, and that in turn activates NF- $\kappa$ B in the epithelial cells. Subsequently, this mediates upregulation of the genes that are associated with anti-apoptosis and angiogenesis in the epithelial cells. Also, molecules which play roles in metastasis such as adhesion molecules, matrix metalloproteinases (MMPs), and chemokines are released from the cells, and so contribute to the development of tumour promotion and progression [234].

Notably, *Netrin-1* was found to be a direct transcriptional target gene of NF- $\kappa$ B activation [236], and the upregulation of Netrin-1 expression was shown to be a major causal factor for tumour development in inflammation-driven colorectal cancer (**Figure 1.10**). This was demonstrated in a mouse model resembling an ulcerative colitis-associated cancer condition, where blocking Netrin-1 prevented colorectal cancer progression while the level of inflammation remained unaffected [235]. Furthermore, a recent study has reported that a major inflammation-associated cytokine, TNF- $\alpha$  which is induced by macrophages in mucosa, can bind tumour necrosis factor receptor superfamily member 1B (1BTNFRSF1B) receptors on colonic epithelial cells [237]. This binding subsequently mediates activation of NF- $\kappa$ B, leading to the production of

Netrin-1 in epithelial cells. This production of Netrin-1 can then allow the cell to avoid undergoing apoptosis by binding to Netrin-1 receptors in an autocrine fashion, causing the cell to survive and proliferate. Anti-TNF- $\alpha$  antibodies were shown to be able to block translocation of NF- $\kappa$ B from the cytosol into the nucleus. This result was thought to occur when the TNF- $\alpha$  signalling-induced phosphorylation of inhibitor of kappa B alpha (I $\kappa$ B $\alpha$ ) was inhibited. In addition to this, the application of NF- $\kappa$ B inhibitor was shown to reduce the level of Netrin-1 production, confirming that *Netrin-1* is a direct target gene for NF- $\kappa$ B. Collectively, these findings highlight an intricate relationship between Netrin-1 and the microenvironment of colorectal cancer progression.

Recently, the Netrin-1 protein level in plasma has been examined in cancer patients to investigate if Netrin-1 can be used as a diagnostic biomarker for cancers. The level of Netrin-1 in plasma is significantly increased in various cancer patients when compared to non-cancer patients who may be affected by other types of diseases [238]. Although the elevated level of Netrin-1 plasma is shown to be directly correlated with the presence of tumour, this level is not influenced by the patient's gender, tumour size or the stage of tumour progression. Hence, Netrin-1 was proposed to be a useful diagnostic biomarker for detecting various human cancer types when they are present at an early stage. Cancers with elevated Netrin-1 levels include brain, breast, liver, prostate and kidney. However, Netrin-1 plasma levels in colon, pancreatic and lung cancers were not found to be elevated, despite previous studies reporting overexpression of Netrin-1 mRNA in those cancer types. For colon cancer, it is understandable that Netrin-1 plasma levels are unperturbed, as the majority of colorectal cancer cases are associated with the loss of Netrin-1 receptors as opposed to enhancing Netrin-1 expression. However, further clarification is required for pancreatic and lung cancers.

In addition to the involvement of Netrin-1 in the tumour microenvironment, recent work on Netrin-1 has identified Netrin-1 as a cytoprotective agent for hypoxia-associated cell transplantation and cell therapy [239]. Mesenchymal stem cells (MSCs) are self-renewable and are capable of differentiating into multiple cell lineages, including connective tissue cells, fat cells, cartilage and

bone cells [240]. Because of this, MSCs have been prime candidates for cell therapy, though the therapeutic effectiveness of MSCs has been limited due to hypoxic injury. A recent study has demonstrated that Netrin-1 can recover umbilical cord blood-derived MSCs (UCB-MSCs) from hypoxic injury [239]. In the presence of Netrin-1, the protection of UCB-MSCs is mediated by Netrin-1 receptors, DCC and integrin  $\alpha 6\beta 4$ , present on UCB-MSCs, and that can initiate anti-apoptotic signalling. Netrin-1 blocks the mitochondrial-mediated apoptotic pathway in hypoxic cells through the expression of heat shock protein 27 (HSP27), which is known to block cytochrome c-dependent activation of caspase-3 [241]. The expression of HSP27 was upregulated by DCC and  $\alpha 6\beta 4$  – dependent AKT and glycogen synthase kinase 3  $\beta$  pathways in the presence of Netrin-1. Collectively, Netrin-1 is proposed to be a potential therapeutic candidate for tissue-regenerative therapy, though its true potential has to be tested with further studies.

**Figure 1.10 Netrin-1 is produced by malignant cells**

Macrophages in stroma produce a major proinflammatory-associated cytokine, TNF- $\alpha$ . The released TNF- $\alpha$  then interacts with TNFRSF1B receptors on epithelial cells and activates a downstream effector, NF- $\kappa$ B. The activated NF- $\kappa$ B transcription factor, in turn, directly activates the transcription of *Netrin-1* gene, which allows cells to proliferate. Furthermore, the secreted Netrin-1 binds its receptors on epithelial tumour cells and activates a number of signalling pathways. These include PI3K-AKT, MEK-ERK, and Rac1/Cdc42 pathways. These pathways induce various cellular effects, such as survival, proliferation, migration and invasion.

**Abbreviations:** N1, Netrin-1; Rac1, ras-related C3 Botulinum toxin substrate 1; Cdc42, cell division cycle 42; PI3K, phosphoinositide 3-kinase; AKT, serine/threonine kinase; MEK, mitogen-activated protein kinase kinase; ERK, extracellular-signal-regulated kinase; NF- $\kappa$ B, nuclear factor  $\kappa$ B; TNF- $\alpha$ , Tumour necrosis factor- $\alpha$ ; TNFRSF1B, tumour necrosis factor receptor superfamily member 1B.

### Colon primary tumour site

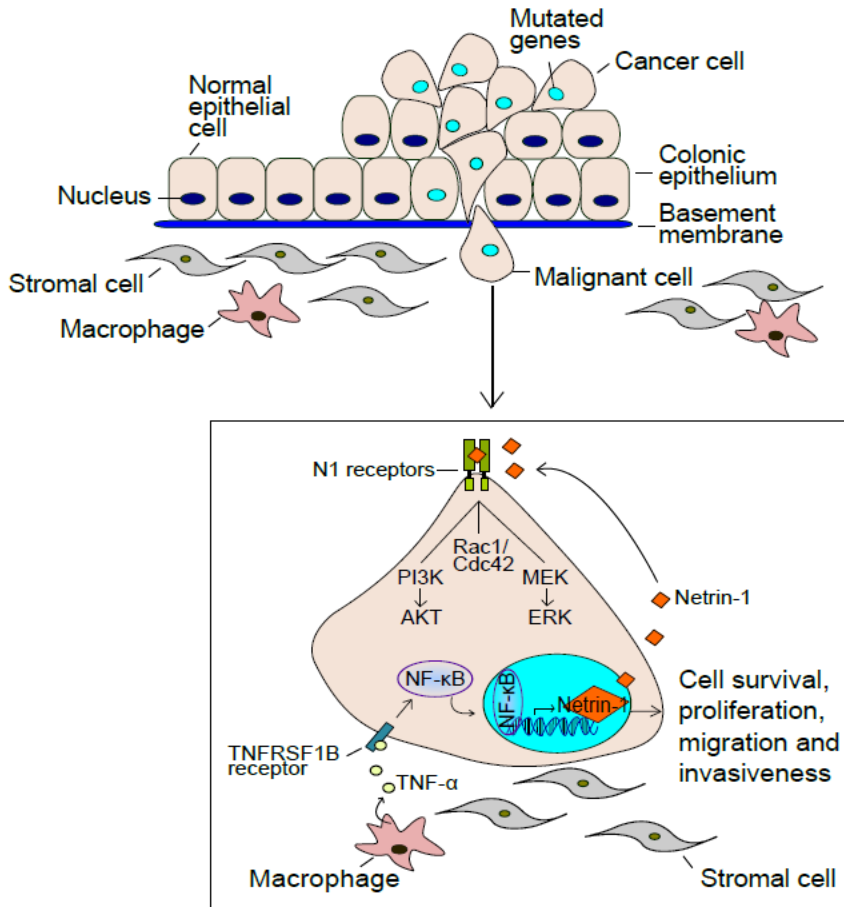


Figure 1.10

### 1.13 Summary

The discovery of roles of Netrin-1 and its receptors in axonal guidance and cell migration has advanced our understanding of CNS development. Netrin-1 has a bi-functional role in neuronal guidance; either chemoattractive or chemorepulsive. These two opposite roles of Netrin-1 are dependent upon the receptor to which Netrin-1 binds. The chemoattractive role as part of its neuronal guidance effect of Netrin-1 and DCC receptors has been revealed in the developing ENS, in addition to the CNS, confirming the importance of Netrin-1 in nervous system development. Meanwhile, an additional role of Netrin-1 as a cell survival factor has been investigated in relation to various cancers, particularly colorectal cancer, and highlighting the notion of Netrin-1 dependence receptors in the intestinal epithelium. Along with this, recent studies have shown that the enteric innervation is disrupted in human colorectal cancers and such damage to the ENS is implicated in the impairment of normal intestinal functions. Based on these observations, it would be intriguing to understand the role of Netrin-1 and DCC/UNC5H receptors in the adult ENS in the context of colorectal cancer. One might speculate that once the ENS is fully established in the adult GIT, the guidance role of Netrin-1 may be unnecessary in adulthood. If so, the presence of Netrin-1 and DCC expression in the adult ENS may be important for promoting neuronal cell survival and nerve regeneration under pathological conditions, including CRC. If their roles in this condition are better understood, it may shed some light on Netrin-1 as a potential neuroprotectant.

## 1.14 Research rationale, aims and hypotheses

Netrin-1 was initially discovered by examining diffusible cues secreted by the floor plate cells during spinal cord development [242], and since then it has been known as a potent axonal and neuronal guidance cue in the developing CNS.

The hallmark of Netrin-1 function is that it serves as either a chemo-attractant or chemo-repellent for different types of axons and neurons. These opposing roles of Netrin-1 are mediated by particular types of Netrin-1 receptors present on axons and neurons. The dynamic expression of Netrin-1 receptors on axons and neurons is directed to find their appropriate targets or prevented from aberrantly growing under Netrin-1 guidance.

Subsequent findings have indicated that Netrin-1 is continuously expressed in the adult CNS and PNS. The role of Netrin-1 in adult nervous system is mostly to maintain the formation of appropriate network connection. In recent years, Netrin-1 function has been found to be involved in nerve regeneration in the adult CNS and PNS. In particular, Netrin-1 has been implicated in neural plasticity and neuronal regeneration in the adult PNS following injury.

In addition, the guidance role of Netrin-1 is shown in developing ENS and the presence of Netrin-1 expression in the adult ENS is noted. However, the localisation of Netrin-1 and its receptors in the adult ENS is not well defined. Furthermore, the role of Netrin-1 in the adult ENS is yet to be elucidated.

Based on the observation that Netrin-1 promotes nerve regeneration after injury in the adult PNS, it is reasonable to hypothesise that Netrin-1 expression in the adult ENS plays a positive role in neuronal and nerve regeneration if damage occurs in the adult ENS under pathological conditions, such as CRC.

Further to the role of Netrin-1 in the nervous system, Netrin-1 expression has been pointed as a regulator in tumourigenesis. This may be a major obstacle for a potential therapeutic use of Netrin-1 for the ENS under CRC condition.

The major aim of this thesis is to determine whether or not Netrin-1 can be used as a neuroprotective agent for the mature ENS under CRC condition.

In this thesis, I hypothesise that Netrin-1 is a potential

candidate as a neuroprotective agent for the mature ENS, and that Netrin-1 treatment can serve as a neuroprotective therapy for the ENS under CRC condition.

To address the major aim of the thesis, the specific aims of the research presented in this thesis are:

- (1) To investigate the neuroprotective effects of Netrin-1 on developed enteric neuronal cells (Chapter 2).
- (2) To verify the effects of Netrin-1 on metastatic properties of colorectal cancer cells (Chapter 3).
- (3) To examine the protective role of Netrin-1 on enteric neurons in the context of colorectal cancer in an *in vitro* system (Chapter 4).
- (4) To test whether or not Netrin-1 treatment has a potential therapeutic use on the mature ENS under CRC condition in an *in vivo* model (Chapter 5).

## Chapter 2

---

**Investigating the effect of Netrin-1 on post-natal enteric neuronal cell line**

## 2.1 Introduction

Adult neurogenesis is the generation of functionally mature neurons that are derived from adult neural stem/progenitor cells [243]. Although neurogenesis is shown to occur throughout adulthood, the occurrence of spontaneous adult neurogenesis is limited to regions in the CNS such as olfactory bulb, subventricular zone and dentate gyrus of the hippocampus [244]. Promoting the endogenous process of adult neurogenesis is often found to be associated with repairing damaged neurons in response to injuries [41, 245].

Adult neurogenesis in the PNS has also been demonstrated. The initial discovery was reported in rats which showed an age-related increase of sensory neuron numbers in dorsal root ganglia [246]. Further investigations concerning adult neurogenesis was conducted by various research groups. The data revealed that an increase in neuron numbers of the myenteric plexus ganglia in the ENS occur in the upstream intestinal loops, following induction of a partial stenosis of the small intestine in rats [244, 245].

Enteric neurons and glial cells in the ENS are derived from neural crest stem cells during embryonic development [41]. Matured neurons and glial cells form a complex network consisting of the myenteric plexus and submucosal plexus in the gastrointestinal tract. This network controls physiological activities including gut motility, secretion and blood flow [17, 247].

Unlike the structurally protected CNS, the ENS resides in the gastrointestinal tract and as a consequence is more vulnerable to injury due to the gastrointestinal tract being exposed to the external environment where it faces various insults such as, mechanical stress of gut motility, infection and inflammation caused by gut pathogens [248, 249]. Hence, regeneration of enteric neurons is an important cellular process for maintaining a healthy ENS as well as neuropathological conditions.

Neurotrophic factors have been shown to play important roles in development, maintenance and repair of the ENS [250]. However, the neurotrophic factors that trigger and regulate adult neurogenesis have yet to be elucidated. In

addition, the mechanism which enables regenerated neurons to be integrated into the existing neural circuits is still unclear.

Netrin-1 was initially discovered in the developing CNS as a diffusible factor, and it acts as a guidance cue for correct axonal pathfinding. The axonal guidance role of Netrin-1 is mediated by activating its receptors that are present on the neuronal cell surface. Interestingly, Netrin-1 binds to many receptors including deleted in colorectal cancer (DCC), Neogenin known as the DCC homologue, UNC5 homologues (UNC5H) family (UNC5H1-4 in rodent; also termed UNC5A-D in human), Adora2b, DSCAM,  $\alpha 6\beta 4$  and  $\alpha 3\beta 1$  integrins [130, 251, 252]. It is now well-established that Netrin-1 acts as an opposing guidance cue depending on which receptors it binds to [124]. For example, DCC and Neogenin receptors induce chemotactic activity of cells towards that of Netrin-1, whereas UNC5H receptors mediate chemo-repulsive activity of the cells in response to Netrin-1 in the embryonic CNS [124, 134, 194]. During the development of the mouse fetal gut, DCC is expressed in growth cones of the vagal sensory axons. Those axons are thought to migrate toward the intrinsic enteric neurons where Netrin-1 is synthesised, thereby forming a communication between the CNS and ENS [188, 189, 195].

In addition to its axon guidance function, Netrin-1 is expressed in non-neural tissues and has been shown to be involved in various cellular processes including proliferation [215], migration [253], differentiation [254] and angiogenesis [221, 224, 255, 256]. Also, it is important as a cell survival factor when it is paired with its receptors. Hence, the effect of Netrin-1 interacting with its receptors has been associated with recovery from ischemic injury [257, 258] and the therapeutic target for cancer cell death in combination with chemotherapy [259].

In this chapter, the effect of Netrin-1 is explored using the mouse immortalised post-natal enteric neuronal (IM-PEN) cell line, which is developed by Professor Srinivasan's Digestive Disease Laboratory [260]. The IM-PEN cells were isolated from the intestines of *H-2K<sup>b</sup>-tsA58* transgenic mice at post-natal day two. This transgenic mouse model harbours a conditional oncogene that is a temperature sensitive (ts) mutant strain of simian virus 40 (SV40) large tumour (T) antigen (TAg), namely tsA58. Increased transcription of this gene is driven

by the mouse class I major histocompatibility complex *H-2K<sup>b</sup>* promoter activation, and that can be elevated by interferons under the permissive temperature at 33°C. As a result, transformation of cells is induced by the expression of thermolabile large TAg [261]. Accordingly, the IM-PEN cells are able to continuously proliferate under the permissive conditions, in addition to being capable of differentiation when the gene is inactivated and the expression of large TAg becomes degraded under the non-permissive conditions. The optimum conditions for IM-PEN cell differentiation had been previously determined by Professor Srinivasan's laboratory. Such conditions were observed when the IM-PEN cells were cultured with 1% serum neurobasal medium in the absence of IFN- $\gamma$  at 39°C for a period of 7 days [260].

An advantage of using this cell line is that they are able to either proliferate or differentiate depending on the ambient temperature conditions. This conditionally temperature-inducible property allows studies to be designed in order to monitor the progression of post-natal neuronal cells from a precursor state to mature state in an *in vitro* setting. The aim of the studies in this Chapter is to investigate the effect of Netrin-1 on IM-PEN cells in both a precursor state and differentiated state and to assess whether or not Netrin-1 could be a possible trophic factor for adult neurogenesis in the ENS.

## **2.2 Materials and methods**

### **2.2.1 Cell culture**

IM-PEN cells were kindly provided by Emory University, Atlanta, USA. In order to propagate IM-PEN cells, cells were cultured at 33°C, using 10% CO<sub>2</sub>, incubated in permissive medium: a Dulbecco's modified eagle medium/F12 (DMEM/F12) containing GlutaMax, N2 supplement, 1% (v/v) antibiotic antimycotic, 10% (v/v) fetal bovine serum (FBS; Invitrogen, Thermo Fisher Scientific), 0.1 mg/mL of Fetuin (Sigma), 1 mg/mL of bovine serum albumin (BSA; Sigma), 20 U/mL of recombinant mouse IFN-gamma, 100 ng/mL of recombinant mouse glial cell line-derived neurotrophic factor (GDNF; Shenandoah Biotechnology). IM-PEN cells were differentiated by culturing them at non-permissive temperature, 40.5°C, using 5% CO<sub>2</sub>, incubated in differentiation medium: a neurobasal-A medium supplemented with B-27 serum free supplement (Invitrogen), 1mM GlutaMax, 1% (v/v) antibiotic antimycotic, 1% (v/v) FBS and 100 ng/mL of recombinant mouse GDNF. In order to differentiate IM-PEN cells, the cells were firstly seeded in permissive medium at 33°C and allow them to grow and reach up to 70% confluency. The medium for the cells was changed from permissive medium to differentiation medium after washing the cells with phosphate-buffered saline (PBS) twice. The cells were then transferred to 40.5°C and the medium was changed each day for a period of 3 days to remove dead cells. Following incubation for 3 days, the differentiation medium was changed every second day.

### **2.2.2 Cell viability assay**

Cell viability was measured using AlamarBlue® cell viability reagent (Thermo Fisher Scientific) according to the manufacturer's instructions. To test the viability of IM-PEN cells cultured at 33°C, cells were seeded at 2000 cells per well on a 96-well plate (cell culture µClear® flat bottom black well) and cultured with permissive medium (10% serum N2 medium with IFN-γ) at 33°C. The viability of IM-PEN cells cultured at 39°C and 40.5°C was tested by seeding the cells at 8000 cells per well and incubating them at 33°C until they reached 70% confluency. Thereafter, the medium was changed to non-permissive medium (1% serum neurobasal medium without IFN-γ). The cells were then further incubated at either 39°C or 40.5°C for 13 days. The medium was changed

every 2-3 days. Eight technical replicates were used in each experiment, and 3 independent biological assays were conducted.

To test the effect of Netrin-1 on IM-PEN cell viability (**Figure 2.10 A**), cells were seeded at 8000 cells per well and cultured overnight at 33°C. On the following day, the permissive medium was removed and the cells were gently washed with PBS three times. The cells were then incubated with serum free medium with Netrin-1 for 24, 48 and 72 hours. At each time-point, AlamarBlue (10% of the final medium volume) was added into each well and incubated for 3 hours. The fluorescence intensity of the AlamarBlue was detected at 545 nm/590 nm (excitation/emission) wavelength by using a microplate reader (Varioskan Flash, Thermo Fisher Scientific). Eight technical replicates were used per Netrin-1 treatment in each experiment, and 3 independent biological assays were conducted.

### 2.2.3 Wound-healing assay

IM-PEN cells were seeded in 24-well plates and cultured at 33°C until a 90% confluent monolayer was formed. The gap was created by scratching the plate with a sterile 200 µl pipet tip. The scraped cells were gently removed by washing with PBS. The experimental media were then introduced. The changes in the gap were monitored by imaging per time-point. A threshold for the gap distance was determined and measured by automated MATLAB. The formula for percentage wound closure is shown as follow:

$$[1 - (\text{the distance at the indicated time}) \div (\text{the distance at time zero})] \times 100$$

### 2.2.4 Immunofluorescence

IM-PEN cells were cultured on coverslips placed in 6 well-plates. The cells were fixed with 2% paraformaldehyde at an indicated time. The cells were pre-fixed with 2% paraformaldehyde for 2 mins. Further fixation was applied using 4% paraformaldehyde for 10 mins at room temperature (RT). The fixed cells were first permeabilised with PBS-Tween 20 (PBS-T; 0.1%, pH7.4) for 10 mins at RT. After washing with PBS (pH7.4), 5% of donkey serum (Sigma) blocking solution consisting of PBS-T (0.05%, pH7.4) was incubated with the cells for 2 hours at RT. Primary antibodies, listed in **Table 2.1**, were diluted in blocking solution and incubated with the cells at 4°C overnight. The cells were then washed with PBS-T (0.05%, pH7.4) for 4 times per 10 min, using a low speed of shaker. The

appropriate fluorescence-labelled secondary antibodies, listed in **Table 2.2**, were incubated with the cells for 1 hour at RT. The cells were washed with PBS-T (0.05%, pH7.4) for 4 times per 10 min, using the low speed of shaker. Nuclei were counterstained with 4',6-diamidino-2-phenylindole (DAPI, 14 nM; ThermoFisher, D1306). For negative control samples, the primary antibody was omitted and a corresponding species secondary antibody was applied. Each coverslip was mounted with mounting medium and confocal microscope was used to visualise and take images. The images were taken systematically random manner with a 40x objective. For each sample group, 7 areas of images were taken per replicate. 3 independent biological assays were conducted.

**Table 2.1 List of primary antibodies used in immunofluorescence assays**

<b>Primary antibody</b>	<b>Host species</b>	<b>Source</b>	<b>Catalouge number</b>	<b>Dilution</b>
Ki67	Rabbit	Abcam	ab16879	1:500
$\beta$ -Tubulin III	Chicken	Abcam	Ab107216	1:1000
PGP9.5	Rabbit	Merck Millipore	AB1761-I	1:1000
GFAP	Rabbit/Goat	Abcam	ab7260/ab53554	1:2000
NeuN	Chicken	Aves Labs	NUN	1:2000
Synaptophysin	Rabbit	Abcam	Ab32127	1:2000

**Table 2.2 List of secondary antibodies used in immunofluorescence assays**

Secondary antibody	Source	Catalogue number	Dilution
Donkey anti-goat rhodamine	Jackson ImmunoResearch Laboratories	705-295-147	1:300
Donkey anti-mouse FITC	Merck Millipore	AP182F	1:300
Donkey anti-rabbit rhodamine	Jackson ImmunoResearch Laboratories	AP182R	1:300
Donkey anti-rabbit FITC	Merck Millipore	AP182F	1:300
Donkey anti-goat FITC	Merck Millipore	AP180F	1:300
Donkey anti-chick FITC	Merck Millipore	AP194F	1:300

### 2.2.5 Western blot and densitometric analysis

The protein samples were collected and suspended with chilled radioimmunoprecipitation (RIPA) buffer (Sigma) containing a protease and phosphatase inhibitor cocktail (Pierce, Thermo Fisher Scientific). The samples were then sonicated for 30 sec for 10 times in between cooling for 2 mins. The sonicated samples were centrifuged at 17000 x g for 25 mins at 4°C, and the supernatant was collected for western blot analysis. The concentration of each sample was quantified by using a BCA protein assay kit (Pierce, Thermo Fisher Scientific). Prior to running an electrophoresis, the samples were reduced by using a reduced reagent (Invitrogen) and heated at 95°C for 5 mins. The reduced samples were then electrophoresed on a 4-12% Bis-Tris mini gel (loaded 15 µg of each sample) with either 3-(N-morpholino) propanesulfonic acid (MOPS) or 2-(N-morpholino) ethanesulfonic acid (MES) buffer according to the manufacturer's instructions (NuPAGE, Invitrogen), and then transferred to (iBlot gel transfer stack, Invitrogen) using iBlot® 2 Dry Blotting System (Invitrogen). The membrane was incubated in blocking buffer (5% skim milk plus TBS-T: 1M tris pH8; 5M NaCl; 0.1% Tween 20) for 1 hours at RT, and incubated with primary antibodies, listed in **Table 2.3**, overnight at 4°C. The

membrane was washed with TBS-T four times at RT, and then incubated with HRP-linked secondary antibodies, listed in **Table 2.4**, for 1 hour at RT. Thereafter, the membrane Bands were incubated with Clarity enhanced chemiluminescence (ECL) western blotting substrate chemiluminescence (Bio-Rad) for 5mins, and then developed with Vilber Lourmat Fusion FX Imaging.

The densitometric values were determined using LI-COR Image Studio Lite (LI-COR biotechnology, USA), and the protein of interest values were normalised by pan-actin expression as a housekeeping protein. The normalised values from 3 independent biological experiments were pooled and shown as mean  $\pm$  SD.

**Table 2.3 List of primary antibodies used in western blot assays**

Primary antibody	Host species	Source	Catalouge number	Dilution
SV40 Large T Ag	Mouse	Abcam [PAb416]	Ab16879	1:1000
Pan-actin	Mouse	ThermoFisher	MA5-11869	1:10,000
PGP9.5	Rabbit	Merck Millipore	AB1761-I	1: 1000
Synaptophysin	Rabbit	Abcam	Ab32127	1:1000
Neogenin	Goat	R and D system	AF1079	1:1000
UNC5H2/B	Goat	R and D system	AF1006	1:1000
Caspase-9	Rabbit	Cell signalling technology	9915	1:1000
Cleaved caspase-9	Rabbit	Cell signalling technology	9915	1:1000
Caspase-3	Rabbit	Cell signalling technology	9915	1:1000
Cleaved caspase-3	Rabbit	Cell signalling technology	9915	1:1000
Cyclin D	Rabbit	Cell signalling technology	ab134175	1:10,000
P27	Rabbit	Abcam	ab62364	1:1000
P21	Rabbit	Abcam	ab109199	1:1000

**Table 2.4 List of secondary antibodies used in western blot assays**

Secondary antibody	Source	Catalogue number	Dilution
Donkey anti-rabbit IgG, HRP-linked	Thermo Fisher Scientific	31458	1:10,000
Goat anti-rabbit IgG, HRP-linked	Cell signalling technology	9915	1:10,000
Horse anti-mouse IgG, HRP-linked	Cell signalling technology	9915	1:10,000
Rabbit anti-goat IgG, HRP-linked	Thermo Fisher Scientific	31402	1:10,000

### 2.2.6 Quantitative RT-PCR

Total RNA was isolated from the IM-PEN cell line by using the Epicentre's MasterPure™ RNA Extraction/purification kit, according to the manufacturer's instructions (Gene Target Solutions). Total RNA concentration was determined by using NanoDrop™ Spectrophotometer (ThermoScientific). RNeasy MinElute Clean up kit (Qiagen) was used to purify the samples when needed. RNA (1 µg) was reverse transcribed into cDNA in a 20 µL reaction by using iScript™ Advanced cDNA Synthesis kit (Bio-Rad). The cDNA synthesis (10 ng/µL) and gene-specific primers were mixed with SsoAdvanced™ Universal SYBR Green Supermix (Bio-Rad) and they were subjected to reverse transcription polymerase chain reaction (RT-PCR; CFX96, Bio-Rad). Amplification parameters were set according to the manufacturer's instructions (Bio-Rad): 95°C for 30 sec, followed by 40 cycles of 95°C for 15 sec, and 60°C for 30 sec, and a final cycle for the melt curve at 65°C to 95°C (increment 0.5°C) for 5 sec. PrimePCR™ PCR primers (Bio-Rad) of mouse UNC5H1, UNC5H2, UNC5H3, UNC5H4 and Netrin-1 were used. The primers for mouse DCC, Neogenin, LC-3 and GAPDH were designed by using NCBI primer-BLAST. Primers used in this thesis are listed in **Table 2.5**. Negative controls such as no template control (NTC) and no reverse transcriptase control (NRT), and a positive control such as brain tissue were included each run of RT-PCR experiment. Experiments were performed in triplicate. PCR products were loaded onto a 2% agarose gel, bands were visualized under UV light (Vilber Lourmat Fusion FX Imaging) by using GelRed™ (Thermo Fisher Scientific) staining.

**Table 2.5 Oligonucleotide sequences used in RT-PCR analysis**

<b>Gene</b>	<b>GenBank accession number</b>	<b>Forward primer</b>	<b>Base number of forward primer</b>	<b>Reverse primer</b>	<b>Base number of reverse primer</b>
<i>Gapdh</i>	<a href="#">NM_001289726.1</a>	5'-GGTCCTCAGTGTAGCCCAAG	905-924	5'-AATGTGTCCGTCGTGGATCT	801-820
<i>L-32 (Rpl32)</i>	<a href="#">NM_172086.2</a>	5'-GACCGATATGTGAAAATTAAGCGAA	127-151	5'-CATCAGGATCTGGCCCTTGA	197-216
<i>Netrin-1</i>	<a href="#">NM_008744.2</a>	5'-TCGCCCCTTGTCATCAAGATT	1624-1643	5'-TGGAGGCCTTGCAATAGGAG	1700-1719
<i>Dcc</i>	<a href="#">NM_007831.3</a>	5'-CACTCTCAACGAACCACCCA	3842-3861	5'-GAGAACACCAACGGTGACCA	3931-3950
<i>Neogenin</i>	<a href="#">NM_008684.2</a>	5'-CCCTGGTCTCTACTCGCTTC	1749-1768	5'-CCTGGCTGGCTGGTATTCTC	1868-1887
<i>Unc5h1</i>	<a href="#">NM_153131.3</a>	5'-ATCAGCCTCCTCATACCCCC	1779-1798	5'-TAGGGGCAACCTCACGTCTT	1855-1874
<i>Unc5h2</i>	<a href="#">NM_029770.2</a>	5'-TAAAAGCCACCCCCTGGAGA	1505-1524	5'-TATACGATCACTCCCACGGC	1593-1612
<i>Unc5h3</i>	<a href="#">NM_009472.4</a>	5'-ATGCAGGCTGCTCCTGACTC	1252-1271	5'-TCCGATACACAAACAGGGCCA	1340-1360
<i>Unc5h4</i>	<a href="#">NM_153135.3</a>	5'-GGCTGTCAGACTCAGGGAAT	957-976	5'-GCCTCCATTACGTAGACCA	1035-1054

### 2.2.7 Flow cytometry (cell staining and data analysis)

Cells were dissociated with TrypLE express (Invitrogen/Gibco). After deactivation of TrypLe and washing with PBS for 3 times, cells ( $1 \times 10^6$  cells per mL) were harvested with a fluorescence-activated cell sorting (FACS) buffer solution (PBS plus 1% FBS). Cell viability was tested by using trypan blue dye and was determined to be above 90%. Cells were fixed and permeabilised using a BD Cytotfix/Cytoperm™ (BD biosciences), according to the manufacturer's instruction. Single-stained compensation bead samples and fluorescence-minus-one samples were included as a control in a 96-well plate. Antibodies used in flow cytometry are listed in **Table 2.6**. Cells were filtered through cell strainer caps (BD Biosciences). The stained cells were analysed by using FACSDiva. Approximately 100,000 – 200,000 cells of IM-PEN cells at 33°C were acquired per replicate, while approximately 10,000 – 20,000 of IM-PEN cells at 40.5°C were acquired. The post-acquisition data analyses including optimise compensation were conducted by using FlowJo (Tree Star Inc., version 9.6.3). Three independent biological experiments were conducted.

**Table 2.6 List of antibodies used in flow cytometry assays**

Antigen	Conjugate	Host species	Clone	Catalogue number	Source	Dilution
CD24	PE-Cy7	Rat	M1/69	580538	BD Pharmingen	1:1200
CD90	APC-Cy7	Rat	OX-7	202519	BioLegend	1:600
CD49b	PE	Rat	DX5	12-5971-82	ThermoFisher (eBioscience)	1:400
CD140a	BV421	Rat	APA5	562774	BD Biosciences	1:200
CD326	BV510	Rat	G8.8	563216	BD Biosciences	1:400
CD45	PerCP/Cy5.5	Rat	30-F11	103132	BioLegend	1:200
GFAP	Alexa Flour488	Mouse	GA5	53-9892-80	ThermoFisher (eBioscience)	1:200
$\beta$ -Tubulin III	eFlour 660	Mouse	2G10-TB3	50-4510-80	ThermoFisher (eBioscience)	1:200

### 2.2.8 Neurite measurement

The cells were fixed with 2% paraformaldehyde at an indicated time and washed with PBS three times. The images were taken with a phase contrast microscope and then they were also labelled with  $\beta$ -Tubulin III. In the case of IM-PEN cells cultured at 33°C, 55 images per group covering the area of 0.7 mm x 0.5 mm per image were examined. Approximately average of 80 cells was counted per images. In the case of IM-PEN cells cultured at 40.5°C, 45 images per group covering the area of 1.4 mm x 1.1 mm per image were examined. Approximately, 50 cells at early time-point and 20 cells at late time-point were counted per image. Three independent biological assays were conducted.

### 2.2.9 Statistical analysis

Results are presented as means  $\pm$  standard deviation (S.D), calculated from the specified numbers (n) of biological replicates. If 'n' represents technical replicates, it is indicated in Figure legends. All experiments were performed in minimum of 3 independent experiments, otherwise specified in Methods or Figure legends. Statistical analysis was performed with Prism software (GraphPad Prism, version 7). Student's *t* test was used for single comparisons, comparing individual data with its control value. Two-way analysis of variance (ANOVA) followed by Tukey's multiple comparisons test or Sidak's multiple comparisons test were used for multiple comparisons. A *p* value of <0.05 was considered statistically significant. The levels of statistical significance were indicated by \**p*<0.05, \*\**p*<0.01, \*\*\**p*<0.001 and \*\*\*\**p*<0.0001.

## 2.3 Results

### 2.3.1 Optimisation of the *in vitro* IM-PEN culture for differentiation

Firstly, the optimisation of the IM-PEN cell culture under both permissive and non-permissive conditions was tested. Consistent with previous observations [260], IM-PEN cells were able to continuously grow at 33°C in the presence of IFN- $\gamma$  with 10% serum to N2 medium, and passaging the cells was required to maintain healthy cell confluency (**Figure 2.1 A**).

On the other hand, when IM-PEN cells were cultured at 39°C in 1% serum neurobasal medium without IFN- $\gamma$ , some initial cell loss was noticed (data not shown). Hence, cell viability tests were conducted under the non-permissive conditions after the cells were seeded and allowed to reach approximately 70% confluency under permissive conditions. Despite the fact that IM-PEN cells were no longer expected to be transformed at 39°C, some delayed cell growth was prominent with a longer incubation time at 39°C (**Figure 2.1 B**). Therefore, the the expression of SV40 large TAg in cells at different incubation temperatures and time points was examined (**Figure 2.1 C-D**). Unexpectedly, a high level of large TAg expression was detected at the temperature of 39°C. Accordingly, the temperature was increased to 40.5°C to allow for proper differentiation to occur. The expression of SV40 large TAg was reduced to a minimum at 40.5°C following 13 days of incubation (**Figure 2.1 D-D'**). The number of surviving IM-PEN cells cultured at 40.5°C showed a steady decline over a period of 5 days. Only a small number of cells remained viable after this time (**Figure 2.1 B**).

During fetal and neonatal development, enteric neurons and glial cells are derived from the neural crest [262]. Neural crest-derived precursor cells are known to be positive for p75<sup>NTR</sup>, which is also known as the low-affinity nerve growth factor receptor [263]. Since IM-PEN cells were isolated from the intestine via p75<sup>NTR</sup> monoclonal antibody magnetic bead immunoselection [260], the expression of more than one cell type were apparent (**Figure 2.2**). Under the permissive conditions, most cells were closely clustered and some loosely attached small circular cells appeared to shine under the light microscope (**Figure 2.2 A**). On the other hand, some cells began to show a neuronal-like appearance by extending a number of processes that connected to other cells during the 10 day incubation period which was conducted under non-permissive conditions at 39°C (**Figure 2.2 B**). When the cells were incubated for 13 days at 40.5°C, they became even more neuronal-like, developing features such as those seen in multipolar and bipolar neurons. Long extended processes were observed in these cells (**Figure 2.2 C**). Neural connection was mostly observed in the corner of the flasks or plates (data not shown).

To ensure the non-permissive temperature for the IM-PEN cells in this study setting is 40.5°C, not as previously reported as 39°C [260], the cells were cultured at 39°C or 40.5°C for various incubation days. The cells were fixed and then labelled with a proliferative marker, Ki67 and neuronal specific marker,  $\beta$ -Tubulin III (**Figure 2.3**). As expected, the expression of Ki67 was evident in IM-PEN cultured at 33°C. The expression of Ki67 was maintained in the cells cultured at 39°C but was diminished at 40.5°C. Taken together, these results suggest that the non-permissive temperature for the IM-PEN cells to be 40.5°C.

**Figure 2.1 Viability of IM-PEN cells under permissive and non-permissive conditions**

**(A)** IM-PEN cells cultured under permissive conditions (33°C, IFN- $\gamma$ , 10% serum to N2 media) showed steady cell proliferation **(B)** IM-PEN cells were initially seeded under the permissive conditions. Once they reached 70% confluency, they were placed to non-permissive temperature (either at 39°C or 40.5°C, in 1% serum to neurobasal media without IFN- $\gamma$ ). Some delay in growth was noted in the cells cultured at 39°C, whilst cell viability was decreased in cells cultured at 40.5°C. The results are shown as mean  $\pm$  SD (n=8 of technical replicates per experiment) and are representative of 3 independent experiments. **(C)** Western blot image showing the expression of SV40 large T antigen present in IM-PEN cells cultured at 33°C. **(D)** Western blot image shows decreased expression of SV40 large TAg in IM-PEN cells cultured at 40.5°C in contrast to cells cultured at 39°C. Images are representative of three independent experiments. The replicate images used for densitometry analysis are shown in **Appendix A**. **(D')** Densitometry analysis of SV40 large T Ag expression in various incubation periods at 39°C versus 40.5°C. The data reported are the mean  $\pm$  SD (n=3).

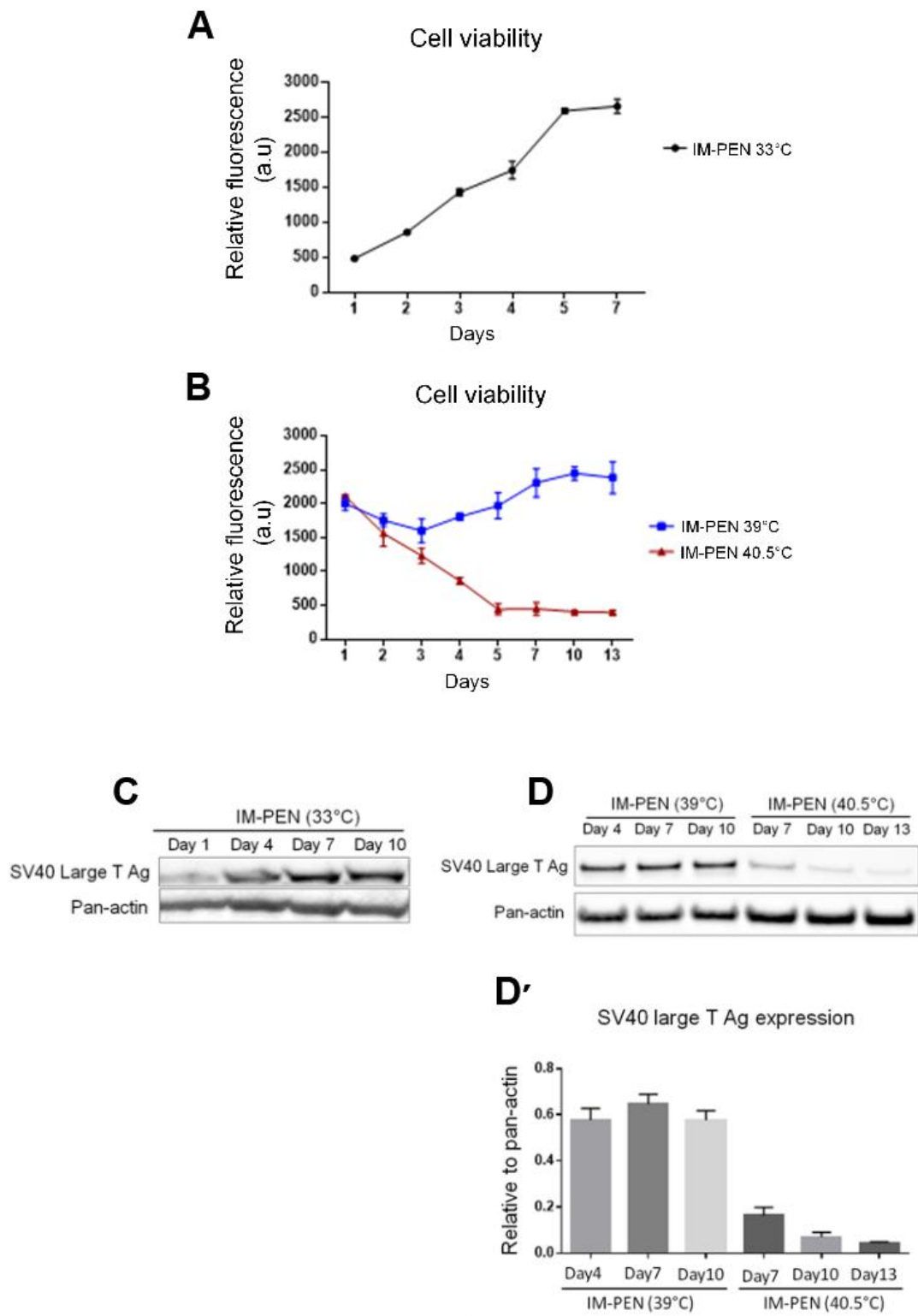


Figure 2.1

**Figure 2.2 Morphological changes in IM-PEN cells under permissive and non-permissive conditions**

Phase contrast microscopic images of **(A)** IM-PEN cells cultured under permissive conditions (33°C with IFN- $\gamma$ ) after seeding, day-1, -4, -7 and -10. **(B)** IM-PEN cells cultured under the non-permissive conditions (39°C without IFN- $\gamma$ ) after seeding, day-1, -4, -7 and -10. **(C)** IM-PEN cells cultured under non-permissive condition (40.5°C without IFN- $\gamma$ ) after seeding, day-1, -4, -7, -10 and -13. Two distinctive phenotypes were noted at day 13; neurite outgrowth from individual neuron (Day 13 a) and neurite elongation of neurons connecting the network (Day 13 b). Scale bar: 100  $\mu$ m. Images are representative of 5 independent experiments.

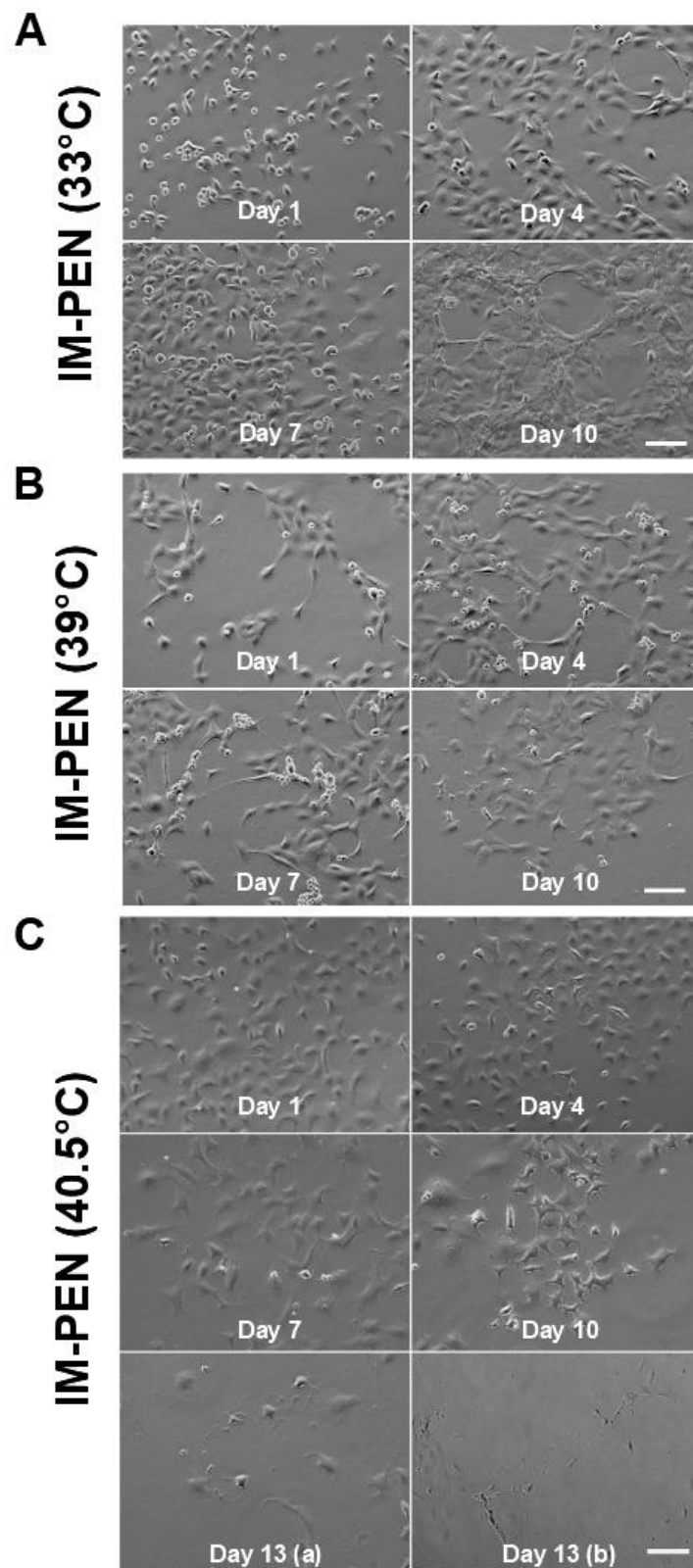


Figure 2.2

**Figure 2.3 The proliferative marker Ki67 and neuronal-specific marker  $\beta$ -Tubulin III expression in IM-PEN cells under permissive and non-permissive conditions**

**(1a-1d)** Immunofluorescence of IM-PEN cells cultured under permissive conditions at 33°C for 7 days. **(2a-2d)** IM-PEN cells cultured under non-permissive conditions at 39°C for 7 days. **(3a-3d)** IM-PEN cells cultured under non-permissive conditions at 39°C for 10 days. **(4a-4d)** IM-PEN cells cultured under non-permissive conditions at 40.5°C for 7 days. **(5a-5d)** IM-PEN cells cultured under the non-permissive condition at 40.5°C for 10 days. **(6a-6d)** IM-PEN cells cultured under the non-permissive condition at 40.5°C for 13 days. **(1a-6a)** Nuclei are labelled with DAPI. **(1b-6b)** Ki67 labelling is shown as green. **(1c-6c)**  $\beta$ -Tubulin III labelling is shown as red. **(1d-6d)** The merged images are shown. Scale bar: 50  $\mu$ m. Images are representative of 3 independent experiments.

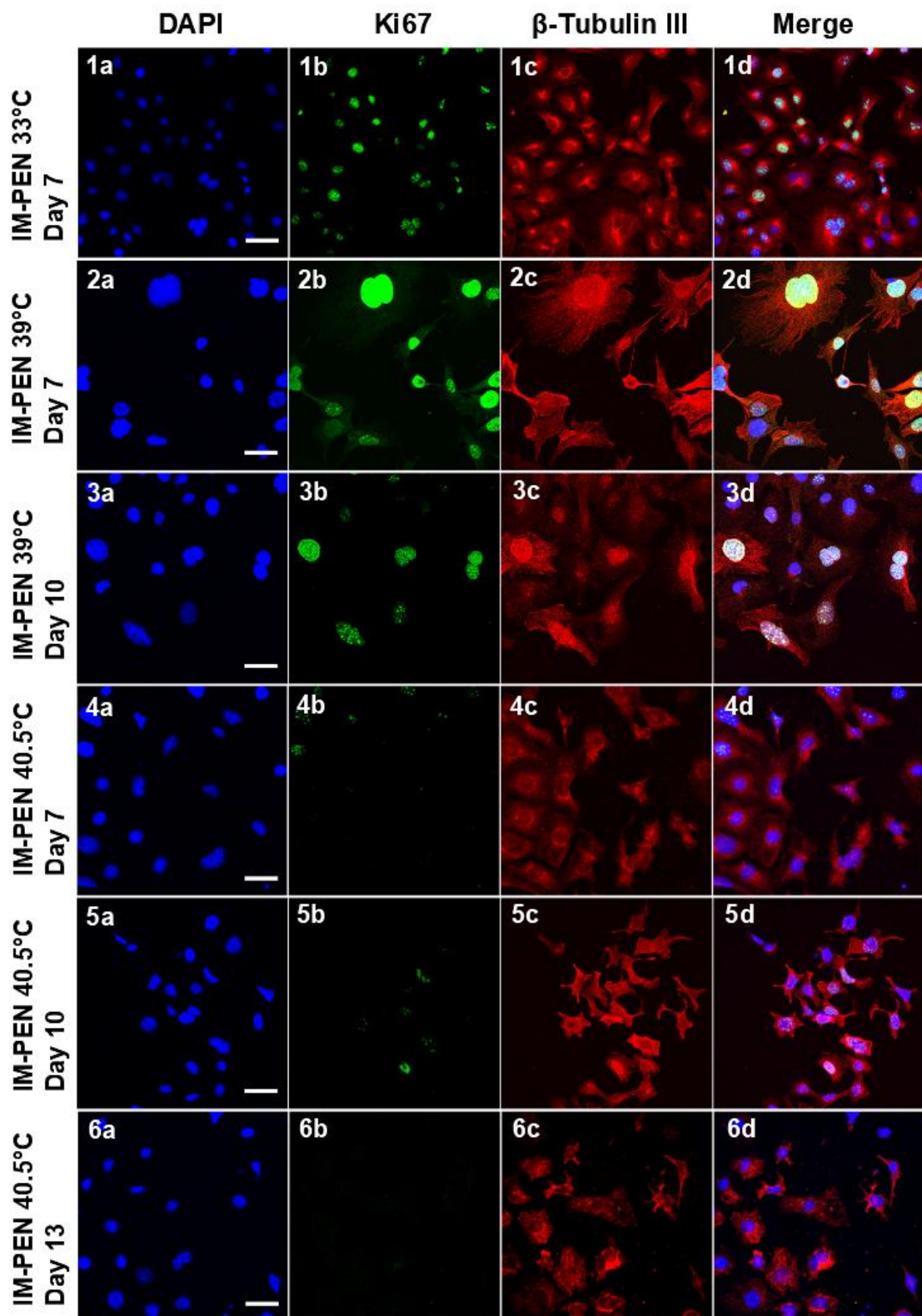


Figure 2.3

### **2.3.2 IM-PEN cells present neuronal markers**

To confirm that IM-PEN cells are neuronal cells, particularly with those cultured at 40.5°C, the expression of neuronal markers such as PGP9.5 and NeuN was demonstrated by immunofluorescence and/or western blotting (**Figures 2.4 and 2.5**). IM-PEN cells cultured at 33°C, 39°C and 40.5°C for various incubation periods, showed similar expression levels of PGP9.5 (**Figure 2.4 A**). The presence of PGP9.5 (**Figure 2.4 B**) and NeuN (**Figure 2.5 B**) expression in cells cultured at 33°C, 39°C and 40.5°C was confirmed by immunofluorescence. In addition, it was expected to see labelling of glial cell marker, GFAP, in IM-PEM cells cultured at 33°C as they are precursor cells. However, surprisingly, GFAP-immunoreactivity was also visible and co-labelled with PGP9.5 in cells cultured at 40.5°C (**Figure 2.4 B**).

Furthermore, the expression of the synaptic vesicle marker, synaptophysin, was examined in those cells to distinguish the differentiated IM-PEN cell from the precursors (**Figures 2.5**). However, synaptophysin was detected across all the cultures and the extent of the expression of this marker did not vary significantly during the course of the incubation period.

**Figure 2.4 Expression of neuronal marker PGP9.5 and glial cell marker GFAP on IM-PEN cells under permissive and non-permissive conditions**

**(A)** A representative western blot image of PGP9.5 expression in IM-PEN cells under various incubation conditions. IMR-32 cell lysate was used as a positive control for PGP9.5 detection. Pan-actin was used as a loading control. **(B)** Immunofluorescence images of IM-PEN cells under the various incubation conditions. All cell nuclei were labelled with DAPI (**1a-4a**). IM-PEN cells were labelled with PGP9.5 shown in red (**1b-4b**) and with GFAP shown in green (**1c-4c**). The merged images are shown (**1d-4d**). Scale bar: 50  $\mu\text{m}$ . Images are representative of 3 independent experiments.

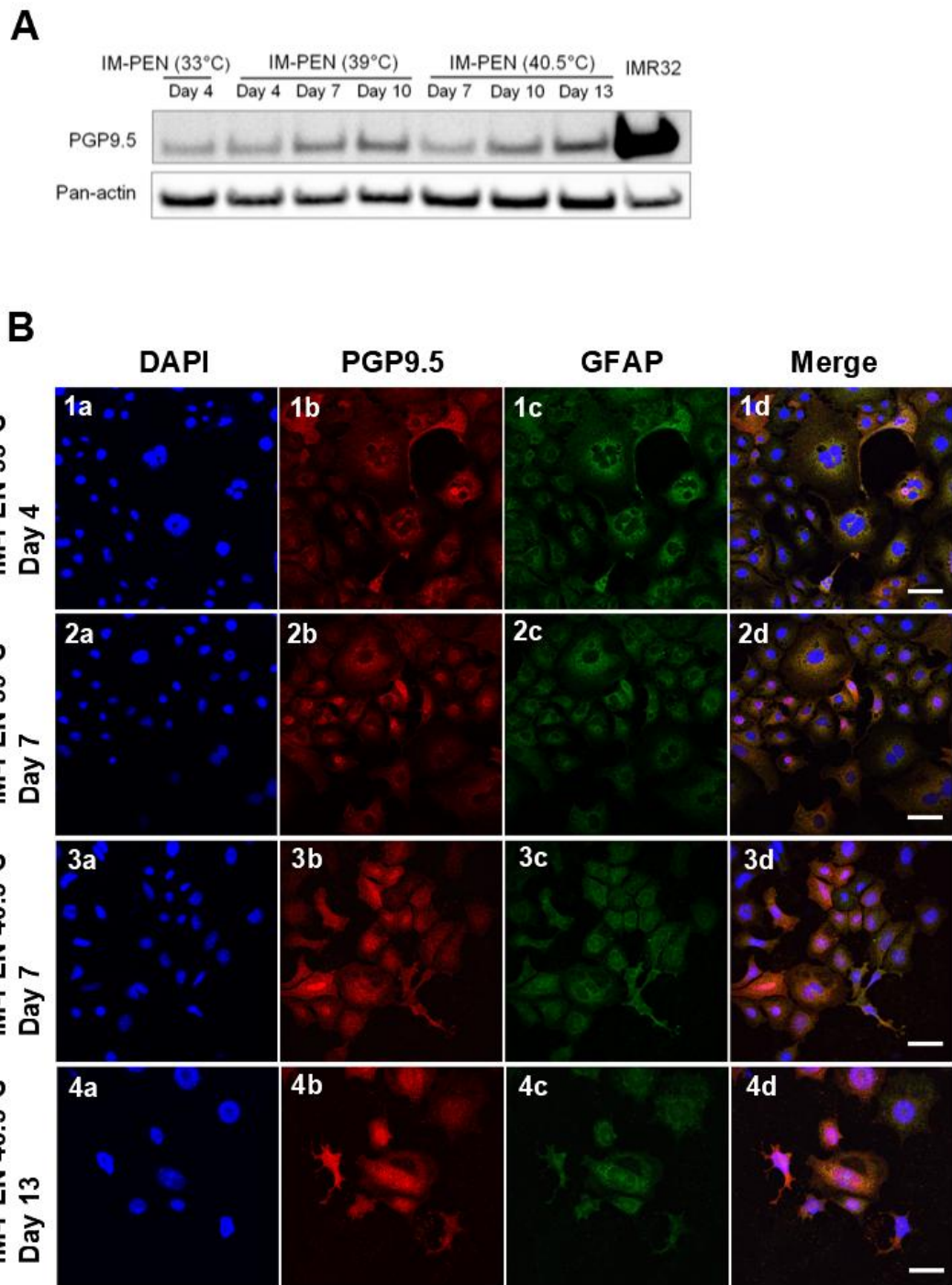


Figure 2.4

**Figure 2.5 Expression of neuronal markers NeuN and Synaptophysin expression on IM-PEN cells under permissive and non-permissive conditions**

**(A)** A representative western blot image of synaptophysin expression found in IM-PEN cells under the various incubation conditions. IMR-32 cell lysate was used as a positive control for synaptophysin detection. Pan-actin was used as a loading control. **(B)** Immunofluorescence images of IM-PEN cells under various incubation conditions were labelled with DAPI, nuclei staining, **(1a-4a)**, NeuN shown in green **(1b-4b)** and synaptophysin shown in red **(1c-4c)**. The merged images are shown **(1d-4d)**. Scale bar: 50  $\mu\text{m}$ . Images are representative of 3 independent experiments.

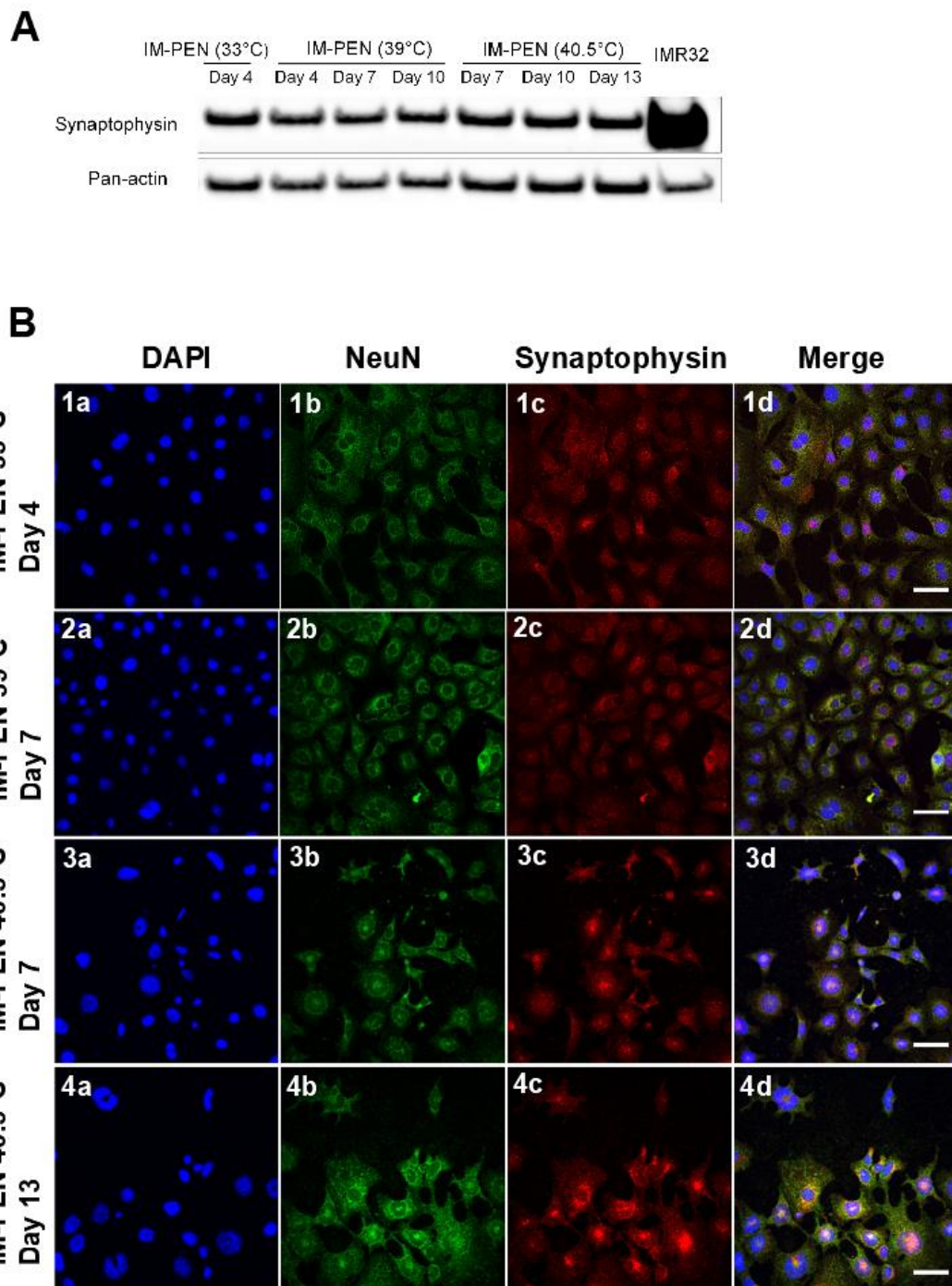


Figure 2.5

### 2.3.3 Characterisation of IM-PEN cell differentiation by flow cytometric analysis

In order to further characterise the neuronal phenotype of IM-PEN cells and their differentiation, a number of cluster of differentiation (CD) molecules were used to stain IM-PEN cells cultured at 33°C and 40.5°C. Those labelled cells together with unlabelled control cells were examined by flow cytometry. The CD molecules are surface proteins, often used to identify cell populations [264]. The antibodies recognising CD surface markers here included, CD24, CD90, CD140a, CD326, CD49b and CD45. Cells were also labelled with intracellular markers such as  $\beta$ -Tubulin III and GFAP.

CD24 is known as a heat-stable antigen and its expression has been a promising marker for mature and differentiated neurons [265]. GFAP is a glial cell marker, and  $\beta$ -Tubulin III is a well-known pan-neuronal marker. IM-PEN cells, cultured at 33°C for 13 days, were found to be predominantly positive for CD24 marker. In addition, GFAP and  $\beta$ -Tubulin III positive cells were also noted as opposed to their corresponding unlabelled cells (CD24+: 92.4  $\pm$  10.0%, \*\*\*\* $p$ <0.0001 vs 0.20  $\pm$  0.1%; GFAP+: 21.7  $\pm$  3.5%, \*\*\* $p$ <0.001 vs 0.5  $\pm$  0.1%;  $\beta$ -Tubulin III+: 31.1  $\pm$  15.3%, \*\* $p$ <0.01 vs 0.1  $\pm$  0.1%) (**Figure 2.6 B-C**).

Overall, only low levels of CD49b, CD90, CD140a, CD326 were expressed by these cells. Cells positive for these individual makers were compared to their corresponding unlabelled cells (CD49b+: 2.1  $\pm$  0.2%, \*\*\* $p$ <0.001 vs 0.05  $\pm$  0.01%; CD90+: 0.5  $\pm$  0.1%, \*\*\* $p$ <0.001 vs 0.03  $\pm$  0.01%; CD140a+: 0.4  $\pm$  0.1%, \*\*\* $p$ <0.001 vs 0.02  $\pm$  0.01%; CD326+: 0.1  $\pm$  0.06% vs 0.01  $\pm$  0.005%) (**Figure 2.6 D**). CD49b is a  $\alpha$ 2 integrin, which labels enteric glia and neural crest stem cells [266]. CD90 is expressed mostly by neurons and some glial cells in the nervous system, but it is also known to label some fibroblasts [267]. In order to clarify whether the CD90-positive staining was specific for either neuronal/glial cells or fibroblasts in these IM-PEN cells, CD140a was also used. CD140a is known to label both mesenchymal stem cells and mouse embryonic fibroblasts, whereas neurons are CD140a-negative [268]. It was found that 2.1  $\pm$  0.2% of IM-PEN cells cultured at 33°C were positive for CD49b. The incidence of CD90-positive cells (0.5  $\pm$  0.1%) and CD140a-positive cells (0.4  $\pm$  0.1%) was similar in these cells (**Figure 2.6 D**). This suggested that the IM-PEN cells

cultured at 33°C include a small population of mouse embryonic fibroblast cells. Furthermore, CD326 known as an epithelial cell adhesion molecule (EPCAM) was used. CD326 is restricted to all simple epithelia in mature murine intestines [269], and a minimal number of IM-PEN cells were positive for CD326 marker ( $0.1 \pm 0.06\%$ ). Finally, CD45 marker was used as a negative control in this experiment, as it is a well-known marker for immune cells such as granulocytes, monocytes, macrophages and lymphocytes [270]. As expected, only a negligible number of IM-PEN cells ( $0.04 \pm 0.01\%$ ) were labelled by CD45 marker.

Previous mouse and human *in vitro* developmental studies have indicated that rising levels of CD24 expression were correlated with maturation of neural differentiation [265, 271]. Particularly, the identification of bivariate CD24 expression, CD24<sup>HI</sup> and CD24<sup>LO</sup> by FACS analysis, was noted in human neural cultures derived from embryonic stem cells during development. It was found that CD24<sup>HI</sup> expressing cells are enriched with differentiated neuronal cells, whereas CD24<sup>LO</sup> expressing cells are associated with immature neural phenotype [265]. Since there was a high incidence of CD24-positive cells in IM-PEN cells cultured at 33°C, the distinct expression levels of CD24 in these cells cultured at 33°C to those cultured at 40.5°C was compared. Notably, it appeared that the size of IM-PEN cells cultured at 40.5°C was much smaller than those cultured at 33°C (**Figure 2.7 A-B**).

Using flow cytometric analysis, the gate for CD24-positive cells was defined using IM-PEN (33°C) unlabelled cells (**Figure 2.7 C1**). The CD24-positive cell populations in IM-PEN cultured at 33°C and 40.5°C were divided into four subsets based on cell size, which was estimated by forward scatter (FSC). Each subset contains forward scatter area of 50K (**Figure 2.7 C2**). The same gates were applied to compare the expression levels of CD24-positive cells cultured at 33°C and 40.5°C. CD24<sup>HI</sup> expressing cells were observed in IM-PEN cells cultured at 40.5°C, whilst CD24<sup>LO</sup> expressing cells were noted in those cells at 33°C. In addition, there was a significant difference in the median fluorescence intensity (MFI) of the CD24 subset-1 between the cells at 33°C and 40.5°C ( $1152.0 \pm 218.9$  vs  $4207.0 \pm 934.90$ , respectively, ### $p < 0.001$ ).

This is because the size of the cells cultured at 40.5°C was significantly smaller than those cultured at 33°C. For this reason, the MFI of the CD24 subset-1 at 40.5°C was compared to the MFI of subset-2, subset-3 and subset-4 at 33°C (4207.0 ± 934.9 vs 2323.0 ± 405.2; 4207.0 ± 934.9 vs 1737.0 ± 113.4; 4207.0 ± 934.9 vs 1715.0 ± 245.3, respectively, \*\*\* $p < 0.001$  for all). These comparisons showed a significant difference in the level of CD24 expression between the cells cultured at 40.5°C versus at 33°C (**Figure 2.7 D**).

CD90 is thought to be expressed mostly, but not exclusively, by neurons. CD24 has been an emerging marker for pure neuron selection. Accordingly, the double-positive staining of CD24 and CD90 was analysed to determine their positive cell proportion in the total IM-PEN cells cultured at 33°C versus 40.5°C (**Figure 2.8 A**). There was no significant difference in the double positive CD24<sup>+</sup>/CD90<sup>+</sup> cells between the ones cultured at 33°C (8.7 ± 4.5) and 40.5°C (5.6 ± 2.5) (**Figure 2.8 B**).

Given that  $\beta$ -Tubulin III is a pan-neuronal marker, the population of double-positive staining of CD24<sup>+</sup>/ $\beta$ -Tubulin III<sup>+</sup> was analysed between cells cultured at 33°C and 40.5°C (**Figure 2.8 C**). This was then compared to the double-positive staining of CD90<sup>+</sup>/ $\beta$ -Tubulin III<sup>+</sup> cell population cultured at 33°C and 40.5°C to seek further clarification of whether or not IM-PEN cell differentiation allow cells to express more of CD90-positive cells (**Figure 2.8 D**).

In the case of IM-PEN cells cultured at 33°C, the population of cells with double-positive staining of CD24<sup>+</sup>/ $\beta$ -Tubulin III<sup>+</sup> was higher (23.4 ± 3.7%, \*\* $p < 0.01$ ) than the population of cells stained for CD90<sup>+</sup>/ $\beta$ -Tubulin III<sup>+</sup> (1.4 ± 0.7%). This suggests that CD24 is a better marker for detecting neuronal cells than CD90 marker. In the case of IM-PEN cells cultured at 40.5°C, there was no significant difference in the populations of cells expressing double-positive staining for CD24<sup>+</sup>/ $\beta$ -Tubulin III<sup>+</sup> versus CD90<sup>+</sup>/ $\beta$ -Tubulin III<sup>+</sup> (10.3 ± 3.2% vs 6.2 ± 2.5%,  $p = 0.53$ ) (**Figure 2.8 E**).

Furthermore, when the double-positive staining of CD24<sup>+</sup>/ $\beta$ -Tubulin III<sup>+</sup> was compared between the cells cultured at 33°C and 40.5°C, approximately two-fold higher population of CD24<sup>+</sup>/ $\beta$ -Tubulin III<sup>+</sup> was shown at 33°C when compared to the ones grown at 40.5°C (23.4 ± 2.5%, \* $p < 0.05$  vs 10.3 ± 3.2%).

However, when the double-positive staining of CD90+/β-Tubulin III<sup>+</sup> was compared between the cells cultured at 33°C and 40.5°C, there was no significant change in the expression of CD90+/β-Tubulin III<sup>+</sup> found in the cells at 33°C when compared to those at 40.5°C ( $1.4 \pm 0.7\%$ ,  $p=0.42$  vs  $6.2 \pm 2.5\%$ ).

Moreover, when the double-positive staining of CD90+/β-Tubulin III<sup>+</sup> at 33°C was compared to the double-positive staining of CD24+/β-Tubulin III<sup>+</sup> at 40.5°C, no significant difference was noted between them ( $1.4 \pm 0.7\%$ ,  $p=0.11$  vs  $10.3 \pm 3.2\%$ ).

Collectively, these data indicated that CD24 was a good indicative marker for neuronal cell lineage of IM-PEN cells. The changes observed in CD24 expression between the precursor stage (33°C) and the differentiated stage (40.5°C day13) represented that IM-PEN cells differentiation cultured at 40.5°C is a suitable to use in the Netrin-1 study.

**Figure 2.6 Flow cytometry analysis of IM-PEN cells cultured at 33°C expressing surface and internal markers**

**(A)** Single cell gating strategy is shown. **(B)** A representative flowcytometry dot plot showing percentage of CD24-, GFAP- and  $\beta$ -Tubulin III-positive staining cells. **(C and D)** IM-PEN cells cultured at 33°C were stained with surface and internal markers; percentage of CD24, GFAP,  $\beta$ -Tubulin III, CD49b, CD90, CD140a, CD326 and CD45 stained cells are shown. The data are shown as the mean  $\pm$  SD (n=3). Student's *t*-test; \*\* $p$ <0.01, \*\*\* $p$ <0.001, \*\*\*\* $p$ <0.0001 vs respective unlabelled cells.

**Abbreviation:** FSC-A, forward scatter-area; SSC-A, side scatter-area; GFAP, glial fibrillary acidic protein.

## A IM-PEN at 33°C single cell gating

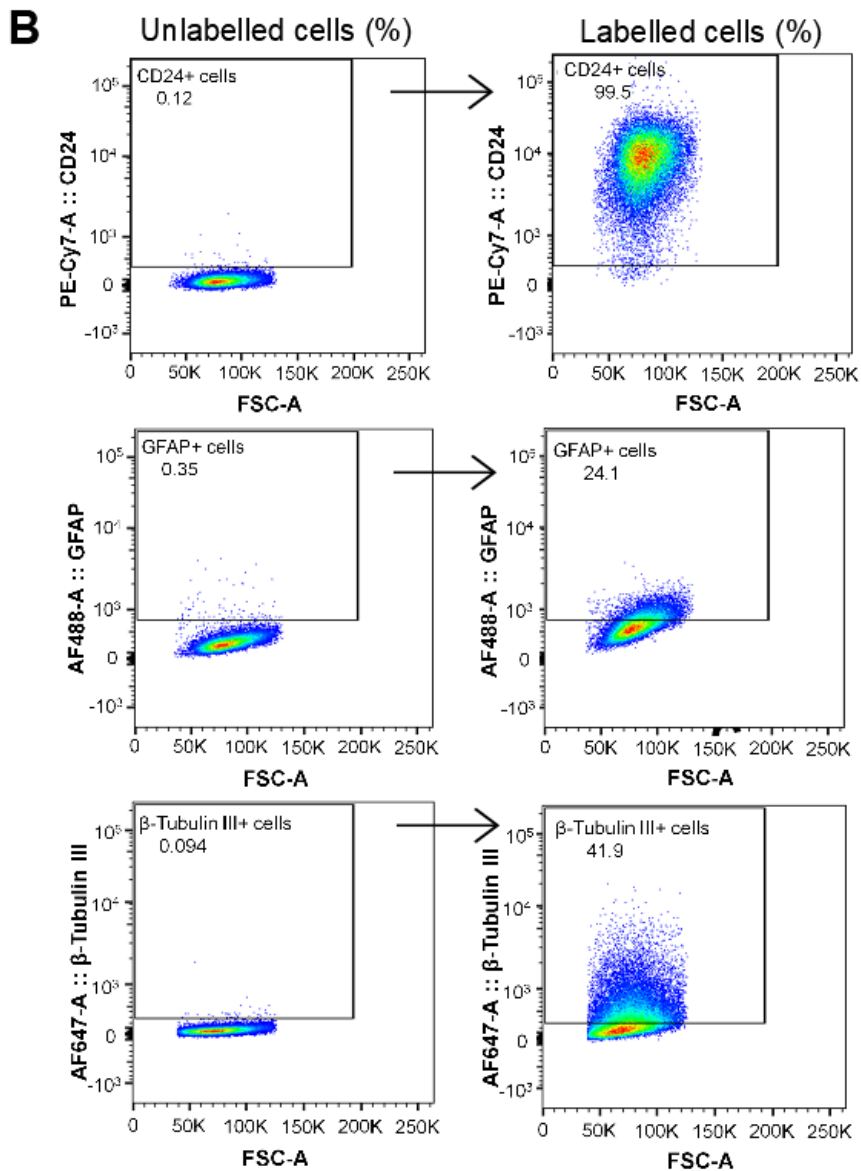
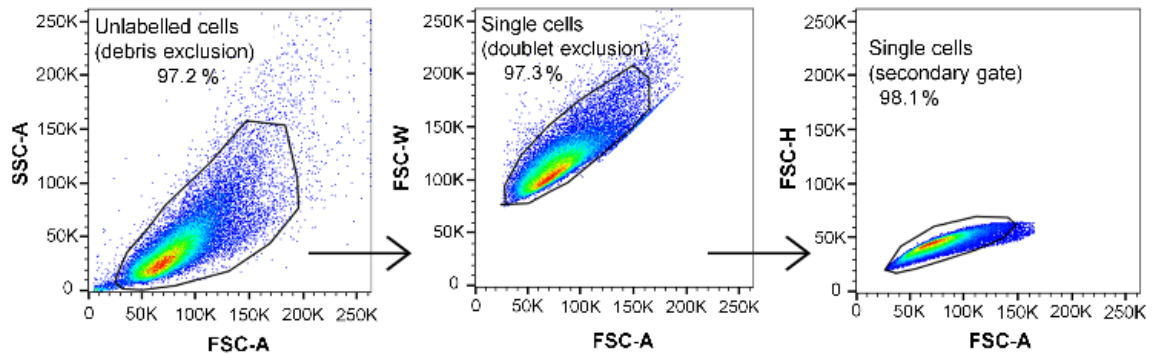


Figure 2.6 A and B

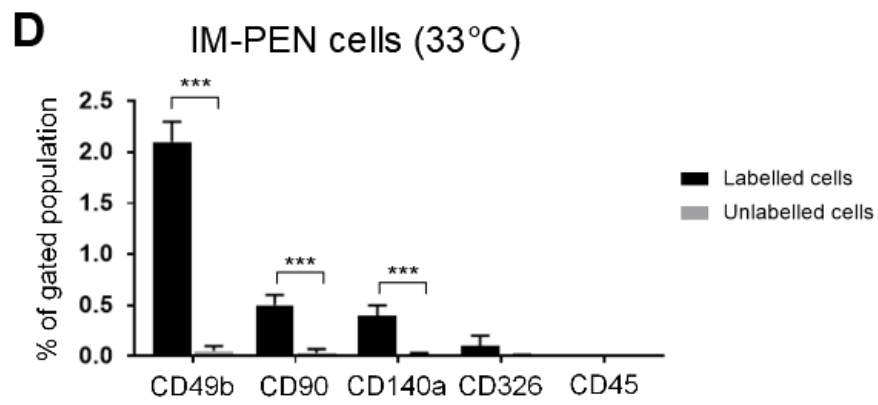
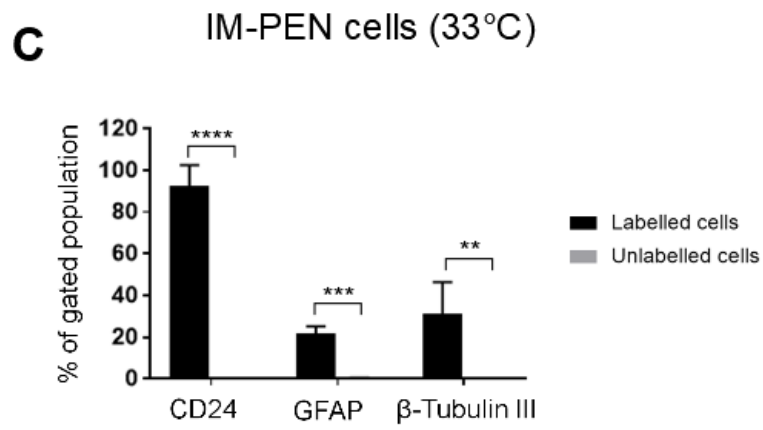


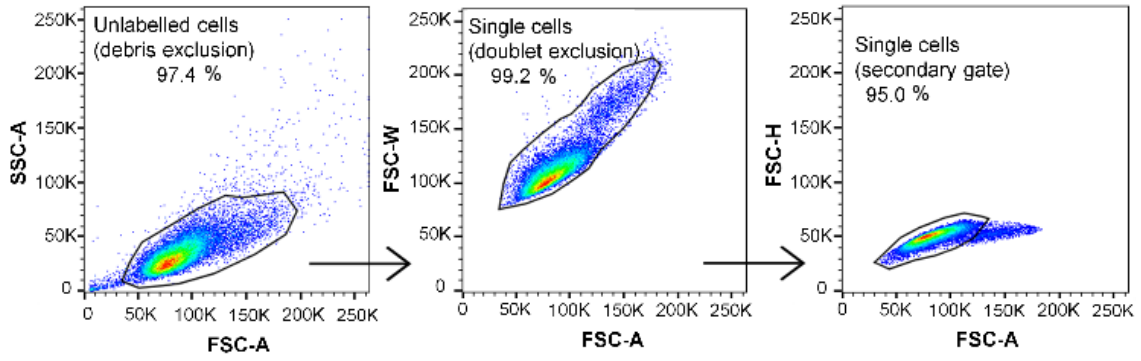
Figure 2.6 C and D

**Figure 2.7 Flow cytometric analysis of CD24-positive IM-PEN cells cultured at 33°C versus 40.5°C**

Single cell gating strategy of IM-PEN cells cultured **(A)** at 33°C, and **(B)** at 40.5°C. **(C1)** gating of CD24-positive region using CD24-unlabelled cells **(C2)** Representative flow cytometry dot plot of CD24 positive cells subsets was gated against the size of the cells at 33°C versus 40.5°C. **(D)** Median fluorescence intensity of the CD24 positive subsets shown in the cells at 33°C versus 40.5°C. The data reported are the mean  $\pm$  SD (n=3). Two-way ANOVA; Sidak's multiple comparisons test; ### $p$ <0.001 vs subset-1 of IM-PEN at 33°C; \*\*\* $p$ <0.001 vs subset-1 of IM-PEN at 40.5°C.

**Abbreviation:** FSC-A, forward scatter-area; SSC-A, side scatter-area; a.u, arbitrary unit.

**A** IM-PEN at 33°C single cell gating



**B** IM-PEN at 40.5°C single cell gating

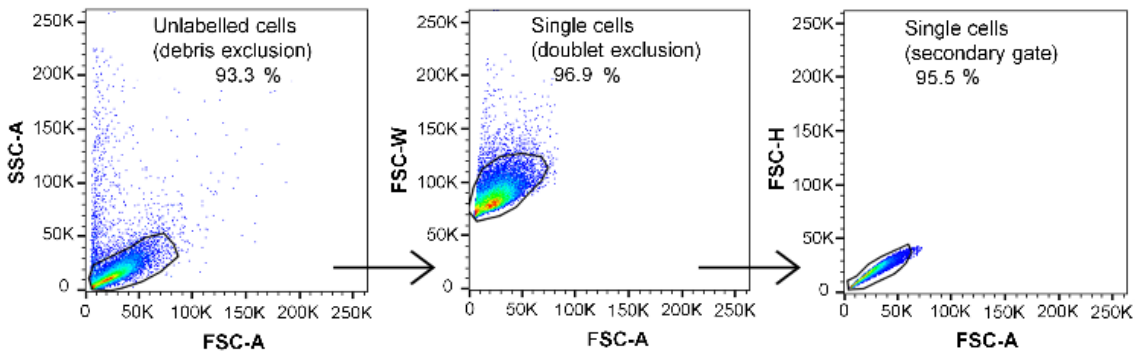
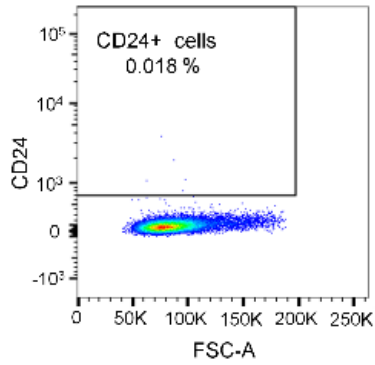
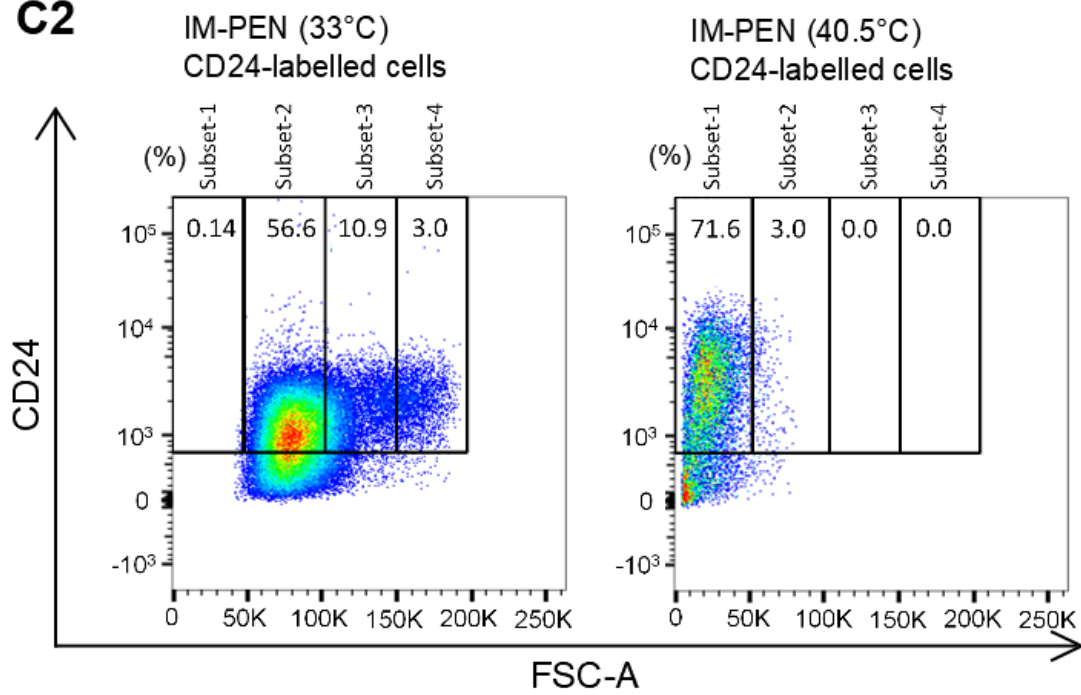


Figure 2.7 A and B

**C1** IM-PEN (33°C) CD24-unlabelled cells



**C2**



**D**

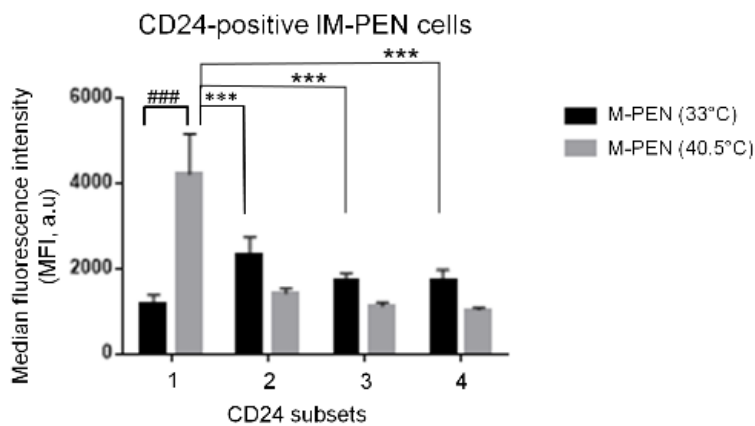


Figure 2.7 C1, C2 and D

**Figure 2.8 Flow cytometric analysis comparing CD90 and CD24-positive IM-PEN cells cultured at 33°C versus 40.5°C**

**(A)** Representative image of CD24+/CD90+ double positive cells cultured at 33°C versus 40.5°C. **(B)** CD24+/CD90+ double positive cells were represented as mean  $\pm$  SD of 3 independent experiments. **(C)** CD24 against  $\beta$ -Tubulin III positive cells at 33°C and 40.5°C were plotted. **(D)** CD90 against  $\beta$ -Tubulin III and CD90 against  $\beta$ -Tubulin III positive cells at 33°C and 40.5°C were plotted **(E)** CD24+/ $\beta$ -Tubulin III double positive cells and CD90+/ $\beta$ -Tubulin III double positive cells shown in IM-PEN cells at 33°C versus 40.5°C. The results are expressed as mean  $\pm$  SD (n=3). Two-way ANOVA; Tukey's multiple comparisons test; \* $p$ <0.05, \*\* $p$ <0.01 vs CD24+/ $\beta$ -Tubulin III+ of IM-PEN at 33°C.

**Abbreviation:** n.s, not significant.

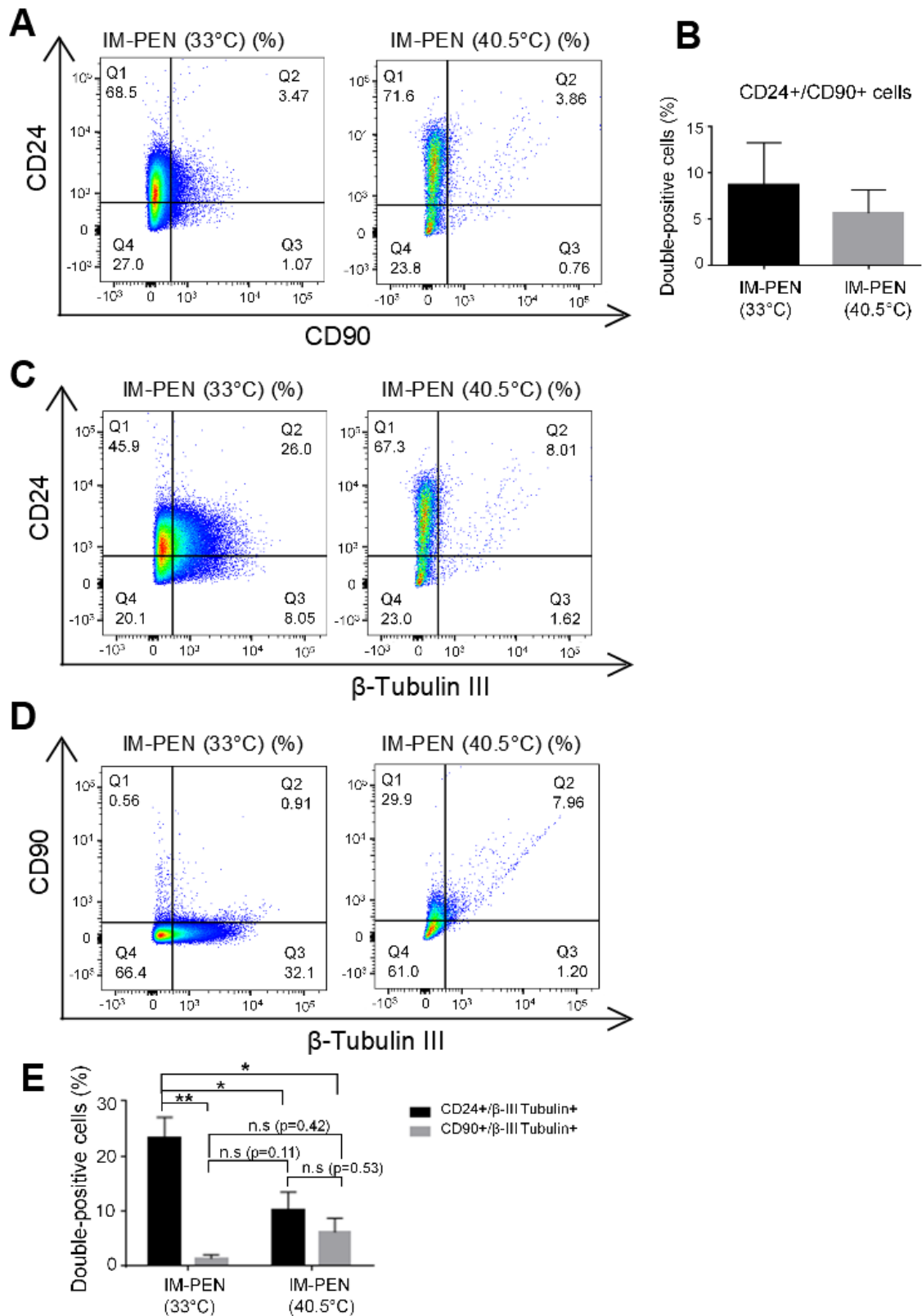


Figure 2.8

#### **2.3.4 Determining the expression of Netrin-1 and its receptors in IM-PEN cells**

To determine whether endogenous Netrin-1 and Netrin-1 receptors are expressed in IM-PEN cells at both the precursor stage (IM-PEN 33°C) and the differentiated stage (IM-PEN 40.5°C day 13), real-time PCR and western blot methods were employed. Firstly, it was important to find a sample that could be used as a positive control, i.e. expressing Netrin-1 and multiple Netrin-1 receptors (UNC5H1, UNC5H2, UNC5H3, UNC5H4, DCC and Neogenin). Young adult mouse brain tissue and mouse embryonic fibroblast (MEF) cells were tested for mRNA expression of Netrin-1 and its receptors (**Figure 2.9 A**). It was found that MEF cells lacked UNC5H1, UNC5H4 and DCC expression whilst brain tissue expresses them all. Hence, brain tissue was used as a positive control for testing mRNA levels of Netrin-1 and its receptors on IM-PEN 33°C and IM-PEN 40.5°C (**Figure 2.9 B-D**). Together with the western blot results (**Figure 2.9 E**), it was shown that IM-PEN precursor cells express UNC5H2 and Neogenin receptors. Similarly, differentiated IM-PEN cells also express UNC5H2 and Neogenin receptors. However, the level of Neogenin receptor expression was minimal in differentiated IM-PEN cells when compared to the level shown in precursor cells (**Figure 2.9 E**). Furthermore, low levels of Netrin-1 mRNA expression were detected in differentiated IM-PEN cells (40.5°C) whilst no expression of Netrin-1 was observed in precursor cells (33°C) (**Figure 2.9 F**). However, Netrin-1 expression in differentiated IM-PEN cells was not readily detected by western blot (data not shown). Since the presence of Netrin-1 receptors is observed in IM-PEN cells at both stages, it is possible to study their biological behaviour by introducing exogenous Netrin-1. In the next section, a range of different concentrations of Netrin-1 was introduced to the IM-PEN precursor cells which were then tested for their cell viability.

**Figure 2.9 The expression of Netrin-1 receptors in IM-PEN cells cultured at 33°C and 40.5°C**

**(A)** RNA was isolated from young adult mouse brain tissue and mouse embryonic fibroblast (MEF) cells. mRNA expression of UNC5H1, UNC5H2, UNC5H3, UNC5H4, DCC and Netrin-1 was assessed to determine a positive control sample. GAPDH was used as a reference gene. **(B)** UNC5H2 mRNA expression was detected in IM-PEN progenitor cells cultured at 33°C. Two technical replicates were used per experiment. The final expression was normalised to the control sample, brain tissue. Two reference genes (GAPDH and L-32) were used. Three independent biological assays were conducted. **(C)** mRNA expression of UNC5H2 and Neogenin was detected in differentiated IM-PEN cells cultured at 40.5°C for 13 days, and **(D)** their amplifications were shown in 2% agarose gel. **(E)** Western blot image showing the expression of UNC5H2 and Neogenin in both IM-PEN 33°C and 40.5°C. Pan-actin was used as a loading control. **(F)** Low level of mRNA expression of Netrin-1 was detected in IM-PEN cells cultured at 40.5°C for 13 days. The data reported are the mean  $\pm$  SD (n=3 of technical replicates per experiment) and are representative of 3 independent experiments.

**Abbreviations:** MEF, mouse embryonic fibroblast; DCC, deleted in colorectal cancer, UNC5H1-4, uncoordinated-5 homologue 1-4.

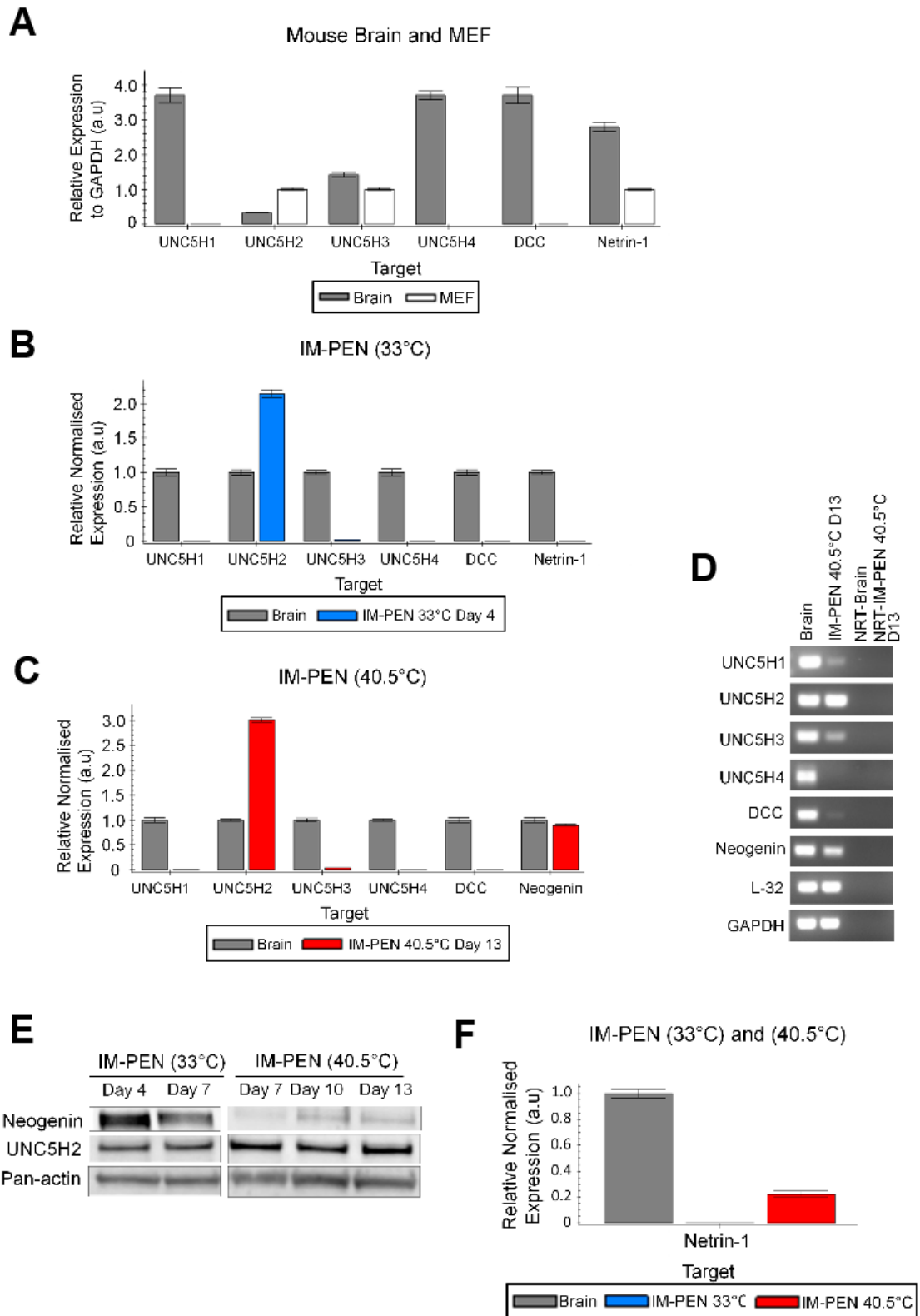


Figure 2.9

### 2.3.5 Netrin-1 does not affect IM-PEN precursor cell proliferation

Netrin-1 is known as a cell survival factor and has been shown to increase proliferation of a number of cell types including Schwann cells [272], oligodendrocyte precursor cells [273] and neuroblast cells [274]. To determine whether Netrin-1 has any influence on IM-PEN precursor cell proliferation, the viability of the cells was tested after introducing a range of Netrin-1 concentrations (**Figure 2.10 A**). Cell viability was measured by an AlarmaBlue indicator that is reduced to the fluorescent molecule, resorufin, during active metabolic activity in healthy living cells. The result indicated that cell viability of IM-PEN precursors was not significantly altered in the presence of Netrin-1 at all concentrations at 24 hour (N50:  $99.5 \pm 3.8\%$ ; N100:  $97.8 \pm 4.8\%$ ; N250:  $101.8 \pm 3.6\%$ ; N500:  $97.2 \pm 3.5\%$  vs  $100 \pm 1.0\%$ ). FBS (5%) was used as a positive control in this assay, and the viability of cells treated with FBS was significantly increased ( $105 \pm 1.1\%$ ,  $p < 0.001$  vs  $100 \pm 1.0\%$ ) at 24 hour.

Similarly, no significant changes of cell viability were observed when cells treated with Netrin-1 at 50 ng/mL of Netrin-1 at both 48 and 72 hours (48 hr:  $98.3 \pm 1.9\%$ ; 72 hr:  $98.8 \pm 4.7\%$ ) or 100 ng/mL of Netrin-1 (48 hr:  $97.1 \pm 2.3\%$ ; 72 hr:  $98.0 \pm 3.7\%$ ) or 250 ng/mL of Netrin-1 (48 hr:  $97.4 \pm 2.9\%$ ; 72 hr:  $97.9 \pm 2.5\%$ ).

Interestingly, reduced cell viability was detected when cells treated with Netrin-1 at 500 ng/mL concentration in comparison to cells treated with PBS, vehicle control at both 48 and 72 hours (48 hr:  $93.0 \pm 1.9\%$ ,  $p < 0.05$  vs  $100 \pm 1.0\%$ ; 72 hr:  $92.9 \pm 2.6\%$ ,  $p < 0.05$  vs  $100 \pm 1.0\%$ ). However, cells treated with FBS (5%) showed a significant increase in cell viability at 48 and 72 hours compared to vehicle control (48 hr:  $107.5 \pm 1.1\%$ ,  $p < 0.001$ ; 72 hr:  $110.9 \pm 1.9\%$ ,  $p < 0.001$  vs  $100 \pm 1.0\%$ ).

Hence, two possibilities are likely; (1) Netrin-1 (500 ng/mL) induces cell death at 48 and 72 hours, or (2) a reduced cellular metabolic activity occurs in cells incubated with Netrin-1 (500 ng/mL) at 48 and 72 hours, as a result of the cells being committed to a quiescent state.

To address the first possibility whether or not adding Netrin-1 (500 ng/mL) led to IM-PEN cell death, apoptotic pathway involving cleaved caspase-3 and cleaved

caspase-9 was examined. Low expression of cleaved caspase-3 and cleaved caspase-9 was noted in the cells incubated with Netrin-1 (500 ng/mL) when compared to the vehicle control containing serum-free media with PBS (**Figure 2.10 B**). This suggests that Netrin-1 at 500 ng/mL unlikely induces cell death.

To address the second possibility whether or not IM-PEN cells underwent to the quiescent state in the presence of Netrin-1 (500 ng/mL), the expression of some proteins that are associated with cell-cycle regulation was examined (**Figure 2.10 B**). It is clear that there is decreased level of cyclin D expression in IM-PEN cells with Netrin-1 (500 ng/mL) at 48 and 72 hours, when compared to the vehicle control and other Netrin-1 concentrations (50 and 100 ng/mL). Furthermore, elevated levels of p27 expression were apparent throughout the samples at 48 and 72 hours as compared to 24 hours. Interestingly, p21 expression was detected only at 24 hours, but not at 48 and 72 hours (**Figure 2.10 C**). Collectively, these results imply that Netrin-1 may be involved in cell cycle regulation.

**Figure 2.10 The effect of Netrin-1 on IM-PEN progenitor cell viability**

**(A)** IM-PEN cells were cultured with serum-free media in the absence or presence of mouse recombinant Netrin-1 at 33°C for 24, 48 or 72 hours. Cell viability was not significantly altered in the presence of Netrin-1 at 24 hour. Netrin-1 at 500 ng/mL reduced cell viability at both 48 and 72 hours. The data are expressed as mean  $\pm$  SD ( $n=8$  of technical replicates were used per experiment) are representative of 3 independent experiments. Two-way ANOVA; Tukey's multiple comparisons test; \* $p<0.05$ , \*\*\* $p<0.001$  vs vehicle control. FBS (5%) was used as a positive control. **(B and C)** Total protein extracted from IM-PEN 33°C cells incubated with Netrin-1 (0, 50, 100 and 500 ng/mL) for the indicated times. Western blot image showing the detection of caspase-9 and cleaved caspase-9 ( $n=3$ ); caspase-3 and cleaved caspase-3 ( $n=3$ ); cyclin D ( $n=3$ ); p27 ( $n=2$ ); p21 ( $n=2$ ). Pan-actin was used as a loading control.

**Abbreviations:** N50: Netrin-1 50 ng/mL; N100: Netrin-1 100 ng/mL; N250: Netrin-1 250; N500, Netrin-1 500 ng/mL.

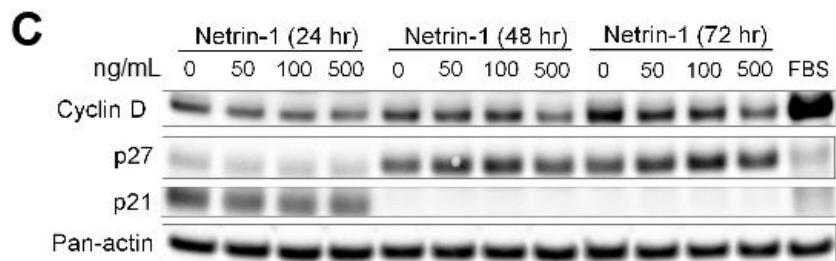
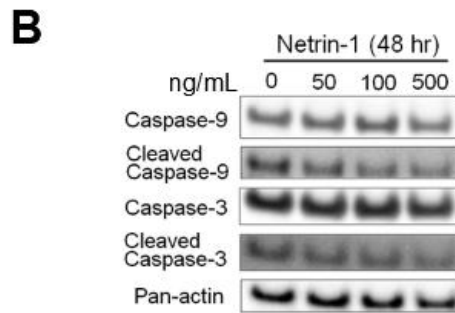
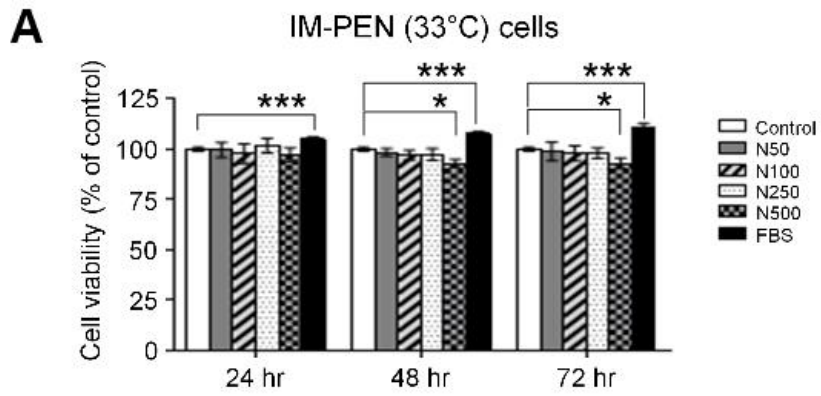


Figure 2.10

### 2.3.6 Netrin-1 effects on IM-PEN cell migration

In the embryonic nervous system, Neogenin mediates chemoattraction in response to Netrin-1 and repulsion in response to RGMa (repulsive guidance molecule). Furthermore, Neogenin has been reported to assist in Netrin-1 dependent neuroblast migration [275]. Since IM-PEN cells express Neogenin, a scratch wound-healing assay was performed to test whether or not Netrin-1 enhances IM-PEN precursor cell migration. Cells were incubated with a range of Netrin-1 concentrations after creating a gap by scratch. The images were taken at 4.5 and 9 hours. The phase contrast images were processed by MatLab. The best angle and threshold of the gap analysis was determined automatically using the MatLab program (**Figure 2.11 A1-A2**). The results indicate that the cells migrate approximately 30% faster in the presence of Netrin-1 at 100 ng/mL ( $37.7 \pm 5.6\%$ ,  $p < 0.05$  vs  $10.6 \pm 5.6\%$ ) as well as 500 ng/mL ( $39.6 \pm 10.8\%$ ,  $p < 0.05$  vs  $10.6 \pm 5.6\%$ ) when compared to the control at 4.5 hour. However, at 9 hour, cells incubated with Netrin-1 at 500 ng/mL slowed the migration rate ( $57.5 \pm 18.5\%$  vs  $48.1 \pm 8.1\%$ ), while cells incubated with Netrin-1 at 100 ng/mL ( $78.8 \pm 14.7\%$ ,  $p < 0.05$  vs  $48.1 \pm 8.1\%$ ) exhibited an approximately 30% faster migration rate than the control (**Figure 2.11 B**). No significant differences were noted when cells were treated with 50 ng/mL of Netrin-1 when compared to the vehicle control at both 4.5 hour ( $14.4 \pm 2.4\%$  vs  $10.6 \pm 5.6\%$ ) and 9 hours hour ( $52.9 \pm 17.0\%$  vs  $48.1 \pm 8.1\%$ ). Cells treated with FBS (10%) were used as a positive control in this assay, and there was a markedly increase in cell migration at both 4.5 hour ( $37.1 \pm 5.1\%$ ,  $p < 0.05$  vs  $10.6 \pm 5.6\%$ ) and 9 hours hour ( $94.3 \pm 7.9\%$ ,  $p < 0.01$  vs  $48.1 \pm 8.1\%$ ).

**Figure 2.11 The effect of Netrin-1 on IM-PEN progenitor cell migration**

**(A1 and A2)** The representative field of migration images are shown. The images are processed by MatLab; each well was marked with a reference line to determine the position of each well. The scratched images were taken by using a phase contrast microscope at intervals 4.5 and 9 hours. The best angle and threshold of the gap analysis was determined and processed automatically using MatLab. **(B)** Wound-healing scratch migration assay was conducted in the absence or presence of Netrin-1 (0, 50, 100, 500 ng/mL). The gap distance is measured by MatLab as a pixel size, which was converted to  $\mu\text{m}$  in distance. The data reported are the mean  $\pm$  SD (n=3). Two-way ANOVA; Tukey's multiple comparisons test; \* $p < 0.05$ , \*\* $p < 0.01$  vs vehicle control. FBS (10%) was used as a positive control.

**Abbreviations:** ctrl, control; N50, Netrin-1 50 ng/mL; N100, Netrin-1 100 ng/mL; N500, Netrin-1 500 ng/mL.

A1

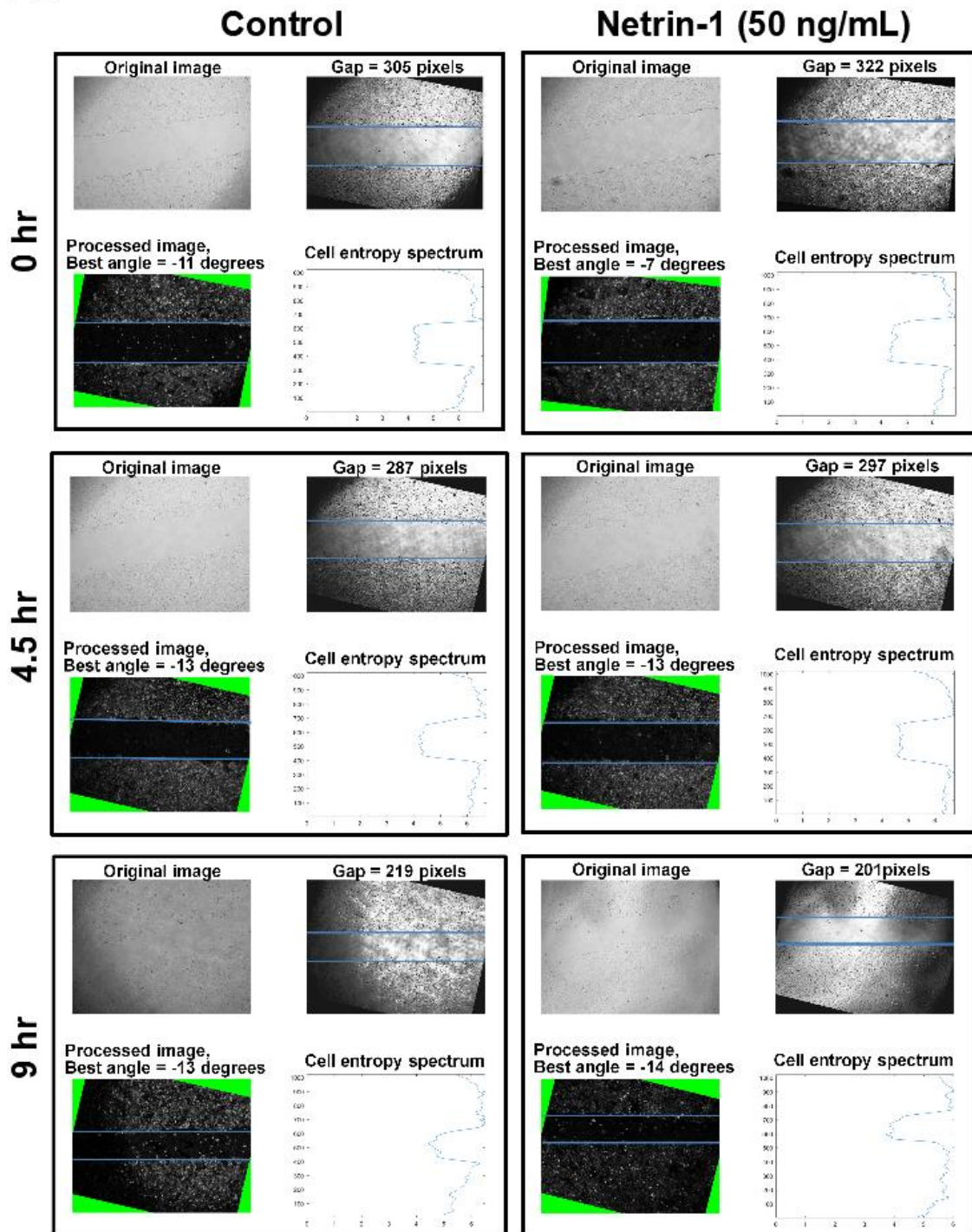


Figure 2.11 A1

A2

Netrin-1 (100 ng/mL)

Netrin-1 (500 ng/mL)

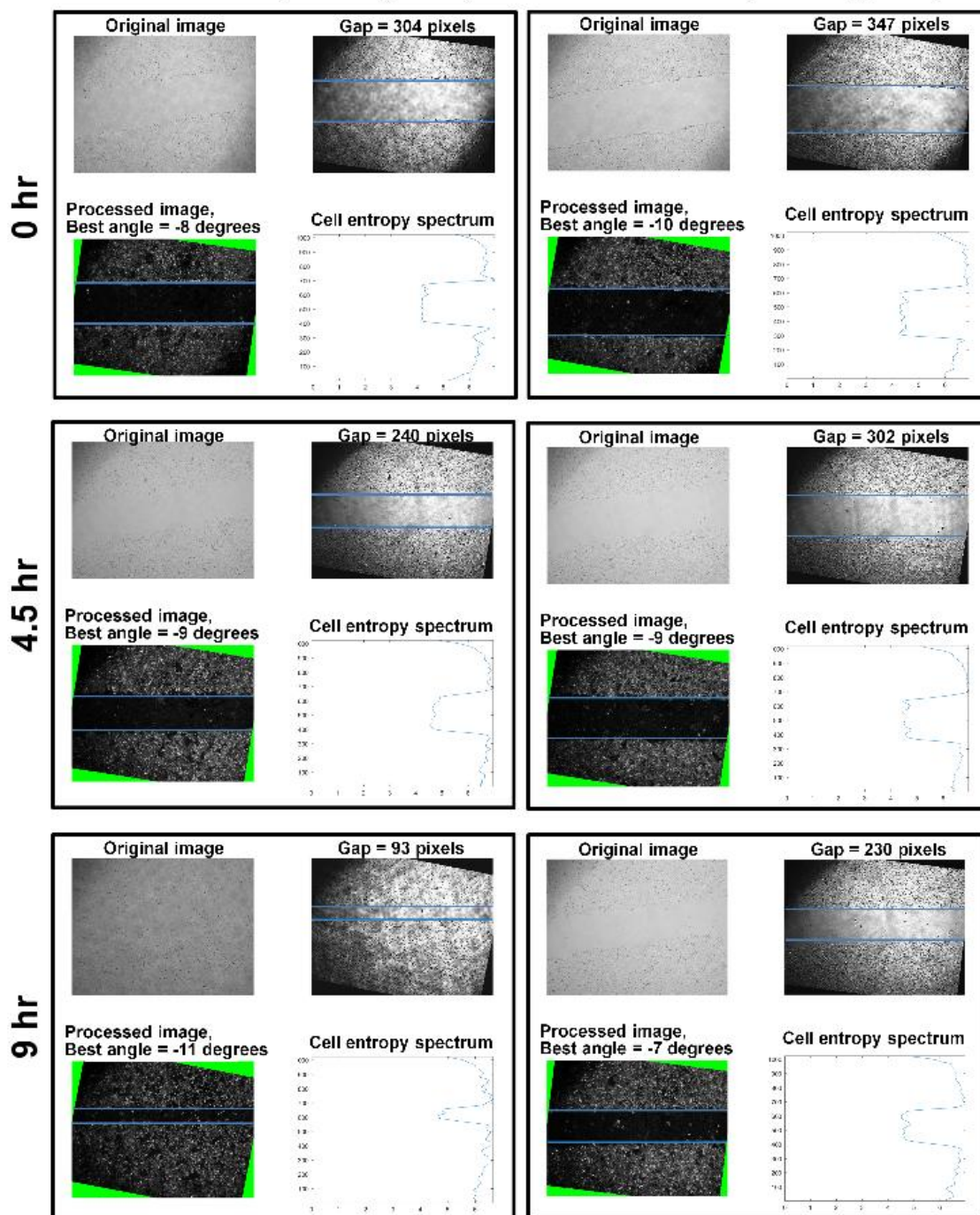


Figure 2.11 A2

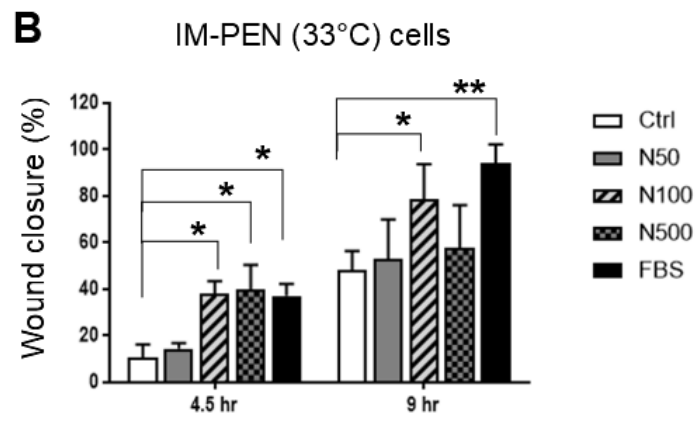


Figure 2.11 B

### 2.3.7 Increased neurite outgrowth of IM-PEN precursor cells in the presence of Netrin-1

IM-PEN cells were seeded and incubated in permissive media for 2 days at 33°C. Netrin-1 (100 ng/mL or 500 ng/mL) was incubated with the cells for 48 hours at 33°C. The phase contrast microscope images were taken to visualise any changes in cell morphology in the presence of Netrin-1. The results showed that the cells incubated with Netrin-1 appeared to develop an extended neurite length, compared to the control (**Figure 2.12 A; 1a-c**). The average length of neurite of IM-PEN precursor cells in the presence of Netrin-1 at the concentration of 100 ng/mL ( $115.4 \pm 15.8 \mu\text{m}$ ,  $p < 0.01$ ) and 500 ng/mL ( $75.8 \pm 18.8 \mu\text{m}$ ,  $p < 0.05$ ) was significantly extended when compared to the control ( $38.7 \pm 8.6 \mu\text{m}$ ) (**Figure 2.12 B**).

Netrin-1 was also introduced to IM-PEN cells cultured at 40.5°C. Two time-points were considered in order to examine the effect of Netrin-1 on those cells; the early time-point for the cells that were undergoing differentiation and the late time-point for the cells that were terminally differentiated. On the basis of the morphology study of the IM-PEN cells under non-permissive conditions shown in the earlier section (**Figure 2.2C**), neurite projections of some cells began to be noticeable at day 4. Hence this time-point was selected as the early time-point to assess the effect of Netrin-1 on early differentiating cells. The late time-point for IM-PEN (40.5°C) cells was chosen to be day 13, because optimally differentiated neurons were evident at day 13 as described in section 2.3.1. To determine whether Netrin-1 enhances neurite outgrowth/branching of the differentiating cells, Netrin-1 was introduced to the IM-PEN (40.5°C) cells at day 4. After 48 hours incubation, the cells were fixed and imaged with a phase contrast microscope and the neurite lengths were measured. The extended neurite outgrowth of these cells in the presence of Netrin-1 (100 ng/mL and 500 ng/mL) was somewhat apparent at the early time-point (**Figure 2.12A; 2a-2c**). However, this was not significant due to the extensive variation in length (control:  $77.8 \pm 15.2 \mu\text{m}$ ; N 100:  $89.9 \pm 23.5 \mu\text{m}$ ; N500:  $95.0 \pm 46.0 \mu\text{m}$ ) (**Figure 2.12 C**). In the case of the terminally differentiated cells, no markedly different neurite outgrowth/branching were noted in the presence of two different concentrations of Netrin-1 used at 100 ng/mL ( $113.2 \pm 12.0 \mu\text{m}$ ) and 500 ng/mL

( $117.3 \pm 18.3 \mu\text{m}$ ) at the late time-point when compared to the control ( $96.7 \pm 12.3 \mu\text{m}$ ) (**Figure 2.12A; 3a-3c and D**).

Neurite outgrowth and elongation are key features of neuronal differentiation [276]. Thus the question arose whether or not Netrin-1 promoted the differentiation process which led to the increase in neurite length of precursor cells, but not differentiated cells. In order to address this question, cells were co-labelled with synaptophysin and  $\beta$ -Tubulin III (also called class III  $\beta$ -Tubulin).  $\beta$ -Tubulin III is one of the six isotypes of the  $\beta$  subunit in the microtubule, which is known to be expressed almost exclusively in neurons. Therefore, it is often used as a neuronal marker [277]. Synaptophysin is an integral membrane protein of the synaptic vesicles that are associated with a particular neuronal function such as releasing and storing of the neurotransmitters. Hence, synaptophysin expression is thought to be an indicator for the presence of neuronal activity and a marker for the differentiated post-mitotic neuronal cells [278]. **Figure 2.13** shows the IM-PEN cells cultured at  $33^\circ\text{C}$  in the presence of Netrin-1 at concentration of 50, 100 and 500 ng/mL respectively. The cells were fixed and then co-labelled with synaptophysin and  $\beta$ -Tubulin III (**Figure 2.13**). Interestingly, the expression of synaptophysin in the cells was detected at all concentrations of Netrin-1 as well as the control. Similar results were obtained for the cells cultured at  $40.5^\circ\text{C}$ , at both early (**Figure 2.14**) and late time-points (**Figure 2.15**).

Collectively, these results suggest that there was no difference in synaptophysin expression between precursor cells and differentiating/differentiated cells. In addition, Netrin-1 does not influence the synaptophysin expression of IM-PEN cells in both a precursor state and differentiating/differentiated state.

**Figure 2.12 Morphological changes in IM-PEN cells cultured at 33°C and 40.5°C in the presence of Netrin-1**

**(A)** IM-PEN cells were cultured at 33°C in the presence of permissive media for 2 days, followed by incubation with **(1a)** vehicle control PBS, or **(1b)** Netrin-1 at 100 ng/mL or **(1c)** Netrin-1 at 500ng/mL for 48 hours. IM-PEN cells were cultured at 40.5°C in the presence of non-permissive media for 4 days, followed by incubation with **(2a)** vehicle control PBS, or **(2b)** Netrin-1 at 100 ng/mL or **(2c)** Netrin-1 at 500ng/mL for 48 hours. IM-PEN cells were cultured at 40.5°C in the presence of non-permissive medium for 13 days, and then the cells were incubated with **(3a)** vehicle control, PBS, or **(3b)** Netrin-1 at 100 ng/mL or **(3c)** Netrin-1 at 500 ng/mL for 48 hours. Scale bar: 100 µm. **(B)** Average neurite outgrowth was measured in IM-PEN cell cultured at 33°C in the presence of Netrin-1 (100 ng/mL or 500 ng/mL). Data represents mean ± SD (n=3). Student's *t*-test; \**p*<0.05, \*\**p*<0.01 vs vehicle control. The average neurite outgrowth was measured in IM-PEN cell cultured at 40.5°C **(C)** early time-point and **(D)** late time-point in the presence of Netrin-1 (100 ng/mL or 500 ng/mL).

**Abbreviations:** N100, Netrin-1 100 ng/mL; N500, Netrin-1 500 ng/mL.

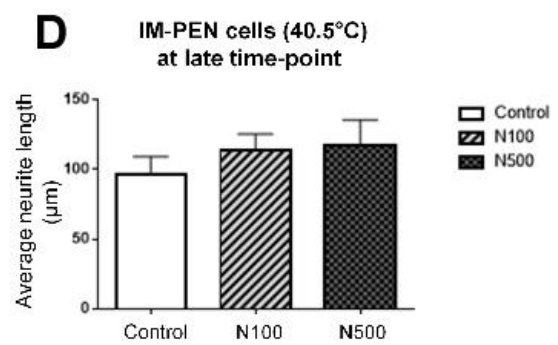
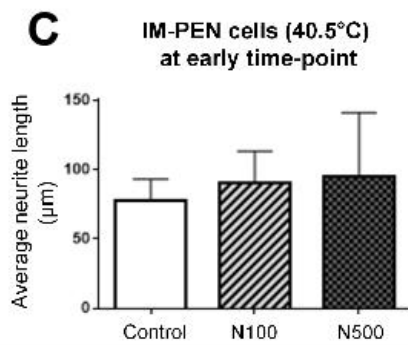
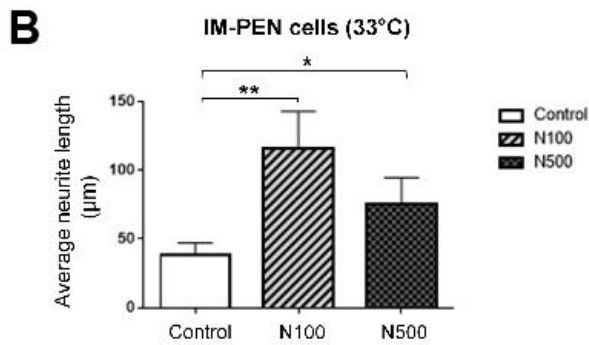
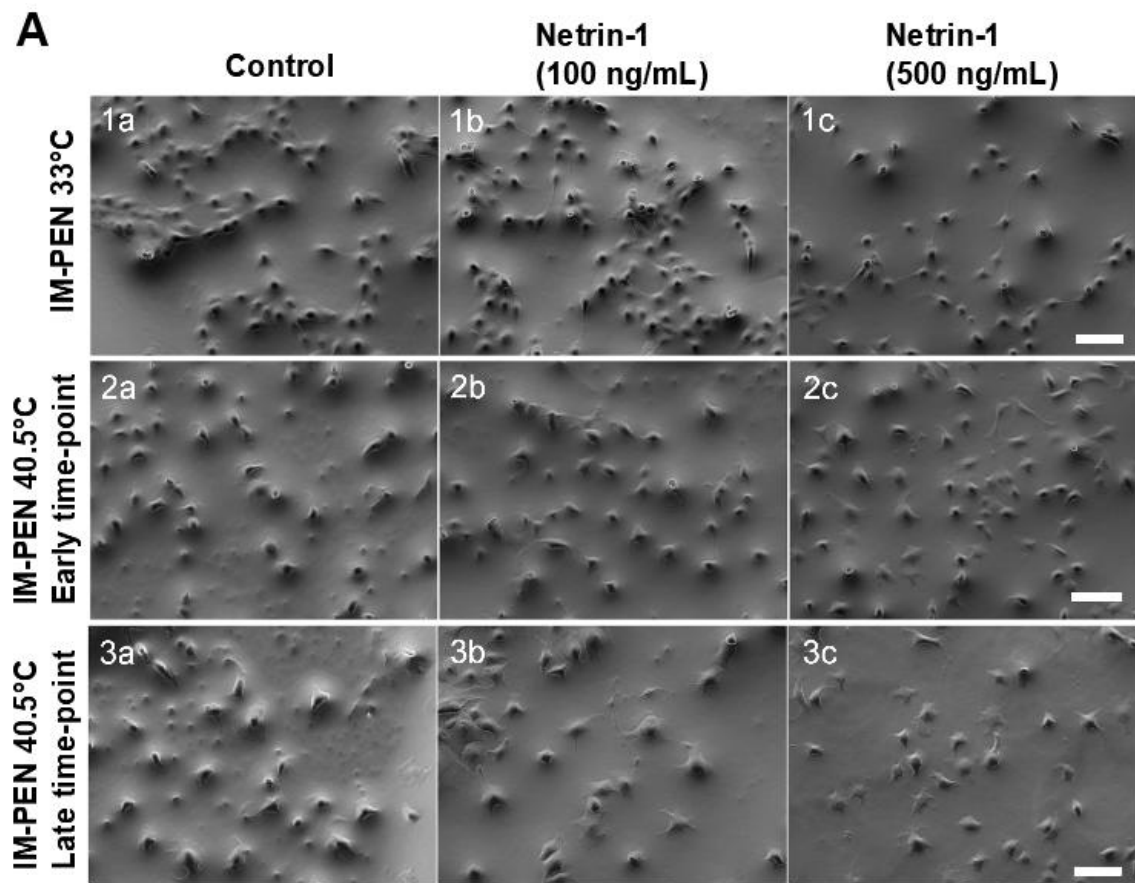


Figure 2.12

**Figure 2.13 Immunofluorescent images of IM-PEN cells cultured at 33°C in the presence of Netrin-1**

IM-PEN cells were cultured at 33°C in the presence of permissive media for 2 days, followed by incubation with **(1a-1c)** vehicle control PBS, **(2a-2c)** Netrin-1 at 50 ng/mL, **(3a-3c)** Netrin-1 at 100ng/mL or **(4a-4c)** Netrin-1 at 500 ng/mL for 48 hr. Synaptophysin labelling is shown as red **(1a-4a)** and  $\beta$ -Tubulin III labelling is shown as green **(1b-4b)**. Nuclei are labelled with DAPI and are shown in merged images **(1c-4c)**. Images are representative of three independent experiments. Scale bar: 50  $\mu$ m.

## IM-PEN (33°C)

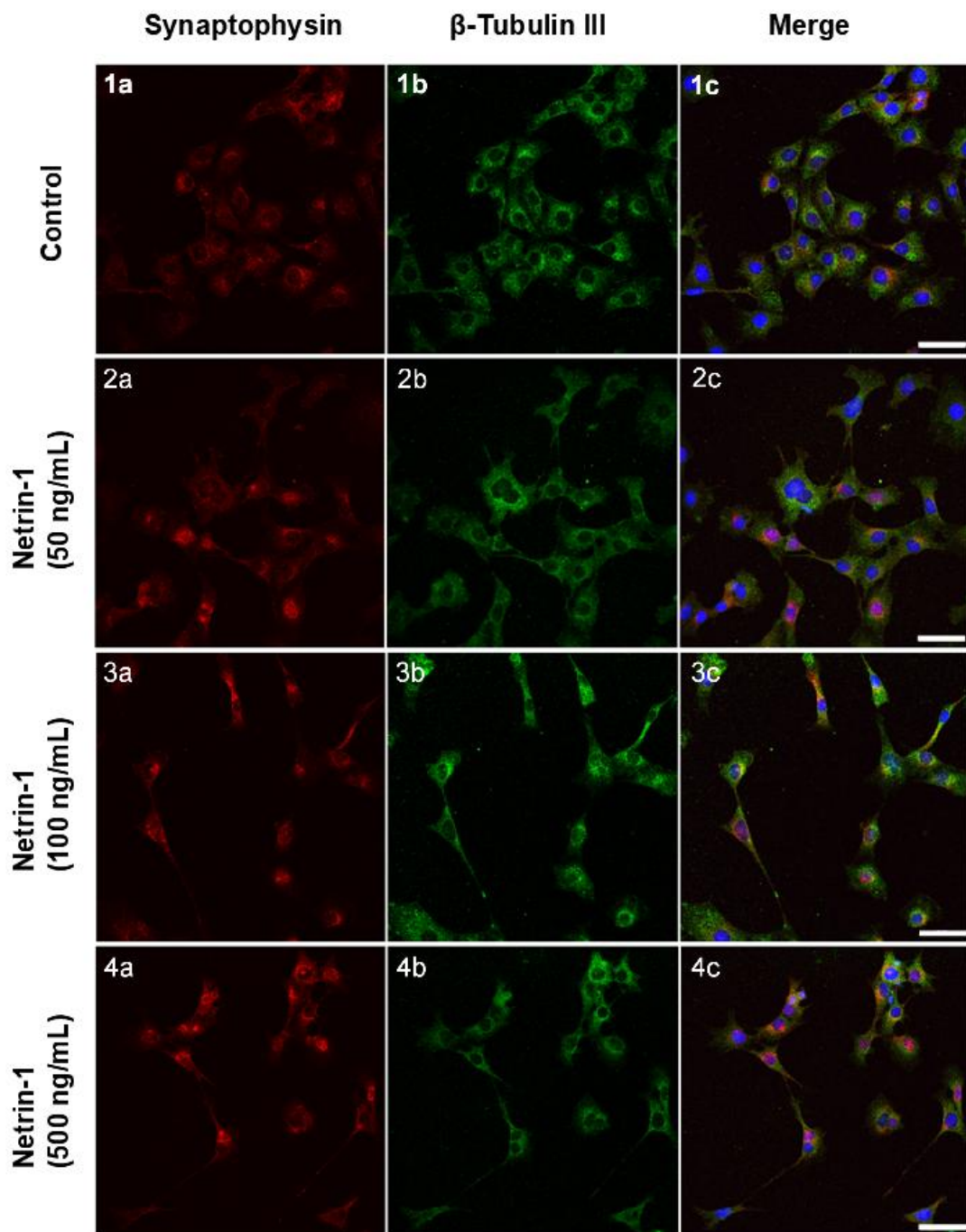


Figure 2.13

**Figure 2.14 Immunofluorescent images of IM-PEN cells cultured at 40.5°C in the presence of Netrin-1 at early time-point**

IM-PEN cells were cultured at 40.5°C in the presence of non-permissive medium for 4 days, followed by incubation with **(1a-1c)** vehicle control PBS, **(2a-2c)** Netrin-1 at 50 ng/mL, **(3a-3c)** Netrin-1 at 100 ng/mL or **(4a-4c)** Netrin-1 at 500 ng/mL for 48 hr. Synaptophysin labelling is shown as red **(1a-4a)** and  $\beta$ -Tubulin III labelling is shown as green **(1b-4b)**. Nuclei are labelled with DAPI and are shown in merged images **(1c-4c)**. Images are representative of three independent experiments. Scale bar: 50  $\mu$ m.

## IM-PEN 40.5°C at early time-point

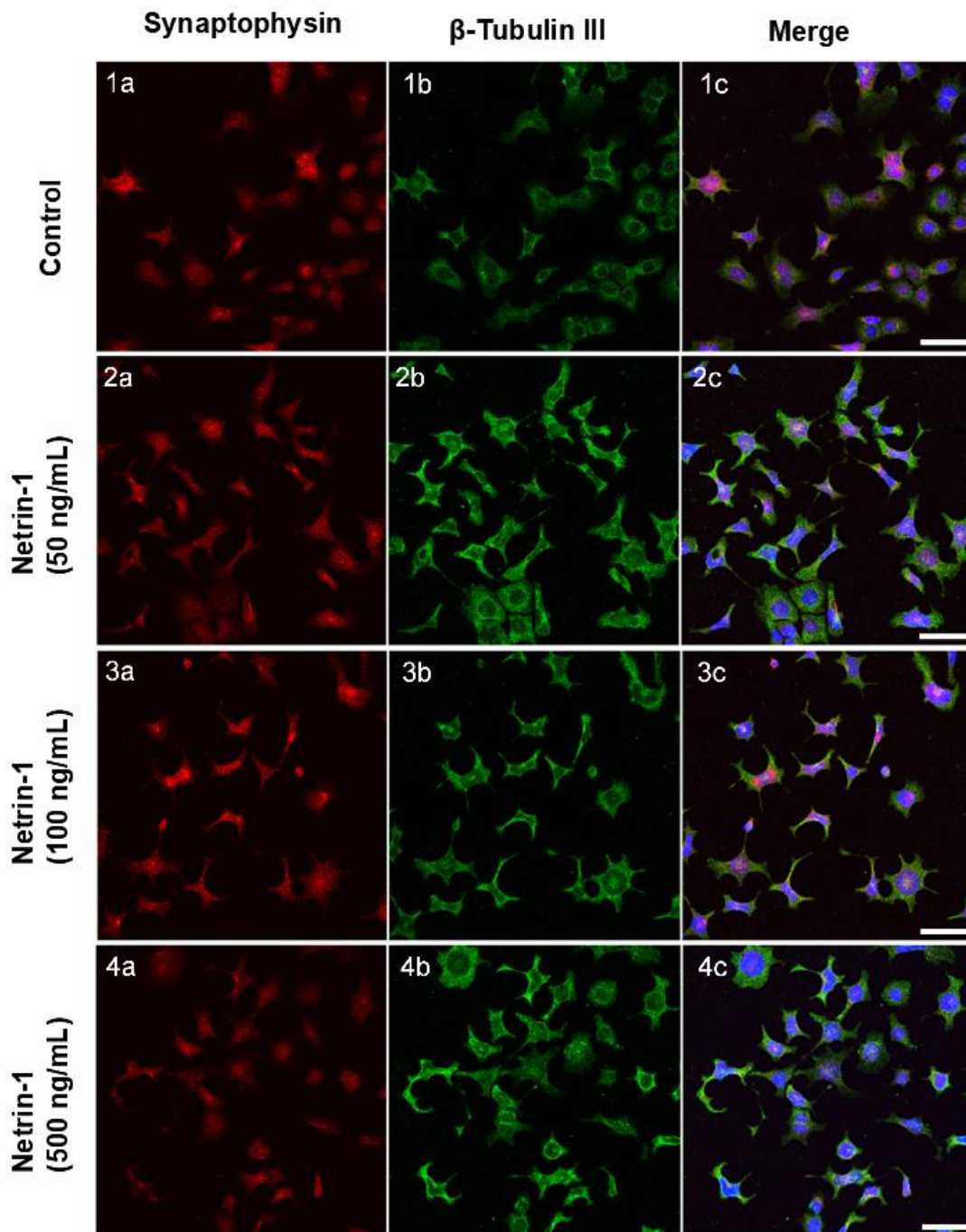


Figure 2.14

**Figure 2.15 Immunofluorescent images of IM-PEN cells cultured at 40.5°C in the presence of Netrin-1 at late time-point**

IM-PEN cells were cultured at 40.5°C in the presence of non-permissive medium for 13 days, followed by incubation with **(1a-1c)** vehicle control PBS, **(2a-2c)** Netrin-1 at 50 ng/mL, **(3a-3c)** Netrin-1 at 100 ng/mL or **(4a-4c)** Netrin-1 at 500 ng/mL for 48 hr. Synaptophysin labelling is shown as red **(1a-4a)** and  $\beta$ -Tubulin III labelling is shown as green **(1b-4b)**. Nuclei are labelled with DAPI and are shown in merged images **(1c-4c)**. Images are representative of three independent experiments. Scale bar: 50  $\mu$ m.

## IM-PEN 40.5°C at late time-point

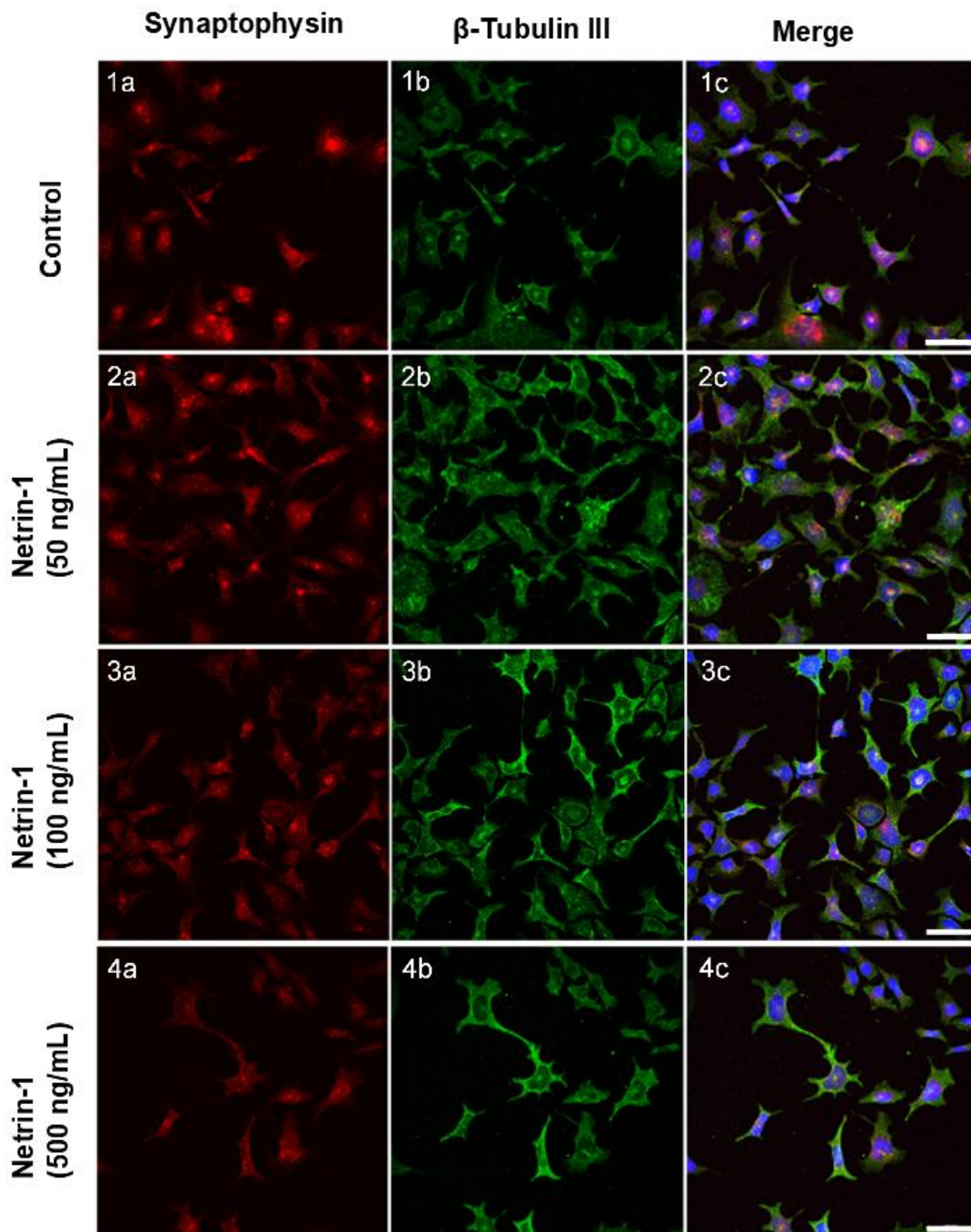


Figure 2.15

### 2.3.8 Flow cytometric analysis of Netrin-1-treated IM-PEN precursor cells

To investigate whether or not treating IM-PEN precursors with Netrin-1 elevates the expression of  $\beta$ -Tubulin III, a FACS analysis was conducted (**Figure 2.16 A-B**). IM-PEN cells cultured at 33°C for 2 days were treated with Netrin-1 (100 ng/mL or 500 ng/mL) for 48 hours. The expression of  $\beta$ -Tubulin III and/or GFAP was analysed. Although there was a slight increase in the fold change of  $\beta$ -Tubulin III positive population in the presence of Netrin-1 (500 ng/mL) when compared to vehicle control, the fold change detected was not significant (N100:  $1.2 \pm 0.3$ ; N500:  $1.3 \pm 0.1$  vs  $1.0 \pm 0.2$ ) (**Figure 2.16 C**). In addition, there was no significant fold change in the GFAP positive population in the presence of Netrin-1 at either concentration of 100 ng/mL ( $1.3 \pm 0.2$ ) or 500 ng/mL ( $1.3 \pm 0.2$ ) in comparison to vehicle control ( $1.0 \pm 0.4$ ) (**Figure 2.16 D**).

**Figure 2.16 Flow cytometric analysis of IM-PEN cells cultured at 33°C in the presence of Netrin-1**

**(A)** Single cell gating strategy is shown. **(B)** IM-PEN 33°C cells incubated with Netrin-1 at the concentration of 100 ng/mL and 500 ng/mL. Analysis showing GFAP-positive staining cells and  $\beta$ -Tubulin III-positive staining cells in the presence of 100 ng/mL and 500 ng/mL. Fold change of **(C)**  $\beta$ -Tubulin III and **(D)** GFAP positive cells in the presence of two different concentrations of Netrin-1 is shown. The results are expressed as mean  $\pm$  SD (n=3).

**Abbreviations:** FSC-A, forward scatter-area; SSC-A, side scatter-area; N100, Netrin-1 100 ng/mL; N500, Netrin-1 500 ng/mL.

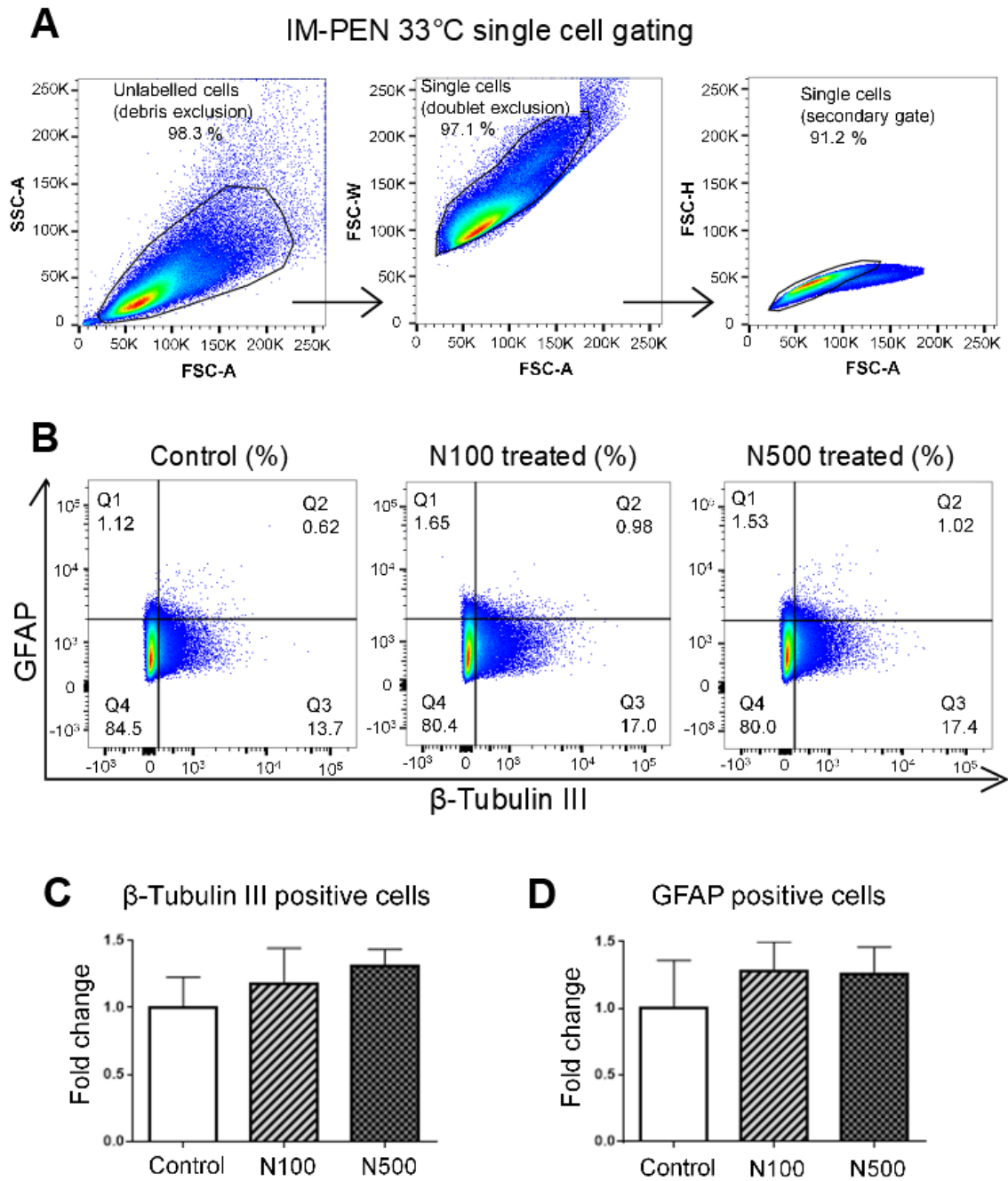


Figure 2.16

## 2.4 Discussion

### 2.4.1 Differentiation of IM-PEN cells

The enteric neurons and glial cells which comprise the ENS in the gut are originally derived from the neural crest [19]. The neural crest are a group of multipotent stem cells derived from the embryonic ectoderm cell layer of the vertebrate species [279]. Enteric neural crest stem cells remain in the ENS of the adult mammalian intestine, and are able to be isolated [41, 247]. Professor Srinivasan's Digestive Disease Laboratory has developed a mouse immortalised post-natal enteric neuronal cell line, IM-PEN. The IM-PEN cells are isolated from the intestines of mice at post-natal day two by using neural crest cell marker, p75<sup>NTR</sup> monoclonal antibody. The IM-PEN cells are generated by the *H-2K<sup>b</sup>-tsA58* transgenic mouse model. These mice harbour a conditional oncogene, SV40 large T antigen, and its expression is thermolabile. Hence, the expression of SV40 large T antigen was dependent on the ambient temperature. Professor Srinivasan's Laboratory reported that IM-PEN cells are able to proliferate under the permissive temperature at 33°C, and they differentiate under the non-permissive temperature at 39°C. The optimal differentiation time-point of the IM-PEN cells was reported to be day 7 at 39°C. [260]. However, the group which originally developed the *H-2K<sup>b</sup>-tsA58* transgenic mouse model showed their non-permissive temperature as 39.5°C, and an abolished expression of SV40 large T antigen at 39.5°C was shown [261]. In agreement with previous reports, IM-PEN cells propagated at 33°C in this study. However, the non-permissive temperature was found to be 40.5°C, instead of 39°C. Furthermore, a time-point which shows the terminally differentiated IM-PEN cells was day 13 at 40.5°C. This was shown by the presence of SV40 large T antigen that was highly expressed at 39°C but decreased to a minimum at 40.5°C on day 13. Furthermore, a time-point which shows the terminally differentiated IM-PEN cells was day 13 at 40.5°C. In addition to SV40 large T antigen expression, a minimal Ki67 expression was observed in IM-PEN cells that were cultured at 40.5°C for 13 days when compared to those cultured at 39°C. Not only was neurite outgrowth/extension observed but also an elongated neurite forming network was observed at 40.5°C on day 13. A neural network was observed mostly in the corners of the plates or flasks, therefore it could not be shown by immunofluorescence

technique using coverslips. This suggests they may form the network better with a matrix support. These cells expressed various neuronal markers such as PGP9.5,  $\beta$ -Tubulin III, NeuN and synaptophysin. Also, GFAP expression was observed in IM-PEN cells cultured at 33°C, 39°C and 40.5°C.

Although synaptophysin was chosen to test the differentiation of the IM-PEN cells, synaptophysin immunoreactivity was also visible in IM-PEN at 33°C, early post-natal neurons. Interestingly, Vannucchi *et al.* reported that the expression of synaptophysin was found in the mouse embryo at E12.5 and its expression was shown to be elevated up to the birth. This is because synaptogenesis occurs during E12.5 til E18.5, and thickening the pre- and post-synaptic membranes is caused by accumulation of synaptic vesicles [280]. A similar finding of the presence of synaptophysin was reported in rat myenteric neurons at E18.5 [281]. In addition, it was revealed that the expression of neuronal differentiation markers can appear at an early stage of differentiation of the adult neural stem cells. This is due to the induction of active membrane properties [282].

Furthermore, it is possible that the indistinguishable expression of synaptophysin in this cell line at 33°C and 40.5°C may be due to the presence of glial cell line-derived neurotrophic factor (GDNF) in the media. Soluble factors produced by the gut mesenchyme such as GDNF are known to promote enteric neuron differentiation [283]. Hence, treatment of rat myenteric neurons with GDNF was found to induce the expression of synaptophysin [284].

#### **2.4.2 Expression of CD surface markers in IM-PEN cells cultured at 33°C and 40.5°C**

In this study, the expression of CD surface markers on IM-PEN cells cultured at 33°C was characterised. Such CD surface markers include CD24, CD90, CD140a, CD326, CD49b and CD45. The IM-PEN cells cultured at 33°C showed a high incidence of CD24-positive cells ( $92.4 \pm 10.0\%$ ). The other CD surface markers that were expressed constituted less than 2.5% of the total cell population. The presence of  $\beta$ -Tubulin III ( $31.1 \pm 15.3\%$ ) and GFAP ( $21.7 \pm$

3.5%) was also identified, suggesting that there are neuronal-specific cells and glial-specific cells at the IM-PEN precursor stage.

Evidence is increasing that neuronal cells show a medium to high level of CD24 expression [264, 265]. The change in the level of CD24 expression was revealed to be a characteristic of neural lineage differentiation of stem cells. In a human embryonic stem cell lineage study, Pruszek *et al.* [265] demonstrated that the combinatory surface marker expression of CD15<sup>+</sup>/CD29<sup>Hi</sup>/CD24<sup>Lo</sup> was shown in neural stem cells. On the other hand, the expression of CD15<sup>-</sup>/CD29<sup>Lo</sup>/CD24<sup>Hi</sup> was indicated in differentiated neurons. Similar to previous studies, with respect to the level of CD24 expression, IM-PEN cells cultured at 40.5°C for 13 day incubation showed an approximately 2-fold increase in the MFI level of CD24 expression, when compared to the ones grown at 33°C. It would be interesting if levels of CD15 and CD29 markers could also be examined in this mouse *in vitro* study to compare with the work of Pruszek *et al.* conducted in human neuronal cell lineage. In addition, culturing cells after FACS cell sorting could also provide a more comprehensive identification of differentiated neurons.

However, there were some limitations involved in working with IM-PEN cells cultured at 40.5°C. Firstly, many cells died during the process of the 13 day incubation at 40.5°C. Therefore it was difficult to collect many cells by day 13. Also the cells did not easily re-adhere to flasks and their viability dropped once they were dissociated. The poor adherence of these cells was not surprising because the precursor cells showed an extremely low expression of adhesion molecule, CD326 (0.06 ± 0.1%). Expression of CD326 was expected to be low, and possibly non-existent, in neuronal cells [264].

Nonetheless, the result from FACS analysis of the CD24 expression, taken together with the study of SV40 T large antigen expression and neuronal marker expression suggested that IM-PEN cells when incubated at 40.5°C for 13 days are terminally differentiated neurons.

### 2.4.3 The effect of Netrin-1 on IM-PEN precursor cell proliferation

Neurogenesis is regulated by extrinsic signals present in the extracellular environment which are essential for governing the coordination of cell division, migration and differentiation [244]. This regulation is often delivered by an interaction between ligands and receptors that are spatiotemporally expressed on cells and their microenvironment [275].

In this study, it was determined that IM-PEN cells cultured at 33°C express Netrin-1 receptors such as UNC5H2 and Neogenin. Netrin-1 receptors are classified as dependence receptors. This means that these receptors mediate two opposing cellular activities such as cell survival or death depending on the presence or absence of their ligand binding, respectively [178]. UNC5H2 is also called UNC5B and has been shown to mediate cell survival in the presence of Netrin-1 in the mammalian central nervous system [285]. Although Neogenin has its own canonical ligand called repulsive guidance molecule (RGM), it also binds to Netrin-1 and mediates cell proliferation and migration [286]. However, introducing various concentrations of Netrin-1 (50, 100 and 500 ng/mL) to IM-PEN cells did not alter their viability at 24 hours. Instead, a reduction in cell viability was detected in the presence of Netrin-1 at 500 ng/mL at 48 and 72 hours. Western blot analysis indicated that expression of cleaved caspase-3 and cleaved caspase-9 was declined in the presence of Netrin-1 (500 ng/mL) when compared to vehicle control. This suggested that cell death was not induced in the presence of Netrin-1 (500 ng/mL).

A recent study concerning mouse olfactory bulb demonstrated that Neogenin is required as a regulator for Netrin-1 mediated neuroblast differentiation. The study of loss-of-function Neogenin (*Neo<sup>gt/gt</sup>*) mice confirmed the fact that neuroblasts in this knock-out mice were unable to undergo terminal differentiation in the presence of Netrin-1 [275].

Given that IM-PEN cells express Neogenin, the reduced cell viability in the presence of Netrin-1 (500 ng/mL) could be due to cells undergoing differentiation and a corresponding reduction in metabolism. Netrin-1 has been associated with cellular differentiation of osteoclasts [287] and mammary gland epithelial cells [288]. The analysis of cell-cycle regulation revealed that

terminally differentiated neurons are arrested in the G0 phase. Therefore, some key regulators involved in cell-cycle progression are shown to be down-regulated [289]. In this study, a decrease in the level of cyclin D expression was apparent in the IM-PEN cells incubated with Netrin-1 (500 ng/mL) at 48 and 72 hours. This suggests that IM-PEN cells may undergo differentiation in the presence of Netrin-1 (500 ng/mL). However, cyclin D expression is thought to increase only in actively cycling cells, but is also required for growth arrest before cells undergo differentiation [289]. Hence, it is difficult to determine whether or not Netrin-1 (500 ng/mL) is involved in IM-PEN cell differentiation by examining cyclin D expression alone.

Furthermore, a significant increase in the level of p27 expression in IM-PEN cells in the presence and absence of Netrin-1 at 48 and 72 hours was evident, when compared to that at 24 hours. On the other hand, an opposite expression of p21 was observed in contrast to the p27 expression.

In the presence of anti-mitogen signals, cell-cycle inhibitors such as p21 and p27 (known as Cip/Kip proteins) are activated [290]. These inhibitors bind to cyclin-cyclin dependent kinases (CDK) complexes and inhibit the catalytic activity of the complexes resulting in cell-cycle arrest [291]. However, p21 and p27 proteins are found to play additional roles in multiple cellular process such as apoptosis, cell fate determination, transcriptional regulation, cytoskeletal remodelling and migration [290]. The p27 protein is found to play a role in neurogenesis by promoting neuronal migration and differentiation in mouse cerebral cortex [292]. On the other hand, the expression of p21 is shown to be associated with preventing apoptosis via blocking cleavage of pro-caspase-3 [293], and decreasing in actin stress fiber formation [294]. There is much information regarding the emerging roles of both p27 and p21 proteins [291], and their expression and roles should be further explored. Additional studies involving signalling pathways may assist in answering questions surrounding the differential expression of p27 and p21 proteins in these cells.

#### **2.4.4 The effect of Netrin-1 on wound-healing cell migration**

Netrin-1 has been shown to play a significant role in directing migration of various cell types, which include endothelial cells [220], leukocytes [252], oligodendrocyte precursor cells [194], and mammary epithelial cells [295].

Similar to the role of Netrin-1 as a guidance cue shown in axonal pathfinding, the cell migration was mediated by Netrin-1 receptors. The migration of cells was directed, either repelled or attracted, in response to Netrin-1 depending on the presence of Netrin-1 receptors on the cells [194].

IM-PEN precursor cells express Neogenin and UNC5H2 receptors. Neogenin has been involved in chemoattractive activity meanwhile UNC5H2 has been associated with chemorepulsive activity in the developing and adult CNS. Neogenin is shown to be required for neural precursor migration in embryo [296] and adult olfactory bulb [275]. The chemorepulsive activity of UNC5H2 was shown to override the chemoattractive activity of DCC, known as homologue of Neogenin in migrating growth cones, in response to Netrin-1 binding [135].

Similar to IM-PEN cells, renal tubular epithelial cells express UNC5H2 and Neogenin but no expression of DCC. A modified chamber migration study of the renal tubular epithelial cells demonstrated that the migration of epithelial cells was increased in response to Netrin-1 with maximum effect shown at 100 ng/mL concentration of Netrin-1 [297].

Concurrent to previous study [297], the migration of IM-PEN cells was enhanced in the presence of Netrin-1. The optimal effect of Netrin-1 in this cell migration was also shown at 100 ng/mL concentration of Netrin-1. However, in response to the 500 ng/mL concentration of Netrin-1, an initial increase in IM-PEN cell migration was observed, and yet eventually the migration was slowed. This dose dependent manner of Schwann cell migration was also reported in the recent work of Lv *et al.* The migration of Schwann cells, the main glial cells in the PNS, was increased to a maximum effect at 100 ng/mL concentration of Netrin-1, instead of 500 ng/mL concentration [253].

This dose dependent manner of cell migration was widely observed in previous migratory studies concerning endothelial cells, which led to conflicting conclusions for the role of Netrin-1 in the past [220, 221, 223, 298]. The best effect of Netrin-1 on endothelial cell migration was observed at as low as 50 ng/mL of concentration, whereas the Netrin-1 concentration as high as 1 µg/mL or above showed either no significant effect of migration or even preventing the

cell migration [299]. Similarly, Schwann cell migration was promoted by Netrin-1 at 100 ng/mL but inhibited by Netrin1 at 500 ng/mL [253], suggesting that cells were responded to Netrin-1 in a dose-dependent manner. The physiological concentration of Netrin-1 was determined in chicken brain and it ranges between 50 ng/mL and 150 ng/mL [298].

#### **2.4.5 The effect of Netrin-1 on a neurite extension of precursor cells and differentiated cells**

Neurite extension is essential for forming networks during development and wiring the nervous system. Netrin-1 is one of the best-described neuronal guidance molecules in the developing CNS. Many studies using *in vivo* and *in vitro* settings have shown that axon outgrowth and elongation are induced by Netrin-1 interacting with its classic chemo-attractant receptor called DCC receptors that are present on the surface of growth cones [300, 301]. Similar to DCC function, Neogenin also mediates a chemo-attraction when it binds to Netrin-1. Upon binding to its tropical ligand RGM, Neogenin inhibits the neurite outgrowth of cerebellar granule neurons in the CNS [302, 303]. It was also shown that UNC5B is constitutively associated with Neogenin and act as a co-receptor for RGMa (one of homolouoes of RGM in vertebrate). UNC5B is found to interact with leukemia-associated guanine nucleotide exchange factor (LARG), which activates RhoA leading to growth cone inhibition of rat cortical neurons [304].

Similar to the CNS, enteric neurons and glial cells express endogenous RGMa and Neogenin *in vivo* [146]. An *in vitro* analysis of co-culturing neurosphere from fetal ENS and RGMa-expressing HEK 293 showed that Neogenin is also inhibits neurite outgrowth of enteric neuronal progenitors in response to RGMa [305].

In this study, IM-PEN precursor cells showed a strong level of Neogenin expression and a moderate level of UNC5H2. In the presence of Netrin-1 (100 ng/mL or 500 ng/mL), IM-PEN precursor cells showed a significant increase in neurite lengths compared to the control. Also, the neurons which exhibit neurite

outgrowth were readily detectable in the presence of Netrin-1 at 100 ng/mL and 500 ng/mL, particularly at 100 ng/mL, when compared to the control (data not shown). This suggested that neurite outgrowth was facilitated by Netrin-1 in IM-PEN precursors. Perhaps the enhanced neurite outgrowth of the IM-PEN precursor cells may be caused by the interaction between Neogenin and exogenously introduced Netrin-1. Further analysis using receptor inhibitors could be a useful strategy to address this point.

Importantly, the work of De Vries *et al.* demonstrated that pre-incubation of Netrin-1 in PC12 cells can prevent the RGMa-dependent growth cone inhibition mediated by Neogenin [306]. Furthermore, upon Netrin-1 stimulation, the level of UNC5B but not neogenin is elevated, and this leads to the recruitment of LARG and RGMa resulting in focal adhesion kinase (FAK) and RhoA activation required for cytoskeleton rearrangements [307].

With respect to IM-PEN differentiated cells, UNC5B expression was readily detectable, whereas a low level of Neogenin was observed. This study showed that there was no significant difference in neurite lengths with IM-PEN differentiated cells in the presence of Netrin-1 at both concentrations.

Possibly, this may be because Netrin-1 was not introduced in a gradient manner. Netrin-1 is a secreted molecule that mediates growth cones to extend toward a high concentration of Netrin-1 in the extracellular matrix [308]. Further investigation addressing this aspect could help to understand the effect of Netrin-1 on both precursors and differentiated cells in a physiological setting.

## **2.5 Summary**

Neurogenesis occurs throughout adulthood and is an essential process for gut tissue maintenance and repair. Neural stem cells are thought to be able to proliferate and differentiate into functioning neurons that can be integrated into existing neural networks under normal condition as well as in response to injury. However, trophic factors that assist in adult neurogenesis are still under investigation.

In this study, Netrin-1 was examined as a potential candidate for a trophic factor that facilitates adult neurogenesis in the gut. The effect of Netrin-1 on the immortalised post-natal enteric neuronal precursors and differentiated cells was investigated. Two important observations were made. The first is that the migration of post-natal neuronal precursor cells was enhanced by the presence of Netrin-1 at a physiological concentration of 100 ng/mL. The second finding is that neurite extension of precursor cells was observed in the presence of Netrin-1. However, the neurite outgrowth of the differentiated enteric neurons was unaffected by Netrin-1.

A future investigation of the underlying mechanisms of the Netrin-1 signalling pathways that relate to neurite extension and migration of enteric neuronal precursors would be most valuable. Understanding this endogenous process is important to elucidate mechanisms underlying neuronal damage caused by injuries and neuropathological conditions as well as the development of therapeutic strategies for effective repair of damaged neurons.

## Chapter 3

---

**The effect of Netrin-1 on colorectal cancer cells:  
*in vitro* study**

### 3.1 Introduction

Netrin-1 is a laminin-related diffusible extracellular protein that binds to its receptors and mediates chemotropic guidance for axons and cell migration during neuronal development [124]. The importance of Netrin-1 signalling in the developing nervous system was highlighted when Netrin-1 loss-of-function or that of its receptors were discovered to be lethal in mice [309].

Subsequent studies have provided that Netrin-1 is also found outside the nervous system and is widely expressed in non-neuronal tissues including lung, pancreas, colon, mammary gland and kidney [310]. In developing non-neuronal tissues, Netrin-1 is found to be associated with morphogenesis by way of guiding cell migration and promoting cell-cell contact and differentiation [288, 311]. In mature non-neuronal tissues, Netrin-1 is involved in the maintenance of regular cellular processes [124]. However, an altered expression of Netrin-1 or Netrin-1 receptors has been implicated in tumorigenesis [126, 215].

Results obtained from *in vitro* and *in vivo* studies utilising Netrin-1 transgenic mice and knock-out systems have demonstrated that tumourigenesis is promoted by either the over-expression of Netrin-1 or a lack of Netrin-1 receptors [215, 312, 313]. These phenomena have been explained by applying the dependence receptor theory proposed by Mehlen *et al.* [158, 177]. Dependent receptors transmit dual signals to the cells depending on their ligand availability. Netrin-1 receptors such as DCC, Neogenin and UNC5H family are discovered to be members of a dependence receptor family [178]. This implies that Netrin-1 receptors mediate cellular survival in the presence of Netrin-1, whereas they induce cellular apoptosis in the absence of Netrin-1. Hence, Netrin-1 acts as a cell survival factor and a regulator for tumourigenesis [162]. Netrin-1 receptors on tumour cells, especially DCC and UNC5B, are considered to be conditional tumour suppressors, since these receptors can mediate cellular apoptosis when unbound to Netrin-1, thus inhibiting tumour growth [314]. However, loss of Netrin-1 receptor expression on tumour cells has been observed to promote tumour growth [215]. This is because tumour cells lose dependent receptor activity that can induce apoptosis. Therefore, loss of Netrin-1 receptors has been demonstrated to be an advantageous event for cancers [215, 315].

Several studies have reported that up-regulation of Netrin-1 is associated with various human cancers such as neuroblastoma [274], breast cancer [316], ovarian cancer [317], and non-small cell lung cancer [318], while down-regulation of Netrin-1 receptors have been demonstrated in colorectal cancer [319], prostate cancer [320] and gastric cancer [321].

Moreover, the impact of Netrin-1 on tumour development is further complicated by the findings that Netrin-1 plays a role in regulating angiogenesis [223, 224, 322] and inflammation [252, 323]. Thereby, the implication of Netrin-1 in relation to metastasis has been highlighted in certain cancer types [234, 324, 325].

However, Netrin-1 expression has been found to be considerably reduced in approximately 50% of brain cancers and prostate cancers [139]. Also, recent studies concerning pancreatic cancer produced conflicting results: increased Netrin-1 expression facilitates pancreatic cancer regression [326], whereas Netrin-1 was believed to promote pancreatic cancer progression [228]. Similarly, Netrin-1 has shown to function as either a pro- or anti-angiogenic factor [298]. Netrin-1 has also been associated with either a pro- or anti-inflammatory response [327-329]. These results imply that the effect of Netrin-1 may be dependent on the cellular context.

In the case of human colorectal cancer, down-regulation of Netrin-1 receptors has been frequently observed as a result of heterozygosity and gene methylation in DCC and UNC5H receptors [319]. On the other hand, Netrin-1 expression was observed to be rarely up-regulated or detectable in sporadic colorectal cancer. Only the fraction of colorectal cancer that was driven by inflammation bowel disease displayed up-regulation of Netrin-1 expression [318].

In order to investigate the possibility of utilising Netrin-1 as a therapeutic neurotropic factor for damaged enteric neurons under colorectal cancer condition, understanding the effect of Netrin-1 on colorectal cancer cells and enteric neurons is of critical importance. In this chapter, the effect of Netrin-1 is studied on murine colorectal carcinoma cell line, CT26 cells. The reason for this is CT26 cells are derived from Balb/c mice, and these cells will be transplanted into syngeneic Balb/c mice in order to generate orthotopic

colorectal cancer mouse model. The consequence of Netrin-1 in the concerned orthotopic mouse model is discussed later in Chapter 5. The aim of the study in this Chapter is to investigate the effect of Netrin-1 on the metastatic properties of CT26 cells at a cellular level.

## **3.2 Materials and methods**

### **3.2.1 Cell culture**

CT26 cells were cultured in DMEM medium containing GlutaMax (Gibco), 1% (v/v) antimycotics/antibiotics (Gibco) and 10% (v/v) FBS (Thermo Scientific) at 37°C, using 5% CO<sub>2</sub> incubator. The medium was changed every second or third day depending on the confluency of the cells. Cells were passaged by removing the media, followed by washing with PBS. Cells were then incubated in 1 mL of TrypLE™ Express (Gibco) until filopodia of the cells were retracted and detached (approximately 10 mins). The flask was gently agitated to detach all the cells from the bottom of the flask. Cells were then resuspended in the complete growth media and were gently mixed. The resuspended cells were pelleted by centrifugation at 1500 rpm for 3 mins. Following the centrifugation, the supernatant was discarded. The pelleted cells were resuspended in PBS, and they were then counted using a haemocytometer. A desired number of cells were seeded into a plate or flask for further experiments. Testing for mycoplasma was routinely conducted by PCR method (*g.Mycoplasma* forward primer: GGCGAATGGGTGAGTAACACG and reverse primer: CGGATAACGCTTGCGACCTATG) or using a MycoAlert™ Mycoplasma Detection kit (Lonza).

### **3.2.2 Quantitative RT-PCR**

The methods for RNA extraction and RT-PCR parameters were described in detail in Chapter 2, section 2.2.6. In brief, total RNA was isolated from the CT26 cell line and a wild-type Balb/c mouse brain tissue by using the Epicentre's MasterPure™ RNA Extraction/purification kit, according to the manufacturer's instructions (Gene Target Solutions). Total RNA concentration was determined by NanoDrop™ Spectrophotometer (ThermoScientific). One µg of RNA was reverse transcribed into cDNA in a 20 µL reaction using iScript™ Advanced

cDNA Synthesis kit (Bio-Rad). The cDNA synthesis (10 ng/ $\mu$ L) and gene-specific primers were mixed with SsoAdvanced<sup>TM</sup> Universal SYBR Green Supermix (Bio-Rad) and they were subjected to RT-PCR (CFX96, Bio-Rad). Mouse primers used in this thesis are listed in **Table 2.5**, Chapter 2. Negative controls such as NTC and NRT, and a positive control such as brain tissue were included each run of RT-PCR experiment. Each primer set was tested in 3 technical replicates and 3 independent experiments were conducted.

### 3.2.3 Western blot

The method for western blot was described in detail in Chapter 2, section 2.2.5. Briefly, cells were serum-starved for 24 hours before they were treated with Netrin-1. Cells were treated with pan-caspase inhibitor (z-VAD-fmk, 20  $\mu$ M; APExBio, AssayMatrix) or caspase-3 inhibitor (z-DEVD-fmk, 20  $\mu$ M; APExBio, AssayMatrix) for 24 and 48 hours. PBS is a vehicle control for Netrin-1. Dimethyl sulfoxide (DMSO; Sigma-Aldrich) is a vehicle control for inhibitors. Cells were also treated with respective vehicle controls for 24 and 48 hours. Following different treatments, cell lysates were collected and the concentration of total protein was quantified by using a BCA protein assay kit (Pierce, Thermo Fisher Scientific). The reduced samples were electrophoresed on a 4-12% Bis-Tris mini gel (loaded 15  $\mu$ g of each sample) with either MOPS or MES buffer according to the manufacturer's instructions (NuPAGE, Invitrogen), and then transferred to Polyvinylidene difluoride (PVDF; iBlot gel transfer stack, Invitrogen) using iBlot<sup>®</sup> 2 Dry Blotting System (Invitrogen). The membrane was incubated in blocking buffer (5% w/v BSA in TBS-tween 20 (1%) for phosphorylated proteins or 5% skim milk in TBS-tween 20 (1%) for non-phosphorylated proteins) 1 hour at RT, and incubated with primary antibodies, listed in **Table 3.1**, overnight at 4°C. The membrane was washed and then incubated with HRP-conjugated secondary antibodies, listed in **Table 3.2**, for 1 hour at RT. Thereafter, the membranes were incubated with Clarity ECL (Bio-Rad) for 5 mins, and then developed with Vilber Lourmat Fusion FX Imaging.

The densitometric values were determined using LI-COR Image Studio Lite (LI-COR biotechnology, USA), and the values were normalised to the experimental control followed by Pan-actin or Lamin B1 expression as a housekeeping

protein. Relative phosphorylated protein expression was normalised by total protein expression. The normalised values from 3 independent biological experiments were pooled and shown as mean  $\pm$  SD.

**Table 3.1 List of primary antibodies used in western blot assays**

Primary antibody	Host species	Source	Catalogue number	Dilution
Neogenin	Goat	R and D system	AF1079	1:1000
UNC5H2/B	Goat	R and D system	AF1006	1:1000
Pan-actin	Mouse	ThermoFisher	MA5-11869	1:10,000
Cyclin D	Rabbit	Cell signalling technology	ab134175	1:10,000
Lamin B1	Rabbit	Cell signalling technology	ab16048	1:1000
Caspase-3	Rabbit	Cell signalling technology	9915	1:1000
Cleaved caspase-3	Rabbit	Cell signalling technology	9915	1:1000

**Table 3.2 List of secondary antibodies used in western blot assays**

Secondary antibody	Source	Catalogue number	Dilution
Donkey anti-rabbit IgG, HRP-linked	Thermo Fisher Scientific	31458	1:10,000
Goat anti-rabbit IgG, HRP-linked	Cell signalling technology	9915	1:10,000
Horse anti-mouse IgG, HRP-linked	Cell signalling technology	9915	1:10,000
Rabbit anti-goat IgG, HRP-linked	Thermo Fisher Scientific	31402	1:10,000

### 3.2.4 Cell viability

CT26 cells were seeded at 8000 cells per well on a 96-well plate and cultured in a complete growth medium. A day after seeding, the cells were washed with PBS followed by incubation in serum-starved DMEM containing a range of different recombinant mouse Netrin-1 (R&D system) concentrations (10, 50, 100, 250 and 500 ng/mL) for a further 24 and 48 hours. For the receptor

blocking assays, cells were pre-incubated with 1 µg/mL of anti-UNC5H2 and/or anti-Neogenin antibodies (R&D system) at 37°C, using 5% CO<sub>2</sub> incubator for 30 mins. Thereafter, the cells were treated with either 100 ng/mL or 500 ng/mL of Netrin-1 in the presence of respective antibodies for 24 hours. AlamarBlue reagent (10 µL/well; Thermo Fisher Scientific) was added into each well and the fluorescence intensity of the AlamarBlue was detected at 545 nm/590 nm (excitation/emission) wavelength using a microplate reader (Varioskan Flash, Thermo Fisher Scientific). Eight technical replicates were used per treatment in each experiment, and 5 independent biological assays were conducted for Netrin-1 treatment, and 3 independent biological assays were performed for Netrin-1 receptor blocking assays.

### **3.2.5 Adhesion assay**

The adhesion assay was performed according to the protocols of Terranova *et al.* [330] and Geng *et al.* [331] with minor modifications. Prior to conducting adhesion assay, 48-well plates (Costar) were coated with rat tail collagen type-I (10 µg/cm<sup>2</sup>; Sigma-Aldrich) overnight at 4°C. After coating, wells were blocked with PBS containing 1% BSA solution for 2 hour at RT, followed by 3 times PBS washing. Cells were harvested and resuspended in serum-free DMEM media containing 0.5% BSA for 30 mins in the incubator (37°C, 5% CO<sub>2</sub>) before adding the cells into wells. For receptor blocking assays, cells were incubated with anti-UNC5H2 and/or anti-Neogenin antibodies (2.5 µg/mL; R&D systems) for 30 mins in the incubator (37°C, 5% CO<sub>2</sub>) prior to adding the cells into wells. Anti-IgG antibody (2.5 µg/mL; Thermo Fisher) was used as a non-specific antibody control for the receptor blocking assays. A single cell suspension (40,000 cells/well) was added into collagen-coated wells and incubated with serum-free DMEM containing Netrin-1 (100 ng/mL or 500 ng/mL) or Fibronectin (500 ng/mL; Sigma-Aldrich) for 45 mins in the incubator (37°C, 5% CO<sub>2</sub>). After incubation, cells were gently washed three times with PBS to remove unattached cells and fixed with 2% paraformaldehyde to count adherent cells. Four areas were randomly selected per well for imaging using an Olympus IX-81 inverted microscope (Olympus, Notting Hill, Australia) with CellSense software. Four independent experiments were performed.

### 3.2.6 Wound-healing migration assay

Wound-healing migration assay was conducted according to the protocol of Liang *et al.* [332] with minor modifications. The method for wound-healing migration assay was described in detail in Chapter 3, section 3.5.3. Briefly, the plate was marked with reference points to obtain the same field of image during the image acquisition. CT26 cells were seeded in 24-well plates and cultured in the incubator (37°C, 5% CO<sub>2</sub>) until a confluent monolayer was formed. The gap was created by scratching the plate with a sterile 200 µl pipet tip. The scraped cells were gently removed by washing with PBS. A mouse recombinant Netrin-1 protein (50, 100, 500 ng/mL) in serum-free DMEM was then introduced to CT26 cells. The changes in the gap were monitored by imaging per time-point (4.5 and 9 hour). For the receptor blocking assay, cells were incubated with anti-UNC5H2 and/or anti-Neogenin antibodies (5 µg/mL; R&D systems) for 30 mins in the incubator (37°C, 5% CO<sub>2</sub>) before scratching the plate with a sterile 200 µl pipet tip. After creating a scratch, cells were gently washed with PBS and then cells were incubated in 500 ng/mL of Netrin-1 with respective antibodies. The images were acquired using an Olympus IX-81 inverted microscope (Olympus, Notting Hill, Australia) with CellSense software. A threshold for the gap distance was determined and measured by automated MATLAB software. The gap distance in pixel was converted into µm distance. The formula for percentage wound closure is shown as follow:

$$[1 - (\text{the distance at the indicated time}) \div (\text{the distance at time zero})] \times 100.$$

### 3.2.7 Statistical analysis

The data are presented as mean ± SD, calculated from the specified numbers of biological replicates (n). If 'n' represents technical replicates, it is indicated in appropriate Figure legends. All experiments were performed in minimum of 3 independent experiments, otherwise specified in Methods or Figure legends. The statistical analysis was performed with GraphPad Prism software. Comparison between treatment groups was examined by Two-way ANOVA with Dunnett's or Sidak's multiple comparisons tests for cell viability assays and wound-healing migration assays; One-way ANOVA with Dunnett's multiple comparisons tests for adhesion assays. A *p* value of <0.05 was considered statistically significant. Level of significance is denoted by \**p*<0.05, \*\**p*<0.01 and \*\*\**p*<0.001.

## 3.3 Results

### 3.3.1 CT26 cells express Neogenin and UNC5H2 receptors

To determine whether murine CT26 cells express Netrin-1 receptors, RT-PCR and western blotting were conducted (**Figure 3.1**). For an RT-PCR analysis, mouse brain tissues were used as a positive control for determining the presence of mRNA expression of Netrin-1 and its receptors in CT26 cells. For a western blot analysis, human IMR32 cell lysate was used as a positive control to verify the presence of Neogenin, UNC5B (human)/UNC5H2 (mouse) protein expression in CT26 cells. Both RT-PCR and western blot analyses indicated that CT26 cells express Neogenin (DCC homologue) and UNC5H2 receptors. However, the expression of other Netrin-1 receptors such as DCC, UNC5H1, UNC5H3, UNC5H4, as well as Netrin-1 was negligible or undetectable in this cell line.

**Figure 3.1 CT26 cells express UNC5H2 and Neogenin receptors**

**(A and B)** A relative mRNA expression of UNC5H2 and Neogenin was shown in murine CT26 cells. mRNA expression of Netrin-1 was negligible in CT26 cells. A mouse *l-c-3* gene was used as a reference gene. mRNA expression of Netrin-1 and its receptors in mouse brain tissue was used as a positive control sample. The data reported are the mean  $\pm$  SD (n=3 of technical replicates per experiment) and are representative of 3 independent experiments. **(C)** Expression of UNC5B (human)/UNC5H2 (mouse) and Neogenin in CT26 cell line was detected by western blot. Total proteins collected from human IMR32 cell line was used as a positive control for Netrin-1 receptors.

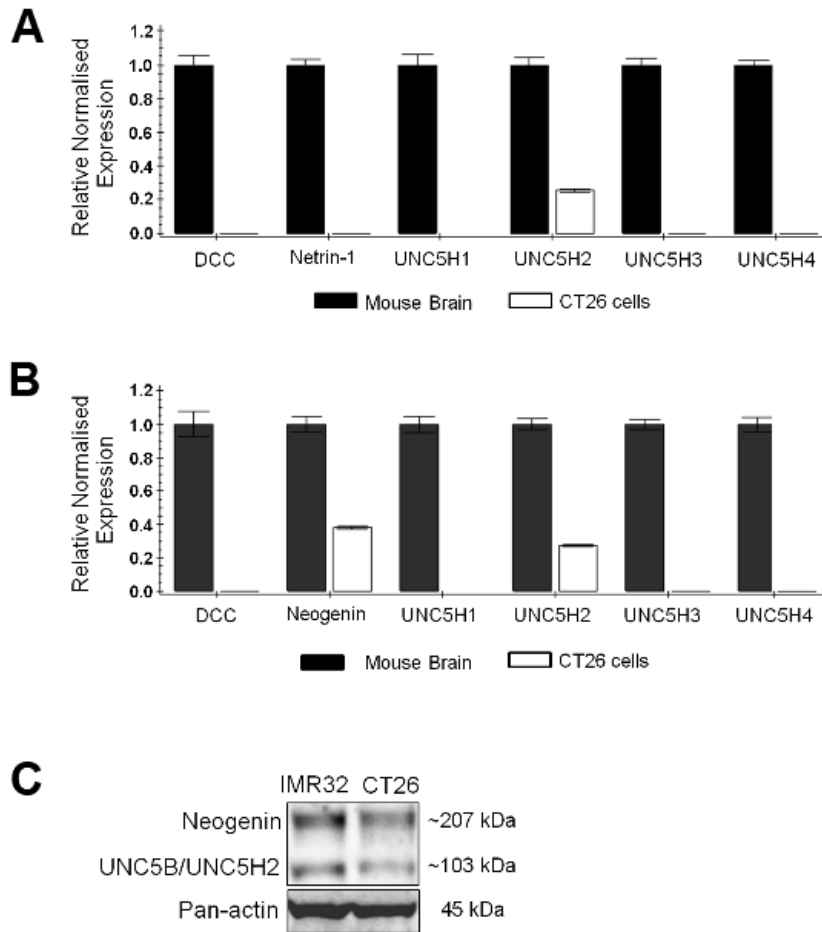


Figure 3.1

### 3.3.2 Netrin-1 increases CT26 cell proliferation

To examine whether or not Netrin-1 functions as a cell survival factor for CT26 cells, the viability of cells was tested subsequent to the treatment of CT26 cells with a range of different concentrations of recombinant Netrin-1 protein (10, 50, 100, 250 and 500 ng/mL) for 24 and 48 hours (**Figure 3.2 A**). The results revealed that a significant increase in the percentage of cell viability was observed in a dose-dependent manner, when CT26 cells were treated with Netrin-1 at the concentrations of 100 ng/mL ( $121.6 \pm 13.5\%$ ,  $p < 0.001$ ), 250 ng/mL ( $145.0 \pm 7.8\%$ ,  $p < 0.001$ ) and 500 ng/mL ( $194.0 \pm 16.4\%$ ,  $p < 0.001$ ) in comparison to cells treated with PBS, vehicle control ( $100.0 \pm 1.0\%$ ), during the 24 hour incubation period. A similar phenomenon was observed when the cells were treated with Netrin-1 for a successive period of 48 hour; a marked increase in the percentage of cell viability was also noted in cells treated with Netrin-1 at the concentrations of 100 ng/mL ( $126.9 \pm 12.5\%$ ,  $p < 0.01$ ), 250 ng/mL ( $153.1 \pm 13.1\%$ ,  $p < 0.001$ ) and 500 ng/mL ( $199.8 \pm 2.8\%$ ,  $p < 0.001$ ) in comparison to control ( $100.0 \pm 1.0\%$ ). Cells treated with 5% of FBS were used as a positive control in this assay (24 hr:  $160.9 \pm 4.4\%$ ,  $p < 0.001$  vs control; 48 hr:  $214.3 \pm 0.6\%$ ,  $p < 0.001$  vs control).

To test whether the viability of CT26 cells in the presence of Netrin-1 is associated with cell proliferation, the expression of cyclin D was examined by immunoblotting (**Figure 3.2 B**). The western blot analysis demonstrated that the expression of cyclin D was increased in accordance with elevating concentrations of Netrin-1. In support of cell viability assay, densitometric analysis revealed an increase in the level of cyclin D protein expression in cells treated with 100 ng/mL (24 hr:  $2.0 \pm 0.7$ ,  $p < 0.05$ ; 48 hr:  $1.7 \pm 0.4$ ,  $p < 0.05$ ), 250 ng/mL (24 hr:  $2.1 \pm 0.7$ ,  $p < 0.05$ ; 48 hr:  $2.0 \pm 0.8$ ,  $p < 0.05$ ) and 500 ng/mL (24 hr:  $2.6 \pm 0.9$ ,  $p < 0.05$ ; 48 hr:  $2.6 \pm 1.1$ ,  $p < 0.05$ ), when compared to control (24 hr:  $1.0 \pm 0$ ; 48 hr:  $1.0 \pm 0$ ).

To investigate whether this observed increase in CT26 cell viability was mediated by UNC5H2 and/or Neogenin receptors in the presence of Netrin-1, these receptors were blocked prior to and during the incubation of cells with two distinct concentrations of Netrin-1 (100 ng/mL or 500 ng/mL) for 24 hours (**Figure 3.2 C**). The antibodies for UNC5H2 and Neogenin were utilised as

blockers, since the epitopes of these antibodies are specific to the Netrin-1 binding sites for UNC5H2 and Neogenin. Hence, incubating the cells with these antibodies prior to and during their treatment with Netrin-1 could interfere with the binding of Netrin-1 to UNC5H2 and Neogenin receptors. Anti-IgG antibody was used as a non-specific antibody control in this assay.

The results indicated that the viability of cells, treated with 100 ng/mL of Netrin-1 subsequent to a blockade of UNC5H2 and/or Neogenin receptors, was significantly reduced (Anti-UNC5H2:  $97.1 \pm 14.6\%$ ,  $p < 0.05$ ; Anti-Neo:  $89.7 \pm 8.9\%$ ,  $p < 0.01$ , Anti-UNC5H2 and Anti-Neo:  $91.4 \pm 6.4\%$ ,  $p < 0.01$ ) when compared to cells treated with 100 ng/mL of Netrin-1 without blocking the receptors ( $118 \pm 12.9\%$ ). However, no significant difference in cell viability was observed when the cells were pre-incubated with IgG blocker ( $106.0 \pm 16.1\%$ ) in comparison to the cells treated with 100 ng/mL of Netrin-1 alone ( $118 \pm 12.9\%$ ).

Similarly, a significant reduction in the viability of cells treated with 500 ng/mL of Netrin-1 was demonstrated in both cases, when the Neogenin alone ( $140.0 \pm 12.5\%$ ,  $p < 0.01$ ) and a combination of Neogenin and UNC5H2 ( $141.0 \pm 17.5\%$ ,  $p < 0.01$ ) were blocked. However, when UNC5H2 alone was blocked, the viability of cells in the presence of 500 ng/mL of Netrin-1 was not significantly reduced ( $147.8 \pm 14.8\%$ ) in comparison to cells treated with 500 ng/mL of Netrin-1 without using blockers ( $168.0 \pm 10.6\%$ ). In addition, no consequential change in cell viability was detected when the cells were pre-incubated with IgG antibody ( $149.2 \pm 19.9\%$ ) in comparison to the cells treated with 500 ng/mL of Netrin-1 alone ( $168.0 \pm 10.6\%$ ).

This observed reduction in cell viability subsequent to receptor blockade was further examined with cyclin D expression in CT26 cells treated with 500 ng/ml of Netrin-1 (**Figure 3.2 D**). Western blot and densitometric analyses demonstrated that expression of cyclin D was significantly reduced when Neogenin ( $0.5 \pm 0.2$ ,  $p < 0.05$ ) but not UNC5B ( $0.7 \pm 0.3$ ) was blocked in comparison to cells treated with 500 ng/mL of Netrin-1 without blockers ( $1.0 \pm 0.0$ ). Also, a significant decrease in cyclin D expression was detected when both UNC5H2 and Neogenin receptors ( $0.5 \pm 0.3$ ,  $p < 0.05$ ) were blocked

simultaneously compared to cells treated with 500 ng/mL of Netrin-1 alone ( $1.0 \pm 0.0$ ).

Previous studies have demonstrated that Netrin-1 inhibits apoptosis of tumour cells by blocking caspase-3 activity [333]. To investigate whether Netrin-1 could inhibit caspase-3 apoptosis of CT26 cell line, the expression of cleaved caspase-3 was examined in the cells treated with Netrin-1 at 100 ng/mL or 500 ng/mL concentrations at 24 and 48 hours (**Figure 3.2 E**). Along with the Netrin-1 treatment, the cells were treated with a pan-caspase inhibitor (z-VAD-fmk) or a caspase-3 inhibitor (z-DEVD-fmk).

Western blot and densitometric analyses indicated a lower level of cleaved caspase-3 expression was detected in the cells treated with Netrin-1 at 100 ng/mL (24 hr:  $0.56 \pm 0.26$ ; 48 hr:  $0.80 \pm 0.17$ ) or 500 ng/mL (24 hr:  $0.19 \pm 0.01$ ,  $p < 0.05$ ; 48 hr:  $0.61 \pm 0.02$ ) when compared to cells treated with PBS, vehicle control (24 hr:  $1.0 \pm 0$ ; 48 hr:  $1.0 \pm 0$ ), especially a significantly low level of cleaved caspase-3 expression was noted in cells treated with 500 ng/mL of Netrin-1 (24 hr:  $0.19 \pm 0.01$ ,  $p < 0.05$ ) at 24 hours compared to control (PBS).

Moreover, as expected, cells treated with the pan-caspase inhibitor (24 hr:  $0.45 \pm 0.4$ ; 48 hr:  $0.59 \pm 0.14$ ) or caspase-3 inhibitors (24 hr:  $0.32 \pm 0.3$ ; 48 hr:  $0.55 \pm 0.27$ ) showed a lower level of cleaved caspase-3 expression at 24 hours and 48 hours when compared to their vehicle control, DMSO (24 hr:  $1.0 \pm 0$ ; 48 hr:  $1.0 \pm 0$ ).

Collectively, these data suggest that Netrin-1 appeared to inhibit caspase-3 apoptosis of CT26 cells, and this may consequently enhance CT26 cell proliferation that is mediated via UNC5H2 and Neogenin activation.

### Figure 3.2 The effect of Netrin-1 on CT26 cell proliferation

**(A)** The viability of CT26 cells was elevated with increasing concentration of Netrin-1. The data are expressed as mean  $\pm$  SD (n=8 of technical replicates per experiment) and are representative of 5 independent experiments. Two-way ANOVA; Dunnett's multiple comparisons test; \*\* $p$ <0.01, \*\*\* $p$ <0.001 vs vehicle control (PBS). FBS (5%) was used as a positive control. **(B)** Western blot and densitometric analyses of cyclin D expression in CT26 cells treated with Netrin-1 for 24 and 48 hours. Densitometry data represent an average fold change normalised to the control sample with  $\pm$  SD (n=3). Two-way ANOVA; Dunnett's multiple comparisons test; \* $p$ <0.05 vs vehicle control. The replicate images used for densitometry analysis are shown in **Appendix A**. **(C)** The viability of CT26 cells in the presence of Netrin-1 (100 ng/mL or 500 ng/mL) was reduced when UNC5H2 (Anti-UNC5H2) and/or Neogenin (Anti-Neo) were blocked. Anti-IgG is used as a negative control as it is a non-specific to Netrin-1 receptors. The data are expressed as mean  $\pm$  SD (n=8 of technical replicates per experiment) and are representative of 3 independent experiments. Two-way ANOVA; Sidak's multiple comparisons test; \* $p$ <0.05; \*\* $p$ <0.01 vs respective Netrin-1 treatment alone. **(D)** Western blot and densitometric analyses show a decrease in expression of cyclin D when UNC5H2 and/or Neogenin were blocked. Lamin B1 was used as a loading control. Densitometry data represent an average fold change normalised to the control sample with  $\pm$  SD (n=3). One-way ANOVA; Dunnett's multiple comparisons test; \* $p$ <0.05 vs N500 treatment alone. The replicate images used for densitometry analysis are shown in **Appendix A**. **(E)** Western blot analysis exhibited difference in expression of cleaved caspase-3 in CT26 cells treated with serum-free media containing Netrin-1 at 100 ng/mL or 500 ng/mL or pan-caspase inhibitor (z-VAD-fmk, 20  $\mu$ M) or caspase-3 inhibitor (z-DEVD-fmk, 20  $\mu$ M) for 24 and 48 hours. PBS is a vehicle control for Netrin-1. DMSO is a vehicle control for inhibitors. Relative expression of cleaved caspase-3/caspase-3 was shown as an average fold change normalised by respective vehicle control sample with  $\pm$  SD (n=2). Two-way ANOVA; Tukey's multiple comparisons test; \* $p$ <0.05 vs vehicle control (PBS). The replicate images used for densitometry analysis are shown in **Appendix A**.

**Abbreviations:** N10: Netrin-1 10 ng/mL; N50: Netrin-1 50 ng/mL; N100, Netrin-1 100 ng/mL; N500, Netrin-1 500 ng/mL; DMSO, dimethyl sulfoxide; a.u, arbitrary unit.

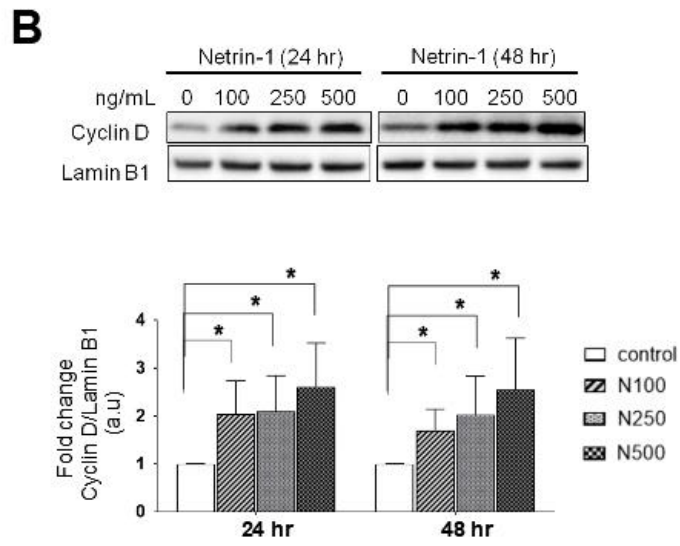
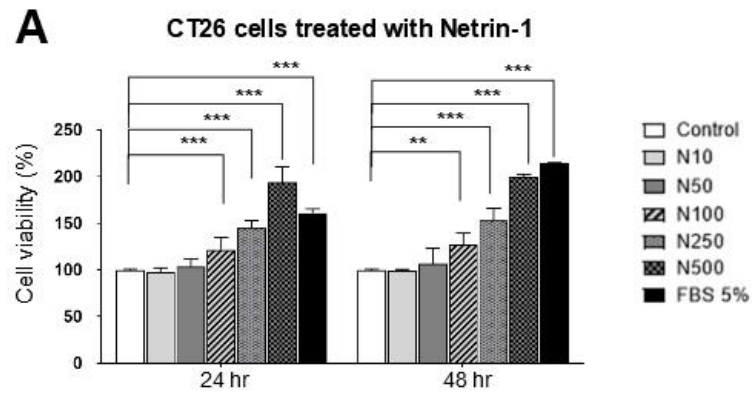


Figure 3.2 A and B

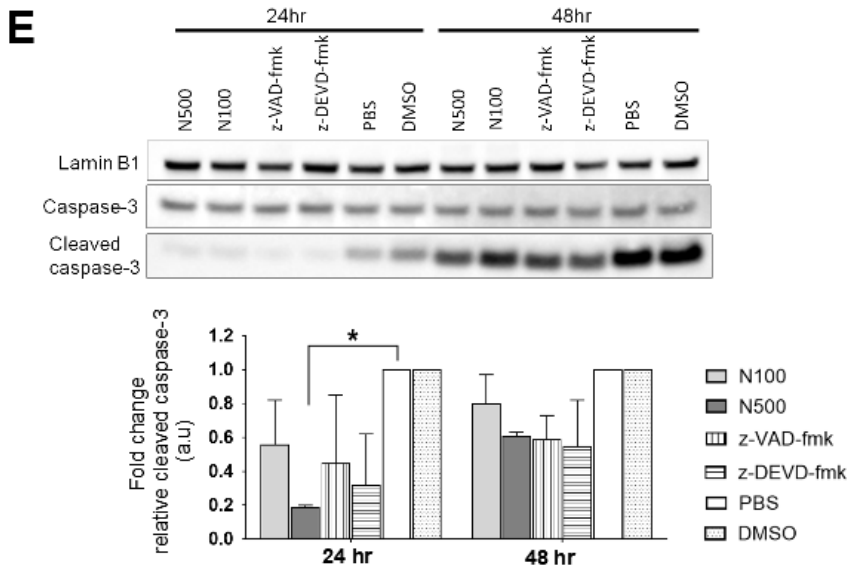
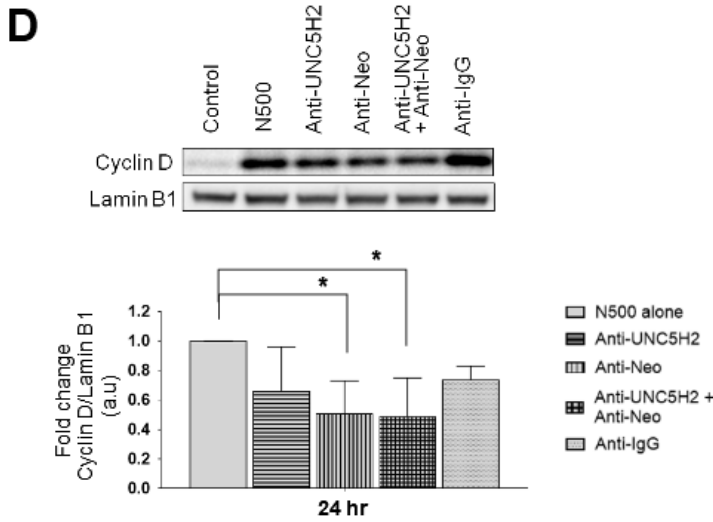
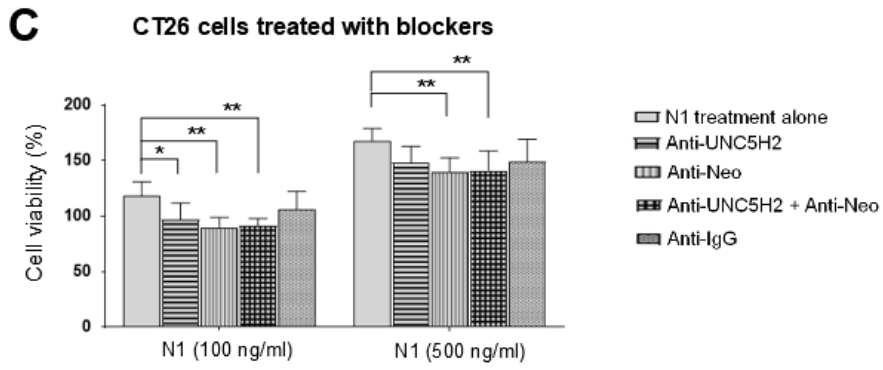


Figure 3.2 C, D and E

### 3.3.3 Netrin-1 contributes to CT26 cell adhesiveness

It has been indicated that Netrin-1 interacts with extracellular matrix elements and it can serve as an adhesion molecule for endothelial cells and pancreatic ductal adenocarcinoma [228]. To examine whether Netrin-1 can function as an adhesion molecule for CT26 cells, an attachment assay was performed. The number of CT26 cells attached to type-I collagen-coated surface in the presence of Netrin-1 at 100 ng/mL ( $1097.2 \pm 111.0$ ,  $p < 0.05$ ) or 500 ng/mL ( $1202.0 \pm 88.0$ ,  $p < 0.001$ ) was significantly increased when compared to control; cells attached to collagen-coated surface in the presence of PBS ( $931.0 \pm 12.8$ ). Cells attached to collagen-coated surface in the presence of fibronectin ( $1284.2 \pm 31.0$ ,  $p < 0.001$  vs control) were used as a positive control in this assay (**Figure 3.3 A-B**).

Furthermore, to examine the involvement of Netrin-1 receptors in CT26 cell adhesion process, the ability of CT26 cells attachment to type-I collagen-coated surface in the presence of Netrin-1 (500 ng/mL) was tested after UNC5H2 and/or Neogenin receptors were blocked with antibodies (**Figure 3.3 C-D**). The result showed that a significant increase in cells attached to collagen-coated surface in the presence of Netrin-1 at 500 ng/mL ( $1171.9 \pm 64.3$ ,  $p < 0.001$ ) when compared to control ( $943.3 \pm 55.4$ ). However, less number of cells were adherent to the collagen-coated surface in the presence of 500 ng/mL of Netrin-1 after blocking of either UNC5H2 or Neogenin receptors individually (Anti-UNC5H2:  $961.2 \pm 65.2$ ,  $p < 0.01$ ; Anti-Neo:  $988.9 \pm 39.5$ ,  $p < 0.01$ ) or simultaneously (Anti-UNC5H2 and Anti-Neo:  $987.1 \pm 64.3$ ,  $p < 0.01$ ) when compared to unblocked cells attached to the collagen-coated surface in the presence of 500 ng/mL of Netrin-1 ( $1171.9 \pm 64.3$ ). Conversely, cells pre-treated with anti-IgG antibodies displayed no differences in cell attachment in the presence of 500 ng/mL of Netrin-1 ( $1054.3 \pm 81.6$ ) when compared to the case of unblocked cells treated with 500 ng/mL of Netrin-1 ( $1171.9 \pm 64.3$ ).

Collectively, these results suggest that Netrin-1 increases CT26 cell adhesiveness, and this process appears to be mediated by UNC5H2 and Neogenin receptors.

### Figure 3.3 The effect of Netrin-1 on CT26 cell adhesion

**(A)** The wells of a tissue culture plate were coated with a matrix element, collagen type-I. CT26 cells were added into the wells and incubated with serum-free media containing PBS (vehicle control) or Netrin-1 (N100 or N500) or Fibronectin for 45 mins in the tissue culture incubator. An increase in a number of adherent cells was shown when they were incubated with Netrin-1 in comparison to cells incubated with PBS. The results are expressed as mean  $\pm$  SD (n=4). One-way ANOVA; Dunnett's multiple comparisons test; \* $p$ <0.05, \*\*\* $p$ <0.001 vs vehicle control (PBS). Fibronectin was used as a positive control (\*\*\* $p$ <0.001 vs vehicle control). **(B)** The images represent the adherent cells in the absence or presence of Netrin-1. Fibronectin was incubated with CT26 cells as a positive control. Scale bar: 200  $\mu$ m. **(C)** CT26 cells were incubated with anti-UNC5H2 and/or anti-Neogenin (2.5  $\mu$ g/mL) for 30 mins prior to culturing in the collagen type-I coated wells. Subsequently, cells were incubated in the presence of Netrin-1 (500 ng/mL) for 45 mins. The number of attached cells was reduced to control level when Netrin-1 receptors were blocked. The data are expressed as mean  $\pm$  SD (n=4). One-way ANOVA; Tukey's multiple comparisons test; ### $p$ <0.001 vs vehicle control (PBS); \*\* $p$ <0.01 vs N500 treatment alone. **(D)** The images represent the adherent cells attached to the collagen-coated surface in the presence of Netrin-1 (500 ng/mL) with or without antibodies pre-incubation. Scale bar: 200  $\mu$ m.

**Abbreviations:** N100, Netrin-1 100 ng/mL; N500, Netrin-1 500 ng/mL; Neo, Neogenin.

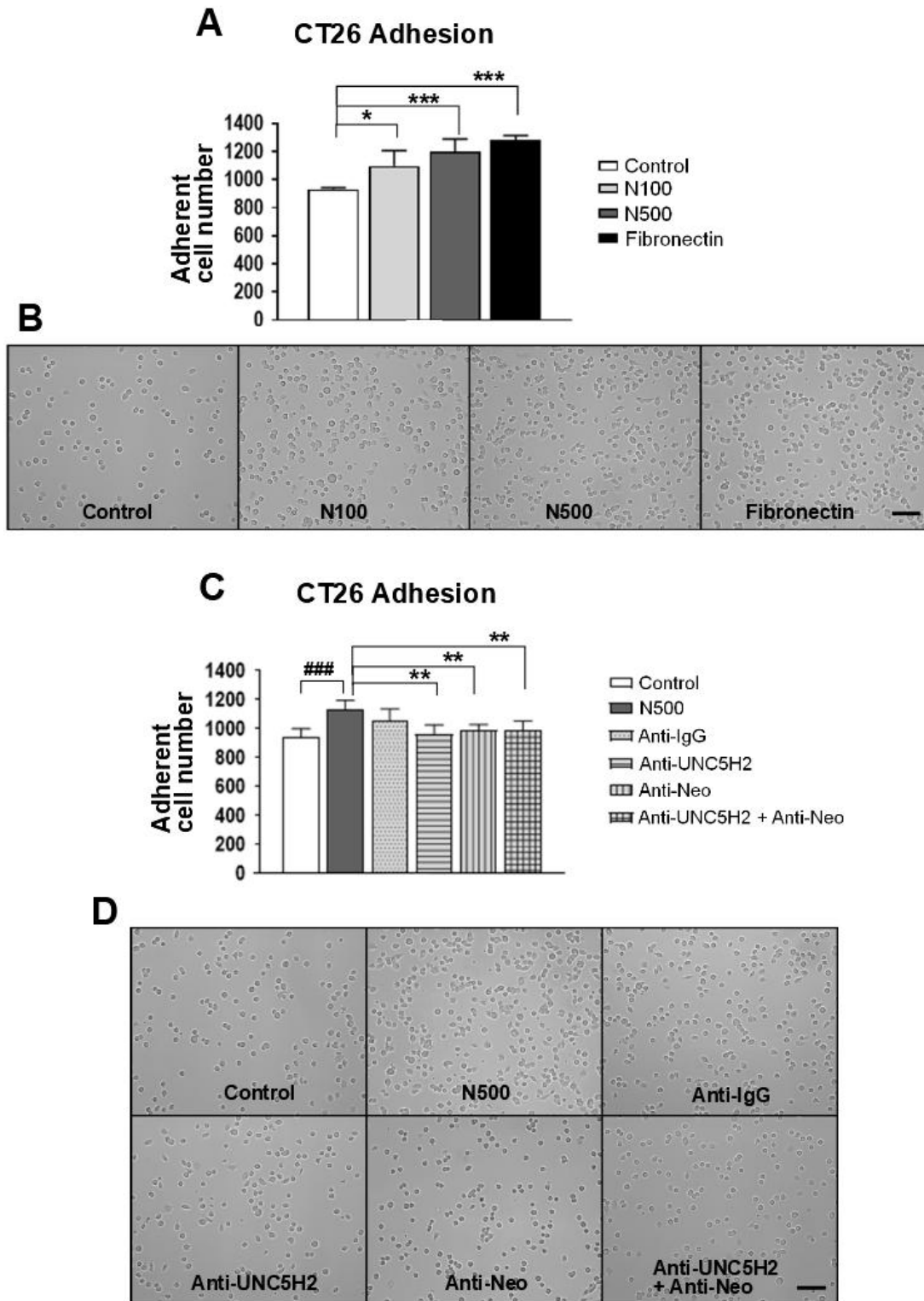


Figure 3.3

### 3.3.4 High concentration of Netrin-1 promotes CT26 cell migration

To investigate whether Netrin-1 promotes CT26 cell migration, a wound-healing migration assay was performed. Subsequent to the creation of a single gap in a confluent monolayer of cells, the cells were incubated with Netrin-1 at varying concentrations of 50, 100 and 500 ng/mL for 4.5 and 9 hours (**Figure 3.4 A1-A3**). The results indicated no significant alteration in the migration of cells in the absence or presence of Netrin-1 at 4.5-hour (N50:  $13.5 \pm 2.4\%$ ; N100:  $15.4 \pm 6.9\%$ ; N500:  $14.1 \pm 10.8\%$ ) when compared to cells incubated with PBS, vehicle control ( $15.7 \pm 1.0\%$ ) (**Figure 3.4 B**). However, cells incubated with 500 ng/mL of Netrin-1 (N500:  $57.3 \pm 4.8\%$ ,  $p < 0.05$ ) exhibited a significant increase in migration when compared to vehicle control ( $36.2 \pm 1.0\%$ ) by 9 hours. No major migratory changes were observed in CT26 cells treated with 50 ng/mL or 100 ng/mL of Netrin-1 compared to vehicle control (N50:  $34.5 \pm 12.9\%$ ; N100:  $30.9 \pm 14.7\%$  vs. control:  $36.2 \pm 1.0\%$ ). Cells treated with FBS were used as a positive control in this assay. As expected, a significant increase in migratory of cells in the presence of FBS was noted compared to vehicle control by 9 hours (4 hr:  $16.8 \pm 5.1\%$ ; 9 hr:  $64.1 \pm 6.1\%$ ,  $p < 0.01$  vs vehicle control).

To examine whether the increased CT26 cell migration in the presence of Netrin-1 (500 ng/mL) was mediated by Netrin-1 receptors, wound-healing migration assays were conducted after blocking UNC5H2 and/or Neogenin receptors with specific antibodies (**Figure 3.5 A**).

Firstly, a number of control groups were used in this assay: (1) cells treated with PBS was a vehicle control group for Netrin-1 (500 ng/ml) treatment; (2) cells treated with 500 ng/mL of Netrin-1 after the application of IgG antibody were used as a negative antibody control group, as Anti-IgG antibody is a non-specific to receptors of interest; (3) cells treated with FBS (10%) was used as a positive control group.

Quantitative analysis indicated that there were no substantial differences in migration of CT26 cells across all treatments at 4.5 hours (control:  $10.2 \pm 1.0\%$ ; N500:  $9.3 \pm 4.1\%$ ; Anti-UNC5H2:  $12.6 \pm 7.1\%$ ; Anti-Neo:  $8.9 \pm 4.3\%$ ; Anti-UNC5H2 and Anti-Neo:  $12.2 \pm 6.3\%$ ; Anti-IgG:  $9.7 \pm 5.5\%$ ; FBS:  $13.4 \pm 5.2\%$ ) (**Figure 3.5 B**).

At 9 hours, cells treated with 500 ng/mL of Netrin-1 alone ( $42.0 \pm 9.8\%$ ,  $p < 0.05$ ) showed a significant increase in cell migration when compared to vehicle control ( $19.7 \pm 1.0\%$ ). However, cells treated with 500 ng/mL of Netrin-1 subsequent to receptor blocking were not significantly altered in cell migration (Anti-UNC5H2:  $36.2 \pm 14.7\%$ ; Anti-Neo:  $34.8 \pm 7.8\%$ ; Anti-UNC5H2 and Anti-Neo:  $33.6 \pm 6.8\%$ ) when compared to cells treated with 500 ng/mL of Netrin-1 without blockers ( $42.0 \pm 9.8\%$ ) (**Figure 3.5 B**).

In addition, cells treated with 500 ng/mL of Netrin-1 subsequent to IgG blocking ( $39.1 \pm 11.9\%$ ) showed no difference in cell migration when compared to cells treated with 500 ng/mL of Netrin-1 alone ( $42.0 \pm 9.8\%$ ) at 9 hours. However, a significant increase in cell migration of cells treated with 500 ng/mL of Netrin-1 subsequent to IgG blocking ( $39.1 \pm 11.9\%$ ,  $p < 0.05$ ) was seen when compared to vehicle control ( $19.7 \pm 1.0\%$ ). Also, a markedly increase in migration of cells treated with FBS ( $46.3 \pm 13.2\%$ ,  $p < 0.01$ ) was noted when compared to vehicle control ( $19.7 \pm 1.0\%$ ).

Based on this observation, UNC5H2 and Neogenin may not be directly involved in Netrin-1 mediated cell migration of CT26 cells. Additional assays will be necessary to clarify the involvement of UNC5H2 and Neogenin receptors in this cancer migration.

### **Figure 3.4 The effect of Netrin-1 on CT26 cell migration**

**(A1-A2)** Wound-healing migration of CT26 cells was performed in the absence or presence of Netrin-1. The control indicates cells treated with PBS (vehicle control). **(A3)** Cells treated with FBS (10%) were used as a positive control in this assay. The representative field of scratched images were shown at 4.5 hour and 9 hour time-points. The images were processed by MatLab; each well was marked with a reference line to determine the position of each well. The scratched images were taken by using a phase contrast microscope at intervals of 4.5 and 9 hours. The threshold of the gap analysis was determined and processed automatically using MatLab. **(B)** Quantitative analysis of the wound closure (%) data are expressed as mean  $\pm$  SD (n=3). Two-way ANOVA; Dunnett's multiple comparisons test; \* $p < 0.05$  vs vehicle control. FBS (10%) was used as a positive control (\*\* $p < 0.01$  vs vehicle control).

**Abbreviations:** N50: Netrin-1 50 ng/mL; N100, Netrin-1 100 ng/mL; N500, Netrin-1 500 ng/mL.

# A1

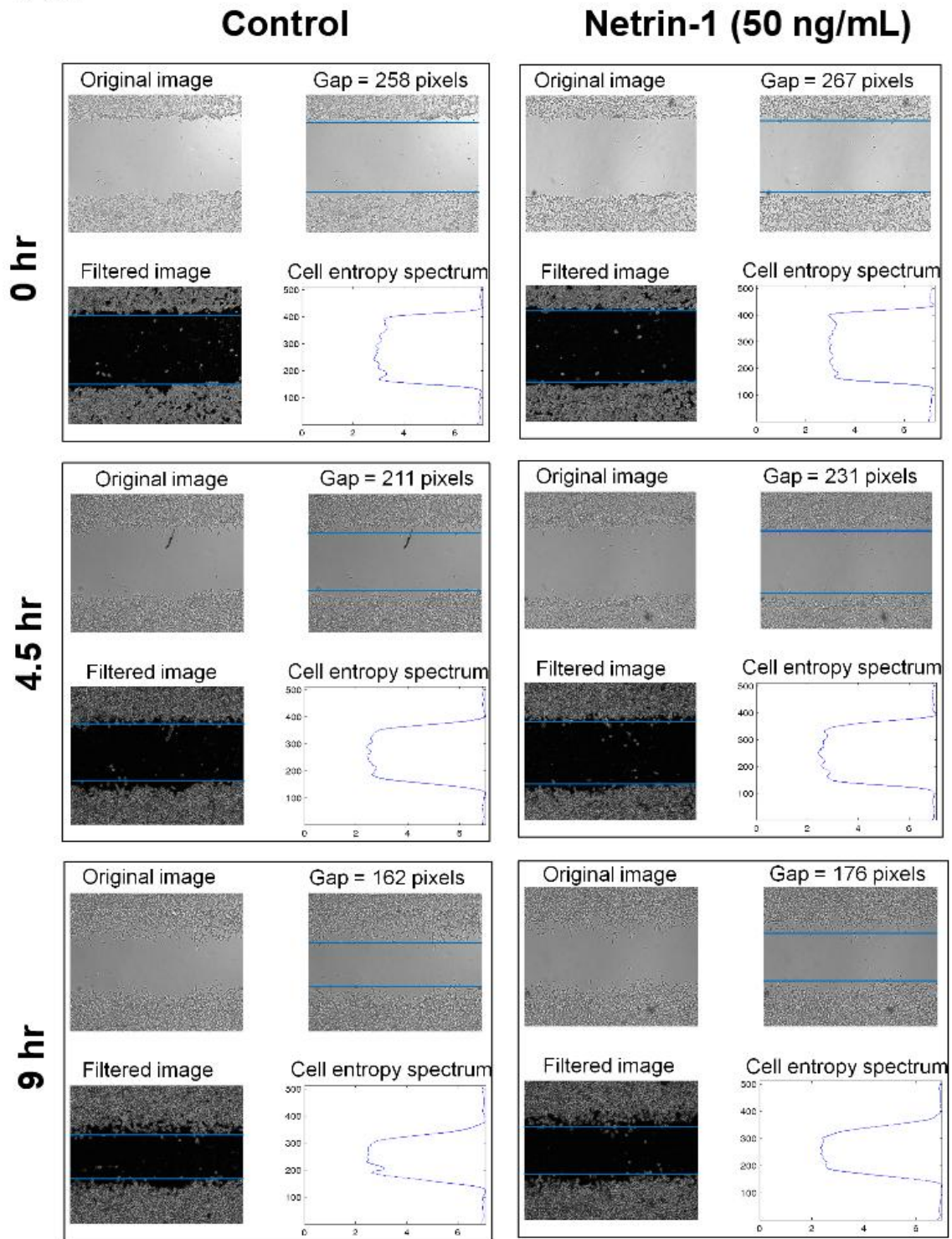


Figure 3.4 A1

# A2

## Netrin-1 (100 ng/mL)

## Netrin-1 (500 ng/mL)

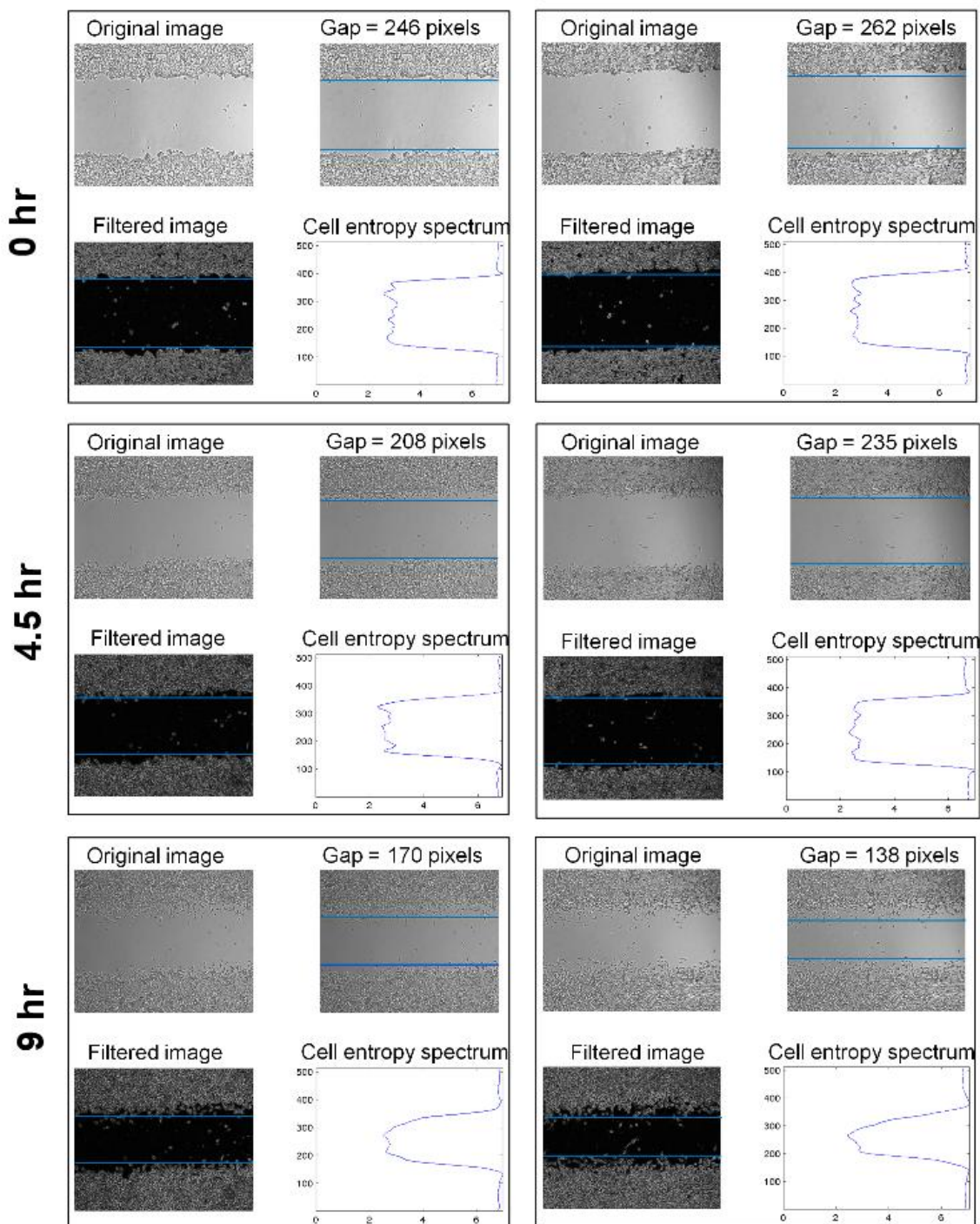


Figure 3.4 A2

**A3**

**FBS**

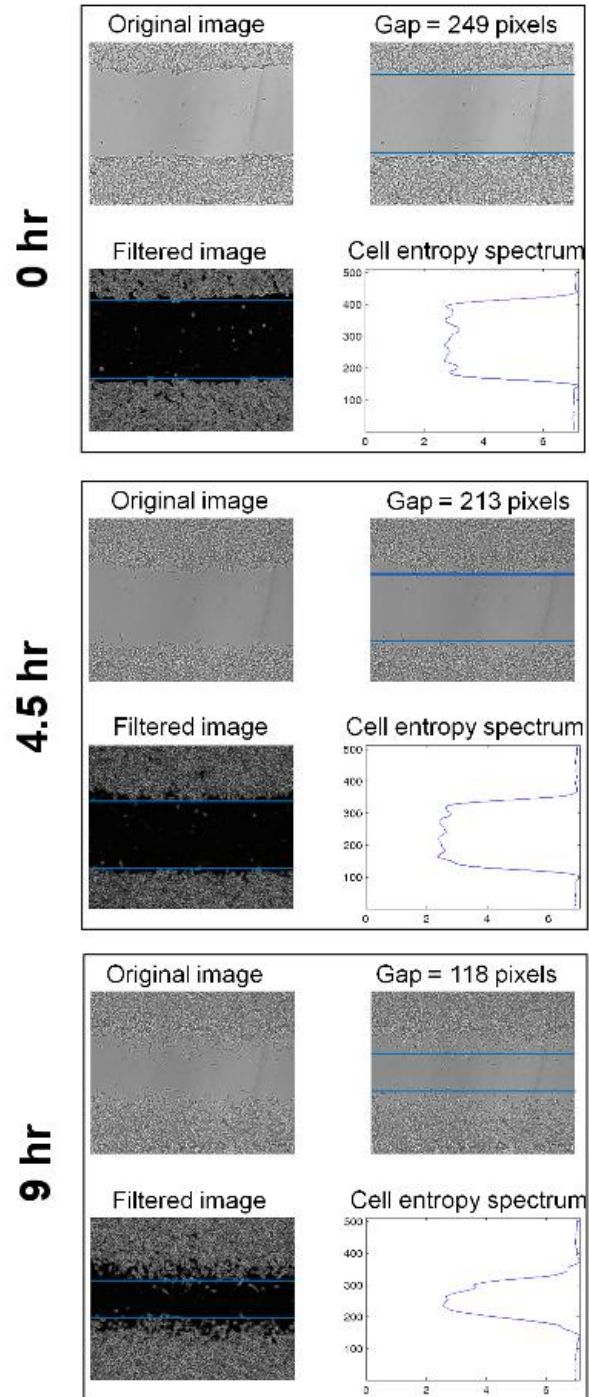


Figure 3.4 A3

**B** CT26 migration  
in the presence of Netrin-1

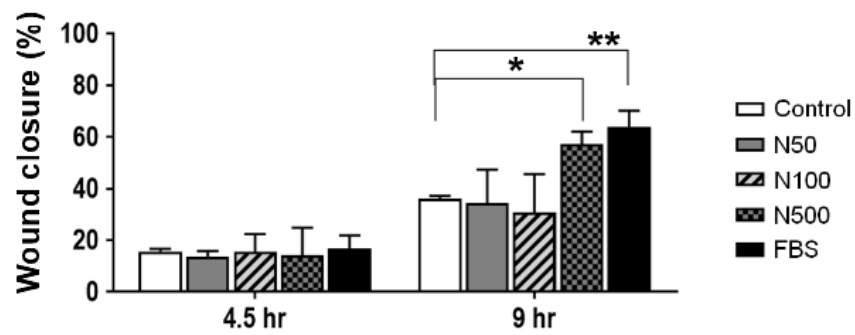


Figure 3.4 B

**Figure 3.5 The effect of CT26 cell migration in the presence of Netrin-1 after blocking Netrin-1 receptors**

**(A1-A3)** Wound-healing migration of CT26 cells was performed in the presence of Netrin-1 (500 ng/mL) subsequent to receptor blockers. UNC5H2 and/or Neogenin receptors were blocked in CT26 cells using specific antibodies (5 µg/mL). Anti-IgG antibody is non-specific to Netrin-1 receptors. A scratch was created and CT26 cells were incubated in 500 ng/mL of Netrin-1 (N500) with respective antibodies, and the ability of CT26 migration was monitored at 4.5 hour and 9 hour time-points. The control indicates cells treated with PBS (vehicle control) without blockers. **(A4)** Cells treated with FBS (10%) without blockers were used as a positive control in this assay. The representative field of scratched images were shown at 4.5 hour and 9 hour time-points. The acquired images were processed by MatLab. The best angle and threshold of the gap analysis was determined and processed automatically using MatLab. **(B)** Quantitative analysis of the wound closure (%); results are expressed as mean ± SD (n=3). Two-way ANOVA; Dunnett's and Tukey's multiple comparisons tests; \* $p < 0.05$ , \*\* $p < 0.01$  vs vehicle control (PBS); n.s groups vs N500 alone. FBS (10%) was used as a positive control.

**Abbreviation:** PBS, phosphate-buffered saline; N500, Netrin-1 500 ng/mL, Anti-UNC5H2, UNC5H2 antibody; Anti-Neo, Neogenin antibody; Anti-UNC5H2 + Anti-Neo, UNC5H2 and Neogenin antibodies; FBS, fetal bovine serum; n.s, not significant.

# A1

## Control

## N500

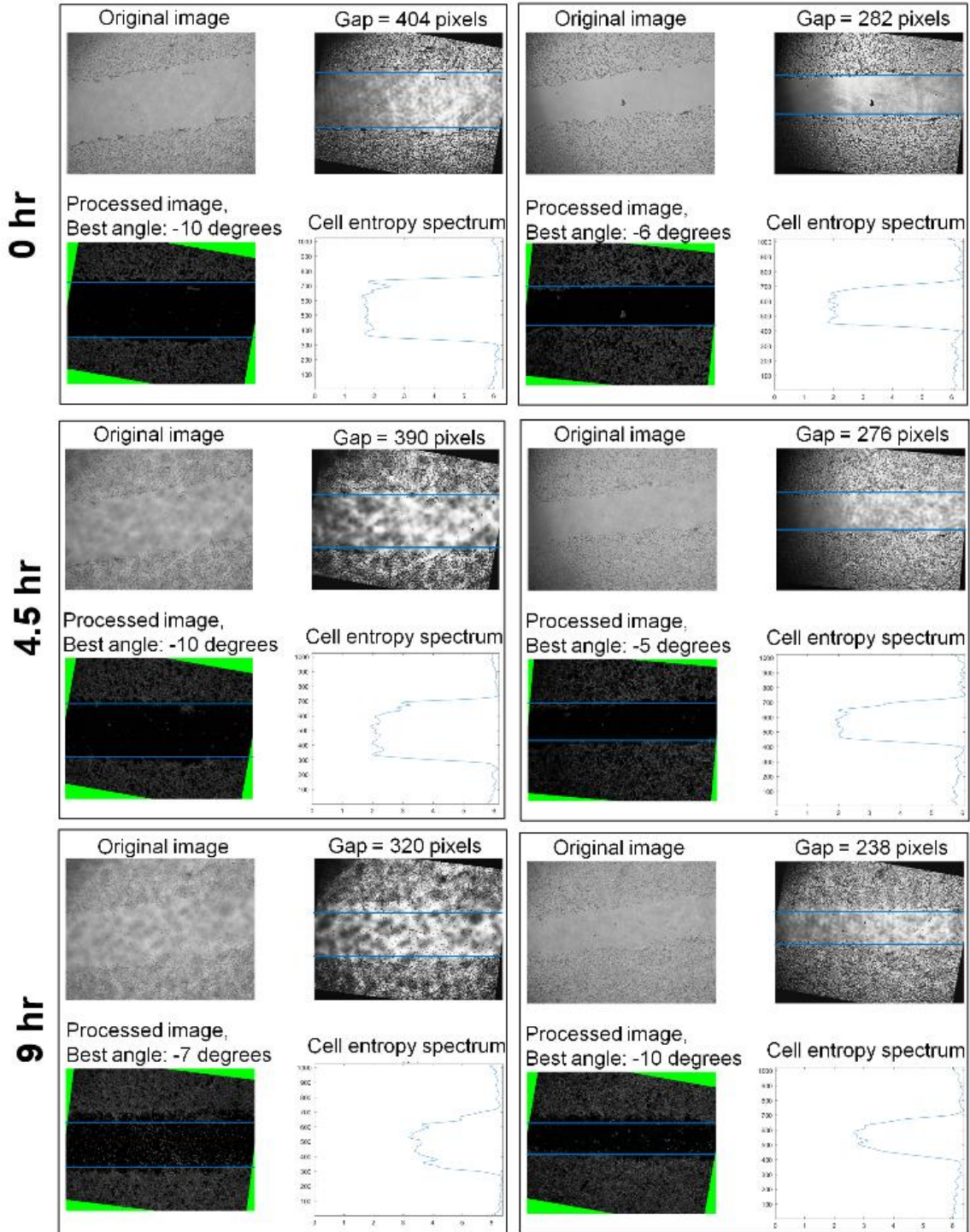


Figure 3.5 A

**A2**

**Anti-UNC5H2  
+ N500**

**Anti-Neo  
+ N500**

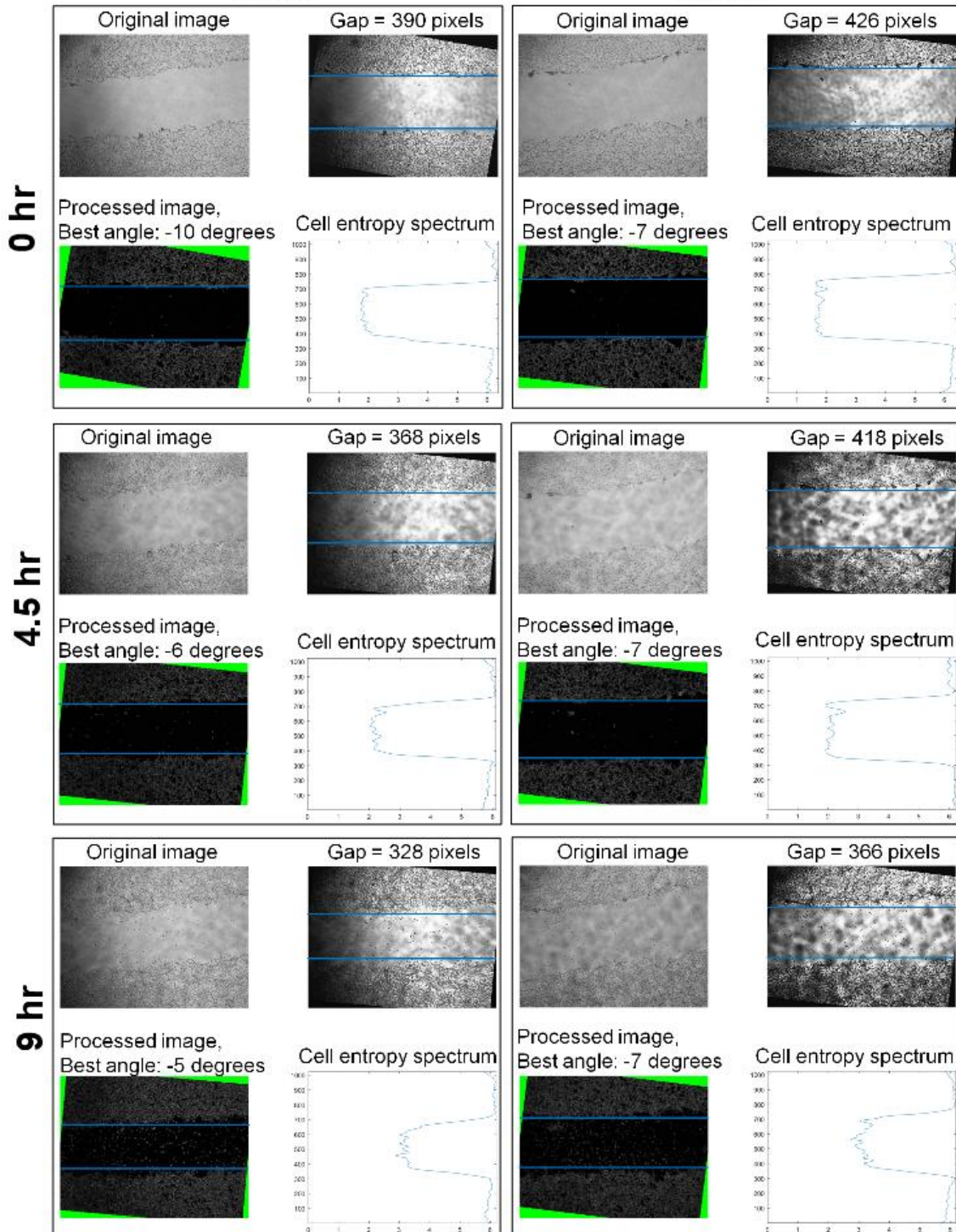


Figure 3.5 A2

**A3**

**Anti-UNC5H2 +  
Anti-Neo + N500**

**Anti-IgG  
+ N500**

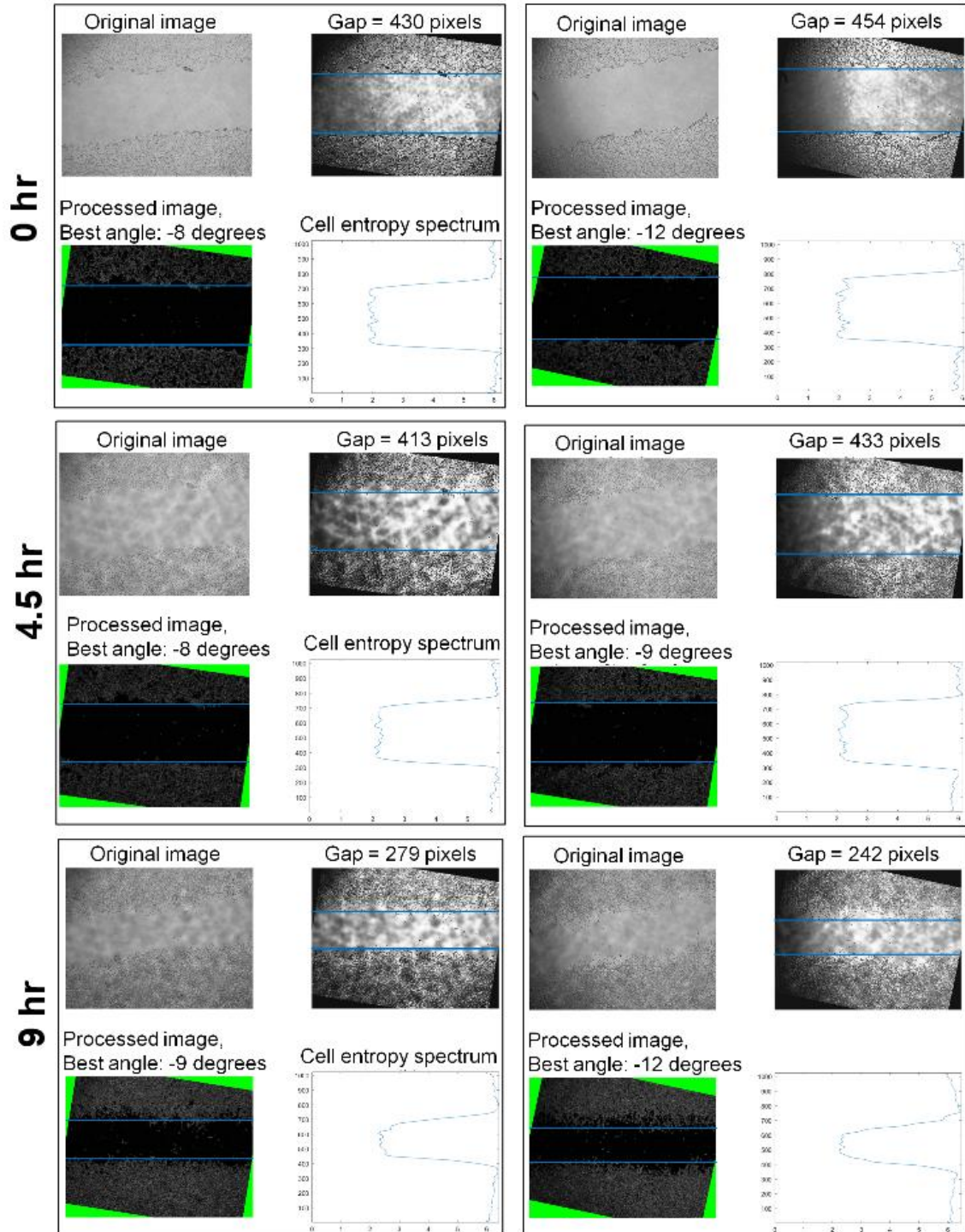


Figure 3.5 A3

# A4

## FBS

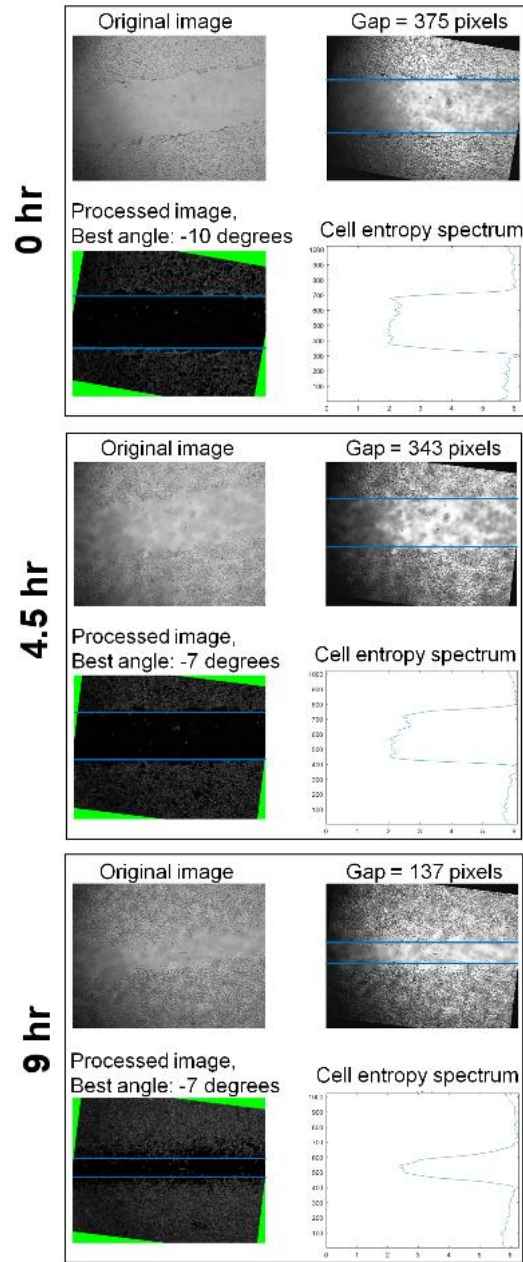


Figure 3.5 A4

**B** CT26 migration in the presence of Netrin-1 (500 ng/mL) subsequent to receptor blocking

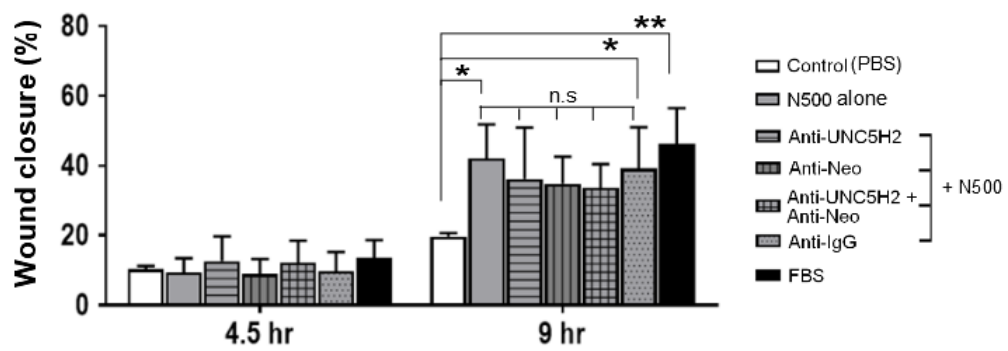


Figure 3.5 B

### 3.3.5 Netrin-1 treatment activates pFAK/pMEK/pERK signalling pathway in CT26 cells

To determine the molecular mechanism for Netrin-1-induced proliferation, adhesion and migration of CT26 cells, a possible signalling pathway that may have been affected by Netrin-1 treatment was examined. Since focal adhesion kinase (FAK) is known to be an early activated molecule in Netrin-1 signalling pathway, changes in phosphorylated FAK expression were examined in CT26 cells treated with 100 ng/mL or 500 ng/mL of Netrin-1 at different time points (0, 5, 15, 30 and 60 mins). Western blot analysis showed a peak expression of phosphorylated FAK at 30 mins, while no changes in total FAK expression were observed in cells treated with Netrin-1 at both concentrations (**Figure 3.6 A**).

One of down-stream of FAK activation pathways is known to be the phosphorylated MEK/ERK pathway [326]. The expression levels of the pFAK/MEK/ERK signalling pathway was examined in cells treated with 100 or 500 ng/mL. In addition, this pathway was examined in cells treated with 500 ng/mL of Netrin-1 after blocking receptors, UNC5H2 and/or Neogenin. Western blot (**Figure 3.6 B**) and densitometric (**Figure 3.6 B'**) analyses revealed a significant increase in the level of phosphorylated FAK in cells treated with 500 ng/mL of Netrin-1 ( $1.32 \pm 0.45$ ,  $p < 0.05$ ) when compared to cells treated with PBS, vehicle control ( $0.45 \pm 0.18$ ). On the other hand, a significant reduction in the level of phosphorylated FAK was noted in cells treated with 500 ng/mL of Netrin-1 after blocking UNC5H2 ( $0.20 \pm 0.01$ ,  $p < 0.01$ ) or Neogenin ( $0.13 \pm 0.10$ ,  $p < 0.01$ ) individually or UNC5H2 and Neogenin ( $0.24 \pm 0.20$ ,  $p < 0.01$ ) simultaneously when compared to cells treated with 500 ng/mL of Netrin-1 without blockers ( $1.32 \pm 0.45$ ). However, the level of phosphorylated FAK was not significantly decreased in cells treated with anti-IgG antibody ( $0.64 \pm 0.45$ ) when compared to cells treated with 500 ng/mL of Netrin-1 ( $1.32 \pm 0.45$ ).

Cells treated with 500 ng/mL of Netrin-1 ( $1.78 \pm 0.29$ ,  $p < 0.05$ ), but not the cells treated with 100 ng/mL of Netrin-1 ( $1.40 \pm 0.8$ ), showed a significant increase in the level of phosphorylated MEK compared to cells treated with vehicle control ( $0.05 \pm 0.03$ ). In the case of blocking receptors (Anti-UNC5H2:  $0.80 \pm 0.50$ ; Anti-Neo:  $0.85 \pm 0.50$ ; Anti-UNC5H2 and Anti-Neo:  $0.9 \pm 0.7$ ), no significant changes were noted when compared to cells treated with 500 ng/mL of Netrin-1

alone ( $1.78 \pm 0.29$ ) or cells treated with vehicle control ( $0.05 \pm 0.03$ ). Similarly, no differences were observed in the case of anti-IgG application ( $1.38 \pm 0.98$ ) when compared to treated with 500 ng/mL of Netrin-1 alone ( $1.78 \pm 0.29$ ) or cells treated with vehicle control ( $0.05 \pm 0.03$ ).

In the case of phosphorylated ERK, a significant increase in the phosphorylation of threonine residue (p44) was noted in cells treated with 500 ng/mL of Netrin-1 ( $2.50 \pm 0.46$ ,  $p < 0.05$ ), but not 100 ng/mL of Netrin-1 ( $1.78 \pm 0.56$ ), when compared to cells treated with vehicle control ( $0.42 \pm 0.39$ ).

However, a significant reduction in the level of threonine residue phosphorylation (p44) was noted in cells treated with 500 ng/mL of Netrin-1 after blocking Neogenin ( $0.60 \pm 0.55$ ,  $p < 0.05$ ) or UNC5H2 and Neogenin ( $0.58 \pm 0.45$ ,  $p < 0.05$ ) simultaneously when compared to cells treated with 500 ng/mL of Netrin-1 without blockers ( $2.5 \pm 0.46$ ). Also, a decreased level of p44 phosphorylation was apparent in cells with UNC5H2 receptor blocking ( $0.88 \pm 1.03$ ), however it was not significantly reduced when compared to cells treated with 500 ng/mL of Netrin-1 alone ( $2.5 \pm 0.45$ ). An application of anti-IgG did not also show a significant reduction in p44 phosphorylation compared to cells treated with 500 ng/mL of Netrin-1 alone ( $1.04 \pm 0.8$  vs  $2.5 \pm 0.46$ ).

Similarly, tyrosine residue (p42) of ERK phosphorylation was significantly elevated in cells treated with 500 ng/mL of Netrin-1 ( $4.90 \pm 1.10$ ,  $p < 0.05$ ), but not the cells with 100 ng/mL of Netrin-1 ( $3.80 \pm 1.30$ ), when compared to vehicle control ( $1.29 \pm 1.18$ ).

The level of phosphorylation of tyrosine residue (p42) was notably reduced in cells treated with 500 ng/mL of Netrin-1 after blocking UNC5H2 ( $1.40 \pm 1.10$ ,  $p < 0.05$ ) or Neogenin ( $1.50 \pm 1.20$ ,  $p < 0.05$ ) individually or UNC5H2 and Neogenin ( $1.36 \pm 1.00$ ,  $p < 0.05$ ) simultaneously when compared to cells treated with 500 ng/mL of Netrin-1 without blockers ( $4.90 \pm 1.10$ ). However, no significant reduction in the level of p44 was noted in cells with anti-IgG antibody ( $1.99 \pm 1.38$ ).

Collectively, the data suggest that pFAK/pMEK/pERK signalling pathway was activated in CT26 cells treated with Netrin-1 at 500 ng/mL, and that this activation was mediated by UNC5H2 and Neogenin receptors.

### **Figure 3.6 Netrin-1 induces the activation of pFAK/pMEK/pERK signalling pathway in CT26 cells**

**(A)** The western blot analysis shows the peak level of phosphorylated FAK expression in CT26 cells at 30 mins following Netrin-1 treatment (100 ng/mL or 500 ng/mL). No changes in expression of total FAK was shown subsequent to the Netrin-1 treatment. Images are representative of 3 independent experiments. Pan-actin was used as a loading control for western blot assays. The replicate images are shown in **Appendix B.** **(B)** The western blot analysis exhibits the levels of pFAK/pMEK/pERK signals in CT26 cells treated with 100 ng/mL or 500 ng/mL of Netrin-1. Also, changes in the levels of pFAK/pMEK/pERK signals in cells treated with Netrin-1 (500 ng/mL) after blocking receptors, UNC5H2 and/or Neogenin receptors, are shown. The total expression of FAK, MEK and ERK exhibited no changes subsequent to the Netrin-1 treatment as well as blocking receptors. Anti-IgG antibody was used as a non-specific antibody control. Images are representative of 3 independent experiments. Lamin B1 was used as a loading control for western blot assays. The replicate images used for densitometric analysis are shown in **Appendix B.** **(B')** Densitometric analysis shows an increase in the level of pFAK/pMEK/pERK signals in CT26 cells treated with 500 ng/mL of Netrin-1. In contrast, a decrease in the levels of pFAK/pMEK/pERK signals in CT26 cells treated with 500 ng/mL of Netrin-1 subsequent to receptor blocking. Relative expression of pFAK/pMEK/pERK was normalised by respective total expressing of FAK/MEK/ERK. The normalised data are presented as mean  $\pm$  SD (n=3). Two-way ANOVA; Tukey's multiple comparisons tests; # $p < 0.05$  vs vehicle control (PBS); \* $p < 0.05$ , \*\* $p < 0.01$  vs N500 alone.

**Abbreviations:** p, phosphorylated; t, total; FAK, focal adhesion kinase; MEK, mitogen-activated protein kinase kinase; ERK, extracellular-signal-regulated kinase; Anti-UNC5H2, UNC5H2 antibody; Anti-Neo, Neogenin antibody, Anti-UNC5H2 + Anti-Neo, UNC5H2 and Neogenin antibodies.

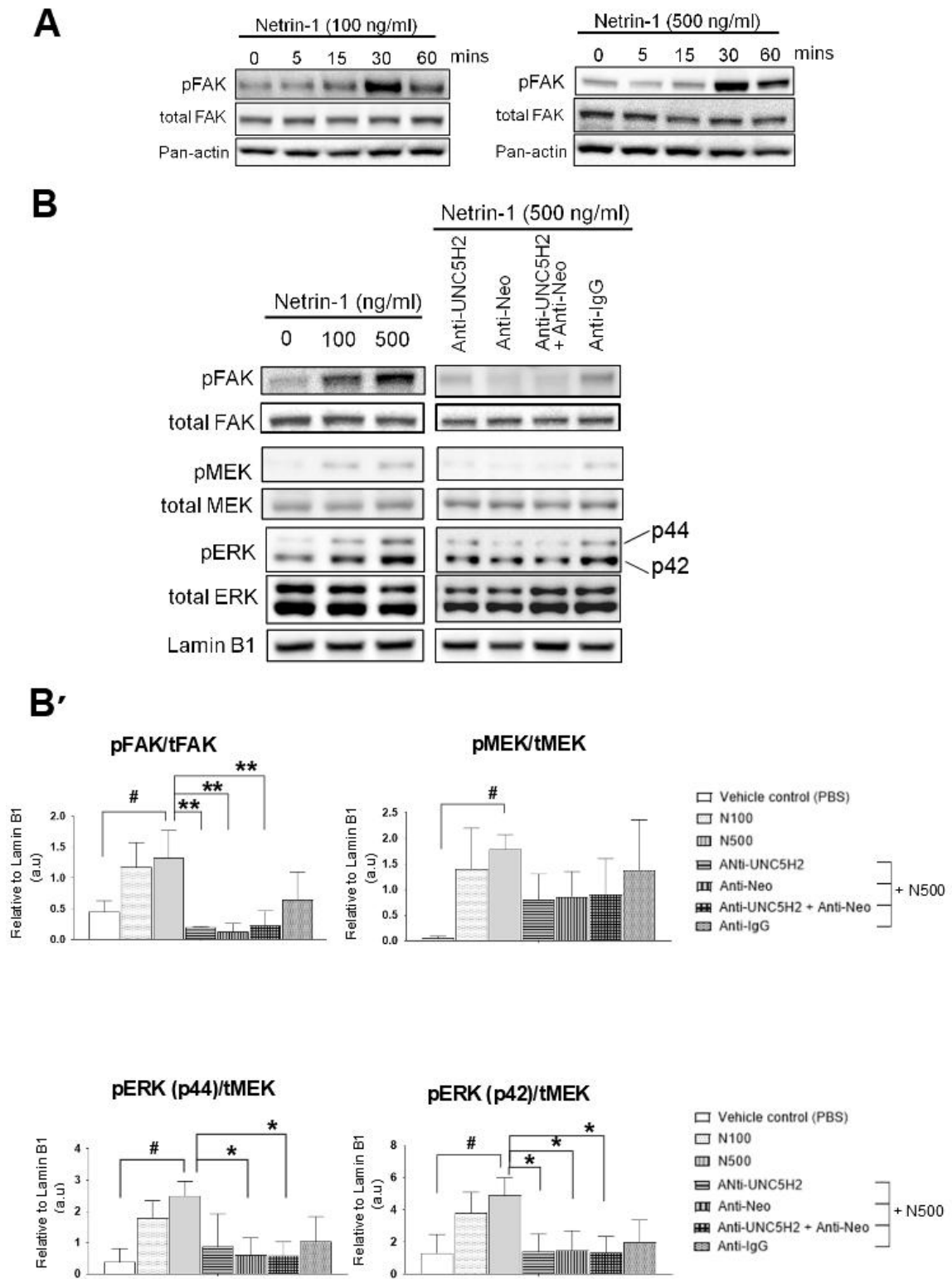


Figure 3.6

## 3.4 Discussion

### 3.4.1 The effect of Netrin-1 on CT26 cell proliferation and adhesion

In this study, it was demonstrated that CT26 cell viability increased when Netrin-1 was exogenously introduced to the cells. Notably, the elevated cell viability was indicated in accordance with increasing concentrations of Netrin-1. This result is consistent with previous studies using various cancer cell lines which were virally transfected with Netrin-1 in order to up-regulate Netrin-1 expression [153]. Furthermore, when UNC5H2 and/or Neogenin receptors in CT26 cells were blocked using specific antibodies prior to the Netrin-1 (100 ng/mL) treatment, the viability of cells was significantly diminished. Interestingly, blocking the combination of UNC5H2 and Neogenin receptors did not display any synergistic inhibition of cell viability in comparison to the case when either UNC5H2 or Neogenin was individually blocked. This may be because some fraction of UNC5H2 and Neogenin receptors are hetero-dimerised in response to Netrin-1 binding [334]. In the case of individual receptor blocking, it appeared that the viability of CT26 cells was not significantly reduced when UNC5H2 receptor alone was blocked prior to the 500 ng/mL of Netrin-1 treatment. This may be because cell viability is more effectively mediated by Neogenin in comparison to UNC5H2. However, further quantitative work is required to clarify their contribution to cell viability. Similar results have been indicated in the previous study of Yin *et al.* [313] that a significant reduction in the proliferative ability of a human gastric cancer cell line, HGC27 cells when *NEOGENIN* but not *UNC5B* gene expression was knocked down. Furthermore, no additional inhibitory effect was reported on HGC27 cell proliferation when both genes were knocked down.

Moreover, the expression of cyclin D and cleaved caspase-3 in CT26 cells was examined following the Netrin-1 (100 or 500 ng/mL) treatment. The level of cyclin D expression was increased, whereas the level of cleaved caspase-3 expression was decreased in the presence of Netrin-1 at both concentrations. These data support the results obtained from cell viability assessment that the increase in cell viability observed in response to Netrin-1 treatment was associated with the inhibition of caspase-3 apoptosis, which ultimately resulted in cell proliferation.

Next, the adhesiveness effect of Netrin-1 on CT26 cells is demonstrated in this Chapter. Cell adhesion is known to be a complex cellular process that involves various molecular interactions [335]. These include receptor-ligand binding, alteration of actin cytoskeletal assembly and disassembly, and modulation of intracellular signalling in response to the surroundings [336]. In metastasis, attachment of tumour cells to the basement membrane is a fundamental initial step [337]. Strongly attached metastatic tumour cells can traverse the basement membrane by releasing matrix metalloproteinases. Hence, they can relocate to a secondary site of the organ [338]. Previous studies have reported that many cells do not easily bind directly to collagen which is one of the basement membrane components. More precisely, cellular adhesion process is facilitated by various attachment proteins such as fibronectin and laminin in the extracellular matrix [330].

Netrin-1 is a laminin-related protein that is diffusible in the extracellular matrix, and it is known to promote adhesion of endothelial cells [231] and certain cancer cells [339]. Previously, it was reported that some tumour cells prefer adhering to collagen type-IV instead of type-I. Conversely, non-metastatic cells prefer attaching to collagen type-I [330]. Based on this information, collagen type-I was chosen to be a coated surface for CT26 cells in order to examine the effect of Netrin-1 as an attachment factor. The results showed that Netrin-1 enhanced the adhesive property of CT26 cells, and that enhanced adhesion was diminished when UNC5H2 and Neogenin receptors were blocked. This suggests that the adhesiveness of CT26 cells in the presence of Netrin-1 is mediated by these receptors.

Further to this adhesion assay using attachment factors, a substrate-attachment adhesion assay was examined where CT26 cells were directly plated onto the Netrin-1-coated surface. Previously it has been indicated that Netrin-1 can also serve as a substrate for endothelial cells [220], pancreatic epithelial cells [340], and pancreatic ductal adenocarcinoma [228]. The protocol for the substrate-attachment assay was adopted from Park et al [220]. However, unlike their study involving endothelial cells, CT26 cell attachment to Netrin-1-coated surface, tested Netrin-1 concentrations ranging from 50, 100 and 500 ng/mL,

was not successful. It was difficult to obtain reproducibility, which has been known to be a common issue for utilising this method [335].

In addition to cell viability and adhesion assays, soft agar colony formation was performed to investigate the effect of Netrin-1 on survival and proliferation of CT26 cells. The soft agar colony formation assay was conducted and the protocol was adapted from a previously published method [341]. Single cells were treated with media containing 1% or 2% FBS and Netrin-1 (100 ng/mL or 500 ng/mL) for 3 weeks. However, CT26 cells incubated with Netrin-1 (500 ng/mL) did not display any differences with respect to the vehicle control (data not shown). Similarly, no differences were found using a collagen type-I coated colony formation assay in the absence and presence of Netrin-1 (data not shown). Further experiments utilising Netrin-1 transfected cells are needed to clarify the effect of Netrin-1 in colony forming efficiency of CT26 cells.

#### **3.4.2 The effect of Netrin-1 on migration of CT26 cells**

Cell migration is an essential cellular process for organogenesis, tissue maintenance and repair under physiological condition [342]. However, this process is also actively involved in cancer metastasis where tumour cells migrate and invade through extracellular matrix into the blood circulation [343].

Netrin-1, originally identified as a neuronal guidance molecule, has also been found to serve as a chemotropic factor for cancer cell migration [344]. Netrin-1 and its receptors have been involved in promoting migration of certain cancer cells [215, 345]. Furthermore, the neuronal guidance role of Netrin-1, either by chemo-attractive or chemo-repulsive, has also been demonstrated in respect of promoting or inhibiting the migration of cancer cells [346-348], endothelial cells [349, 350] and immune/inflammatory cells [351, 352]. Typically, these opposing guidance roles of Netrin-1 were mediated by the same types of Netrin-1 receptors that are activated in cancer cells. For example, increased migration and invasion of gastric cancer cells (BGC823 and MKN45 cell lines with over-expression of Netrin-1) were demonstrated through the activation of Neogenin receptors [313]. Additionally, a human bladder cancer cell line (5637) with up-regulated UNC5B expression displayed a reduced migratory activity [353].

Here, a wound-healing migration analysis showed that enhanced CT26 cell migration was detected when a high concentration of Netrin-1 (500 ng/mL) was applied. However, it was unable to detect an invasive migratory behaviour of CT26 cells towards 500 ng/mL of Netrin-1 compared to control using a Matrigel-coated Transwell migration (data not shown). Additional assays are required to confirm this lack of invasiveness of CT26 cells in response to Netrin-1.

Furthermore, to examine whether UNC5H2 and/or Neogenin were involved in the modulation of CT26 cell migration in the response to Netrin-1, blockade of these receptors was conducted. The results showed that no significant changes in the migratory activity of CT26 cells were observed when UNC5H2 and/or Neogenin receptors were blocked in wound-healing migration assay. This might be because of the chosen concentration of antibodies for blocking Netrin-1 receptors in this assay was insufficient. An alternative reason may be because Netrin-1 receptors were not directly responsible for promoting CT26 cell migration. Previously, few studies have shown that integrin proteins such as  $\alpha 6\beta 4$  and  $\alpha 3\beta 1$  also bind to Netrin-1 [310, 354], and these integrins were shown to mediate neuronal and epithelial cell migration in response to Netrin-1 [326, 355, 356]. Subsequently, integrins were considered to serve as a co-receptor for UNC5B and thereby modulating mesenchymal-epithelial interaction in response to Netrin-1 [357]. In order to clarify the direct involvement of UNC5H2 and Neogenin in CT26 cell migration, testing cell lines with down-regulated Netrin-1 receptors using siRNA may be a useful strategy to address this question.

#### **3.4.3 The effect of Netrin-1 on CT26 cells via activation of pFAK/pMEK/pERK pathway**

Previous studies have provided evidence that FAK molecule is constitutively bound to Neogenin receptors at the intracellular domain of the P3 motif [306]. When Netrin-1 binds to Neogenin, Src kinases are recruited to the phosphorylated tyrosine 1,467 amino acid residue of the receptor, and they promote phosphorylation of the Src and FAK kinases [164, 358].

In this study, an increase in the level of FAK phosphorylation was detected when Netrin-1 was added into CT26 cells. Similar results were demonstrated in human gastric cancer cell lines expressing both Neogenin and UNC5B

receptors [313]. Over-expression of Netrin-1 in certain gastric cancer cell lines (HGC27 and AGS cells) led to an increase in the level of FAK phosphorylation. Conversely, reduced FAK phosphorylation was observed when Netrin-1 was knocked down in those cell lines [313]. In addition to gastric cancer cells, increased FAK phosphorylation was detected in human pancreatic cancer cells, MiaPaCa II, when either the cells were induced to express up-regulation of Netrin-1 or the cells were treated with a recombinant Netrin-1 [326].

Following FAK phosphorylation, the AKT pathway was shown to be activated in gastric cancer cells expressing up-regulation of Netrin-1 [313]. The authors indicated that Netrin-1 activating Neogenin mediates gastric cancer cell proliferation and invasion through PI3K/AKT signalling pathway [313]. However, Netrin-1 treated CT26 cells in our study did not appear to involve the AKT pathway since no phosphorylation of AKT was detected (data not shown). On the other hand, the level of MEK and ERK phosphorylation was increased in CT26 cells treated with 500 ng/mL of Netrin-1. Conversely, the level of phosphorylated MEK and ERK expression was reduced when UNC5H2 and/or Neogenin receptors were blocked prior to the cells being treated with Netrin-1, suggesting that the MEK/ERK pathways are associated with the activation of UNC5H2 and Neogenin receptors in CT26 cells following the Netrin-1 treatment.

The studies of An *et al.* [326] have also indicated that when MiaPaCa II cells expressing UNC5B and Neogenin were treated with Netrin-1, MEK/ERK signalling pathways were modulated, while the PI3K-AKT pathway was unchanged.

However, a modulation of the MEK/ERK pathway that was observed in our study is in contrast to the results obtained by An *et al.* [326]. Although the authors have indicated that Netrin-1 activated c-RAF kinase, which is up-stream of MEK kinase, the expression of MEK/ERK phosphorylation in MiaPaCa II cells was found to be reduced in response to Netrin-1. A further detail was provided that UNC5B in MiaPaCa II cells were responsible for mediating FAK activation, which in turn, stimulated nitric oxide (NO) production. The production of NO promoted protein phosphatase 2A (PP2A) activity, which dephosphorylate MEK/ERK expression and c-Jun inhibition resulting in down-regulation of

integrin  $\beta 4$ . As a consequence, the authors [326] suggested that Netrin-1 suppresses pancreatic cell growth and adhesion, while it does not affect proliferation and apoptosis of pancreatic cells.

In colorectal cancer, PP2A is commonly inhibited [359], and the relationship of PP2A and Netrin-1 has not been demonstrated. However, during angiogenesis regulation, PP2A-mediated dephosphorylation of DAP kinase is associated with UNC5H2/B-induced apoptosis of endothelial cells in the absence of Netrin-1 [360].

Although some studies have indicated that Neogenin acts as a co-receptor for UNC5H2 [361], it appears that the receptor type, which is dominated in the cell line, may cause a different cellular response to Netrin-1. It is uncertain which receptor type (UNC5H2 or Neogenin) was taking a lead role in CT26 cells in response to Netrin-1. Further work will be required to clarify the down-stream of MEK/ERK pathways.

### **3.5 Summary**

A potential metastatic effect of Netrin-1 was investigated in CT26 cells expressing UNC5H2 and Neogenin receptors. Unlike other studies utilising the cell lines with modulating Netrin-1 expression, the effect of Netrin-1 on wild-type CT26 cells was examined by treating the cells with a recombinant Netrin-1. This is to understand the CT26 cell behaviour in response to Netrin-1, prior to investigating the effect of Netrin-1 in an orthotopic colorectal mouse model induced with the CT26 cells (Chapter 5).

CT26 cells treated with Netrin-1 exhibited an increase in proliferation and adhesion properties. These properties were mediated by UNC5H2 and Neogenin receptors in response to Netrin-1, since blockade of those receptors diminished the proliferative and adhesive effect of Netrin-1 on CT26 cells. Furthermore, wound-healing migration of CT26 cells was promoted in response to a high concentration of Netrin-1. However, the colony formation and invasiveness of CT26 cells in response to Netrin-1 was not detected, and additional work is needed to confirm these metastatic properties.

Following Netrin-1 treatment, pFAK/MEK/ERK signalling pathway was activated. This pathway is known to be involved in promoting cell survival and migration. In addition, activation of pFAK/MEK/ERK pathway was shown to be mediated by UNC5H2 and Neogenin receptors.

Further molecular studies are required to determine underlying mechanisms of metastatic properties of CT26 cells in response to Netrin-1.

## Chapter 4

---

**The effect of colorectal cancer conditioned media on neuronal cells in *in vitro* system**

## 4.1 Introduction

Peripheral neuropathy, the damage of peripheral nerves, has been a major complication in cancer patients receiving chemotherapy. Many studies have found that peripheral neuropathy is induced by chemotherapeutic agents, which have been shown to cause neurotoxicity as an adverse effect of targeting and killing rapidly dividing cancer cells [362-364]. Recent reports have found that 30% to 40% of patients undertaking chemotherapy suffer from neuropathic symptoms such as abnormal sensory function, pain or loss of motor control [362, 365, 366].

Importantly, Byette-Davis *et al.* have suggested that peripheral neuropathy observed in colorectal cancer patients is not solely caused by chemotherapeutic agents; instead, the presence of cancer, the disease itself, is an initial contributing factor for neuropathy [367]. Extensive quantitative sensory testing of 52 colorectal cancer patients with no pre-existing neuropathic disease found that these patients had already shown subclinical neuropathy deficits in sensorimotor function, thermal stimuli and touch sensation detection before chemotherapy [367].

The work of Godlewski provided the first morphological evidence of colorectal cancer damaging the ENS [368]. Immunohistochemical analysis of specimens obtained from colorectal cancer patients before chemotherapy and/or radiotherapy indicated that an invasive tumour destroys the intestinal wall and disrupts the submucosal and myenteric plexus as the tumour expands. The myenteric plexus of the colon sections near the tumour, in particular, showed a reduced number of neurons, a noticeably smaller size of the network or rarely visible nerve fibres. Disappearance of the submucosal plexus surrounded by tumours was reported in the case of dispersed invasion of carcinoma. In addition, there were no detectable elements of the ENS in some solid tumour cases. Subsequently, Kozłowska *et al.* investigated possible mechanisms by which atrophy of the myenteric plexus is induced in cancer invasion [369] and suggested that neither apoptosis nor necrosis is directly responsible for the observed atrophy of the myenteric plexus in the vicinity of colorectal cancer. The cause of atrophy of the myenteric plexus is yet to be elucidated.

In this thesis, the effect of colorectal cancer on the enteric nervous system is recapitulated in an *in vitro* system to understand the direct effect of colorectal cancer cells on the enteric neurons without involvement of the complex immune responses that are normally present in an *in vivo* system. If the damaged ENS, which was seen in the invasive cancer, was not solely due to the physical growth of the tumour driving a distortion of the tissue layers, the secreted factors released from the colorectal cancer cells may be affecting the enteric neurons. To test this hypothesis, enteric neuronal cells were incubated with the colorectal cancer conditioned media and the viability and apoptosis of enteric neuronal cells were examined.

## **4.2 Materials and methods**

### **4.2.1 IM-PEN cell culture**

IM-PEN cell line culture method and culture media at 33°C and 40.5°C were described in detail in chapter 3, section 3.2.1. Briefly, IM-PEN cells cultured at 33°C were incubated in permissive medium (PM): a DMEM/F12 medium containing GlutaMax, 1% (v/v) antibiotic antimycotic, 10% (v/v) FBS, 0.1 mg/mL of Fetuin, 1 mg/mL of BSA, 20U/mL of recombinant mouse IFN-gamma, 100 ng/mL of recombinant mouse GDNF. IM-PEN cells cultured at 40.5°C were incubated in differentiation medium: a neurobasal-A medium supplemented with B-27 serum free supplement, 1mM GlutaMax, 1% (v/v) antibiotic antimycotic, 1% (v/v) FBS and 100 ng/mL of recombinant mouse GDNF.

### **4.2.2 CT26 cells conditioned media**

Murine colorectal cancer CT26 cells were maintained at 37°C, using 5% CO<sub>2</sub>, and incubated with a DMEM medium containing GlutaMax, 1% (v/v) antibiotic antimycotic, 10% (v/v) FBS. The medium was changed every second or third day depending on the confluency of the cells. To collect CT26 cells conditioned media, cells from passage between 4 and 6 were incubated in their regular medium. They were cultured until 65% confluence at 37°C, using 5% CO<sub>2</sub>. After washing adherent CT26 cells with PBS three times, the medium was replaced with a fresh serum free medium: DMEM medium containing GlutaMax, 1% (v/v) antibiotic antimycotic and 1% (w/v) bovine serum albumin (BSA). This

conditioned media (CM) from CT26 cells was harvested at 48 hour incubation. The harvested CM was then centrifuged at 5000 rpm for 10 min at 4°C followed by filtering the CM using a 0.2 µm sterile syringe filter to remove any residual cell contamination. The filtered CM was kept frozen in aliquots at -20°C no longer than a two-week period. The aliquots were thawed only once each time prior to use. CM from the same batch was used per experiment.

### **4.2.3 Cell viability**

IM-PEN cells were seeded at  $1 \times 10^4$  cells per well on a 96-well plate, and they were cultured in PM containing supplements at 33°C. A day after seeding, the cells were washed with PBS twice to remove residual PM. The cells were then incubated for further 24 hours with different types of testing media indicated in Figure 4.1; serum free media (SFM), CM, 1:1 (SFM:CM), 1:1 (N100), 1:1 (N500), 1:1 (z-DEVD-fmk). In the case of 1:1 (z-DEVD-fmk), the cells were treated with an irreversible caspase-3 inhibitor (20 µM of z-DEVD-fmk; ApexBio) for 1 hour prior to incubation with 1:1 media for 24 hours. AlamarBlue reagent (10 µL/well; Thermo Fisher Scientific) was added into each well and the fluorescence intensity of the AlamarBlue was detected at 545nm/590nm (excitation/emission) wavelength by using a microplate reader (Varioskan Flash, Thermo Fisher Scientific). Eight technical replicates were used per treatment in each experiment. Three independent experiments were conducted.

### **4.2.4 Immunofluorescence**

Immunofluorescent protocol was described in detail in Chapter 3, section 3.2.4. In brief, IM-PEN cells were cultured on poly-D-lysine coated coverslips placed in 6 well-plates. The cells were fixed and permeabilised. They were then incubated with blocking solution for 2 hours at RT. Cells were then incubated with primary antibodies against neurofilament-heavy chain (NF-H) (chicken, 1:1000, Aves Labs, USA) and cleaved caspase-3 (rabbit, 1:1000, Cell Signalling Technologies, USA) overnight at 4°C. Cells were washed in PBS-T (0.05%, pH7.4) for 4 x 10 min at RT. Cells were incubated with species-specific secondary antibodies labelled with different fluorophores, such as Donkey anti-chicken-FITC (1:300, Merck Millipore) and Donkey anti-rabbit-rhodamine (1:300, Jackson ImmunoResearch Laboratories) for 1 hour at RT dark. Following secondary antibody incubation, cells were washed with PBS-T

(0.05%, pH7.4) for 4 x 10 min, and nuclei were counterstained with DAPI. Each coverslip was mounted with fluorescent mounting medium. Secondary antibody controls were conducted. Cleaved caspase-3 immunoreactive cells were counted in total area 2 mm<sup>2</sup> using ImageJ plugin.

#### **4.2.5 Imaging**

Immunofluorescent images were taken using a confocal microscope (Nikon Lidcombe, Australia) with NIS element software. Z-stack images were acquired at a normal thickness of 0.5 µm with a 20x objective. Random 8 areas of images (total area of 2 mm<sup>2</sup>) were taken per treatment group. The images of phase contrast were taken using an Olympus BX53 microscope (Olympus, Notting Hill, Australia) with CellSense software.

#### **4.2.6 Statistical analysis**

Results are presented as means ± SD, calculated from the specified numbers (n) of biological replicates. If 'n' represents technical replicates, it is indicated in Figure legends. All experiments were performed in minimum of 3 independent experiments, otherwise specified in Methods or Figure Legends. The statistical analysis was performed using GraphPad software (GraphPad Prism version 7.0 for Windows). Comparison between treatment groups was examined by one-way ANOVA with Tukey's multiple comparisons test. A *p* value of <0.05 was considered statistically significant. The levels of statistical significance were indicated by \**p*<0.05, \*\**p*<0.01 and \*\*\**p*<0.001.

### **4.3 Results**

#### **4.3.1 The effect of colorectal cancer conditioned media on post-natal enteric neuron precursors**

To investigate whether or not colorectal cancer causes damage to enteric neurons, enteric neuronal cells were incubated with colorectal cancer cell conditioned media (CM). CM was produced by culturing CT26 cells in DMEM containing 1% BSA for 48 hours. The effect of CM was tested on the post-natal enteric neuronal cell line, IM-PEN cells which were cultured at two different temperatures. IM-PEN cells grown at 33°C show characteristics of enteric

neuronal precursors, whereas IM-PEN cells cultured at 40.5°C display characteristics of differentiated enteric neurons.

Normally, IM-PEN cells at 33°C require a permissive medium (PM), which consists of DMEM/F12 containing N2 supplements, growth factors such as GDNF, IFN- $\gamma$  and 10% FBS. These supplementary materials were needed for growth and survival of the enteric neuronal precursors. CT26 cells were cultured in DMEM containing 10% FBS for their growth. To test the effect of factors secreted from CT26 cells; that are released into CM, FBS was removed and 1% BSA was added in DMEM to ensure the basic survival of the cells. Because these two cell lines were grown in a different type of medium, it was necessary to demonstrate that IM-PEN cells could be compatible with DMEM in the absence of FBS and they could survive in that medium.

After seeding IM-PEN cells on a 96-well plate, the cells were incubated with either PM or DMEM containing 1% BSA in the absence of FBS for 24 and 48 hours at 33°C. An AlamarBlue assay was conducted to test IM-PEN cell viability on those media (**Figure 4.1 A**). Surprisingly, the results showed that the viability of cells was similar when the cells were incubated in either PM or DMEM in the absence of FBS for a 24 hour period at 33°C. However, a slight increase in cell viability was noticed when the cells were incubated in PM without FBS as opposed to DMEM without FBS for a 48 hour incubation period at 33°C.

Based on the observation that those different media had not affected the viability of IM-PEN cells cultured at 33°C during 24 hour incubation, it was decided that DMEM in the absence of FBS, also called here as a serum free medium (SFM) containing 1% BSA was used as a negative control medium.

The effect of CM on the viability of IM-PEN cells at 33°C was examined at the 24 hour incubation time point (**Figure 4.1 B**). The results indicated that a notable decrease in cell viability was shown in the presence of CM ( $69.9 \pm 5.9\%$ ,  $p < 0.001$ ) in comparison to SFM. Given that CM was a two-day old medium while SFM was a fresh medium at the time when they were individually introduced to the IM-PEN cells, this may have caused a possible variation in the viability result. Hence, in order to minimise that difference in the media, CM was combined with a fresh SFM in a 1:1 ratio and this mixed media, indicated here

as 1:1, were introduced to the cells and incubated for further 24 hours. Still, IM-PEN cells that were incubated in 1:1 media showed significantly less viability ( $83.9 \pm 8.8\%$ ,  $p < 0.01$ ) than the negative control, SFM. This suggests that the CT26 CM reduces the viability of enteric neuronal precursors.

In order to investigate whether Netrin-1 could assist in the viability of enteric neuronal precursors, a recombinant mouse Netrin-1 protein was introduced at concentrations of either 100 ng/mL or 500 ng/mL in combination with 1:1 media (**Figure 4.1 B**). However, no significant difference in the viability of cells was observed in the presence of Netrin-1 at both the 100 ng/mL and 500 ng/mL concentrations ( $81.6 \pm 6.9\%$  and  $88.0 \pm 10.7\%$ , respectively) when compared to 1:1 media in the absence of Netrin-1 ( $83.9 \pm 8.8\%$ ). **Figure 4.1 C** shows the images of IM-PEN cells, which were seeded on a 96-well plate and incubated with different types of media tested for the cell viability assay. Those media were also tested on IM-PEN cells seeded on a 6-well plate and the images are shown in **Figure 4.1 D**. A noticeable blebbing was observed in the cells incubated in CM and 1:1 media. Also, fewer cells were adhered to the wells when the cells were incubated in either of CM or 1:1 media as opposed to SFM. In the presence of Netrin-1 both at 100 ng/mL and 500 ng/mL concentrations, elongation of neurites was evident when compared to the cells incubated in 1:1 media.

The next investigation was conducted to determine whether or not the reduced viability of enteric neuronal precursors observed in the presence of CM was caused by apoptosis instead of cell cycle arrest. An assay for immunofluorescent labelling of cleaved caspase-3 was conducted on IM-PEN cells after the IM-PEN cells were incubated with various testing media including SFM, CM, 1:1, 1:1 (N100), 1:1 (N500) and 1:1 (z-DEVD-fmk) for 24 hours at 33°C (**Figure 4.2 A**). The results showed that there was a significant increase in the percentage of neurons that were immunoreactive to cleaved caspase-3 in the presence of CM ( $85.0 \pm 4.3\%$ ,  $p < 0.001$ ) and 1:1 ( $79.0 \pm 7.1\%$ ,  $p < 0.001$ ) when compared to SFM ( $8.0 \pm 4.0\%$ ) (**Figure 4.2 B**).

Remarkably, when the cells were incubated in 1:1 media containing a high concentration of Netrin-1 (500 ng/mL), here indicated as 1:1 (N500), a significant reduction in the percentage of neurons that were immunoreactive to

cleaved caspase-3 was observed ( $45.0 \pm 8.7\%$ ,  $p < 0.001$ ) in comparison to the cells incubated in 1:1 media alone ( $79.0 \pm 7.1\%$ ) (**Figure 4.2 B**). However, no significant difference in the percentage of cleaved caspase-3 immunoreactive neurons was found in the cells incubated in 1:1 media containing 100 ng/mL of Netrin-1 ( $78.5 \pm 8.2\%$ , n.s.) when compared to the cells incubated in 1:1 media alone ( $79.0 \pm 7.1\%$ ).

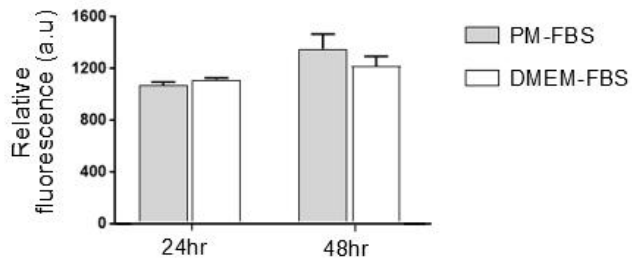
In addition, when the cells were pre-treated with an irreversible caspase-3 specific inhibitor, z-DEVD-fmk, followed by 1:1 media incubation for 24 hours, the percentage of neurons that were positive for cleaved caspase-3 was markedly reduced ( $5.0 \pm 3.0\%$ ,  $p < 0.001$ ). This result was found to be similar to the percentage of cleaved caspase-3 positive neurons observed in SFM ( $8.0 \pm 4.0\%$ ). Collectively, the data suggest that CM induces caspase-3 activation in enteric neuronal precursors, while Netrin-1, when present at a high concentration, was able to inhibit active caspase-3 in the precursors.

**Figure 4.1 Cell viability test and imaging of IM-PEN precursors cultured in CRC conditioned media with or without Netrin-1**

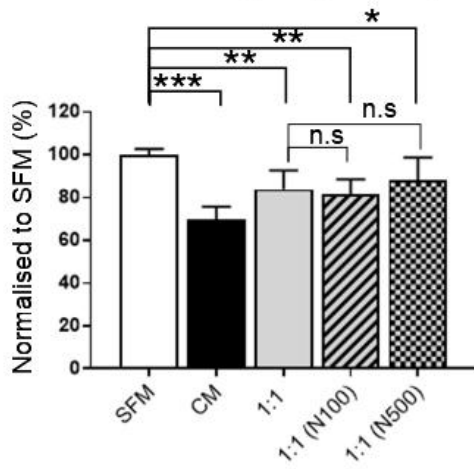
**(A)** Cell viability of IM-PEN cells cultured in a permissive medium in the absence of FBS (PM-FBS) as opposed to a DMEM medium in the absence of FBS (DMEM-FBS) at 33°C. **(B)** IM-PEN cells were seeded on a 96-well plate and cultured at 33°C with different types of testing media. The testing media include SFM, CM, 1:1, 1:1 (N100) and 1:1 (N500). The results are expressed as mean  $\pm$  SD (n=8 of technical replicates per experiment) and are representative of three independent experiments. One-way ANOVA; Tukey's multiple comparisons test; \* $p$ <0.05, \*\* $p$ <0.01, \*\*\* $p$ <0.001 vs SFM. **(C)** After the viability test, the cells that were treated with different types of media were imaged using a phase contrast microscope. **(D)** Phase contrast microscopic images showing changes in morphology of IM-PEN cells that were incubated in different types of media at 33°C. Scale bar: 100  $\mu$ m. Images are representative of three independent experiments.

**Abbreviations:** SFM, serum free DMEM medium; CM, conditioned media from CT26 cells; 1:1, the mixed medium of SFM and CM in a 1 to 1 ratio; 1:1 (N100), the mixed medium of SFM and CM containing 100 ng/mL Netrin-1; 1:1 (N500), the mixed medium of SFM and CM containing 500 ng/mL Netrin-1.

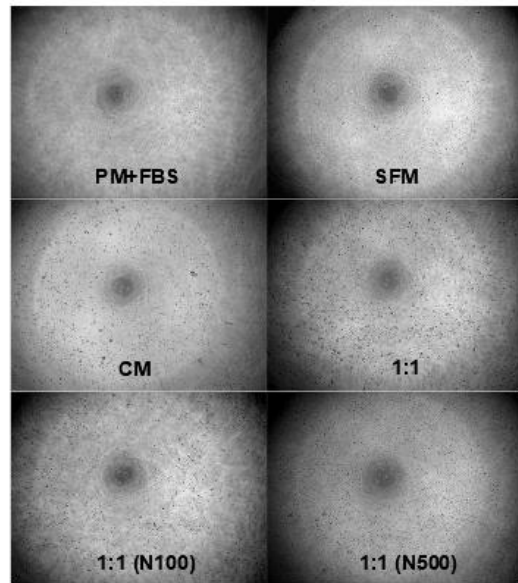
**A** IM-PEN cell (33°C) viability



**B** IM-PEN cell (33°C) viability



**C**



**D**

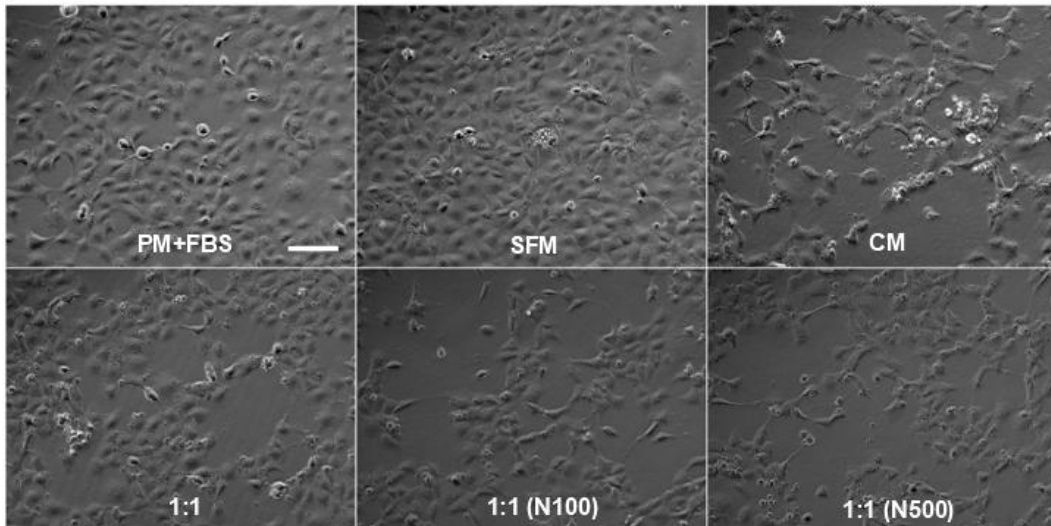


Figure 4.1

**Figure 4.2 Cleaved caspase-3 expression in IM-PEN precursors after incubation in conditioned media with or without Netrin-1**

**(A)** Representative images of immunofluorescence staining for NF-H and cleaved caspase-3 on IM-PEN cells cultured at 33°C. DAPI was used for nuclei staining. Prior to staining, the cells were incubated in different types of testing media for 24 hours. The testing media include SFM, CM, 1:1, 1:1 (N100), 1:1(N500) and 1:1 (z-DEVD-fmk). NF-H was labelled as counter staining for IM-PEN cells. The z-stack images were taken by confocal microscopy using a 20x objective. Scale bar: 100 µm. Images are representative of three independent experiments. **(B)** The number of positively stained cells for cleaved caspase-3 over the number of NF-H/DAPI stained cells was counted and that value was expressed as a percentage. The results are represented as mean ± SD (n=3). One-way ANOVA; Tukey's multiple comparisons test; \*\*\* $p < 0.001$  vs SFM; ### $p < 0.001$  vs 1:1.

**Abbreviations:** SFM, serum free DMEM medium; CM, conditioned media from CT26 cells; 1:1, the mixed medium of SFM and CM in a 1 to 1 ratio; 1:1 (N100), the mixed medium of SFM and CM containing 100 ng/mL Netrin-1; 1:1 (N500), the mixed medium of SFM and CM containing 500 ng/mL Netrin-1; 1:1 (z-DEVD-fmk), the mixed medium of SFM and CM after treating the cells with z-DEVD-fmk; NF-H, neurofilament-heavy chain.

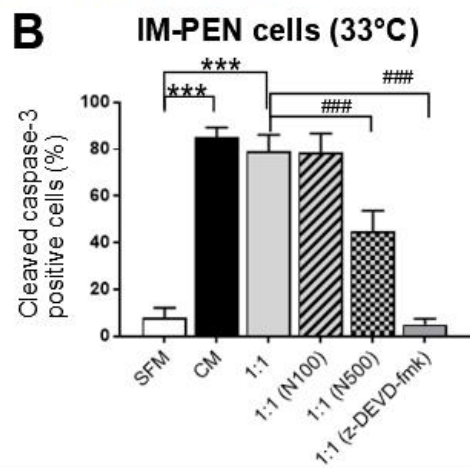
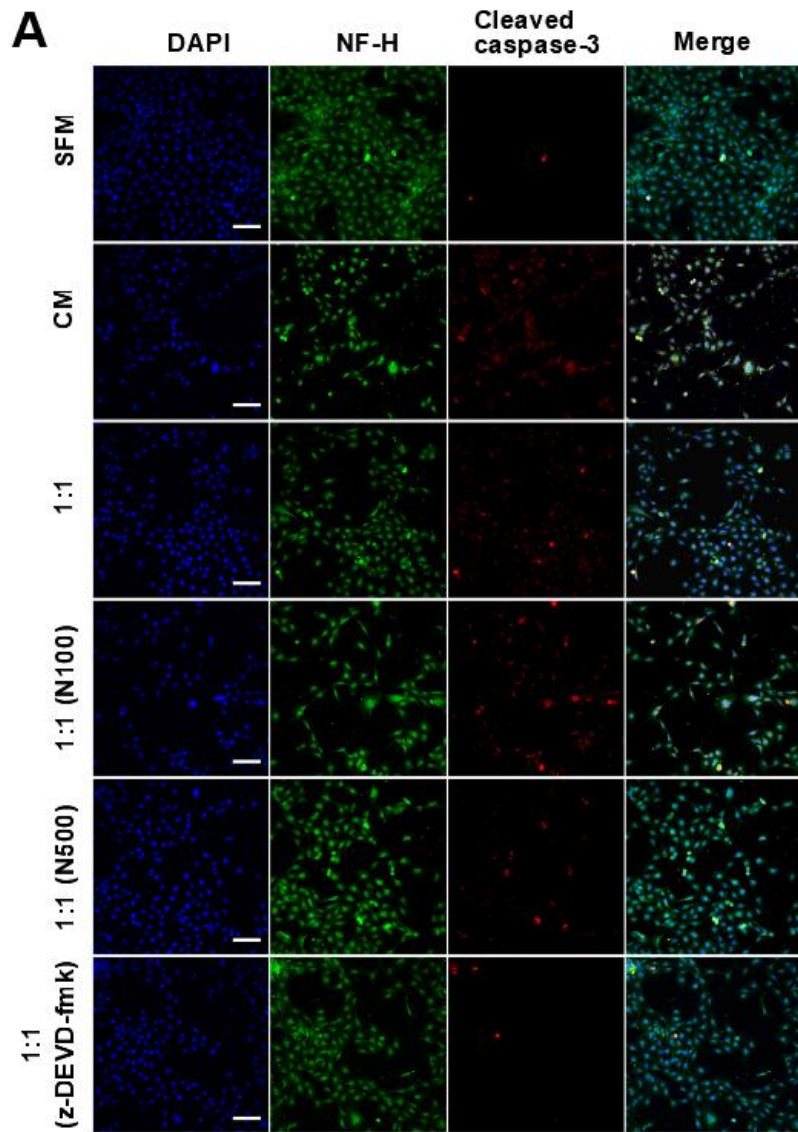


Figure 4.2

### 4.3.2 The effect of colorectal cancer conditioned media on post-natal differentiated enteric neurons

To induce differentiation, IM-PEN cells were incubated with their optimal differentiation medium (DM), which consists of Neurobasal-A medium supplemented with B-27, GDNF and 1% FBS for 4 days at 40.5°C. After incubation for 4 days, the cells were incubated for a further 24 hours with various testing media including DM, CM, and a mixed medium of DM and CM in a 1:1 ratio, indicated here as 1:1, 1:1 (N100), 1:1 (N500) and 1:1 (z-DEVD-fmk).

To examine whether or not CM induces apoptosis in those early differentiated enteric neuronal cells, an immunofluorescent assay labelling cleaved caspase-3 was conducted on IM-PEN cells after the cells were incubated at 40.5°C with testing media indicated the above. The immunofluorescent images were taken using a confocal microscope (**Figure 4.3 A**). The analysis of cleaved caspase-3 immunoreactivity indicated that the cells incubated with CM alone showed a significant increase in the percentage of neurons that were positive for cleaved caspase-3 ( $64.4 \pm 6.9\%$ ,  $p < 0.001$ ) when compared to the cells incubated with their optimal medium, DM ( $10.9 \pm 4.8\%$ ) (**Figure 4.3 B**). However, when the cells incubated in 1:1 media ( $14.3 \pm 5.7\%$ ) were examined, it was found that the percentage of cleaved caspase-3 immunoreactive cells was rather similar to the percentage of cells that were incubated in DM. This may suggest that the elevated level of cleaved caspase-3 observed with the cells incubated in CM was likely due to medium incompatibility. Alternatively, this may also suggest that the composition of DM medium and/or factors secreted from the neuronal cells were able to counteract the apoptotic pathway that was induced by CM. Nonetheless, it is difficult to conclude from these data whether or not CM causes apoptosis of IM-PEN cells at 40.5°C.

In addition, no significant difference in the percentage of cleaved caspase-3 positive neurons in the presence of Netrin-1 at both concentrations of 100 ng/mL and 500 ng/mL ( $17.4 \pm 8.7\%$  and  $16.0 \pm 4.1\%$ , respectively) was observed when compared to the cells that were incubated in 1:1 media alone ( $14.3 \pm 5.7\%$ ) as well as those in DM ( $10.9 \pm 4.8\%$ ). Furthermore, no notable changes in the percentage of cells that was positive for cleaved caspase-3 was

found when the cells were incubated with 1:1 media after z-DEVD-fmk inhibitor treatment ( $7.1 \pm 1.8\%$ ).

Collectively, additional assays will need to be conducted in order to determine the effect of CM on the differentiated neurons. In addition, further tests will be required in order to ascertain the effect of Netrin-1 on differentiated neuronal survival. In the following discussion section, details of possible factors that may have contributed to this equivocal result are provided. A description of further assays that could be carried in order to clarify these research questions is discussed.

**Figure 4.3 Cleaved caspase-3 expression in IM-PEN differentiated cells after incubation in conditioned media with or without Netrin-1**

**(A)** Representative images of immunofluorescence staining for NF-H and cleaved caspase-3 on IM-PEN cells cultured at 40.5°C. DAPI was used for nuclei staining. Prior to staining, the cells were cultured at 40.5°C for 4 days. Following day, the cells were incubated in different types of testing media for a further 24 hours. The testing media include DM, CM, 1:1, 1:1 (N100), 1:1 (N500) and 1:1 (z-DEVD-fmk). NF-H was labelled as counter staining for IM-PEN cells. The z-stack images were taken by confocal microscopy using a 20x objective. Scale bar: 100 µm. Images are representative of three independent experiments. **(B)** The number of cleaved caspase-3 immunoreactive neurons was counted over NF-H/DAPI immunoreactive neurons and presented as a percentage of the total number of neurons. The results are represented as mean ± SD (n=3). One-way ANOVA; Tukey's multiple comparisons test; \*\*\* $p < 0.001$  vs DM; n.s groups vs DM.

**Abbreviations:** DM, differentiation medium; CM, conditioned media from CT26 cells; 1:1, the mixed medium of DM and CM in a 1 to 1 ratio; 1:1 (N100), the mixed medium of DM and CM containing 100 ng/mL Netrin-1; 1:1 (N500), the mixed medium of DM and CM containing 500 ng/mL Netrin-1; 1:1 (z-DEVD-fmk), the mixed medium of DM and CM after treating the cells with z-DEVD-fmk; NF-H, neurofilament-heavy chain; n.s, no significance.

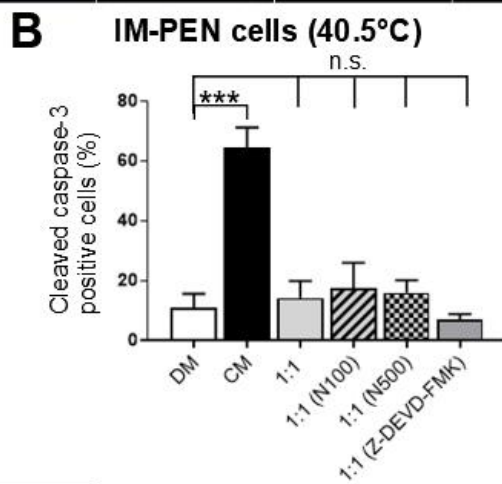
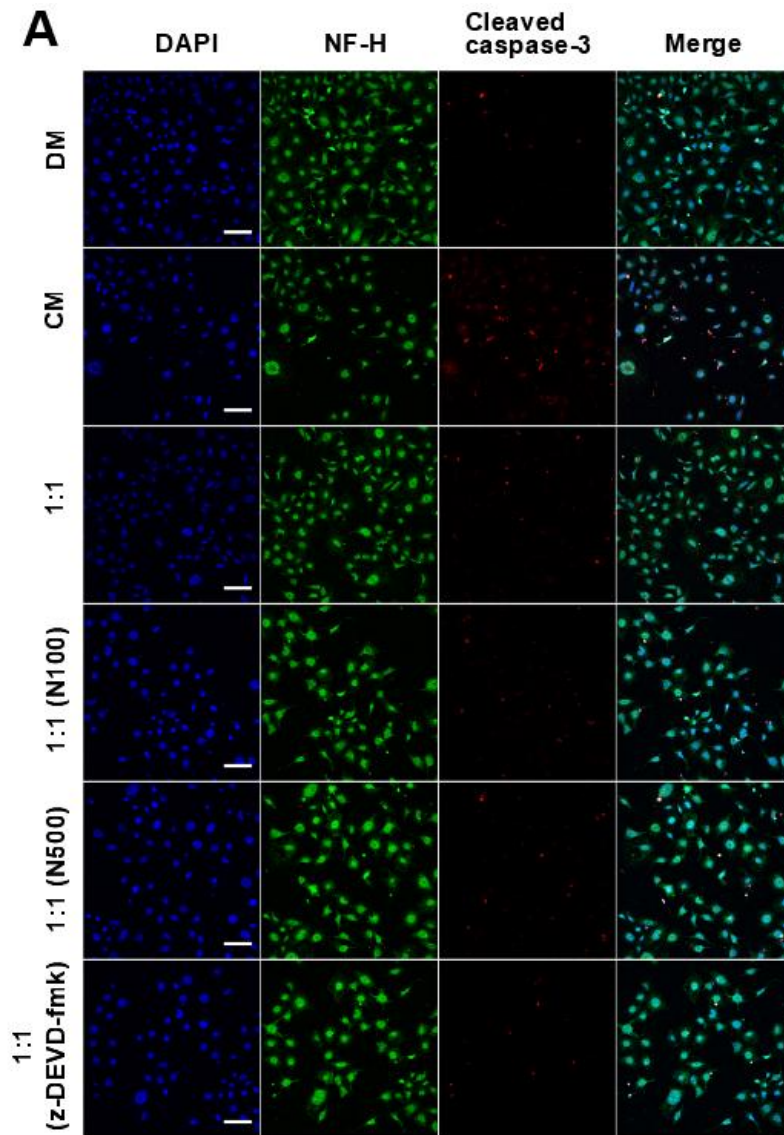


Figure 4.3

## 4.4 Discussion

### 4.4.1 The effect of colorectal cancer conditioned media and Netrin-1 on caspase-3 activation in enteric neuronal precursors

Conditioned media containing secreted factors has been used to identify important biological effects in a range of different cell types. Some factors, that were secreted from cells have been found to play a crucial role in intercellular communication, hence they have been recognised as an effective source for understanding cellular responses [370]. For example, CM containing factors released from embryonic rat retina were found to induce differentiation of adult rat hippocampus-derived neural stem cells [371]. CM collected from astrocytes present at the injury site of a rat brain were shown to mediate selective astrocytic lineage differentiation among adult neural stem/progenitor cells [372].

In this thesis, the effect of CM generated by CT26 murine colorectal cancer cells was examined on the murine post-natal enteric neuronal precursors, IM-PEN cells which were cultured at 33°C. It was demonstrated that CM reduced the viability of enteric neuronal precursor cells after incubation for 24 hours. In the presence of CM, blebbing of the cells was observed. Membrane blebbing is a well-known feature associated with apoptosis. This morphological observation taken together with cell viability test results led us to investigate whether or not the reduced cell viability which was detected was caused by apoptosis.

An assay for testing the presence of active caspase-3 was conducted using an immunofluorescent method on the precursor cells after incubating them with 100% CM or 50% CM (1:1 media). The percentage of cleaved caspase-3 immunoreactive cells was significantly increased when the cells were incubated with CM and 1:1 media. On the other hand, when the cells were incubated in 1:1 media after treatment with caspase-3 inhibitor, z-DEVD-fmk, a marked decrease in the percentage of cells that were positive for cleaved caspase-3 was found. This suggests that the secreted factors from CT26 cells induce active caspase-3 in enteric neuronal precursors.

It is noteworthy that originally the function of active caspase-3 was thought to be associated with apoptosis. However, over a decade ago, caspase-3 has been found to play additional roles in neural development of the CNS, and these other roles are unrelated to apoptotic function [373]. The non-apoptotic functions of caspase-3 activation in neuronal cells have been associated with neural stem cell differentiation [374], synaptic plasticity and dendrite pruning [375]. On the other hand, inhibiting caspase-3 activation was shown to reduce neurite extension and errors in axonal targeting in chick auditory brainstem [376].

If the increased level of active caspase-3 observed in the precursor cells was due to differentiation process, the reduction in cell viability may be due to cell cycle arrest or metabolic state of the cells.

To ensure that whether or not the level of cleaved caspase-3 immunoreactivity in this assay is responsible for mediating apoptosis, additional experiments will be required in the future. For example, assays that allow us to examine DNA fragmentation by propidium iodide (PI)-labelled FACS analysis, a terminal deoxynucleotidyl transferase dUTP nick-end labelling (TUNEL) assay, 8-hydroxyguanosine labelling and caspase-3 activity assay would complement to clarify the results obtained in this thesis.

Notably, when Netrin-1 was introduced in combination with 1:1 media, the viability of the cells was not improved. However, the percentage of cells that were positive for cleaved caspase-3 significantly declined when the cells were incubated in 1:1 media containing a high concentration of Netrin-1 (500 ng/mL). This phenomenon was not observed when a low concentration of Netrin-1 (100 ng/mL) was used.

Similar results have been shown in previous studies, that is, that Netrin-1 can suppress active caspase-3, thereby inhibiting apoptosis. For example, Netrin-1 administration in mice was able to inhibit p53 and caspase-3 activation present in ischemia-induced apoptosis in the brain and kidney injury [377]. Netrin-1 addition was also shown to reduce caspase-3 activity in human endothelial cell apoptosis under serum starvation [224]. Netrin-1 transgenic mice displayed a

lack of caspase-3 activation in diabetes-induced tubular epithelial cell apoptosis [327].

In addition to inhibiting apoptosis, the role of Netrin-1 has recently been found to induce differentiation of various cell types including human embryonal carcinoma cells [254], mammary epithelial cells [378], osteoclast cells [287], neural and glial precursors in the olfactory bulb [379].

It may be possible that no changes in cell viability were observed, when Netrin-1 was applied, because the Netrin-1 may have been affecting the differentiation of precursor cells instead of affecting cell survival. This may partially explain why elongated neurites were observed with those precursors in the presence of Netrin-1. Further tests will be needed to clarify this in the context of CM.

#### **4.4.2 The effect of colorectal cancer conditioned media on caspase-3 activation in differentiated enteric neurons**

An AlamarBlue assay was attempted to determine the effect of CM on the viability of IM-PEN cells cultured at 40.5°C. The immortalised IM-PEN cells underwent differentiation during a period of incubation in DM at 40.5°C. As discussed in chapter 3, when IM-PEN cells were incubated for 4 days at 40.5°C they began to differentiate at an early stage. Terminally differentiated cells were those incubated for 13 days at 40.5°C. Hence, it would be ideal if CM could be tested on IM-PEN cells that were incubated for both 4 days and 13 days at 40.5°C. However, as shown Figure 3.1 C in chapter 3, the viability of the cells which were cultured at 40.5°C declined dramatically during the period from day 1 to day 5. From day 5 onwards, the viability of cells remained steady but at a low level. Because of the significant loss of cell viability in their optimal medium at that temperature, efforts to conduct an AlamarBlue cell viability test on those differentiated cells incubated in CM using a 96-well plate were unsuccessful.

However, it was possible to perform an immunofluorescent assay which was conducted by seeding IM-PEN cells on a poly-D-lysine coated coverslips fitted

in a 6-well plate, and the cells were cultured for 4 days at 40.5°C. This method resulted in the enhanced attachment of the cells to the coated coverslips, thereby there were a sufficient number of cells present on day 4. Those cells which had adhered to the coverslips were then incubated with testing media for a further 24 hours.

Unlike the test conducted on the IM-PEN cells at 33°C, DMEM in the absence of FBS was not chosen as a control medium in the case of IM-PEN cells cultured at 40.5°C. This is because, even though IM-PEN cells were incubated with their optimal DM containing 1% FBS, instances of cell death were noticed during the differentiation process on incubating day 4 and 5 at 40.5°C. For this reason, the CM was combined with a fresh DM in a 1:1 ratio, indicated here as 1:1, and introduced to the IM-PEN cells on day 5 at 40.5°C. After incubation for 24 hours, the immunoreactivity of cleaved caspase-3 was examined on those cells which began to differentiate at the early stage.

The results showed that the cells which were incubated in CM, as opposed to DM, showed a significant increase in the percentage of neurons positive for cleaved caspase-3. However, when the 1:1 media were introduced to the cells, the percentage of cleaved caspase-3 immunoreactive neurons was shown to be similar to the percentage that was shown in optimal DM. This observation indicated that CM induces neither cell death nor enhances cell survival. If CM was causing the neuronal death, a greater level of cleaved caspase-3 immunoreactivity would be expected in the case of cells incubated in 1:1 media as compared to the ones in DM. However, this result was not observed. Therefore, the apparent elevated cleaved caspase-3 immunoreactivity that was seen in the cells incubated with CM alone would be mostly likely due to media incompatibility.

A further plausible alternative explanation of these results is that the composition of DM and/or the factors, which were secreted by neurons during the incubation in 1:1 media (DM:CM), may be able to counteract the activating apoptotic pathway of the neurons that was being induced by CM.

GDNF is a growth factor that promotes neuronal cell survival and differentiation, and it was included in the DM medium for IM-PEN cells. The characterisation studies of IM-PEN cells conducted by Anitha *et al.* indicated that the IM-PEN cells cultured at 39°C, as opposed to the ones cultured at 33°C, showed a notable increase in Ret expression by RT-PCR [260]. Ret is a tyrosine kinase receptor for GDNF. When one of the co-receptors, GFR $\alpha$ 1-4, forms a complex with Ret and GDNF, Ret activates intracellular signalling pathways including the PI3K/Akt pathway and the Ras/ERK1/2 MAPK pathway. The former pathway is shown to modulate cell survival and the latter is involved in neuronal differentiation [380, 381]. The work of Burke *et al.* [382] indicated that GDNF aids the viability of dopamine neurons by inhibiting natural apoptosis which occurs in the substantia nigra during the postnatal period. It is conceivable that the presence of GDNF in DM may have prevented neurons from undergoing apoptosis induced by CM.

Studies conducted by Noda *et al.* [383] revealed that conditioned media produced by culturing human lung cancer cell line, HARA-B cancer cells was able to inhibit proliferation of primary culture neurons derived from mouse cerebral cortex. However, conditioned media generated by culturing primary mouse microglia attenuated HARA-B cancer cell proliferation. Microglia are known as a type of neuroglial cells located in the CNS. Importantly, when microglial cells were added into the co-culture of cancer cells and neurons, microglial cells were able to rescue the disturbed neuronal survival. Hence, the authors suggested that the microglia has a neuroprotective role. However, factors secreted from microglia and providing neuroprotection are yet to be determined.

In addition to the neuroprotective role of microglia in the CNS, enteric glial cells in the ENS have also been found to protect enteric neurons [384]. The co-culture experiments conducted by Abdo *et al.* have demonstrated that the increased level of active caspase-3 immunoreactivity found in the neuroblastoma cells, caused by dopamine neurotoxicity, actually declined when neuroblastoma cells were co-cultured with enteric glial cells.

Also, a similar result was observed when neuroblastoma cells displaying dopamine-induced neurotoxicity, were incubated in CM generated by enteric

glial cells. The authors have found that glutathione released from enteric glial cells is a factor that inhibits neuronal cell death induced by oxidative stress. However, the neuroprotective role of glutathione was only effective when oxidative stress was occurring in the presence of reduced glutathione [385].

In chapter 3 of this thesis, IM-PEN cells cultured at 33°C and 40.5°C are reported to have shown positive GFAP immunoreactivity, suggesting that there was an enteric glial cell population present in the IM-PEN cell line. Based on the co-culture studies of Abdo *et al.*, one might speculate that some factors released from the enteric glial cells-derivative of IM-PEN precursors in the presence of CM may have played a neuroprotective role. Further work will be necessary to identify those factors secreted from IM-PEN cells in the presence of CM.

Alternatively, if the significant increase in the cleaved caspase-3 immunoreactivity shown in the presence of CM alone was due to media incompatibility, this means then the CM, as represented in 1:1 media, may not be responsible for the level of cleaved caspase-3 immunoreactivity shown in those differentiated cells.

If so, this *in vitro* result is in agreement with earlier clinical studies conducted by Kozłowska *et al.* [369]. Their immunohistochemistry analysis was performed on specimens removed from CRC patients. The myenteric neurons were labelled with active caspase-3 and caspase-8 antibodies in the tissue sections that were close to tumour invasion sites as compared to those that were distant from the tumour. It was found that there was a similar level of caspase-8 immunoreactivity in those sections that were either distal or close to the tumour invasion sites. Also the same phenomenon was observed with active caspase-3 immunoreactivity, suggesting that the atrophy of the myenteric plexus noticed in CRC invaded tissues was not caused by apoptosis. The authors also examined the possibility that necrosis may have been responsible for the observed atrophy of the myenteric plexus. However, lack of mononuclear cell infiltration and random macrophage distribution around the invasive tumour sites did not support their hypothesis. Hence, the authors also concluded that necrosis was not the process explaining the atrophy of the myenteric plexus in the CRC invaded tissues. Based on those observations, the authors have drawn our

attention to the importance of understanding the relationship of neuropeptides present in the myenteric plexus and thus the role played by neuropeptides in cancer progression.

In this thesis, the effect of Netrin-1 was examined on IM-PEN cells cultured at 40.5°C by adding a concentration either of 100 ng/mL or 500ng/mL of Netrin-1 in the 1:1 media. However, there was no apparent difference in the percentage of cleaved caspase-3 immunoreactive neurons that were incubated in the 1:1 media in the absence or presence of Netrin-1. Further studies are required to demonstrate the effect of Netrin-1 in the context of neurons and cancer interaction. This is addressed in Chapter 5 using an *in vivo* model.

As shown *in vitro* studies performed by Noda *et al.* [383] and Abdo *et al.* [385], direct co-culturing CT26 cells with IM-PEN cells may be a valuable investigative tool for the future. Also, Introducing Netrin-1 into this co-culturing system could bring complementary findings. If factors such as media compatibility and culture temperature can be compromised between IM-PEN cells and CT26 cells, then the co-culture system will advance our understanding of the interaction between enteric neurons and colorectal cancer. Advances in this area could also lead to a greater understanding of the role played by Netrin-1 in the context of the interacting enteric neurons and the cancer.

## 4.5 Summary

Many studies have reported that colorectal cancer patients receiving chemotherapy suffer from neuropathic symptoms such as sensations of numb and tingling extremities, sensitivity to cold and heat, stomach pain, constipation and diarrhoea [386-388]. These neuropathic symptoms were initially thought to be side effects caused by the chemotherapy-induced neurotoxicity [364, 389]. However, clinical studies have found that the cancer itself actually plays a subclinical role in neuropathy [367-369]. Factors contributing to the neuropathy that were caused directly from cancer are yet to be elucidated.

In this thesis, the effects of CM containing secreted factors from colorectal cancer cells on enteric neuronal cells were examined. The results showed that CM reduced the viability of enteric neuronal precursor cells. The increase in the

immunoreactivity of active caspase-3 was found when the cells were incubated with CM for 24 hours. However, a significant decrease in the immunoreactivity of active caspase-3 was observed when the cells were incubated with CM in the presence of Netrin-1 at a high concentration, 500 ng/mL, but not at a low concentration, 100 ng/mL.

Introducing CM to enteric neurons that were differentiated at an early stage did not appear to affect the level of active caspase-3 immunoreactivity. In addition, no changes in the active caspase-3 immunoreactivity were found in differentiated neurons when they were incubated in CM containing Netrin-1 at both high and low concentrations.

The expression of active caspase-3 in neuronal precursors could represent the induction of neuronal differentiation instead of activating apoptosis. Therefore, additional experiments are required to clarify the meaning of having active caspase-3 expression present in neuronal precursors under the condition of CM.

Once the effects of colorectal cancer cells on enteric neurons are better understood, this may shed light on the development of novel therapeutic strategies for treating colorectal cancer patients.

## Chapter 5

---

**Netrin-1 treatment in an orthotopic colorectal cancer mouse model: pilot study**

## 5.1 Introduction

The enteric nervous system (ENS) is essential for the proper functioning of the digestive tract [7]. The ENS is the largest division of the autonomic nervous system that innervates the wall of the gastrointestinal tract (GIT). It is capable of controlling local functions of the GIT, independent of extrinsic signals from the central nervous system (CNS). Such functions include intestinal wall movement, water/electrolyte absorption and secretion, and local blood supply regulation [7, 13, 184].

The ENS is composed of two major ganglionated plexuses: the submucosal plexus and myenteric plexus [390]. The submucosal plexus lies within the connective tissue of the submucosa, and regulates secretion of fluid and blood flow. The myenteric plexus lies between the longitudinal and circular muscle layers, and plays a role in gut motility by controlling the activity of the smooth muscle cells. The ganglia containing enteric neurons are connected by internodal strands (bundles of nerve cell processes), and hence form a network of two ganglionated plexuses in the digestive tract [17, 19, 390, 391].

Changes in ENS structure have been frequently reported in many colonic diseases, such as inflammatory bowel disease and Hirschsprung's disease [17, 184]. In addition, the work of Godlewski examining human colorectal cancer (CRC) tissues has revealed that enteric innervation was disrupted, and that enteric neurons have disappeared near the region of the tumour [368]. It was suggested that such damage to the ENS, when it occurs during the course of intestinal carcinoma, may lead to the impairment of normal intestinal function. As a consequence, these deficits may be responsible for CRC patients experiencing clinical symptoms, such as constipation and diarrhoea [368]. Furthermore, these clinical symptoms have also been manifested in CRC patients undergoing chemotherapy treatment [392]. This could be due to the fact that commonly used anti-cancer chemotherapeutic agents including oxaliplatin, cisplatin and 5-fluorouracil, have been associated with neurotoxicity side-effects, such as enteric neuropathy [393, 394], paresthesia and paralysis [395]. However, to date, in order to manage neurotoxicity, chemotherapy dose-limitation has been primarily used as a solution to the problem for patients [396]. For this reason, identification and/or development of neuroprotective

treatments is imperative, as such treatments would reduce neurotoxicity, improve tolerability to chemotherapy, and the quality of life for CRC patients.

The most ideal candidates for neuroprotection would be factors that induce axonal growth, and/or decrease neuronal death. One such candidate, Netrin-1, a secreted chemotrophic molecule that mediates axonal outgrowth and axon orientation [397], could be an effective neuroprotectant.

Netrin-1 is an evolutionarily conserved laminin-related protein that is diffusible in the extracellular matrix [124]. The major role of Netrin-1 has been shown to be a neuronal guidance cue, either a chemo-attractant or chemo-repellant, during the development of the CNS. These two opposite roles of Netrin-1 are found to be dependent upon the receptor to which Netrin-1 binds. It has been shown that in response to Netrin-1 binding, the DCC receptors mediate chemo-attractive activity [125, 126, 398], whereas the homo-dimerised UNC5H receptors, or the hetero-dimerized DCC and UNC5H receptor complex, is found to mediate a chemo-repulsive activity [125, 126, 174]. The chemo-attractive role of Netrin-1 and DCC has been revealed in the developing ENS. However, their expression and their role have yet to be elucidated in the *adult* ENS.

Further to the chemotropic role of Netrin-1 in the neuronal tissues, subsequent discovery of Netrin-1 expression in non-neuronal tissues has highlighted that Netrin-1 serves as a cell survival factor [126]. This role of Netrin-1 has been further investigated in various tumour cell models, and it was revealed that Netrin-1 is involved in regulating tumourigenesis [126]. This is because DCC and UNC5H receptors are found to be a functional family of dependence receptors. Such receptors are able to determine the cellular status depending on the ligand availability; either cellular survival in the presence of ligand or cell death in the absence of ligand [126, 161, 234].

In CRC, down-regulation of DCC and UNC5H receptors has been observed [399, 400]. On the other hand, decreased Netrin-1 expression has been reported in CRC except for the case where increased Netrin-1 expression was noted in inflammation-induced colorectal cancer [139].

However, the effect of Netrin-1 in the adult ENS, in the context of CRC, has not been investigated. The ENS is embedded in the wall of the GIT, hence the neuronal and non-neuronal tissues are inseparable in the gut.

Netrin-1 could be a neuroprotective factor for damaged ENS under the CRC condition, it is also important to consider the notion that the effect of Netrin-1 may be associated with tumourigenesis. Here, an *in vivo* study was conducted to investigate the effect of Netrin-1 treatment on (1) CRC progression and (2) expression of Netrin-1 and its receptor in the myenteric plexus in the colon from healthy and CRC mice.

## **5.2 Materials and methods**

### **5.2.1 Animals**

Male Balb/c mice aged 6-10 weeks (18-25 g) were purchased from the Animal Resources Centre (WA, Australia). Mice were housed in a controlled environment where autoclaved cages, bedding, food and water were provided. They were maintained on a daily 12-hour dark and light cycle at 22°C. Mice were acclimatised for a minimum of 3 days prior to commencing any experiments. All surgical and experimental procedures were conducted in accordance with the guidelines approved by the Victoria University Animal Experimentation Ethics Committee (AEETH21/11).

### **5.2.2 Cell culture**

CT26 cells were cultured in Dulbecco's Minimal Essential Medium (Life technologies) supplemented with 10% heat/inactivated fetal bovine serum (ThermoFisher), and they were maintained at 37°C humidified incubator with 5% CO<sub>2</sub>. CT26 cells were passaged four times before harvesting from 75-80% confluent cultures by a brief exposure to TrypLE Express. Cells were washed with phosphate-buffered saline (PBS pH7.4; Gibco, Life technologies) and the viable cells were then counted ( $1 \times 10^6$  cells per mouse) by trypan blue exclusion using a hemocytometer. Cells were resuspended in Matrigel (BD Biosciences) on ice. Mycoplasma test (Lonza) for CT26 cells was conducted prior to harvesting cells.

### **5.2.3 Orthotopic colorectal cancer mouse model**

All the surgical instruments were autoclaved and the surgical procedures were performed in sterile environment. Mice were anaesthetised with the combination of ketamine (80 mg/kg) and xylazine (10 mg/kg) prior to surgery. The abdominal fur was clipped around the surgical area and Betadine was applied to prevent a topical infection. The abdomen was covered by the sterile drape in order to avoid contamination of the incision. Approximately a 1.5 cm long midline skin incision along the lower abdomen was made. The caecum was gently pulled out from the incision with a pair of forceps and hydrated the exteriorised caecum with 0.9% sodium chloride during the entire procedure. Using a binocular surgical microscope the CT26 cells ( $1 \times 10^6$ ) that were resuspended in 25  $\mu$ L of Matrigel (BD Biosciences) on ice, were injected in the caecal wall using a 27G insulin syringe. The caecum was returned to the abdominal cavity and the incision was sutured. Temgesic (0.05 mg/kg) and Carprofen (5 mg/kg) were administered post-operation. Before returning the mice to the animal house, the mice were placed on heating pads and carefully monitored until they recovered from the anaesthesia.

### **5.2.4 Netrin-1 administration**

The tumour-bearing mice were grouped into; (1) saline-treated (vehicle control; n=4), (2) 1  $\mu$ g of Netrin-1-treated (n=3) and (3) 4  $\mu$ g of Netrin-1-treated (n=4). Each group received 0.2 mL treatment via intraperitoneal (i.p.) injection. The recombinant mouse Netrin-1 protein (R&D Systems) group was given either 1 or 4  $\mu$ g per mouse. Vehicle group was given saline. Each mouse received this treatment daily at a set time for a period of 6 days. On the 6<sup>th</sup> day, mice were euthanised by cervical dislocation 5 hours after given the final Netrin-1 injection.

### **5.2.5 Enzyme-linked immunosorbent assay**

The levels of recombinant mouse Netrin-1-his tag protein in plasma were determined using a His-Tag Protein ELISA Kit (Cell Biolabs), according to the manufacturer's instructions. All measurements were made in duplicate in a single plate for an absorbance reading by a microplate reader (Varioskan Flash, Thermo Fisher Scientific).

### **5.2.6 Hematoxylin and eosin staining**

The paraffin embedded tissues were sectioned at 5 µm thickness. The tissue sections were stained for a standard hematoxylin and eosin (H&E) staining. After baking the sections for 1 hour at 65°C, the sections were immersed in xylene (2 x 5 min), 100% ethanol (2 x 3 min), 90% ethanol (2 min), 70% ethanol (2 min), rinsed in distilled water, hematoxlin (5 min), rinsed in distilled water, acid alcohol (1 sec), Scott's tap water (1 min), eosin (3 sec), rinsed in tap water, 100% ethanol (2 x 1 min), xylene (2 x 5 min), and mounted with distyrene plasticizer xylene, DPX (Sigma).

### **5.2.7 3,3'-diaminobenzidine immunohistochemistry**

The paraffin embedded tissues were sectioned at 5 µm thickness. The tissue sections were baked for 1 hour at 60°C, deparaffinised with xylene (2 x 5 min) and rehydrated in graded ethanol concentration; 100% ethanol (2 x 5 min), 70% ethanol (5 min), 50% ethanol (5 min), and 30% ethanol (5 min). The sections were permeabilised using 0.1% TritonX-100. Antigen retrieval was conducted using citrate buffer pH6 at 95°C for 20 mins. Endogenous peroxidase was quenched with 0.3% (v/v) H<sub>2</sub>O<sub>2</sub> in PBS solution. Blocking buffer (mouse IgG blocking reagent followed by 2.5% normal horse serum) was used according to the manufacturer's recommendations (M.O.M. kit, Vector Laboratories). The sections were incubated with the primary antibodies against 6x-His tag (1:200, ab18184, Abcam), Ki67 (1:1000, ab15580, Abcam) and CD31 (1:1000, ab28364, Abcam) at 4°C overnight. Following 3 x 10 min washes in PBS-T (tween 20, 0.05%), they were incubated with the secondary antibody according to the manufacturer's recommendations (ImmPRESS Anti-Rabbit IgG reagent, Vector Laboratories). Following 3 x 10 min washes in PBS-T, the tissue sections were developed using 3,3'-diaminobenzidine (DAB) detection kit (DAB Peroxidase Substrate, Vector Laboratories). After the final washing step, the sections were counterstained with hematoxylin and dehydrated with graded ethanol concentration; 30% ethanol (2 min), 50% ethanol (2 min), 70% ethanol (2 min), and 100% ethanol (2 min) followed by xylene (2 x 5min). The sections were mounted with DPX.

### 5.2.8 Wholemout immunofluorescence

The intermediate to distal colon tissues were removed from mice. The tissues were placed in a PBS solution containing an L-type calcium channel blocker, nifedipine (3  $\mu$ M) that was supplied with carbogen for 20 min. The tissue sections were cut open along the mesenteric border, maximally stretched and pinned into a silicon coated dish. Tissues were fixed in a Zamboni's fixative (2% formaldehyde and 0.2% picric acid) solution at 4°C overnight. The tissues were then washed for 3 x 10 min in dimethyl sulfoxide (Sigma-Aldrich) followed by 3 x 10 min in PBS to remove fixative. Subsequently tissues were dissected to expose myenteric plexus and they were incubated with 10% donkey serum (Merck Millipore) diluted in 0.1% PBS-tween 20 for 1 hour at RT. Tissues revealing myenteric plexus were incubated with primary antibodies (**Table 5.1**) at 4°C overnight. When double- or triple-labelling was conducted in the wholemount preparations, the primary antibodies that were raised in different species were used. Following 3 x 10 min washes in a 0.1% PBS-tween 20 solution, tissues were labelled with different fluorophores donkey secondary antibodies, listed in **Table 5.2**, for 1 hour at RT. Tissues were washed 3 x 10 min in PBS-tween 20 (0.1%). Before the final washing step, the fluorescent nucleic acid stain 4'-6-diamidino-2-phenylindole (DAPI, 14 nM; ThermoFisher, D1306) was introduced to the tissues for 1 min. Tissues were mounted onto glass slides with fluorescent mounting medium (DAKO). Negative control lacking primary antibodies was conducted for the antibodies used in this study.

**Table 5.1 List of primary antibodies used in immunofluorescence assays**

Primary antibody	Host species	Source	Catalogue number	Dilution
PGP9.5	Rabbit	Merck Millipore	AB1761-I	1:1000
DCC	Goat	Santa Cruz (A-20)	Sc-6535	1:500
Netrin-1	Rabbit	Santa Cruz (H-104)	Sc-20786	1:500
$\beta$ -Tubulin III	Chicken	Abcam	Ab107216	1:1000
ChAT	Goat	Merck Millipore	AB144P	1:500
nNOS	Goat	Novus Biologicals	NB100-858	1:500

**Table 5.2 List of secondary antibodies used in immunofluorescence assays**

Secondary antibody	Source	Catalogue number	Dilution
Donkey anti-goat rhodamine	Jackson ImmunoResearch Laboratories	705-295-147	1:300
Donkey anti-mouse FITC	Merck Millipore	AP182F	1:300
Donkey anti-rabbit rhodamine	Jackson ImmunoResearch Laboratories	AP182R	1:300
Donkey anti-rabbit FITC	Merck Millipore	AP182F	1:300
Donkey anti-goat FITC	Merck Millipore	AP180F	1:300
Donkey anti-chick FITC	Merck Millipore	AP194F	1:300

### 5.2.9 Imaging

The images of wholemount preparations were taken using an Eclipse Ti confocal laser scanning microscope (Nikon, Lidcombe, Australia) with NIS element software. Fluorophores were visualised using a 488 nm excitation filter

for fluorescein isothiocyanate (FITC), a 561 nm excitation filter for Alexa 594, a 405 nm excitation filter for DAPI, and a 640 nm excitation filter for Alexa 647. Three-dimensional (Z-series) images of the wholemount preparations were acquired at a normal thickness of 0.5  $\mu\text{m}$ , with 20x (dry, 0.75) or 40x (oil immersion, 1.3) or 100x (oil immersion, 1.45) objective lenses. The images of DAB-IHC and H&E staining sections were taken using an Olympus BX53 microscope (Olympus, Notting Hill, Australia) with CellSense software.

#### **5.2.10 Neural cell counting and quantitative analysis**

The immunoreactive neuronal cell counting was performed according to the method published previously [401]. The immunoreactivity (IR) of a deleted in colorectal cancer (DCC), Netrin-1, neuronal nitric oxide synthase (nNOS) and cholin acetyltransferase (ChAT) positive neurons was assessed against IR of  $\beta$ -Tubulin III or protein gene product 9.5 (PGP9.5) positive neurons in the myenteric plexus in total area of  $2\text{mm}^2$ . Eight randomly chosen images per preparation were taken with a 20x objective. The acquired images were captured with identical exposure setting. The co-localisation of Netrin-1/nNOS and Netrin-1/ChAT positive neurons was counted manually per ganglion in images (512 x 512 pixels per image) using ImageJ plugin. (average 30 ganglia in total area of  $2\text{mm}^2$  per preparation). Thresholding for each channel was determined based on a single fluorophore labelling, and that calibrated threshold was applied to analyse double-labeling preparations as well as strong and weak intensity using MatLab software (The Mathworks, USA).

#### **5.2.11 Statistical analysis**

Results are presented as mean  $\pm$  SD from 3 to 4 animals or minimum of three replicate per condition. GraphPad Prism 7 software was used for statistical analysis. One-way ANOVA followed by Tukey's multiple comparisons test or Kruskal-Wallis and Dunn's multiple comparison tests; two-way ANOVA followed by Tukey's multiple comparisons test were used;  $p$  value less than 0.05 was considered significant. The levels of statistical significance are denoted by \* $p < 0.05$ , \*\* $p < 0.01$  and \*\*\* $p < 0.001$ .

## 5.3 Results

### 5.3.1 Netrin-1 treated colorectal cancer orthotopic mouse model

The orthotopic mouse model of CRC has been able to replicate features shown in the human CRC condition. Such features, including regional and distal organ metastasis (i.e. lymph-node, liver, lung and abdominal metastases) have frequently been reported in previous studies involving the orthotopic CRC mouse model [402, 403]. The technique used in this study involved injecting a cancer cell suspension into the caecal wall. The images from **Figure 5.1** represent the surgical procedure that we used to generate the orthotopic CRC mouse model. A suspension of CT26 ( $1 \times 10^6$ ) cells was implanted into the caecum wall of a syngeneic Balb/c mouse under anesthesia. The CT26 cell line is a murine colon carcinoma that shares a molecular hallmark with human colorectal carcinoma cells [404]. Following the successful injection of CT26 cells into the caecal wall, the formation of a fluid-filled blister called a bulla was visible as shown in **Figure 5.1 E**. The presence of the bulla indicates that there was no accidental intra-luminal injection and/or post-injection spillage of the cells during the procedure. In this study, a single injection site was made in the caecal wall, and the caecum was returned to the abdominal cavity. One mouse was euthanized due to a surgery complication, hence no assessment was available in this case. The tumour implantation for the remaining eleven mice was successful.

A pilot assay for Netrin-1 treatment on the orthotopic CRC mouse model was conducted. On the seventh day following surgery, tumour-bearing mice were given different types of treatments. The treatments include saline (vehicle control), a low concentration of Netrin-1 (1  $\mu\text{g}/\text{mouse}$ ), and a high concentration of Netrin-1 (4  $\mu\text{g}/\text{mouse}$ ). Mice were injected daily with one of the three types of treatment intraperitoneally for a period of six days. In order to avoid any possible bias, littermates per cage were injected with a different treatment instead of allocating a particular treatment to all littermates from a particular cage.

To the best of our knowledge, this is the first study involving the introducing a recombinant mouse Netrin-1 protein into orthotopic CRC mice, instead of using

transgenic mice. Furthermore, introducing Netrin-1 via intraperitoneal (i.p.) injection as a route of administration has not been widely conducted in literature. Therefore, in the next section, data involving the investigation of the levels of Netrin-1 present in the plasma of those CRC mice are presented.

**Figure 5.1 Surgical procedures for orthotopic mouse model of colorectal cancer**

**(A)** A mouse was anaesthetised and the abdominal fur was clipped. **(B)** The mouse was covered with a sterile drape and a midline laparotomy was conducted and **(C)** caecum was exteriorised from the abdominal cavity. **(D)** CT26 ( $1 \times 10^6$ ) cells resuspended in 25  $\mu\text{L}$  of cold Matrigel were injected into the caecal wall using an insulin syringe. **(E)** A successful injection of CT26 cells showed bulla formation. **(F)** The caecum was returned to the abdominal cavity and the incision was sutured.

## Orthotopic colorectal cancer mouse model

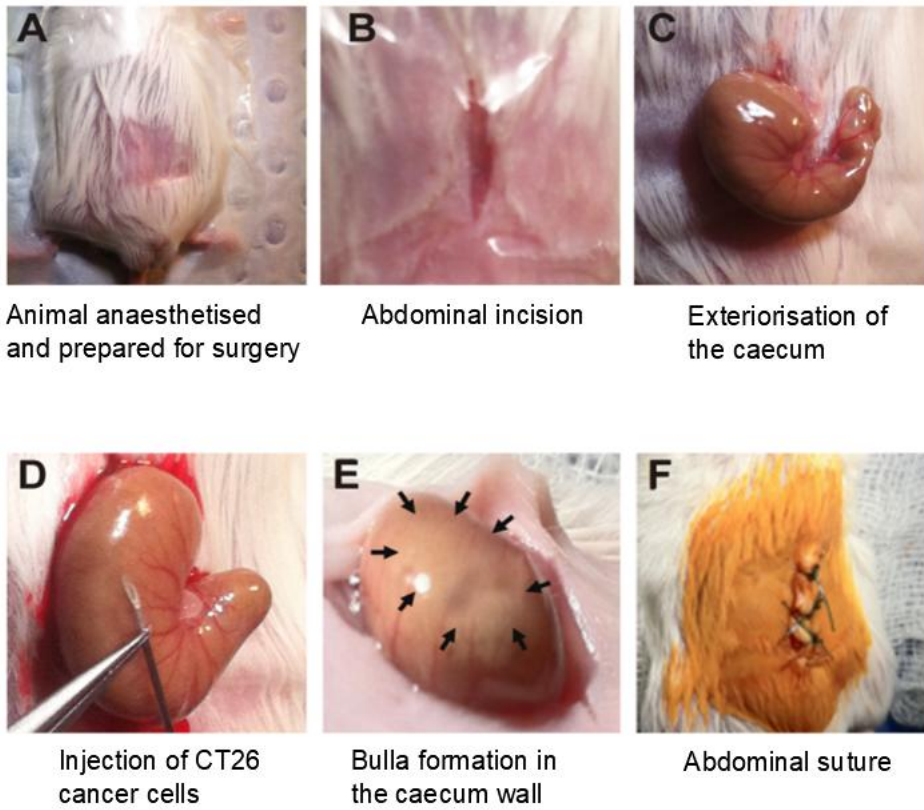


Figure 5.1

### 5.3.2 Recombinant mouse Netrin-1 protein in plasma

In previous *in vivo* studies, the recombinant mouse Netrin-1 protein was often administered intravenously instead of intraperitoneally. Hence, there is lack of information concerning the bioavailability of Netrin-1 via i.p. injection in mice. To determine a desired concentration of Netrin-1 for administration by i.p. injection, the level of Netrin-1 in plasma was examined using an ELISA assay (**Figure 5.2**). The recombinant mouse Netrin-1 that was used in this study has a ten-His tag conjugated to its C-terminus. In order to distinguish between the endogenous Netrin-1 and exogenously introduced Netrin-1, a His-tag ELISA was performed.

There was a significant increase in the level of Netrin-1-His tag in the plasma of the CRC mice treated with 4  $\mu\text{g}$  Netrin-1 ( $2.63 \pm 0.60 \mu\text{g/mL}$ ,  $n=4$ ,  $p<0.01$ ) when compared to the CRC mice treated with saline ( $0.02 \pm 0.01 \mu\text{g/mL}$ ,  $n=4$ ). Also, there was a marginally significant increase in the level of Netrin-1-His tag in the plasma of the CRC mice treated with 4  $\mu\text{g}$  of Netrin-1 ( $2.63 \pm 0.60 \mu\text{g/mL}$ ,  $n=4$ ) when compared to the CRC mice treated with 1  $\mu\text{g}$  of Netrin-1 ( $0.48 \pm 0.31 \mu\text{g/mL}$ ,  $n=3$ ,  $p=0.0501$ ). These data suggest that almost half of the initial concentration of Netrin-1 appeared to be present in the circulation of the mice following the initial Netrin-1 i.p. injection.

It has long been established that substances deposited into the peritoneal cavity will first be absorbed into the portal circulation [405]. Also, it has been reported that liver tissues express an endogenous Netrin-1 as well as Netrin-1 receptors [406]. Therefore, the liver tissues were examined to see whether or not there was any deposit of Netrin-1-His tag in mice. The DAB-IHC results indicated that Netrin-1-His tag was shown in the liver tissues from the mice that were treated with both 1  $\mu\text{g}$  and 4  $\mu\text{g}$  of Netrin-1 (**Figure 5.3**). Positive DAB staining was prominent around the realm of the portal vein area in the liver tissues from the mice treated with Netrin-1. Taken together, these data suggest that recombinant mouse Netrin-1 introduced into these mice had circulated in the blood system.

**Figure 5.2 The levels of His-tagged Netrin-1 in plasma from Netrin-1-treated mice**

The concentrations of his-tagged Netrin-1 were measured by competitive ELISA ( $R^2=0.9822$ ). Duplicates per assay and two biological repeats were conducted. One-way ANOVA followed by Kruskal-Wallis and Dunn's multiple comparison tests for statistical analysis. A significant increase in the level of His-tagged Netrin-1 in the CRC mice treated with 4  $\mu\text{g}$  of N1 in comparison to the CRC mice treated with saline (\*\* $p<0.01$ ).

**Abbreviations:** CRC, colorectal cancer; N1, Netrin-1.

### His-tagged Netrin-1 plasma level

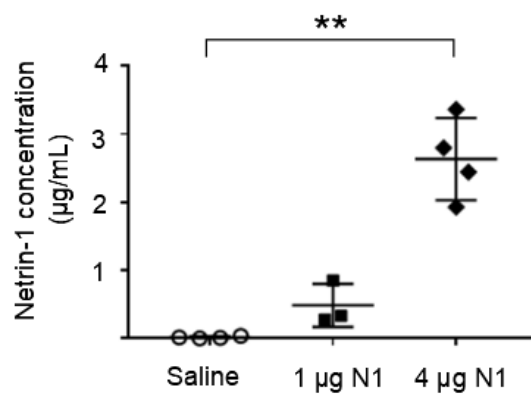


Figure 5.2

**Figure 5.3 3,3'-diaminobenzidine immunohistochemistry of liver tissues from the CRC mice treated with Netrin-1**

The liver tissues removed from the CRC mice, that were treated with **(A)** saline (n=4 mice), **(B)** 1 µg of N1 (n=3 mice), and **(C)** 4 µg of N1 (n=4 mice), were stained with anti-His antibody-DAB (brown). Haematoxylin was used as a counter stain. Scale bar: 100 µm.

**Abbreviations:** DAB, 3,3'-diaminobenzidine; CRC, colorectal cancer; N1, Netrin-1.

## Liver tissues

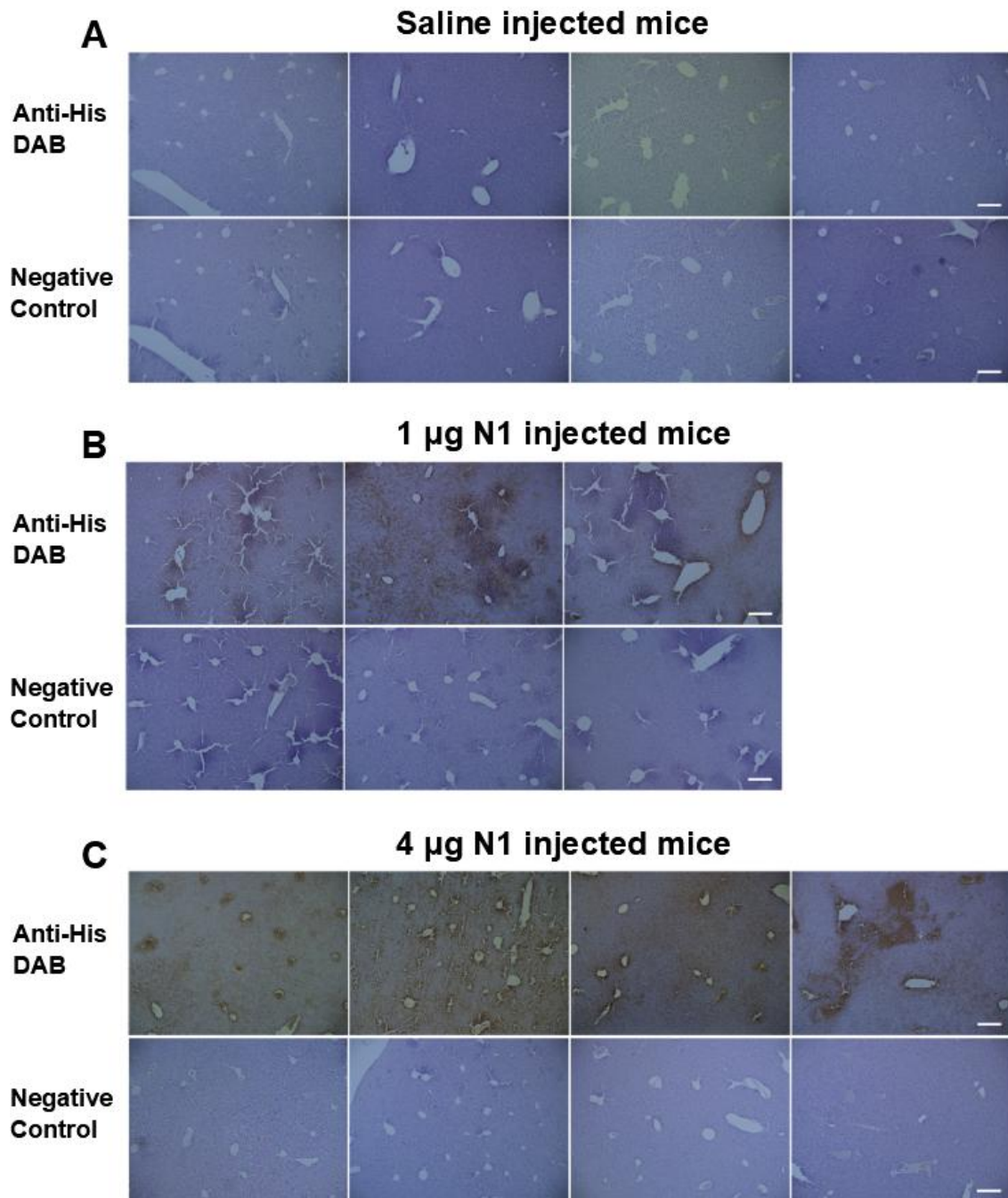


Figure 5.3

### 5.3.3 Primary tumour growth in the caecum with or without Netrin-1 treatment

To investigate whether addition of Netrin-1 enhances tumour growth and/or metastasis of the colorectal cancer, mice were firstly implanted with CT26 tumour cells on their caecum wall. After allowing the tumour to grow for 6 days, either a low or high concentration of Netrin-1 (1  $\mu\text{g}$  or 4  $\mu\text{g}$ , respectively) was injected intraperitoneally into those tumour-bearing mice for a period of six days. **Figure 5.4 A** shows images of the caecum from individual tumour-bearing mice treated with saline or 1  $\mu\text{g}$  of Netrin-1 or 4  $\mu\text{g}$  of Netrin-1. The tumour polyps that were developed from an initial single CT26 injection site on caecum wall were counted (**Figure 5.4 B**). The mice treated with 4  $\mu\text{g}$  of Netrin-1 ( $3.7 \pm 2.3$ ,  $p < 0.05$ ), but not the mice treated with 1  $\mu\text{g}$  of Netrin-1 ( $10.3 \pm 7.8$ ), had a significantly lower number of tumours polyps on their caecum when compared to saline treated vehicle control mice ( $22.3 \pm 7.0$ ). In this pilot assay, the three statistical numbers for the mice treated with 1  $\mu\text{g}$  of Netrin-1 were accountable due to one mouse loss from the surgical complication.

To examine the characteristics of CT26 tumour growth on the caecal wall in the presence or absence of Netrin-1 treatment, the caecum tissue from each mouse was harvested for the H&E staining. The three out of four CRC mice treated with saline exhibited not only growth of the tumours inoculated in their caecum wall but also tumour cells were aggressively invaded into lamina propria, submucosa and muscle layers (**Figure 5.5 A 1a-1d**). Metastasis of the tumour cells into the colon tissues was evident in all of the CRC mice that received saline treatment (**Figure 5.5 A 2a-2d**). The caecum tissues from the CRC mice treated with 1  $\mu\text{g}$  of Netrin-1 also showed an invasive tumour growth in their caecum wall (**Figure 5.5 B 3a-3c**). However, only one in three CRC mice treated with 1  $\mu\text{g}$  of Netrin-1 showed metastasis of the tumour cells from the caecal wall to the colon tissue (**Figure 5.5 B 4c**). On the other hand, the tumour growth appeared to be much less invasive in the caecum tissues from the CRC mice treated with 4  $\mu\text{g}$  of Netrin-1 (**Figure 5.5 C 5a-5c**), except for one mouse which exhibited a massive tumour growth (**Figure 5.5 C 5d**). In addition, there was no obvious infiltration of tumour cells into the colon tissues in three out of four CRC mice treated with 4  $\mu\text{g}$  of Netrin-1 (**Figure 5.5 C 6a-6d**).

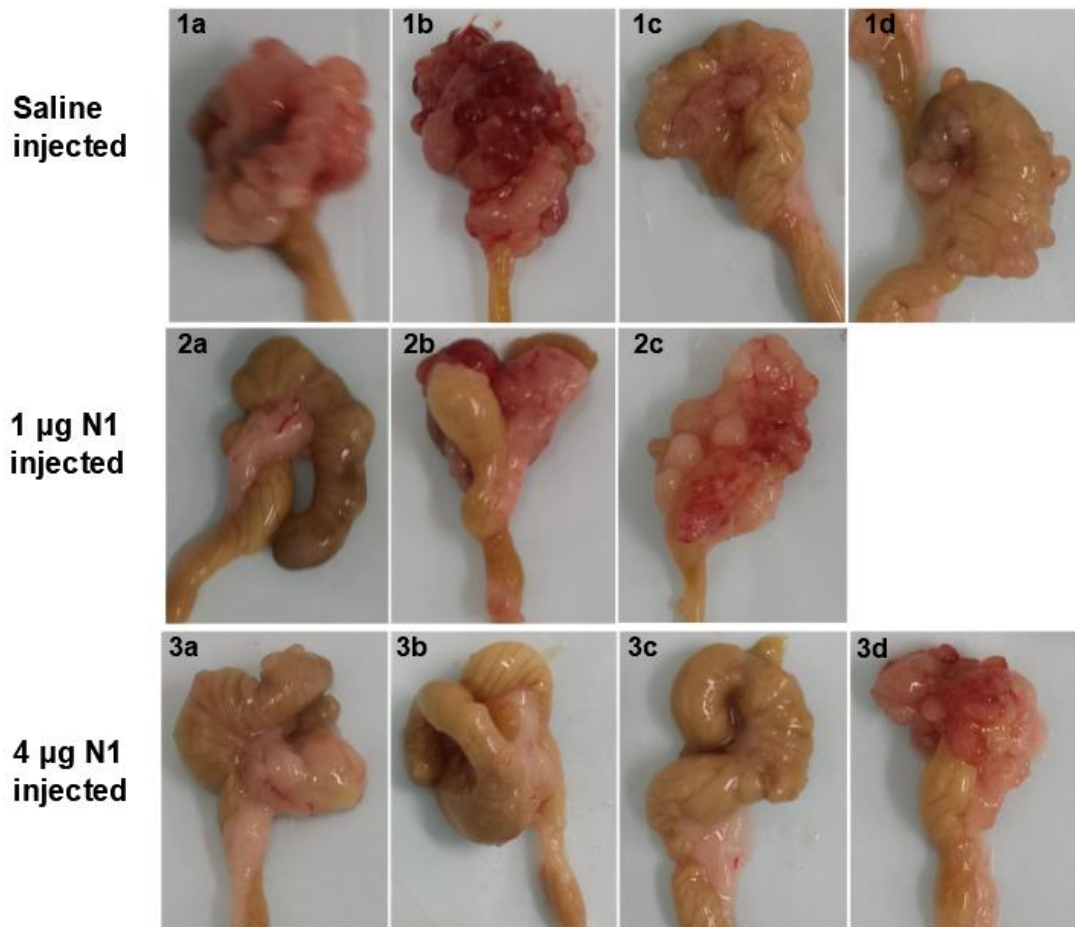
The tumour regions of the caecum tissues were confirmed by Ki67 labelling (**Figure 5.6 A 1a-1d, B 3a-3c and C 5a-5d**). The tumour neovascularisation of the caecum was examined by CD31 immunohistochemical staining (**Figure 5.6 A 2a-2d, B 4a-4c and C 6a-6d**). The majority of the caecum tissues exhibited CD31 expression and this was seen near the region of tumour mass. The intense staining of CD31 was predominantly observed in the caecum tissues from the CRC mice treated with saline, whereas weaker staining of CD31 was noticed in the CRC mice treated with 4  $\mu$ g of Netrin-1 (**Figure 5.6 C 6a-6c**). Collectively, these data suggest that a high concentration of Netrin-1 inhibits the primary tumour growth and progression in the CRC mice.

The effect of Netrin-1 treatment on the ENS under the CRC condition was also investigated in this study. Prior to undertaking that investigation, the presence of Netrin-1 and its receptor, DCC in the *adult* ENS of the healthy gut was examined and the outcomes were shown in the following results section.

**Figure 5.4 Caeca from the CRC mice in the absence or presence of Netrin-1 treatment**

**(A)** Images of CT26 cells-implanted caeca taken from the mice treated with or without Netrin-1 for a 6-day period. The caecum tissues removed from the CRC mice, that were treated with **(1a-1d)** saline (n=4 mice), **(2a-2c)** 1 µg of N1 (n=3 mice), and **(3a-3d)** 4 µg of N1 (n=4 mice). **(B)** The number of tumour polyps on the caeca was counted per group that received saline or 1 µg of N1 or 4 µg of N1 treatment. Data represented as mean ± SD, Student's *t* test; \**p*<0.05.

## A CT26-implanted caecum



## B Caecum tumour polyps

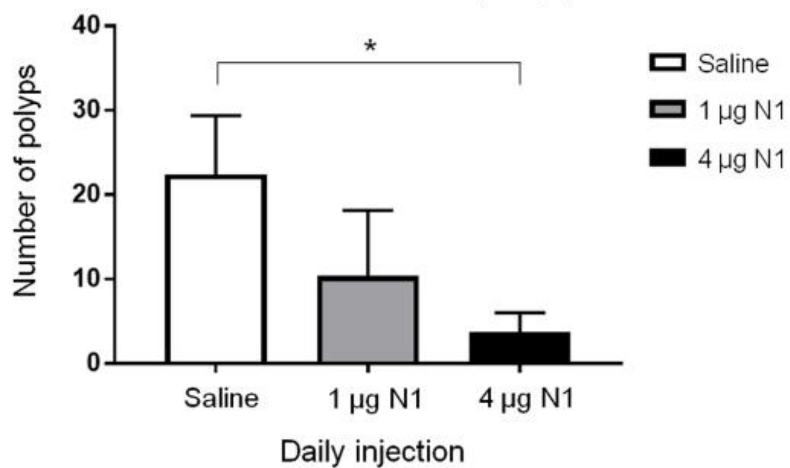


Figure 5.4

**Figure 5.5 Hematoxylin and eosin staining of caecum and colon tissues from Netrin-1 or vehicle-treated CRC mice**

The caecum and colon tissues from the CRC mice that received a treatment of **(A)** saline, **(B)** 1  $\mu\text{g}$  of N1, and **(C)** 4  $\mu\text{g}$  of N1, were stained with H&E staining. Scale bar: 25  $\mu\text{m}$

**Abbreviations:** CRC, colorectal cancer; N1, Netrin-1; H&E, hematoxylin and eosin.

# Colorectal cancer mice

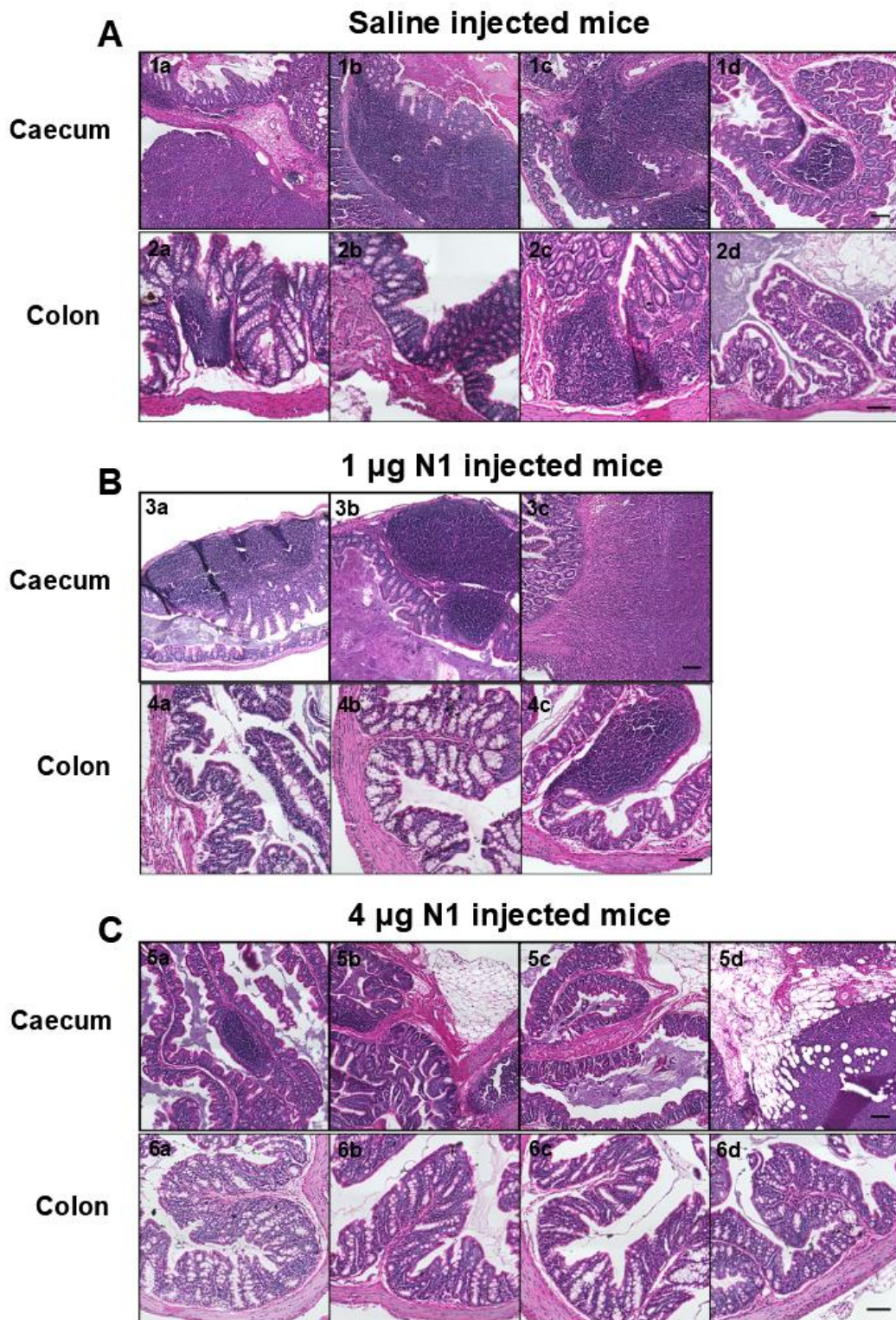


Figure 5.5

**Figure 5.6 3,3'-diaminobenzidine immunohistochemistry of caecum and colon tissues from Netrin-1 or vehicle-treated CRC mice**

The caecum and colon tissues taken from the CRC mice treated with saline **(A)**, 1 µg of N1 **(B)**, and 4 µg of N1 **(C)** were stained with Ki67 and CD31 marker labelled with DAB (brown). Haematoxylin was used as a counter stain. Scale bar: 25 µm.

**Abbreviations:** CRC, colorectal cancer; N1, Netrin-1; DAB, 3,3'-diaminobenzidine.

# CT26-implanted caecum

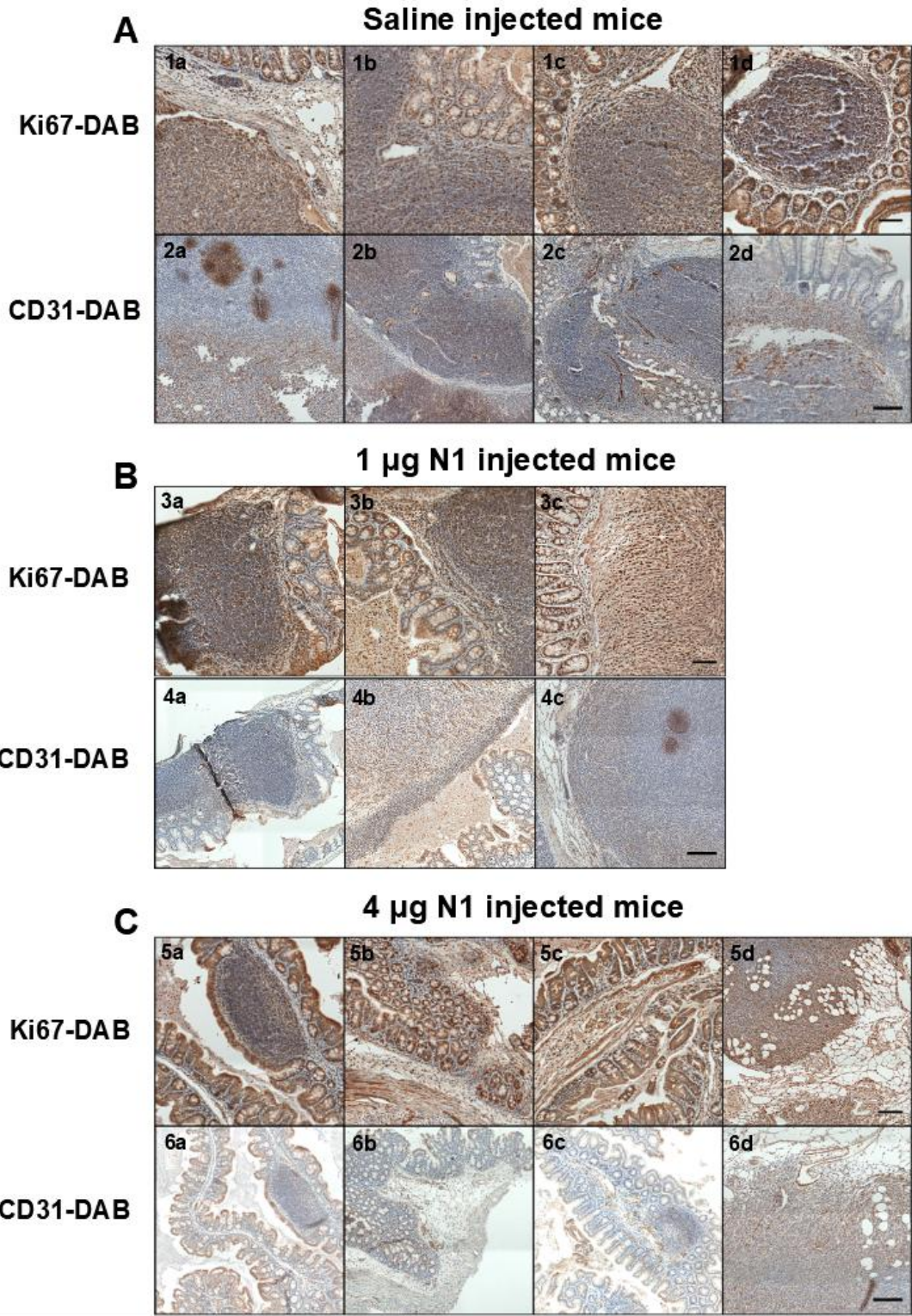


Figure 5.6

#### **5.3.4 Defining the expression of Netrin-1 and its receptor, DCC, in the myenteric plexus of the colon from healthy adult mice**

In order to investigate the role of Netrin-1 in the adult ENS, firstly it is important to confirm whether Netrin-1 receptors such as DCC and/or UNC5H2 are present in the adult ENS. This is potentially the first to determine whether or not DCC expression remains in the mature ENS; that is after the ENS has been fully developed in the organism. The young adult mice (6-10 weeks old, n=6 mice) were used to examine whether or not DCC is expressed in their ENS. In particular, myenteric neurons were the focus of this investigation since they play an essential role in intestinal motility. A wholemount preparation of mice colon tissues revealing myenteric plexus was labelled with DCC immunofluorescence. This wholemount preparation minimised detection of DCC expression from other tissue layers of the colon section. This was achieved by dissecting the tissue layers, such as colonic epithelium, mucosa, submucosa and circular muscle layers. Thereby, only the myenteric plexus was revealed on the longitudinal muscle layer.

The results showed that DCC-immunoreactivity (IR) was distinctively apparent in the myenteric plexus (**Figure 5.7**). DCC staining was co-localised with the neuronal marker, protein gene product 9.5 (PGP9.5) that labels neuronal cell bodies and processes. The IR for DCC was clearly shown in the cytoplasm of the neuronal cell bodies and nerve processes, notably in the internodal strands forming a nerve plexus. This was also detected by the co-localization of DCC staining combined with another neuronal marker specific to the neurofilament-heavy chain (NF-H). In addition to neuronal markers, co-labelling of DCC and a glial cell marker using intermediate filament glial fibrillary acidic protein (GFAP) was tested to see if this observed DCC expression was specific to the enteric neurons or was shared with glial cells. The enteric glial cells are located in close proximity to the enteric neurons within the ganglia, and the glial cell fibers embrace neurons and nerve fibers in the ENS [407]. The GFAP-IR was shown to outline the DCC-immunoreactive enteric neurons and internodal strands. At a high magnification, the expression of DCC was clearly observed in the cytoplasm of the neurons. Some small punctuated structures (arrowheads) were exhibited along where the glial cell fibers embraced the neurons (**Figure 5.7 5b-d arrowheads**). However, it appeared some glial cell fibers lack the

DCC-IR (**Figure 5.7, 5b-d arrows**). Collectively, these data suggest that DCC receptors are expressed in the myenteric neurons and processes.

Next, the expression of Netrin-1 was examined to see whether Netrin-1 is produced in the mature ENS. The wholemount immunofluorescent labelling of Netrin-1 indicated that Netrin-1 expression was clearly observed in the myenteric plexus (**Figure 5.8**). Similar to the DCC expression, the Netrin-1-IR was found to be co-localised with PGP9.5 and NF-H, suggesting that Netrin-1 is expressed in enteric neurons and processes. The Netrin-1-IR was primarily detected in the cytoplasm of the nerve cell bodies, and those Netrin-1 positive neurons showed both strong and weak staining. There were also many punctate structures surrounding individual neurons within a ganglion (**Figure 5.8 4c-5c and Figure 5.9 2c-c'**). To see whether those punctate structures of Netrin-1-IR were associated with glial cells, GFAP was co-stained with Netrin-1. As expected, Netrin-1-positive neurons and processes were outlined by the GFAP-IR. However, it was difficult to determine whether glial cells also express Netrin-1.

Since the IR of both DCC and Netrin-1 was found to be in almost all neurons and nerve processes, a double-labelling of DCC and Netrin-1 was conducted to confirm this localisation. The staining of both markers was clearly co-localised in the myenteric plexus (**Figure 5.9**). Notably, it was evident that within a ganglion, some neurons exhibited stronger Netrin-1-IR in their cytoplasm than others. Also, it appeared to show IR of Netrin-1 in the varicose axons (**Figure 5.9 3c-c'**). Taken together, these observations prompted us to investigate whether Netrin-1 expression is associated with certain neuronal subtypes. In the following section, the data concerning expression of Netrin-1 in relation to the expression of choline acetyltransferase (ChAT) and neuronal nitric oxide synthase (nNOS) in the colonic myenteric plexus are presented.

**Figure 5.7 Localisation of DCC receptors in the myenteric plexus of the colon from healthy young adult mice**

The myenteric plexus of the colon tissues were stained with DAPI, nuclei staining (**1a-5a**), neuronal markers, PGP9.5 (**1b and 4b**) and NF-H (**2b**), as well as a glial marker, GFAP (**3b and 5b**). DCC receptors (**1c-5c**) were labelled and the merged images (**1d-5d**) demonstrate the co-localisation of neuronal and glial markers with DCC receptors. Filled arrowheads in **5b-5d** indicate the co-localisation regions of GFAP and DCC markers, whilst arrows indicate lack of co-localisation of GFAP and DCC markers (**5b-5d**). Scale bar: 100  $\mu\text{m}$  (**1a-3d**); 25  $\mu\text{m}$  (**4a-5d**). (n=5 animals).

**Abbreviations:** DCC, deleted in colorectal cancer; PGP9.5, protein gene product 9.5; NF-H, neurofilament-heavy chain; GFAP, glial fibrillary acidic protein; DAPI, 4',6-diamidino-2-phenylindole.

## Myenteric plexus of healthy colon tissues

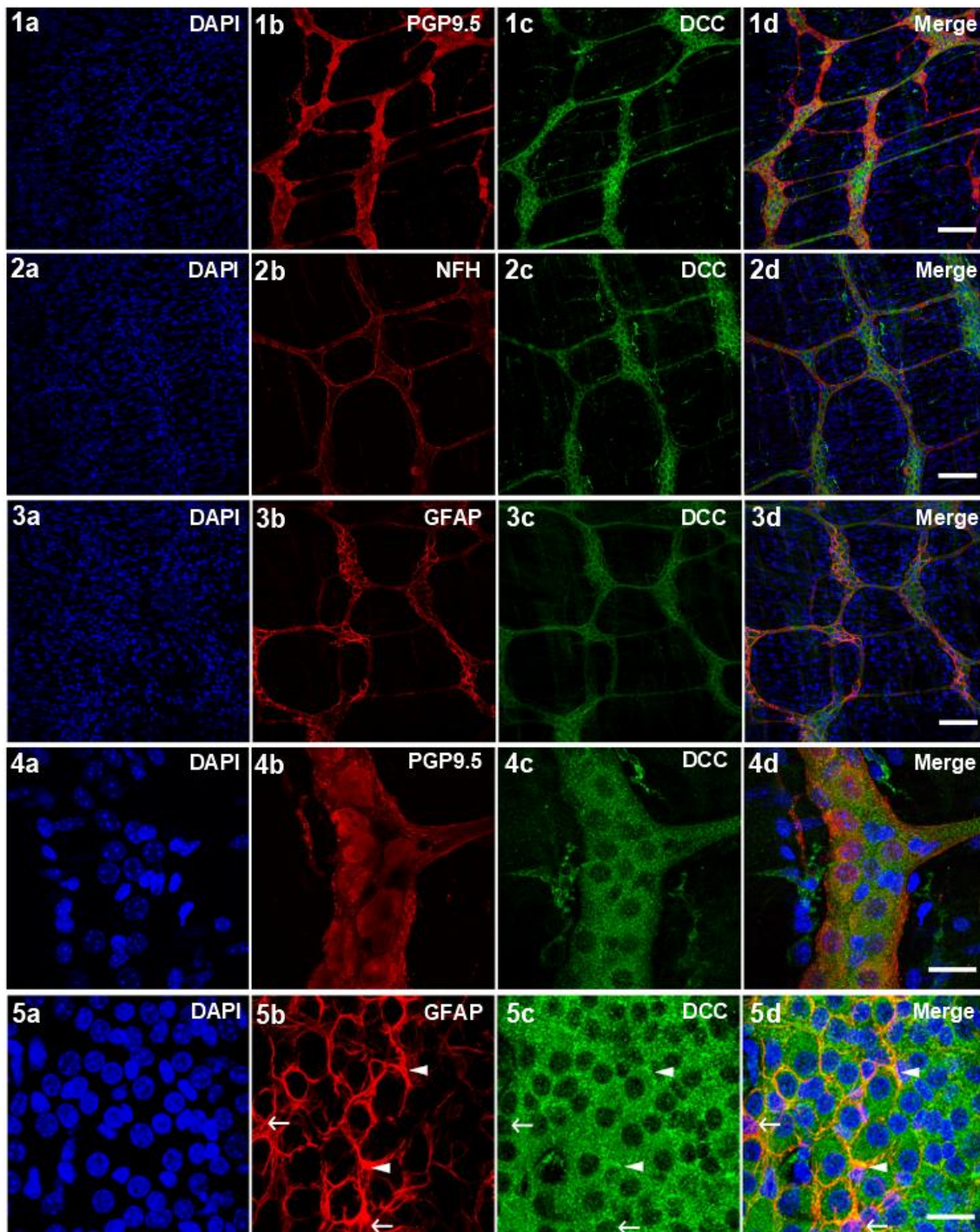


Figure 5.7

**Figure 5.8 Localisation of Netrin-1 in the myenteric plexus of the colon from healthy young adult mice**

The myenteric plexus of the colon tissues were stained with DAPI, nuclei staining (**1a-5a**), neuronal markers, PGP9.5 (**1b and 4b**) and NF-H (**2b**), as well as a glial marker, GFAP (**3b and 5b**). Netrin-1 (**1c-5c**) was labelled and the merged images (**1d-5d**) demonstrate the co-localisation of neuronal and glial markers with Netrin-1. Scale bar: 100  $\mu\text{m}$  (**1a-3d**); 25  $\mu\text{m}$  (**4a-5d**), (n=5 animals).

**Abbreviations:** PGP9.5, protein gene product 9.5; NF-H, neurofilament-heavy chain; GFAP, glial fibrillary acidic protein; DAPI, 4',6-diamidino-2-phenylindole.

## Myenteric plexus of healthy colon tissues

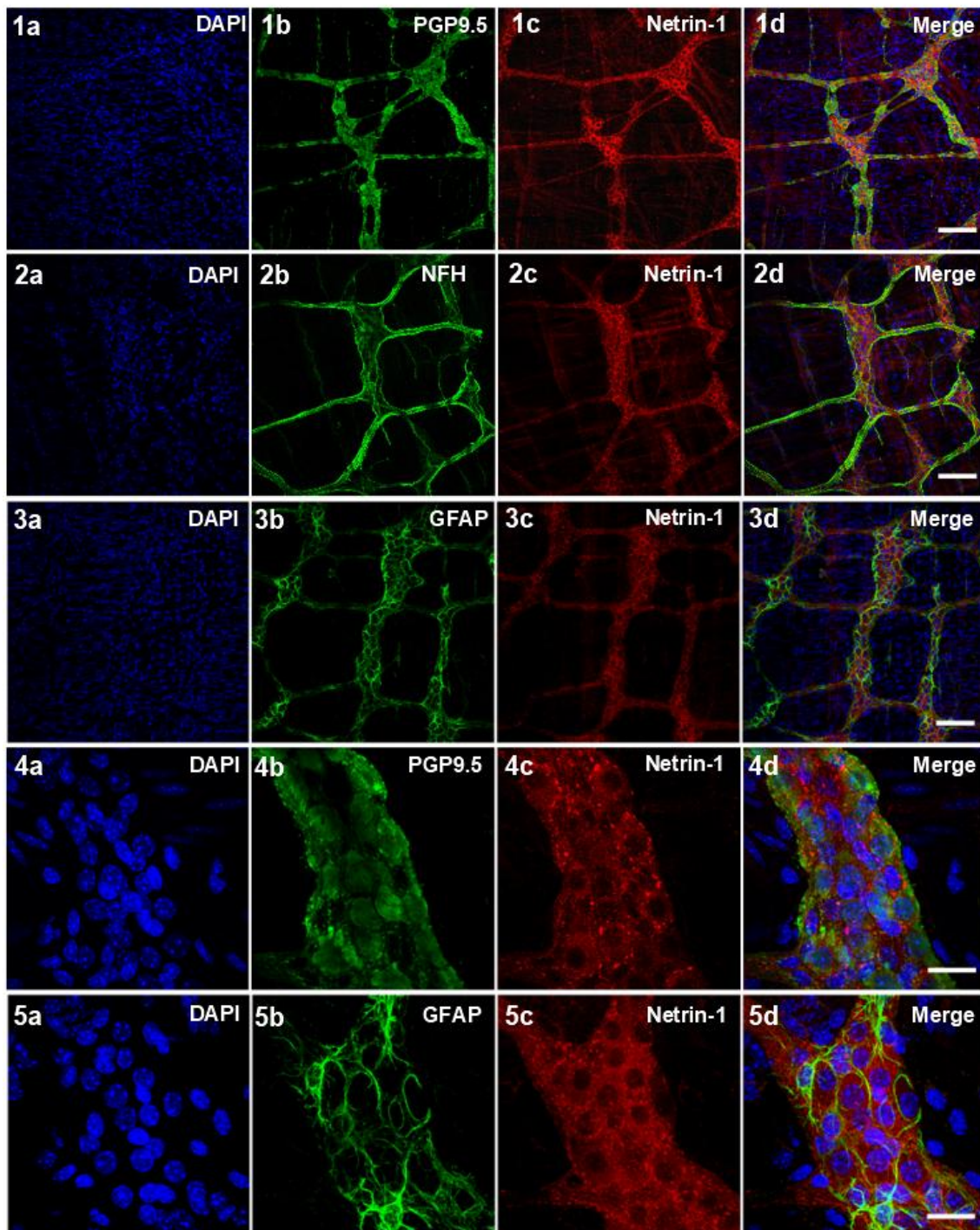


Figure 5.8

**Figure 5.9 Co-localisation of DCC-IR and Netrin-1-IR in the myenteric plexus of the colon from healthy young adult mice**

The myenteric plexus of colon tissues were stained with DAPI, nuclei staining (**1a-3a**), DCC receptors (**1b-3b**) and Netrin-1 (**1c-3c**). The merged images (**1d-3d**) demonstrate the co-localisation of DCC receptors and Netrin-1. The inserted box area of **2c** is shown with a high magnification view (**2c'**) and it highlights the punctated structure around the cell body. The arrows in **3c'** indicate the IR of Netrin-1 on varicosities. Scale bar: 100  $\mu\text{m}$  (**1a-1d**); 25  $\mu\text{m}$  (**2a-2d**), Scale bar: 50  $\mu\text{m}$ , (n=5 animals/group).

**Abbreviations:** DCC, deleted in colorectal cancer; IR, immunoreactivity; DAPI, 4',6-diamidino-2-phenylindole.

## DCC and Netrin-1 expression in healthy colon tissues

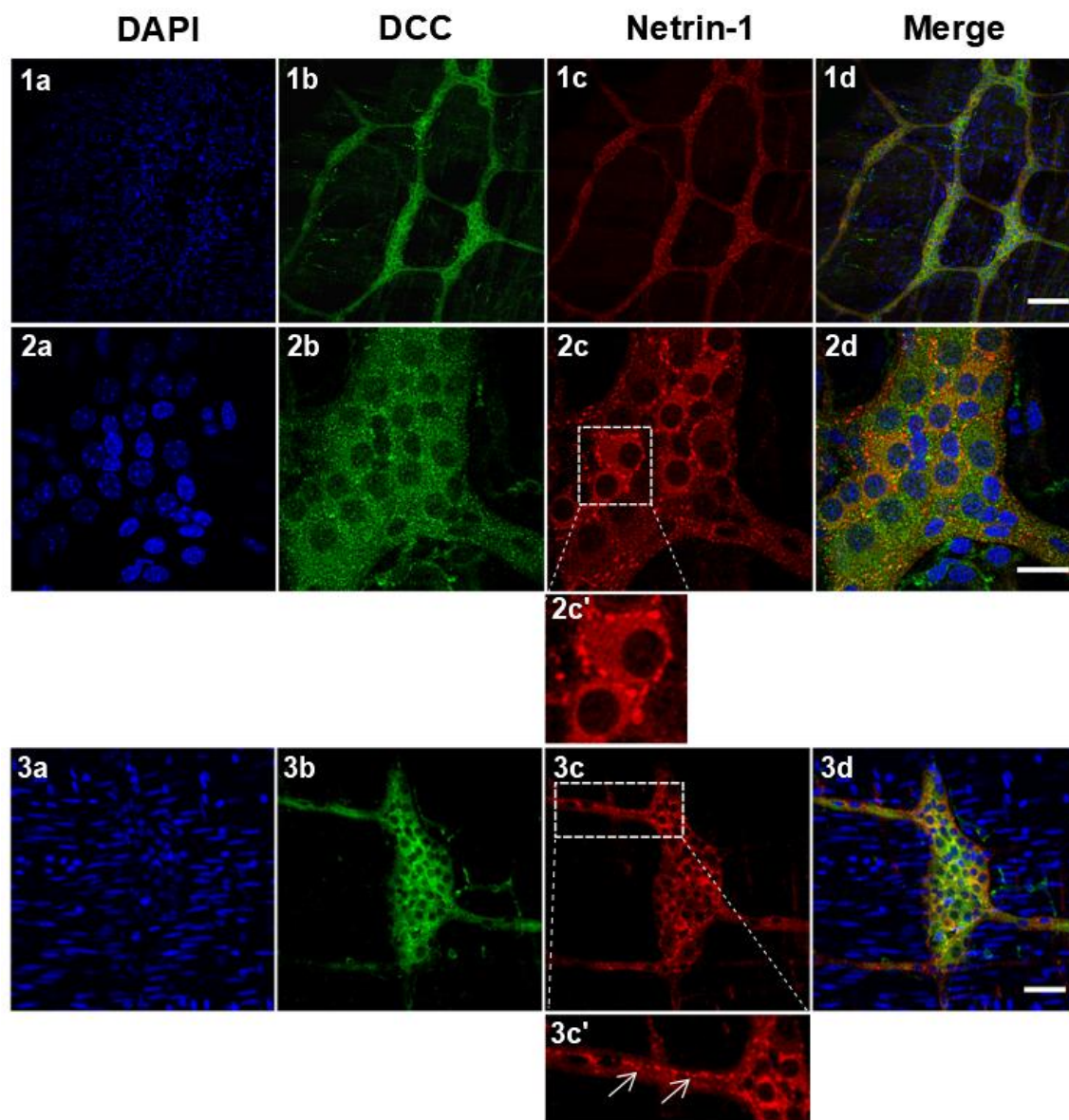


Figure 5.9

### 5.3.5 Identifying the co-expression of Netrin-1 with ChAT and nNOS in the myenteric plexus of the colon from healthy adult mice

The motility of the gut is controlled by excitatory and inhibitory motor neurons, which are identified by neurochemical coding such as ChAT and nNOS, respectively [19, 408]. These ChAT and nNOS markers were used to test whether or not the Netrin-1-positive neurons overlap with either of those two markers in the myenteric plexus of the colon in healthy young adult mice. As discussed in previous section 5.3.4, the Netrin-1-IR was found in the myenteric plexus, and this time it was indicated by showing the co-localisation of Netrin-1 with a pan-neuronal marker,  $\beta$ -Tubulin III (**Figure 5.10**). Also, the IR of ChAT was shown to co-localised with the  $\beta$ -Tubulin III marker, and the majority of myenteric neurons were stained with the ChAT marker in the myenteric plexus. Similar to what had been seen in the case of Netrin-1-positive neurons, there were either strongly or weakly stained ChAT-positive neuronal cell bodies in ganglia. The co-staining of Netrin-1 with ChAT was conducted in the myenteric plexus of the colon tissues to confirm their overlapping population. Although the majority of the Netrin-1-positive and ChAT-positive neurons were shown to overlap, 4 different combinations of stained neurons were observed and were indicated as arrows and arrowheads in **Figure 5.10 A 3a'-3c'**. These were grouped and they include neurons that were: (1) strongly Netrin-1-positive but ChAT-negative (N1<sup>++</sup>/ChAT<sup>-</sup>, filled arrowheads); (2) Netrin-1-negative but strongly ChAT-positive (N1<sup>-</sup>/ChAT<sup>++</sup>, empty arrowheads); (3) strongly Netrin-1-positive but also weakly positive for ChAT (N1<sup>++</sup>/ChAT<sup>+</sup>, filled arrows); (4) weakly Netrin-1-positive but also strongly positive for ChAT (N1<sup>+</sup>/ChAT<sup>++</sup>, empty arrows). The groups 3 and 4 were combined into one group, namely N1<sup>+(+)</sup>/ChAT<sup>+(+)</sup>, since those neurons expressed both Netrin-1 and ChAT markers (**Figure 5.10 B**).

The quantified results showed that either weakly or strongly co-stained neurons for both Netrin-1 and ChAT markers, N1<sup>+(+)</sup>/ChAT<sup>+(+)</sup>, were found to be  $73.3 \pm 3.1\%$ . On the other hand, the non-overlapping population which means the neurons positive only for either Netrin-1 or ChAT marker were shown to be 26.7

$\pm 3.1\%$ . This included the population of N1<sup>++</sup>/ChAT<sup>-</sup> ( $19.2 \pm 3.0\%$ ) and the population of N1<sup>-</sup>/ChAT<sup>++</sup> ( $7.5 \pm 3.1\%$ ).

Next, in order to examine whether or not the strong Netrin-1-positive neurons overlap with nNOS-positive neurons in the myenteric plexus of the colon from healthy young adult mice, the nNOS marker was co-labelled with Netrin-1 marker (**Figure 5.11**). The result showed that the proportion of neurons that were strongly positive for Netrin-1 was  $43.1 \pm 3.8\%$ . The proportion of neurons that were positive for nNOS was  $32.0 \pm 3.6\%$ . The proportion of neurons that were positive for both nNOS and strong Netrin-1 markers was  $30.2 \pm 4.5\%$ . This suggests that a high expression of Netrin-1 is associated with the nNOS phenotype in the myenteric plexus of the colon.

**Figure 5.10 Co-localisation of Netrin-1-IR and ChAT-IR in the myenteric plexus of the colon from healthy young adult mice**

**(A)** The myenteric plexus of the colon tissues were triple-labelled with  $\beta$ -Tubulin III, Netrin-1 and ChAT, and the images indicate labelling of  $\beta$ -Tubulin III and Netrin-1 (**1a-1c**);  $\beta$ -Tubulin III and ChAT (**2a-2c**); and, Netrin-1 and ChAT (**3a-3c**). The inserted box areas of **3a-3c** are shown with a high magnification view (**3a'-3c'**). In **3a'-3c'**, the filled arrowhead indicates the neuronal cell bodies that are strongly Netrin-1-positive, but ChAT-negative (N1+/ChAT-). The empty arrowhead in **3a'-3c'** indicates the neuron that is Netrin-1-negative but strongly ChAT-positive (N1-/ChAT+). The filled arrow in **3a'-3c'** indicates the neuron that is strongly Netrin-1-positive but also weakly positive for ChAT (N1+/ChAT+). The empty arrow in **3a'-3c'** indicates the neuron that is weakly Netrin-1-positive but also strongly positive for ChAT (N1+/ChAT+). (Strongly positive: ++; weakly positive: +). Scale bar: 100  $\mu$ m (**1a-3c**). **(B)** The proportion of the immunoreactive neurons for N1+/ChAT-, N1-/ChAT+ and N1+(+)/ChAT+(+) were measured in the total area of 2mm<sup>2</sup>. The population of N1+(+)/ChAT+(+) represents the populations of both N1+/ChAT+ and N1+/ChAT+. Data represented as mean  $\pm$  SD (n=3 animals).

**Abbreviations:** ChAT, choline acetyltransferase; N1, Netrin-1; +, weakly positive; ++, strongly positive; +( ), both weakly and strongly positive; -, negative.

## Netrin-1 and ChAT expression in healthy colon tissues

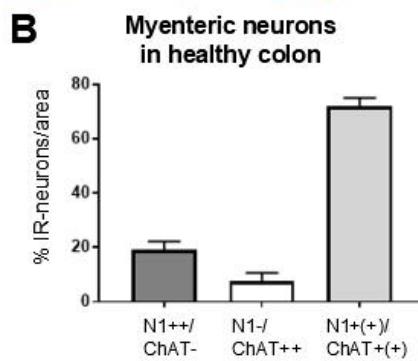
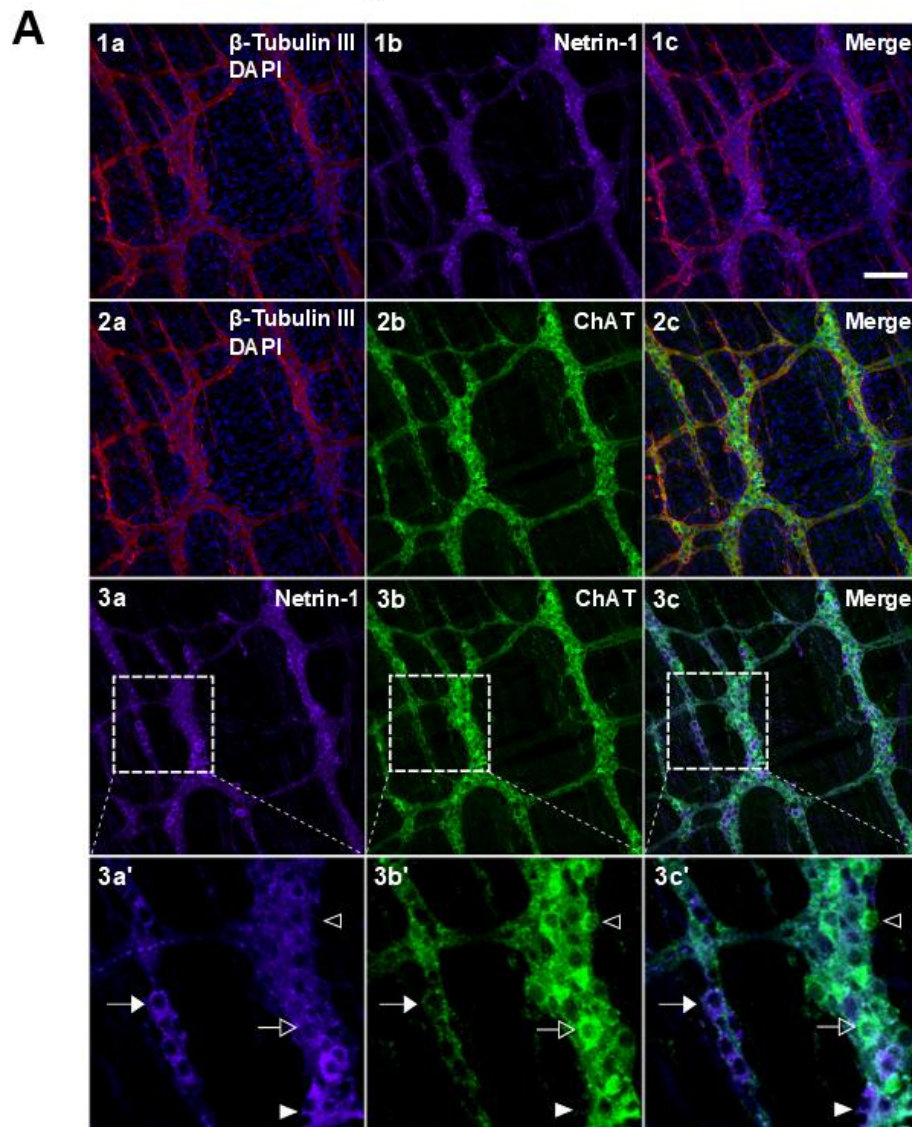


Figure 5.10

**Figure 5.11 Co-localisation of Netrin-1-IR and nNOS-IR in the myenteric plexus of the colon from healthy young adult mice**

**(A)** The myenteric plexuses of the colon tissues were triple-labelled with  $\beta$ -Tubulin III, Netrin-1 and nNOS, and the images indicate labelling of  $\beta$ -Tubulin III and Netrin-1 (**1a-1c**);  $\beta$ -Tubulin III and nNOS (**2a-2c**); and, Netrin-1 and nNOS (**3a-3c**). The inserted box areas of **3a-3c** are shown with a high magnification view (**3a'-3c'**). In **3a'-3c'**, the filled arrowhead indicates a strong Netrin-1-immunoreactive neuron that was co-stained with nNOS (N1++/nNOS+). The empty arrowhead in **3a'-3c'**, indicates a weak Netrin-1-immunoreactive neuron that did not show nNOS-immunoreactivity (N1+/nNOS-). (Strongly positive: N1++; weakly positive: N1+). The arrow in **3b'** indicates a nNOS-positive neuron with flat lamella dendrites. This is known as a characteristic of mature nNOS enteric neurons. Scale bar: 50  $\mu$ m (**1a-3c**). Scale bar: 100  $\mu$ m. **(B)** The proportion of the immunoreactive neurons for N1++, nNOS+ and N1++/nNOS+ were measured within the total area of 2mm<sup>2</sup>. Data represented as mean  $\pm$  SD (n=3 animals).

**Abbreviations:** nNOS, neuronal nitric oxide synthase; N1, Netrin-1; +, weakly positive; ++, strongly positive; +( ), either weakly or strongly positive; -, negative.

## Netrin-1 and nNOS expression in healthy colon tissues

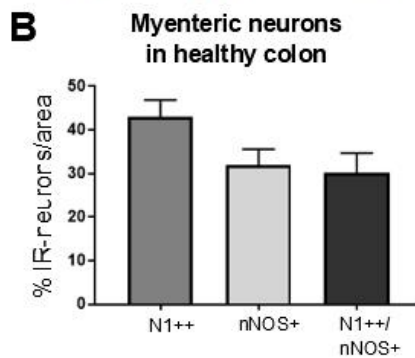
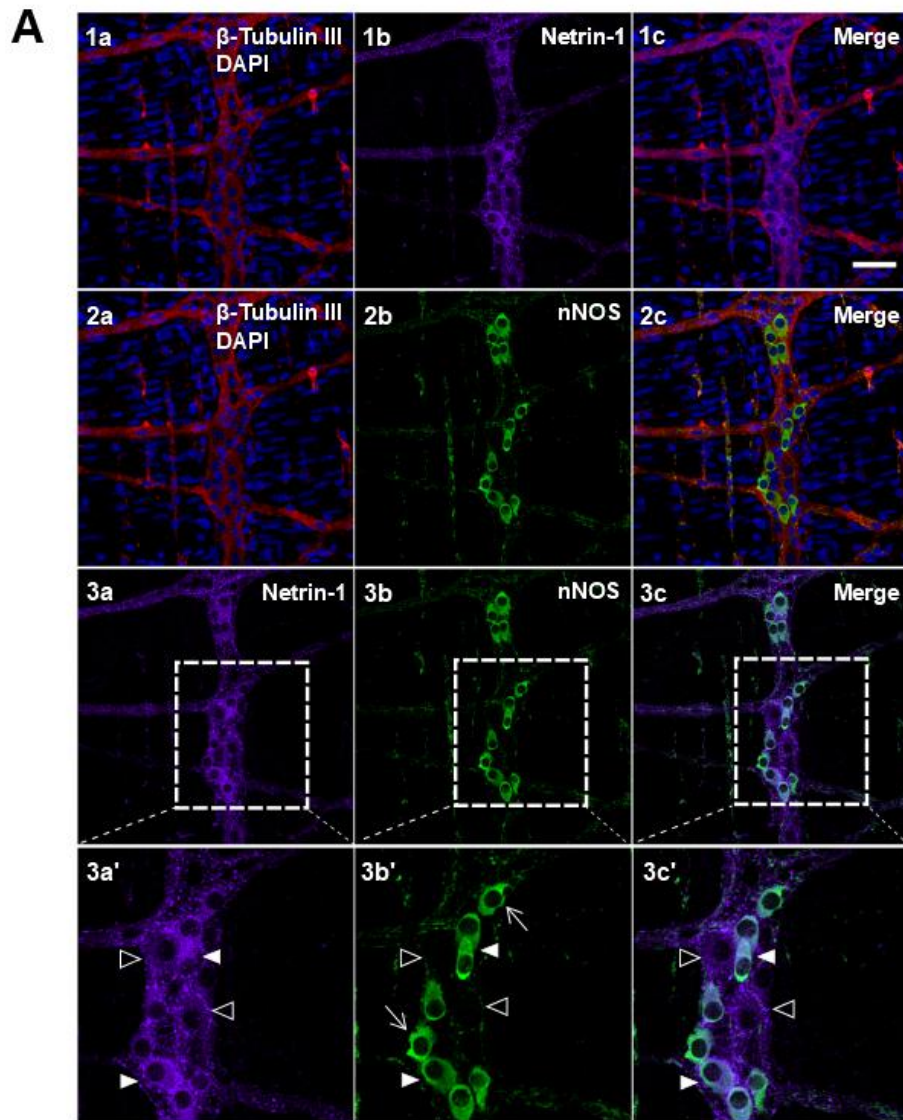


Figure 5.11

### **5.3.6 The expression of DCC and Netrin-1 in the colonic myenteric plexus of colorectal cancer mice with or without Netrin-1 treatment**

Since this current study has revealed the presence of DCC expression in the myenteric plexus of the colon tissues, it was possible to examine the expression of DCC in the myenteric plexus under the CRC condition. Furthermore, it was valuable to explore whether there would be any changes to the DCC expression in the myenteric plexus when Netrin-1 was exogenously introduced to the CRC mice. Two concentrations (1  $\mu\text{g}$  or 4  $\mu\text{g}$ ) of Netrin-1 (N1) were injected daily to the CRC mice as previously described in the methods and material section 5.2. The result of a wholemount preparation for the immunofluorescent labelling indicated that DCC expression in the myenteric plexus of the colon in CRC mice was found to be similar to the one that was seen in the healthy control mice (**Figure 5.12**). The IR of DCC was clearly shown in the cytoplasm of the neuronal cell bodies and processes. Furthermore, there were no obvious changes to DCC expression in the myenteric plexus of CRC mice regardless of whether or not they received Netrin-1 treatment (**Figure 5.12; 2b, 3b and 4b**).

The expression of Netrin-1 was also examined in the myenteric plexus of the colon in CRC mice in the presence and absence of Netrin-1 treatment. Similar to the healthy control mice, the presence of Netrin-1-IR in myenteric neurons and processes was evident under those conditions (**Figure 5.13**). Particularly, the weak and strong Netrin-1 staining of the cell bodies was still observed in CRC with or without Netrin-1 treatment.

**Figure 5.12 DCC-IR in the myenteric plexus of the colon from Netrin-1 or vehicle-treated CRC mice**

The myenteric plexus of the colon tissues taken from healthy mice (**1a-1c**). The myenteric plexus of the colon tissues from the CRC mice treated with saline (**2a-2c**), 1 µg of N1 (**3a-3c**), 4 µg of N1 (**4a-4c**). The tissues were labelled with β-Tubulin III marker in conjunction with DAPI (**1a-4a**) and DCC marker (**1b-4b**). The merged images are shown (**1c-4c**). Scale bar: 100 µm (n=3 animals).

**Abbreviations:** DCC, deleted in colorectal cancer; IR, immunoreactivity; N1, Netrin-1; DAPI, 4',6-diamidino-2-phenylindole.

## DCC expression in the CRC mice treated with or without Netrin-1

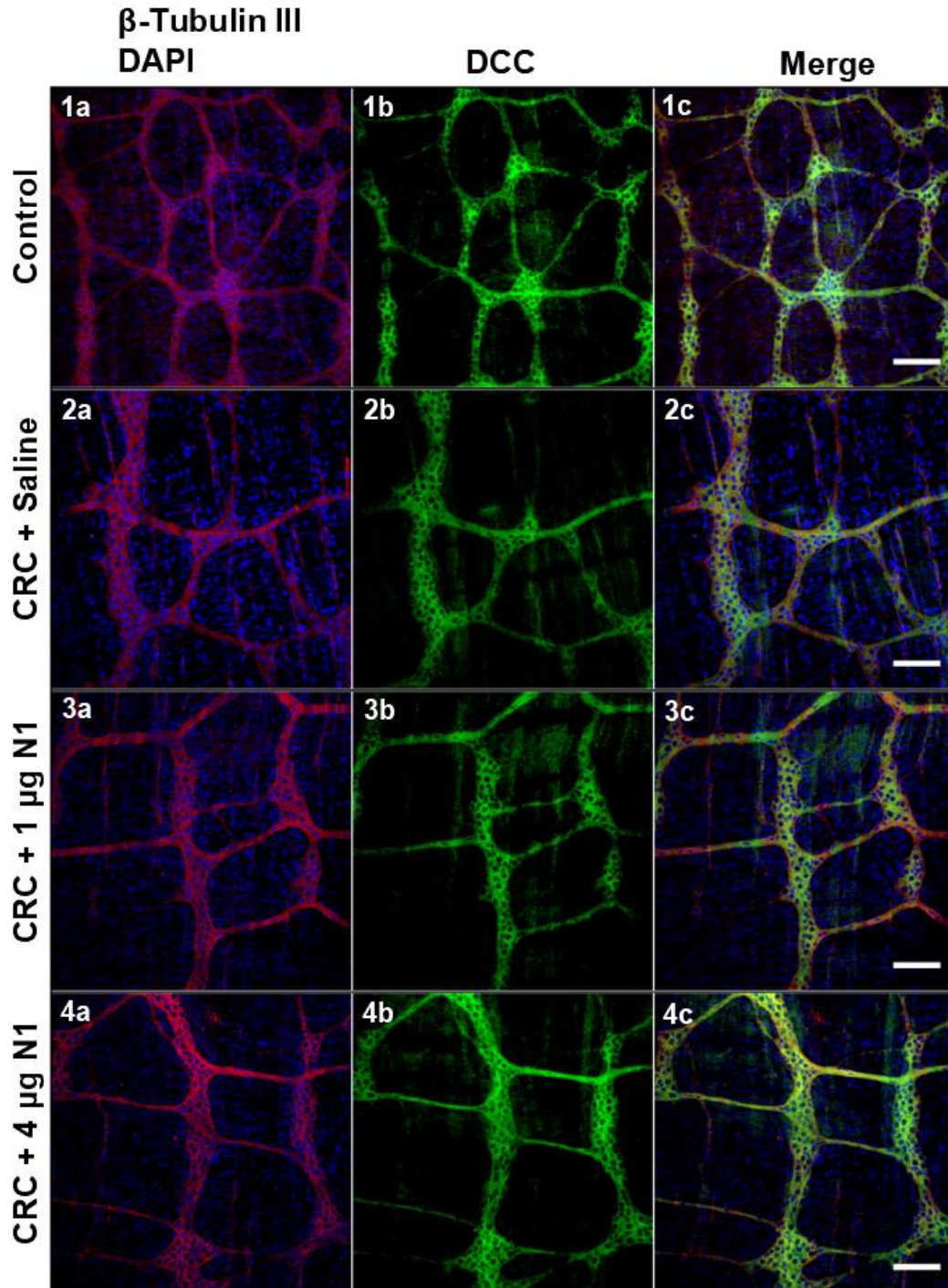


Figure 5.12

**Figure 5.13 Netrin-1-IR in the myenteric plexus of the colon from Netrin-1 or vehicle-treated CRC mice**

The myenteric plexus of the colon tissues taken from healthy mice **(1a-1c)**. The myenteric plexus of the colon tissues from the CRC mice treated with saline **(2a-2c)**, 1 µg of Netrin-1 (N1) **(3a-3c)**, 4 µg of N1 **(4a-4c)**. The tissues were labelled with β-Tubulin III marker in conjunction with DAPI **(1a-4a)** and Netrin-1 marker **(1b-4b)**. The merged images are shown **(1c-4c)**. Scale bar: 100 µm (saline, n=4; 1 µg of N1, n=3; 4 µg of N1, n=4).

**Abbreviations:** IR, immunoreactivity; CRC, colorectal cancer; N1, Netrin-1; DAPI, 4',6-diamidino-2-phenylindole.

## Netrin-1 expression in the CRC mice treated with or without Netrin-1

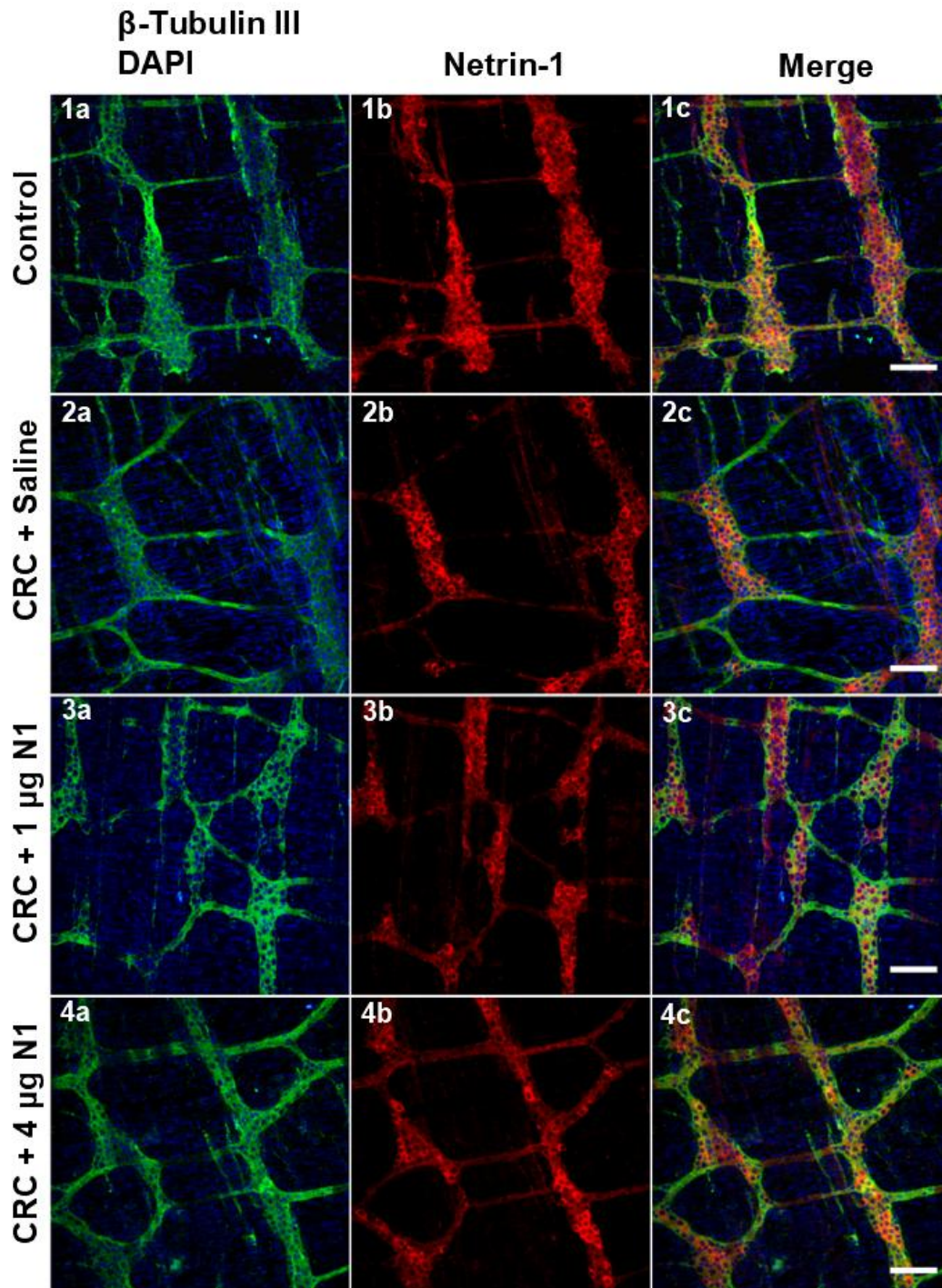


Figure 5.13

### 5.3.7 The co-expression of Netrin-1 and nNOS in the colonic myenteric plexus of colorectal cancer mice with or without Netrin-1 treatment

Previously in our healthy mice study, it appeared that some correlation existed between the nNOS expression and the strong Netrin-1-IR in the neuronal cell bodies in the healthy control mice. This relationship was explored under the CRC condition with or without Netrin-1 treatment to see whether there may be any changes in their expression. The co-staining of Netrin-1 and nNOS results indicated that the nNOS-positive neurons were the ones that also stained for the strong Netrin-1-IR under the CRC condition with or without Netrin-1 treatment (**Figure 5.14**). The quantitative analysis revealed that  $43.1 \pm 3.8\%$  myenteric neurons in control tissues were shown to be positive for the strong Netrin-1-IR. However, this strong Netrin-1-IR was reduced under the CRC conditions. A significant reduction in the population of neurons positive for strong N1-IR, was observed in the CRC mice received saline treatment ( $34.7 \pm 2.0\%$ ,  $p < 0.01$ ) and  $1 \mu\text{g}$  of Netrin-1 treatment ( $33.8 \pm 1.3\%$ ,  $p < 0.01$ ) when compared to the healthy control ( $43.1 \pm 3.8\%$ ). However, this reduction in strong Netrin-1-IR shown in the mice treated with  $4 \mu\text{g}$  of Netrin-1 ( $37.2 \pm 5.3\%$ ) was not significant (**Figure 5.15**).

Furthermore, no significant difference in the population of neurons that were positive for nNOS was noted in the CRC mice regardless of the treatments (saline:  $31.8 \pm 1.6\%$ ,  $1 \mu\text{g}$  N1:  $30.1 \pm 2.7\%$  and  $4 \mu\text{g}$  N1:  $30.2 \pm 2.0\%$ ). Also, approximately 30% of neurons tested positive for both nNOS and strong Netrin-1-IR in all conditions (saline:  $29.3 \pm 2.2\%$ ,  $1 \mu\text{g}$  N1:  $29.3 \pm 2.3\%$  and  $4 \mu\text{g}$  N1:  $29.9 \pm 1.4\%$ ) (**Figure 5.15**). Collectively, these data indicated that similar to what had been seen in the case of healthy control mice, the majority of nNOS-positive neurons were also found to be positive for a strong Netrin-1-IR in CRC conditions.

**Figure 5.14 Co-localisation of Netrin-1-IR and nNOS-IR in the myenteric plexus of the colon from Netrin-1 or vehicle-treated CRC mice**

The myenteric plexus of the colon tissues taken from healthy mice (**1a-1c**). The myenteric plexus of the colon tissues from the CRC mice treated with saline (**2a-2c**), 1 µg of N1 (**3a-3c**), 4 µg of N1 (**4a-4c**). The tissues were labelled with Netrin-1 and nNOS markers. Netrin-1 labelling is shown red (**1a-4a**) and nNOS labelling is shown green (**1b-4b**). The merged images of Netrin-1 and nNOS are shown (**1c-4c**). Scale bar: 100 µm (saline, n=4; 1 µg of N1, n=3; 4 µg of N1, n=4).

**Abbreviations:** nNOS, neuronal nitric oxide synthase; CRC, colorectal cancer; N1, Netrin-1.

## Netrin-1 and nNOS expression in the CRC mice treated with or without Netrin-1

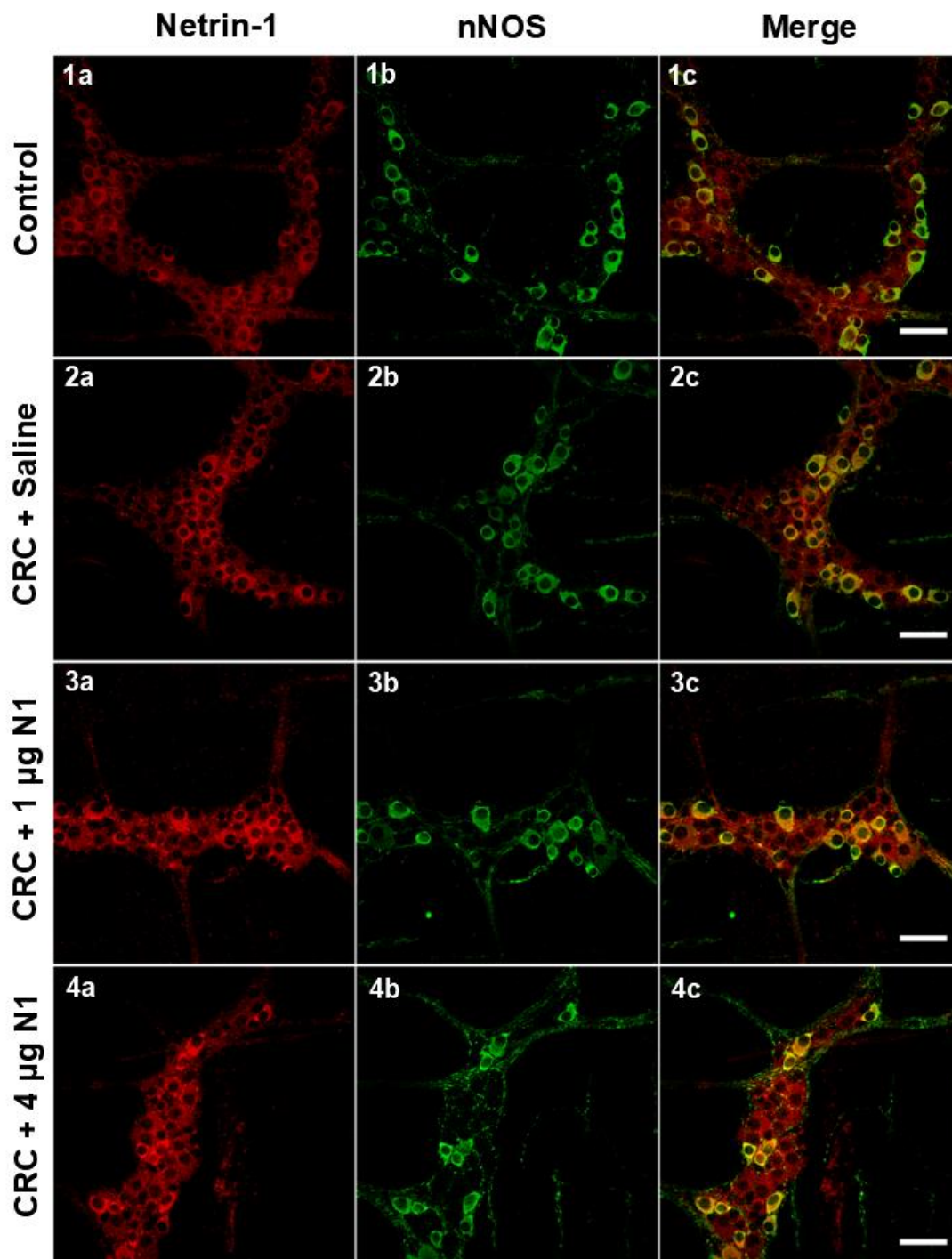


Figure 5.14

**Figure 5.15 Netrin-1-IR and nNOS-IR in the myenteric plexus of the colon tissues from Netrin-1 or vehicle-treated CRC mice**

The population of neurons that were positive for either strong Netrin-1 (N1++) or nNOS (nNOS+) and both strong Netrin-1 and nNOS (N1++/nNOS+) were counted within 2mm<sup>2</sup> area. Those three populations of neurons, that were found in the control healthy mice, were compared with the CRC groups treated with saline, 1 µg N1 and 4 µg of N1. Two-way ANOVA followed by Tukey's multiple comparisons test was used. Data represented as mean ± SD, \*\**p*<0.01 (saline, n=4; 1 µg of N1, n=3; 4 µg of N1, n=4).

**Abbreviations:** IR, immunoreactivity; nNOS, neuronal nitric oxide synthase; N1, Netrin-1; +, weakly positive; ++, strongly positive; ANOVA, analysis of variance.

**Netrin-1-IR and nNOS-IR neurons  
in the myenteric plexus**

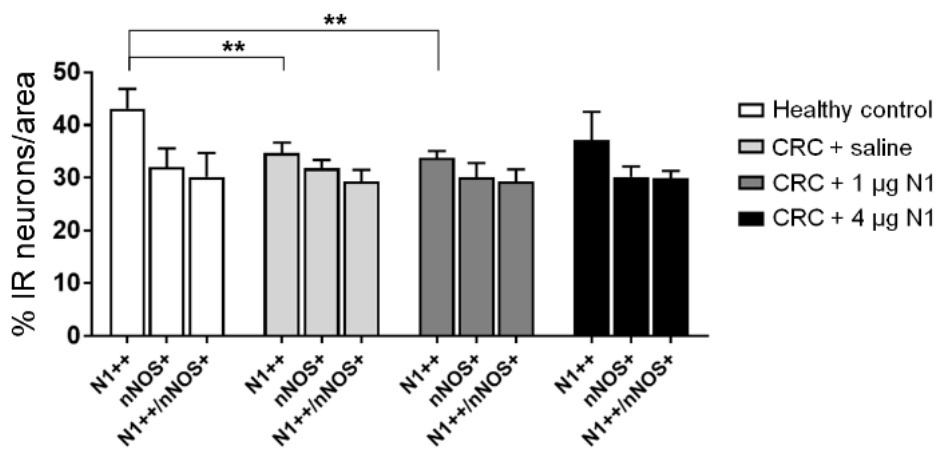


Figure 5.15

### 5.3.8 The co-expression of Netrin-1 and ChAT in the colonic myenteric plexus of colorectal cancer mice with or without Netrin-1 treatment

The expression of ChAT in relation to Netrin-1-positive neurons was examined in the myenteric plexus of CRC mice colon tissues to see whether or not Netrin-1 treatment influenced the expression of those two markers. Similar to our healthy mice study (section 5.3.5), four different combinations of stained neurons were observed in CRC mice with or without Netrin-1 treatment (**Figure 5.16**). Again, neurons expressing either N1<sup>++</sup>/ChAT<sup>+</sup> or N1<sup>+</sup>/ChAT<sup>++</sup> markers were combined into a one group namely, N1<sup>+(+)</sup>/ChAT<sup>+(+)</sup> for the quantitative analysis, since those neurons express both markers.

Quantitative analysis indicated that there was no statistically significant changes in the N1<sup>-</sup>/ChAT<sup>++</sup> population among all conditions (control: 7.5 ± 3.1%, saline: 10.5 ± 2.9%, 1 µg N1: 12.8 ± 6.0% and 4 µg N1: 11.3 ± 3.9%) (**Figure 5.17 A**). However, the N1<sup>++</sup>/ChAT<sup>-</sup> population was found to be markedly elevated in the case of CRC mice with all treatments (saline: 28.0 ± 2.3%,  $p < 0.001$ ; 1 µg N1: 25.0 ± 1.2%,  $p < 0.05$ ; and 4 µg N1: 23.8 ± 0.5%,  $p < 0.05$ ) when compared to the control mice (19.2 ± 3.0%). Of those CRC mice, there was a significant increase of the N1<sup>++</sup>/ChAT<sup>-</sup> population in the CRC mice with saline treatment (28.0 ± 2.3%,  $p < 0.05$ ) when compared to the CRC mice with 4 µg of Netrin-1 treatment (23.8 ± 0.5%) (**Figure 5.17 B**). With respect to the overlapping populations of Netrin-1 and ChAT markers, N1<sup>+(+)</sup>/ChAT<sup>+(+)</sup>, those overlapping populations were significantly reduced in the CRC mice with all conditions (saline: 61.5 ± 3.2%,  $p < 0.001$ ; 1 µg N1: 62.2 ± 5.5%,  $p < 0.05$ ; and 4 µg N1: 64.9 ± 2.4%,  $p < 0.05$ ) when compared to the control mice (73.3 ± 3.1%) (**Figure 5.17 C**). Collectively these data indicate that ChAT expression has been decreased in the CRC mice regardless of the treatment.

**Figure 5.16 Co-localisation of Netrin-1-IR and ChAT-IR in the myenteric plexus of the colon from Netrin-1 or vehicle-treated CRC mice**

The myenteric plexus of the colon tissues taken from healthy mice (**1a-1c**). The myenteric plexus of the colon tissues from the CRC mice treated with saline (**2a-2c**), 1 µg of N1 (**3a-3c**), 4 µg of N1 (**4a-4c**). The tissues were labelled with Netrin-1 and ChAT markers. Netrin-1 labelling is shown red (**1a-4a**) and ChAT labelling is shown green (**1b-4b**). The merged images of Netrin-1 and ChAT are shown (**1c-4c**). Scale bar: 100 µm (saline, n=4; 1 µg of N1, n=3; 4 µg of N1, n=4).

**Abbreviations:** IR, immunoreactivity; ChAT, choline acetyltransferase; N1, Netrin-1.

## Netrin-1 and ChAT expression in the CRC mice treated with or without Netrin-1

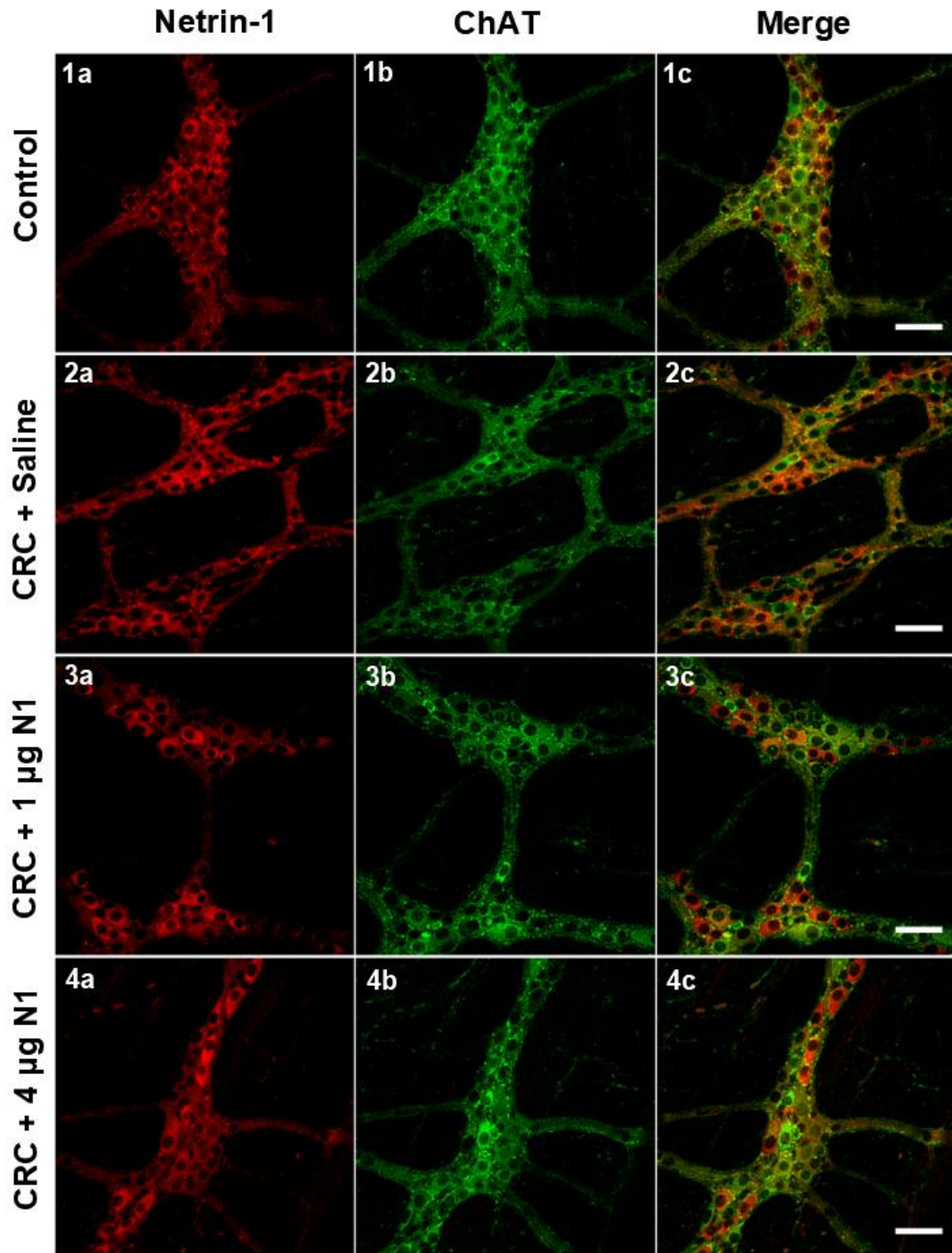


Figure 5.16

**Figure 5.17 Quantitative analysis of Netrin-1-IR and ChAT-IR co-localisation in the myenteric plexus of the colon tissues from Netrin-1 or vehicle-treated CRC mice**

**(A)** The proportion of neurons, that were Netrin-1-negative but strongly positive for ChAT-IR (N1-/ChAT++), was found in the colonic myenteric plexus from healthy mice and the CRC mice treated with saline, 1 µg of N1 and 4 µg of N1. The IR of neurons was measured within the total area of 2mm<sup>2</sup>. Data represented as mean ± SD. **(B)** The proportion of neurons, that were strong Netrin-1-positive but ChAT-negative (N1++/ChAT-), was found in the colonic myenteric plexus from healthy mice and the CRC mice treated with saline, 1 µg of N1 and 4 µg of N1. The IR of neurons was measured within the total area of 2mm<sup>2</sup>. Data represented as mean ± SD (\**p*<0.05, \*\*\**p*<0.001 vs control; #*p*<0.05 vs CRC + saline). **(C)** The proportion of neurons, that were positively stained for both Netrin-1 and ChAT markers; either weakly or strongly positive for Netrin-1-IR as well as either weakly or strongly positive for ChAT-IR (N1+(+)/ChAT+(+)), was found in the colonic myenteric plexus from healthy mice and the CRC mice treated with saline, 1 µg of N1 and 4 µg of N1. The IR of neurons was measured within the total area of 2mm<sup>2</sup>. Data represented as mean ± SD (\**p*<0.05, \*\**p*<0.01 vs control) (saline, n=4; 1 µg of N1, n=3; 4 µg of N1, n=4).

**Abbreviations:** IR, immunoreactivity; ChAT, choline acetyltransferase; N1, Netrin-1; +, weakly positive; ++, strongly positive; +(+) , both weakly and strongly positive; -, negative.

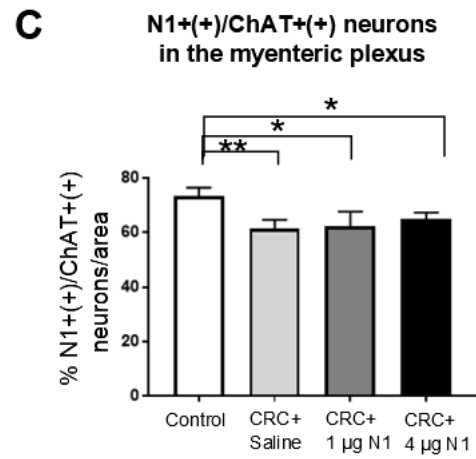
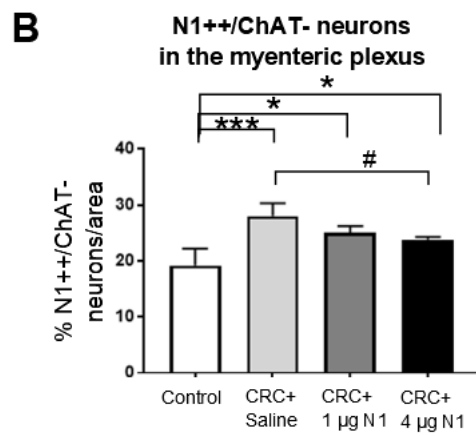
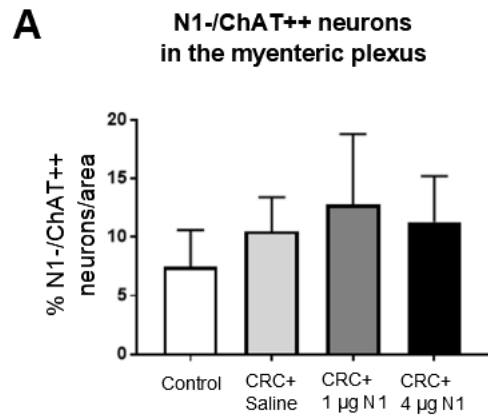


Figure 5.17

## 5.4 Discussion

### 5.4.1 The effect of Netrin-1 treatment on primary tumour growth and progression

Netrin-1 receptors are found to belong to a family of dependence receptors [178]. This means that Netrin-1 receptors mediate cell survival in the presence of Netrin-1, while the receptors trigger apoptosis in the absence of Netrin-1. Hence, Netrin-1 has been identified as a cell survival factor. The interaction of Netrin-1 and its dependence receptor has been elegantly shown in the healthy adult colonic epithelium of the crypts [209]. It is found that DCC receptors are evenly distributed along the epithelium, whereas expression of Netrin-1 is shown to form a gradient in the colonic crypts. A high expression of Netrin-1 is shown at the crypt base, where the compartment of stem cell and transit-amplifying progenitors is located. On the other hand, a low expression of Netrin-1 is indicated at the tip of the crypts, where apoptotic cells are shed off to the lumen [160]. This Netrin-1 gradient was further examined to see whether Netrin-1 is a key player for maintaining epithelial homeostasis by regulating DCC-induced apoptosis. Using the transgenic mice with a constitutively active Netrin-1 gene in the gut revealed that Netrin-1 and its receptors are involved in colorectal tumour progression by two opposing events: gain of Netrin-1 and loss of Netrin-1 receptors [153, 162, 409]. Up-regulated Netrin-1 mediates cell survival signals and confers a selective advantage for tumour cells to become metastatic cancer cells [410]. The *in vivo* study using the gut specific Netrin-1 transgenic mice backcrossed with mutated adenomatous polyposis coli genetic background mice,  $APC^{+/1638N}$ , showed that enforced expression of Netrin-1 enhanced transition of adenoma to adenocarcinoma. This tumour progression was shown to be merely mediated by reduction in intestinal epithelial cell death. Other cellular processes such as proliferation and differentiation were not affected by up-regulation of Netrin-1, and consequently the global epithelial structure was not disturbed [153].

The other event, involving the loss of Netrin-1 receptors, is frequently observed in human sporadic colorectal cancer [411]. The loss of Netrin-1 receptors represents the loss of the dependence receptors, which are capable of mediating apoptosis, resulting in enhanced tumour cell survival [400]. Similarly,

transplanting DCC-deficient tumour cells into mice lungs exhibited elevated tumour cell survival as opposed to DCC-proficient tumour cell transplantation [410]. This is because DCC-deficient tumour cells lack the capacity to undergo pro-apoptotic activity. Collectively, the current dogma is that DCC receptors are known to be a conditional tumour suppressor, and Netrin-1 is a tumourigenic regulator.

On the contrary, this current study demonstrated that introducing a high concentration of Netrin-1 in CRC mice inhibited the primary CRC tumour growth and progression. The CRC mice treated with 4 µg of Netrin-1 indicated a significantly lower number of tumour polyps on their caeca when compared to the CRC mice treated with saline. Furthermore, H&E staining results revealed that the tumour cells implanted in the caeca from the majority of mice treated with 4 µg of Netrin-1 appeared to be lacking tumour growth, when compared to the ones from the mice treated with saline and 1 µg of Netrin-1. Furthermore, metastasis of tumour cells from the caecum to the colon was observed in all CRC mice that received saline treatment. On the other hand, only one CRC mouse from each of the 1 µg and 4 µg of Netrin-1 treatment groups showed metastases to the colon.

In addition to the H&E staining data, the Ki67-immunohistochemistry results indicated vast numbers of Ki67-positive cells in the tumour regions of caeca thus confirming the highly aggressive nature of the tumour. This was shown in the caecum tissues from the CRC mice treated with saline and 1 µg of Netrin-1, but not treated with 4 µg of Netrin-1. Also, angiogenesis marker, CD31-positive regions were more readily detected in the caecum tissues from the mice treated with saline and 1 µg of Netrin-1 in comparison to the ones from the mice treated with 4 µg of Netrin-1.

There may be two major reasons why our results contradict the current dogma that the increase of Netrin-1 expression induces tumour progression. Firstly, Netrin-1 was introduced to the surgically operated CRC orthotopic mouse model. This means that this CRC was not induced by genetic alteration, such as loss of DCC heterozygosity. Although CT26 cells that were inoculated in the caecum do not express DCC, they nevertheless express other types of Netrin-1

dependence receptors, such as UNC5H2 and Neogenin (data shown in Chapter 2). Therefore, CT26 cells do not lack conditional tumour suppressors.

Secondly, recombinant mouse Netrin-1 protein and murine colorectal cancer CT26 cells were introduced to wild-type syngeneic Balb/c mice instead of immunocompromised mice. Hence, it would be expected that these wild-type mice would have raised an immune response to the CT26 cells and Netrin-1. There has been accumulating data revealing that Netrin-1 is associated with regulating inflammation. Generally, Netrin-1 has been associated with anti-inflammatory response. Netrin-1 is found to inhibit leukocyte migration [412] and dampen the inflammation response to the local injury site. A similar anti-inflammatory effect of Netrin-1 has been reported in the condition of pancreatitis [413], peritonitis [414], and inflammatory bowel disease [415]. Furthermore, Netrin-1 is shown to attenuate acute colitis by limiting leukocyte and neutrophil recruitment [416]. However, Netrin-1 has also been associated with T cell recruitment into acute inflammatory sites resulting in a pro-inflammatory response [417].

Further work is necessary with an increased number of mice. This will provide us a better understanding of these preliminary results to a higher degree of confidence. Also, setting up a time-point assay for this study would be useful, especially with respect to assessing primary tumour growth. This will allow us to understand whether or not introducing 4 µg of Netrin-1 may have reduced the primary tumour growth.

#### **5.4.2 Intrinsic expression of Netrin-1 and DCC in the colonic myenteric plexus of healthy and CRC mice**

The work of Ratcliffe *et al.* has indicated that the Netrin-1 receptor, DCC was found to express in the growth cones of the vagal sensory axons during the development of mice fetal gut. These axons were migrated toward the intrinsic enteric neurons where Netrin-1 was thought to be synthesised. Hence, a neural network between the central nervous system and the enteric nervous system is formed during development [188, 189]. However, the presence of DCC and

Netrin-1 expression and their role in the mature ENS of the *adult* gut have not been elucidated.

To the best of our knowledge, this is the first study to present the localisation of DCC and Netrin-1 in the mature ENS. The wholemount preparation of immunofluorescence labelling indicated that Netrin-1 and the chemo-attractive Netrin-1 receptor, DCC, were expressed in the myenteric plexus of the colon in healthy young adult mice. This was demonstrated by double-labelling of Netrin-1 or DCC with neuronal markers such as PGP9.5, NF-H and  $\beta$ -Tubulin III. The vast majority of all myenteric neurons were positive for DCC and Netrin-1. Also, double-staining of Netrin-1 and DCC showed that both markers were clearly co-localised in the cytoplasm of the neuronal cell bodies and processes.

Particularly, those Netrin-1-positive neurons showed both strong and weak staining in their cytoplasm. This observation led us to examine whether or not there was any potential relationship between Netrin-1 expression with other subtypes of neurons, such as excitatory and inhibitory motor neurons. This is discussed in more detail in the next section 5.4.3.

Moreover, some punctate structures from Netrin-1-IR were notably observed on the edges of the neuronal cell bodies and along the processes; possibly they are varicosities of the axons. The axonal varicosity refers to swelling of the axon which occurs at the synapse where neurotransmitters are contained and released [418]. Often successive varicosities are distributed along an axon [419]. Synaptophysin is a synaptic vesicle marker that has been found in myenteric ganglia and nerve fibers including varicosities in human and rat ENS [420]. The vesicular acetylcholine transporter (VACHT) is a neurotransmitter transporter that functions to load acetylcholine (ACh) into synaptic vesicles in the cleft [421]. Previous studies have shown the staining of synaptophysin and VACHT markers in enteric neurons and they appear granular and/or punctuated structure within the neuronal fibers and enteric glial cells [407, 422], similar to what Netrin-1-IR had shown in this study. Further neurochemical coding of Netrin-1 with synaptophysin and VACHT may be worth examining in the future.

Co-labelling of DCC or Netrin-1 and a glial cell marker, GFAP was tested to see whether or not glial cells also express DCC and/or Netrin-1. However, it was

unclear to answer this question using GFAP. GFAP was chosen because its expression is known to be rich in mature enteric glial cells [401, 423]. However, additional glial cell markers such as calcium binding protein, S100 $\beta$  or transcription factor SRY box-containing gene 10, (SOX10) may help to further clarify this question, as those markers were known to use for purpose of counting glial cells [424].

In addition to DCC, the chemo-repulsive Netrin-1 receptor, UNC5H2 was also examined in this study. Although some IR of UNC5H2 in myenteric ganglia was detected, the staining of UNC5H2 was rather indefinable (data not shown).

It has been reported that DCC expression is markedly reduced in CRC due to the loss of heterozygosity and an aberrant gene methylation in DCC [425]. Also, down-regulation of Netrin-1 expression was generally monitored in CRC except for the CRC case that was driven by inflammation. In that case, up-regulation of Netrin-1 expression was noted [139, 235]. Furthermore, gaining of Netrin-1 expression was found to be associated with the intestinal tumour progression in mice [137]. However, none of this information directly addressed the question of expression of DCC and Netrin-1 in the ENS. Hence, our pilot study of the CRC mouse model in the absence and presence of Netrin-1 treatment was conducted to examine the effects of CRC on the expression of DCC and Netrin-1 in the ENS. Also, the effect of Netrin-1 treatment on the expression of DCC and Netrin-1 in the ENS of CRC mice was examined.

Results of these investigations indicated that both DCC and Netrin-1 expression could be clearly observed in the myenteric neuronal cell bodies and processes of the colon under the CRC condition both in the absence and presence of Netrin-1 treatment. However, the population of neurons that stained strongly positive for Netrin-1 significantly decreased in CRC mice when compared to healthy control mice. This difference in the strong Netrin-1-IR is discussed in detail in relation to the nNOS expression in the following section.

### 5.4.3 Correlation between Netrin-1 expression and the phenotypes of nNOS- and ChAT-positive neurons in the myenteric plexus

The ENS is composed of many different functional types of enteric neurons in mammals [19]. Motility of the gut is regulated by the neuronal circuitry of the myenteric plexus. The subtypes of myenteric neurons in the mouse have been characterised by neurochemistry and electrophysiology [426, 427]. The subtypes include inhibitory and excitatory motor neurons, ascending and descending interneurons and intrinsic sensory neurons. Among those, two major subtypes of myenteric neurons are involved in regulating motility: inhibitory motor neurons expressing nNOS and excitatory motor neurons expressing ChAT. Nitric oxide (NO) is an inhibitory neurotransmitter that is synthesised by the enzyme, nNOS, present in the inhibitory motor neurons [428], whereas ACh is an excitatory transmitter that is produced by ChAT in the excitatory motor neurons [429]. In this thesis, nNOS and ChAT expression are examined in relation to Netrin-1 expression in the myenteric neurons.

This thesis showed that in healthy control mice, nearly 45% of neurons were found to be positive for *strong* Netrin-1 (N1++) in their cytoplasm. Approximately 30% of neurons were positive for nNOS (nNOS+). Of those 45% of neurons expressing strong Netrin-1, around 67% of them were also positive for nNOS (N1++/nNOS+), which is approximately 30% of the total number of neurons. On the other hand, in the cases of CRC mice treated with saline and 1 µg Netrin-1, the proportion of those strong Netrin-1-positive neurons (N1++) was significantly decreased to approximately 35%. As well, the proportion of neurons expressing nNOS (approximately 30% nNOS+) was similar in all CRC conditions. Of those 35% of neurons expressing strong Netrin-1 (N1++) in the CRC mice, around 86% of them were also positive for nNOS (N1++/nNOS+). This indicated that nNOS-positive neurons were also found to express strong Netrin-1 in all conditions (**Figure 5.18 A**).

Collectively, the data suggest that the proportion of neurons expressing nNOS has been delineated by the proportion of neurons expressing strong Netrin-1 in the CRC condition, and thereby the population of neurons expressing both nNOS and strong Netrin-1 has been considerably increased from 67% to 86%.

Since there was no loss of total neuron numbers observed under the CRC condition, this reduction in the population of neurons expressing strong Netrin-1 is not likely due to the loss of neurons. It suggests that there must be a shift in the density of strong Netrin-1-positive neurons to weak Netrin-1-positive neurons in the CRC condition. In the case of CRC mice treated with 4  $\mu$ g Netrin-1, a somewhat similar phenomenon to the other CRC conditions was observed, but it was not regarded as being significant.

In addition, there were some notable changes in the expression between Netrin-1 and ChAT under the condition of CRC with or without Netrin-1 treatment. A schematic diagram (**Figure 5.18 B**) shows an example of the changes in proportion of three different subpopulations: neurons expressing N1-/ChAT++, N1++/ChAT- and N1+(+)/ChAT+(+), in the healthy mice as well as in the context of the CRC mice treated with saline. Here, the proportion of those three subpopulations in the total number of neurons is discussed with respect to each condition. Also, the individual subpopulation type from the control group was compared to its corresponding subpopulation type in the CRC with or without Netrin-1 treatment.

Firstly, with regard to the subpopulation of N1-/ChAT++, no statistically significant changes were observed. However, when comparing this subpopulation from the control group to the ones from CRC conditions (**Figure 5.18 B**, green column), the subpopulation of N1-/ChAT++ was increased by approximately 40% (saline treated), 70% (1  $\mu$ g of N1 treated) and 50% (4  $\mu$ g of N1 treated) in the context of CRC condition.

Despite the rise in this N1-/ChAT++ subpopulation, when only the ChAT-positive neurons were considered, overall ChAT-positive neurons were found to have decreased by approximately 10% under the CRC condition with all treatments. This was analysed by the proportion of N1-/ChAT++ subpopulation together with the proportion of the N1+(+)/ChAT+(+) subpopulation.

Secondly, a significant increase in the subpopulation of N1++/ChAT- in CRC conditions was noted when compared to healthy control (**Figure 5.18 B**, red column). This subpopulation became larger by approximately 50% (saline

treated), 30% (1 µg of N1 treated) and 20% (4 µg of N1 treated) in the context of the CRC condition. Interestingly, the CRC mice treated with Netrin-1 showed less ChAT-negative neurons when compared to the CRC mice treated with saline.

Collectively, these data indicate that a decrease in ChAT-positive neurons as well as an increase in ChAT-negative neurons occurred under CRC conditions with all treatments. This suggests that there was a reduction in ChAT expression in the context of CRC. A similar observation was reported in the studies in Walker 256 carcinosarcoma cell-bearing rats, where a marked decrease in ChAT-immunoreactive myenteric neuronal cell bodies in the small intestine in the presence of cancer was found [430].

Thirdly, with respect to the subpopulation of N1+(+)/ChAT+(+), there were noticeable changes in the proportion of this expression. Of nearly 75% neurons expressing N1+(+)/ChAT+(+) subpopulation in control group was significantly reduced to 60-65% in the CRC condition regardless of the treatment. When this N1++/ChAT- subpopulation was compared to those with the CRC condition (**Figure 5.18 B**, yellow column), it was reduced to approximately 15% (saline treated), 15% (1 µg of N1 treated) and 10% (4 µg of N1 treated) under the CRC condition. Interestingly, in the context of CRC, the loss in the proportion of this subpopulation appears to have been accompanied by an increase in the proportion of the other two subpopulations, N1-/ChAT++ (green column) and N1++/ChAT (red column). This suggests that there is greater separation of Netrin-1 and ChAT co-expression in neurons under the CRC condition. Hence, it led to increase in the number of neurons expressing either Netrin-1 or ChAT alone.

Although no considerable loss of neurons was observed in the context of the CRC condition, a decrease of approximately 5% was observed in the population of Netrin-1-positive neurons that were either strongly or weakly staining under the CRC condition regardless of Netrin-1 treatment. The work of Godlewski *et al.* reported that atrophy of myenteric plexus has been reported in the region proximal to a tumour invasion but not in the region distal to the tumour [368]. Possibly, undetected loss of enteric neurons in the CRC condition in this study

may have occurred because the chosen colonic segments for the wholemount preparation had not yet been invaded by the tumour.

It has been reported that more than one neurotransmitter co-exists in the neurons, and most neurotransmitters and the neurotransmitter-synthetic enzymes are differentially expressed in different subtypes of enteric neurons [21]. Despite the opposing roles of nNOS and ChAT, the co-localisation of these two enzymes has been found in the subpopulation of enteric neurons in all species studied including mice, guinea-pig and humans [431]. In the human colon, it was found that nearly 50% of myenteric neurons express ChAT and 40% express nNOS. Approximately 4% of the myenteric neurons express both nNOS and ChAT [432]. Given this information, it is possible that the subpopulation of N1<sup>++</sup>/ChAT<sup>-</sup> may represent the N1<sup>++</sup>/nNOS subpopulation. The triple-neurochemical labelling of Netrin-1, nNOS and ChAT could not be conducted in this study, because both nNOS and ChAT antibodies were raised in the same species (goat). However, further work involving this triple-labelling may be useful to determine those observed changes in the relationship of nNOS and ChAT in relation to Netrin-1 expression, in the context of the CRC condition.

In this thesis, CRC mice showed an overall decrease in the proportion of ChAT-positive neurons when compared to healthy controls. However, no significant changes in the proportion of neurons immunoreactive for individual nNOS and Netrin-1 were observed in CRC mice when compared to healthy controls. Interestingly, our study found that the proportion of ChAT immunoreactive neurons that are also expressing Netrin-1 was reduced in CRC mice. Also, a greater proportion of neurons exhibited lack of co-labelling of ChAT and Netrin-1 in CRC mice in comparison to healthy controls.

Changes in neurochemical phenotypes associated with gastrointestinal dysfunction have been reported in previous studies. For example, a decrease in the proportion of ChAT immunoreactive neurons, meanwhile an increase in the proportion of nNOS immunoreactive neurons in all regions of the colon have been exhibited in the case of slow transit constipation in patients [433]. This phenomenon has been linked to the observation of disordered peristalsis in

patients experiencing slow transit constipation due to the reduced propagating contractions of the bowel.

In the case of human diabetes, a reduction in the proportion of inhibitory neurons is found to be greater than the proportion of excitatory neurons in diabetic colons [434]. A selective loss of nNOS expressing neurons is noted in the diabetic colons when compared to healthy controls. Also, an overall decrease in cholinergic neurons is found in the diabetic colons in comparison to controls. As a consequence, impaired colonic motility is reported in diabetic patients and this may have induced symptoms such as colonic spasms and constipation.

Consistent with our findings, a notable reduction in the proportion of ChAT immunoreactive neurons in the myenteric plexus was observed in the case of cancer-related cachexia animal model using Walker 256 tumour-bearing rats. This phenomenon has been linked to an intestinal dysfunction during cachexia [430].

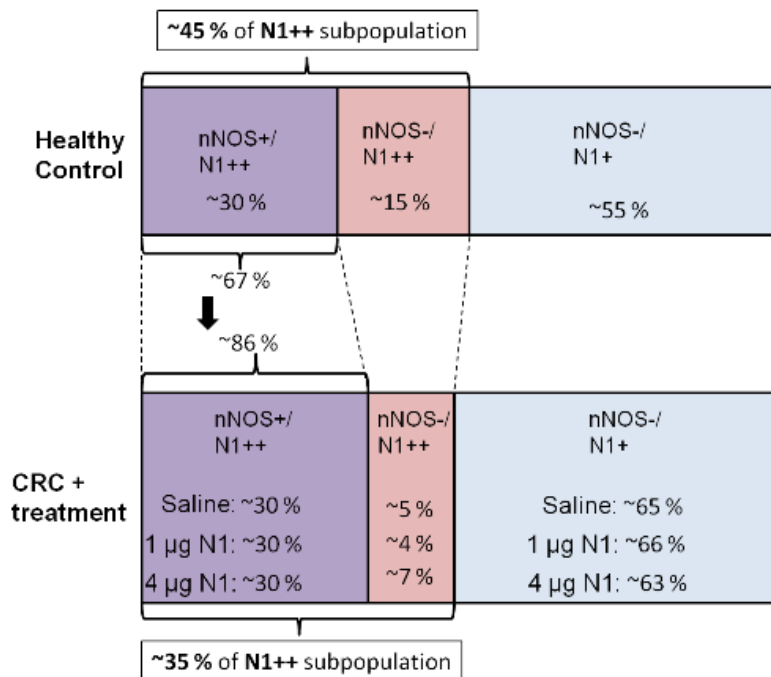
Understanding the contribution of Netrin-1 to phenotypic changes in the nNOS and ChAT phenotypes in CRC condition would be a valuable aspect for a therapeutic target.

**Figure 5.18 A schematic diagram indicating changes in relationship between Netrin-1-IR, nNOS-IR, and ChAT-IR in CRC mice with or without Netrin-1 treatment**

**(A)** Changes in strong Netrin-1 expression in relation to nNOS expression in the context of CRC condition. **(B)** Changes in 3 different immunoreactive neuronal proportions; N1-/ChAT++, N1++/ChAT- and N1+(+)/ChAT+(+).

**Abbreviations:** N1++: strong N1-positive; N1+: weakly N1-positive; N1+(+): either strongly or weakly positive; N-: N1-negative; ChAT++: strong ChAT-positive; ChAT+(+): either strongly or weakly positive; ChAT-: ChAT-negative.

## A Netrin-1 and nNOS expressing neurons



## B Netrin-1 and ChAT expressing neurons

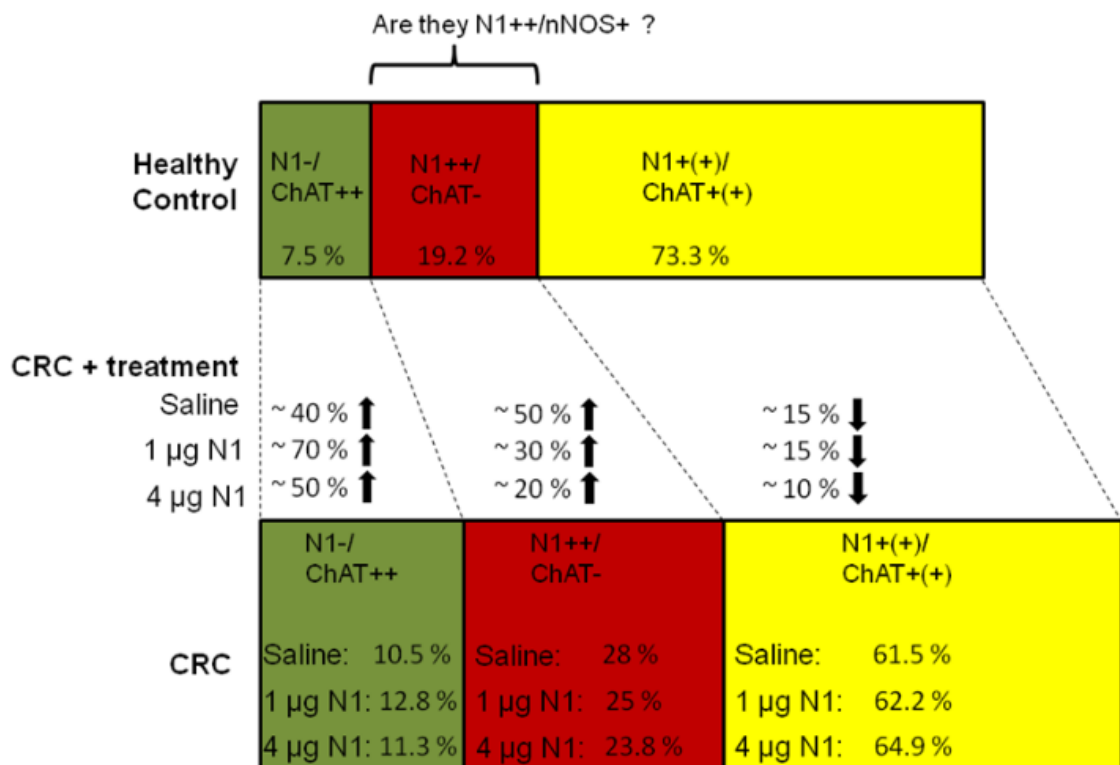


Figure 5.18

## 5.5 Summary

Atrophy of the myenteric plexus in CRC patients has been observed. The damage of enteric neurons during the course of intestinal carcinoma may be responsible for the impairment of normal intestinal function. In order to prevent damage to both enteric neurons and regenerate neural innervations, it is possible that Netrin-1 could be an effective neuroprotectant in these circumstances. However, the caveat associated with this molecule is that it also regulates tumourigenesis.

Two major roles of Netrin-1 have been previously revealed: a neuronal guidance cue and a cell survival factor. The neuronal guidance effect of Netrin-1 has been extensively studied in the developing CNS. The cell survival effect of Netrin-1 has been investigated in relation to various cancers. However, there is a significant gap in our understanding of the role of Netrin-1 and its receptors in the mature ENS in the context of colorectal cancer.

In this thesis, an *in vivo* pilot assay was designed to test whether Netrin-1 could be a possible neuroprotectant for the ENS under the CRC condition. The orthotopic CRC tumour-bearing mice were treated with Netrin-1. Netrin-1 treatment in the CRC mice inhibited the primary tumour growth and progression.

In addition, it was difficult to detect whether or not Netrin-1 treatment caused neuroprotection of the ENS in the CRC mice. This is because no obvious structural damages of myenteric plexus were seen in the CRC mice groups regardless of Netrin-1 treatment when compared to wild-type mice using an immunofluorescent assay.

Furthermore, results presented in this thesis show that Netrin-1 and DCC are expressed in the myenteric plexus of the colon in healthy adult mice. The expression of Netrin-1 and DCC was not changed under the CRC condition. The differential expression of Netrin-1 was observed in certain enteric neuronal cell bodies in the myenteric ganglia. This expression was found to be associated with nNOS and ChAT expression. Under the CRC condition, there

was change in the proportion of Netrin-1 expressing neurons co-localised with nNOS and ChAT.

Although it was found that introducing Netrin-1 via i.p. injection was successful in achieving an increasing Netrin-1 expression in blood circulation, the effect of Netrin-1 treatment did not appear to contribute to the changes in the ENS under the CRC condition. Further studies investigating molecular mechanisms underlying the effects of Netrin-1 treatment on CRC tumour inhibition and changes in the ENS observed in this study are warranted.

# Chapter 6

---

## General discussion and future directions

## **6.1 General comments**

The ENS is an intricate network providing innervations to the GIT and is responsible for regulating vital functions of the GIT, including peristalsis, absorption and secretion [435]. Developmental studies have revealed that the failure of the ENS development and/or absence of the ENS in a region of the colon lead to a severe disruption of the gut function resulting in lethal consequence [436]. Many GIT diseases concerning enteric neuropathy such as inflammatory bowel disease [437] and Chagas disease [438] have been extensively investigated, and yet there is currently no treatment available for enteric neuropathy. Atrophy of the ENS induced by CRC has also been reported in clinical CRC studies [368]. However, this phenomenon has not been well understood. Also, only a few studies on this topic have been conducted up-to-date [369]. This may be because many investigators focus on perineural invasion in the context of cancer [65], instead of enteroneuropathic consequence.

Netrin-1 is one of the best known CNS neuronal guidance molecules. We examined an undefined role of Netrin-1 in the mature ENS. Furthermore, it was investigated whether Netrin-1 can serve as a neuroprotectant for the mature ENS under CRC condition.

## **6.2 The effect of Netrin-1 treatment on the post-natal enteric precursors and differentiated neurons**

The role of Netrin-1 as an axonal guidance cue has been well-established in the CNS. In the past decade, a few studies have demonstrated that Netrin-1 also serves as a guidance molecule in the developing ENS; Neural-crest precursor cells were guided by Netrin-1 to form enteric neuronal plexus [127]. Also, the formation of vagal sensory afferent innervations to the gut was guided by Netrin-1 [439]. Although the role of Netrin-1 in the mature ENS is claimed to be a cell survival factor, this has not been previously investigated.

In this thesis, we examined the role of Netrin-1 in immortalised post-natal enteric neuronal cells, which can show the cellular properties of either

precursors (IM-PEN cells at 33°C) or differentiated neurons (IM-PEN cells at 40.5°C) depending on the changes in temperature and permissive media conditions. Chapter 2 demonstrated that Netrin-1 at a concentration of 50, 100 and 250 ng/mL did not promote the proliferation of enteric neuronal precursor cells. Interestingly, treating the enteric precursors with a high concentration of Netrin-1 (500 ng/mL) induced a significant reduction in cell viability at 48 and 72 hour incubation time points. This phenomenon was not shown to be caused by cell death, since the expression level of cleaved caspase-3 and -9 was decreased in the presence of Netrin-1. Instead, it was thought to be caused by precursor cells undergoing differentiation following a high concentration of Netrin-1 treatment.

In recent years, studies have indicated that Netrin-1 plays a role in cellular differentiation in various tissues. For example, Mediero and colleagues [307] showed that Netrin-1 acting upon UNC5B receptors on osteoclast precursors was essential for osteoclast differentiation in both murine and human species. Additional evidence indicating the role of Netrin-1 in cell differentiation was observed in human embryonal carcinoma (EC) cells [254]. The EC is a germline tumour derived from pluripotent cells. Upon exogenously introduced Netrin-1 treatment, EC cells showed reduced transcription factor Cripto-1, which was associated with the EC cell transformation. Moreover, EC cells treated with Netrin-1 showed neuronal-like morphology with the expression of neuronal markers such as  $\beta$ -Tubulin III, Nestin, and neurotransmitter GABA [254].

In this thesis, cell cycle regulatory proteins such as cyclin D, p21 and p27 were examined in the precursors treated with Netrin-1 to address our hypothesis that Netrin-1 induces enteric precursor cell differentiation. The level of cyclin D was reduced when the cells were treated with 500 ng/mL of Netrin-1. However, the differential level of p27 and p21 expression was uncertain to support our hypothesis. Further analysis using receptor inhibitors or FACS analysis could be useful strategies to clarify the role of Netrin-1 in the differentiation of enteric precursor cells.

Furthermore, it was demonstrated that the migration of precursors was promoted in the presence of Netrin-1 (100 ng/mL and 500 ng/mL) by 4.5 hours. The migratory property of precursors was continuously increased following 100

ng/mL of Netrin-1 treatment by 9 hours. However, this migration was slowed when precursors were treated with 500 ng/mL of Netrin-1 by 9 hours.

Moreover, precursor cells treated with either 100 ng/mL or 500 ng/mL of Netrin-1 displayed an increase in the average neurite length. However, no significant changes were observed in the average neurite length of the differentiated neurons treated with Netrin-1.

Overall, post-natal enteric precursors showed increased migratory property and neurite outgrowth in response to Netrin-1 treatment. However, it was difficult to detect the effect of Netrin-1 on differentiated neurons by using our *in vitro* model. The major difficulty was to obtain a substantial number of fully differentiated neurons, as many cells die during the process of the immortalised cells undergoing differentiation. Additional experiments utilising primary enteric neuronal culture may have been useful in this research. This is discussed further in detail in section 6.6.1.

In addition to *in vitro* studies, the effect of Netrin-1 treatment on the ENS under CRC mice was demonstrated in Chapter 5. There were no obvious differences in the ENS of the CRC mice treated with Netrin-1 when compared to the CRC mice treated with saline. Possible reasons why Netrin-1 treatment was unaffected in the ENS in the context of CRC are further discussed in detail in section 6.6.2.

### **6.3 Intrinsic Netrin-1 expression in the myenteric plexus of healthy young adult mice**

The expression of DCC in the ENS has been noted since early 2000, when Seaman *et al.* have demonstrated that DCC expression is present in the developing mouse of the PNS, in particular, at the early phase of development of the ENS [440]. This finding highlighted that DCC and Netrin-1 signalling is not limited to the CNS. Subsequent studies have described that vagal neural crest-derived precursors, which colonise the gut and form the ENS, were found to express DCC [127]. During the colonisation, precursors initially establish the myenteric plexus and then the subset of those cells undergo a perpendicular

secondary migration toward mucosa to form the submucosal plexus and pancreatic ganglia. The migration of this subset was guided by Netrin-1 originated from the mucosal layer of the gut and pancreas [127]. In addition to vagal neural crest-derived precursors, vagal sensory axons were found to up-regulate the expression of DCC at a certain developmental period, so that the sensory afferent innervation to the fetal gut can be mediated by Netrin-1 guidance [439]. It was further demonstrated that the sensory afferent innervations to the gut were only possible in the ganglionic regions, whereas no progressive innervations were made when the fibers reached the aganglionic regions. Importantly, *in vitro* studies have revealed that the enteric neural crest-derived cells (ENCC) do not express Netrin-1, but they synthesize Netrin-1 once they give rise to enteric neurons. Therefore, DCC-expressing vagal sensory afferent fibers were able to connect with the intrinsic enteric neurons expressing Netrin-1 [189]. Collectively, the authors have indicated that DCC/Netrin-1 signalling plays a pivotal role in establishing the ENS during development. Subsequent studies have indicated that Netrin-1 expression is present in the neural unit of the adult gut [441]. However, the localised expression of DCC and Netrin-1 and the role of Netrin-1 in the mature ENS have not been fully unravelled.

In Chapter 5 of this thesis exhibited the localised expression of DCC and Netrin-1 in the colonic myenteric plexus of the healthy adult mice was demonstrated. The immunofluorescence analysis of the wholemount colon tissue preparations revealed that the expression of DCC and Netrin-1 overlapped in the myenteric plexus, and their expression included almost all enteric ganglia and processes. Some strong Netrin-1-immunoreactivity (IR) was observed along the varicose axons as well as in the outer rim of individual neurons within the ganglion. Especially, the Netrin-1-IR was detected in the cytoplasm of the nerve cell bodies with some showing strong or weak staining. Nearly 45% of the enteric neurons in the myenteric plexus indicated strong Netrin-1-IR in their cytoplasm.

The observed differential intensity of Netrin-1 expression in the myenteric neurons was further investigated in relation to two major neuronal subtypes, excitatory (ChAT) and inhibitory (nNOS) muscle motor and interneurons, that

regulate intestinal motility. This is to explore whether a strong Netrin-1 expression contributes to determining certain neuronal subtypes. The results presented in Chapter 5 indicated that the majority of Netrin-1 expressing neurons also expressed ChAT. However, a small population of approximately 19% showed the neurons which were strongly Netrin-1-positive but ChAT-negative. In contrast, around 8% displayed the neurons which were Netrin-1-negative but strongly ChAT-positive.

In the case of NOS-expressing subtype, almost all of NOS-positive enteric neurons were found to also be labelled for strong Netrin-1-immunoreactivity. This suggests that there is a strong correlation between Netrin-1 and nNOS expression in the colonic myenteric plexus of the healthy mice.

The functional significance of this differential level of Netrin-1 expression in various subpopulations of enteric neurons needs to be further explored.

This Netrin-1 expression in relation to ChAT and NOS expression was further investigated in the context of cancer with or without Netrin-1 treatment. This is discussed in the following section 6.4.

## **6.4 The effect of Netrin-1 treatment on the ENS in the context of colorectal cancer**

The first histological evidence revealing the disrupted ENS in the CRC tissues was demonstrated by Godlewski [368]. Consistent findings were subsequently reported by Kozłowska *et al.* [369] and the authors indicated the atrophy of myenteric plexus near the CRC regions; a reduced number of neurons per plexus and a smaller size of the myenteric plexus were found in the proximity to the cancer invasion. Importantly, those examined CRC tissue samples were taken from patients who had no chemo- and/or radio-therapy or a second serious illness. This highlights the key issue that enteric neuropathy was induced by CRC. The authors initially hypothesized that the observed atrophy of the ENS is caused by apoptosis and/or necrosis. However, there was lack of difference in both caspase-3 and caspase-8 immunoreactive neurons found in the CRC region of the tissues, as opposed to the ones shown in the non-CRC

region of the corresponding tissues. Also, the unclear pattern of macrophage and mononuclear cells were observed in the CRC regions. Together, the authors suggested that the atrophy of the ENS was caused by neither apoptosis nor necrosis event. The effect of CRC on the enteric neurons was investigated in *in vitro* setting to reassess whether CRC induces enteric neuronal death.

### ***Enteric neuronal cells treated with Netrin-1 under CRC conditioned media***

In Chapter 4 of this thesis, the effect of Netrin-1 treatment on the enteric neurons, in the presence of conditioned media (CM) containing factors secreted from CRC, was investigated. The results indicated that when enteric neuronal precursors were incubated with conditioned media, the viability of precursors was significantly reduced. Furthermore, caspase-3 activation in the enteric neuronal precursors was induced by CM. Although treating the precursor cells with Netrin-1 did not improve the viability of the cells, the percentage of cleaved caspase-3-immunoreactive neurons significantly declined in the presence of a high concentration of Netrin-1 (500 ng/mL). This suggests that Netrin-1 is able to inhibit the caspase-3 activation, which was induced by CM, in the precursors.

In the case of examining the differentiated neurons, no significant changes in the level of active caspase-3-IR were found. Furthermore, there was no obvious difference in the percentage of cleaved caspase-3 positive neurons, following Netrin-1 treatment at both high and low concentrations.

It is important to note that caspase-3 activation in neuronal cells could also be associated with the cellular differentiation [374]. Hence, it is difficult to conclude whether the observed reduced cell viability in the presence of CM was directly caused by apoptosis. Additional apoptotic assays such as TUNEL assay and Propidium iodide (PI)-labelled FACS analysis will be helpful to clarify this observation.

Interesting information was provided by the work of Ranigiah and colleagues (2009) using a new biologically targeted approach to discover and validate protein biomarkers that were released from cell lines and mouse models [442]. The authors provided the information involving the entire secreted proteomes of the CT26 cell line and normal young adult mouse colon cell line, YAMC. The

authors also conducted a comparable analysis on the differential expression of the released proteins from CT26 and YAMC cell lines. When compared to the secretome of YAMC, 20 proteins were found to be over-expressed in the secretome of CT26. Among those 20 proteins released from CT26, cathepsin L and secreted phosphoprotein 1 were shown to be largely absent in the secretome of YAMC. Cathepsin L is a cysteine protease, and it is shown to be involved in an apoptotic and autophagic process of Quinolinic acid-induced neuronal death [443] and 6-hydroxydopamine-induced apoptosis of neuroblastoma cells [444]. Furthermore, those abundant 20 proteins are found to be involved in pathways associated with cellular development, including cell growth and death, motility, cell communication, as well as the nervous system functions. Given this information, it might be interesting to determine the effect of those individual 20 proteins on enteric neurons.

### ***The myenteric plexus in CRC mice treated with Netrin-1***

In Chapter 5, the localisation of DCC and Netrin-1 expression in the colonic myenteric plexus of CRC mice was demonstrated. The results showed that no obvious structural changes in the colonic myenteric plexus were observed in the CRC mice. This might be because invasive tumour regions were not found in the collected wholemount preparation. The localised DCC and Netrin-1 expression in the enteric ganglia and processes was unchanged in CRC mice when compared to wild-type control. However, the subpopulation of the neurons expressing strong Netrin-1 found in wild-type was reduced from approximately 45% to 35% in all CRC groups with or without Netrin-1 treatment. Furthermore, no difference in the distribution of the neurons expressing nNOS (approximately 30%) was observed in all CRC groups regardless of Netrin-1 treatment in comparison to the wild-type control.

Consistent with what was seen in the wild-type, nNOS-positive neurons were also shown to be labelled for strong Netrin-1. Of those 35% of neurons expressing strong Netrin-1 in CRC groups, around 86% of them were also positive for nNOS (N1<sup>++</sup>/nNOS<sup>+</sup>), which is approximately 30% of the total number of neurons. Overall, subpopulation totalling 67%, which express both nNOS and strong Netrin-1 found in wild-type control, was found to increase to a total of around 86% in CRC groups regardless of Netrin-1 treatment.

In addition to Netrin-1 and nNOS co-expression, the distribution of the subpopulation expressing both ChAT and Netrin-1 was examined in CRC mice. The results showed that the subpopulation of approximately 75%, expressing both ChAT and Netrin-1 found in the wild-type, was reduced to approximately 62% (saline treated), 62% (1 µg of N1 treated) and 65% (4 µg of N1 treated) under the CRC condition.

Furthermore, subpopulations totalling around 30%, which express either ChAT or Netrin-1 found in the wild-type, were shown to increase to a total of approximately 40% in CRC groups regardless of Netrin-1 treatment.

Collectively, for the markers of nNOS and ChAT, the data suggested that the CRC condition induced an increase in subpopulation size that express either Netrin-1 or ChAT marker, but a decrease in subpopulation size co-expressing Netrin-1 and ChAT markers. It is unclear what causes this phenomenon to occur at this stage. Further mechanistic studies are needed to clarify the shifts in the expression of these 3 markers under CRC condition. Overall, it appeared that exogenous Netrin-1 treatment did not significantly affect the enteric neurons which intrinsically express Netrin-1, nNOS and ChAT in this CRC mouse model. Additional work involving colonic motility assessment and an electrophysiology analysis of neuronal functions may enable to better understand the role of Netrin-1 in specific neuronal subpopulations in the adult ENS in the context of CRC condition.

## **6.5 The effect of Netrin-1 treatment on colorectal cancer cells and in *in vivo* model of colorectal cancer**

Chapter 2 results indicate that Netrin-1 induces migration and neurite outgrowth of post-natal enteric neuronal precursor cells. Data presented in Chapter 4 provide evidence that Netrin-1 inhibits the caspase-3 activation occurring in precursors under CRC conditioned media. Collectively, the data suggest that Netrin-1 could be a useful factor for promoting adult enteric neurogenesis under pathological conditions, such as cancer. However, there is a caveat of using Netrin-1 as a neurotrophic factor and/or neuroprotectant for the enteric neurons under CRC condition. This is because Netrin-1 has also been shown to play a

regulatory role in tumourigenesis [126]. This regulatory role of Netrin-1 is largely based on either association or dissociation between Netrin-1 and its dependence receptors on tumour cells [215].

The majority of human CRC have displayed down-regulation of Netrin-1 dependence receptors such as DCC and UNC5H via genetic and epigenetic alteration [160]. If tumour cells harbour Netrin-1 dependence receptors under a limited and/or absent Netrin-1 condition, tumour cell survival and proliferation can be inhibited by dependence receptor-induced apoptosis. However, loss and/or inactivation of those Netrin-1 dependence receptors can cause the tumour cells to lose ability to undergo apoptosis in the absence of Netrin-1, which ultimately results in tumour development. Hence, down-regulated DCC and UNC5H have been associated with tumour progression as a consequence of decreased tumour apoptosis [211].

In addition to CRC, the cancer profiling analysis revealed that down-regulation of the human UNC5A-C receptors was observed in various cancers including lung, kidney, breast, ovary, uterus and stomach cancers [210]. Moreover, UNC5H receptors are found to be a direct transcriptional target for the tumour suppressor p53 in various cell lines. The p53-dependent apoptosis is shown to be induced by UNC5H expression in the absence of Netrin-1, and that was reverted in the presence of Netrin-1 [153]. Up-regulation of UNC5B in bladder cancer was found to inhibit proliferation and migration. Transplantation of over-expressing UNC5B bladder cancer cells into nude mice showed a reduction in cancer progression [353].

As Netrin-1 being known as a cell survival factor, over-expression of Netrin-1 has been associated with tumour progression [274]. For example, transgenic mice that constitutively over-express Netrin-1 in the gut exhibited spontaneous hyperplastic and neoplastic lesions. When up-regulation of Netrin-1 was genetically enforced in the *adenomatous polyposis coli* mutant mice, which produce spontaneous adenomas, malignancies were observed [137].

Similarly, Netrin-1 over-expressing glioblastoma cells displayed stem-like cell property and enhanced invasiveness in vivo [312]. In addition, Netrin-1 over-expression is found in metastatic but not in non-metastatic breast cancer cell

lines. Metastasis of the Netrin-1 over-expressing breast cancer was suppressed in both cases when Netrin-1 siRNA and receptor blockers, such as decoy soluble receptor ectodomains, were added [445]. Collectively, it was proposed that targeting Netrin-1 or its receptors and/or disrupting the interaction between Netrin-1 and its receptors could be a useful strategy for anti-cancer therapy.

However, the Netrin-1 dependence receptor theory is well-suited to explain the causal effect for many cancer types, in particular, in genetically modified settings. A few contradictory results have been observed. For example, Netrin-1 is reduced or absent in approximately 50% of brain tumours and neuroblastomas [139]. Netrin-1 and its receptors such as DCC and Neogenin were also reduced in prostate cancer [153]. In an earlier study, over-expression of Netrin-1 was found to mediate pancreatic adenocarcinoma progression [228]. However, a recent study showed over-expression of Netrin-1 induced regression of pancreatic cancer [326]. This discrepancy is yet to be determined.

In Chapter 3 of this thesis, the effect of Netrin-1 treatment on CT26 colorectal carcinoma cells was demonstrated. This examination was important to assess the behaviour of CT26 cells in culture in response to Netrin-1, since CT26 cells were chosen for induction of orthotopic CRC in Balb/c mice followed by Netrin-1 treatment (Chapter 5).

#### ***Colorectal cancer cells treated with Netrin-1***

Introducing exogenous Netrin-1 to CT26 cells in culture showed an increase in cell proliferation and adhesion. These cellular properties were shown to be mediated by UNC5H2 and Neogenin receptors on CT26 cells in response to Netrin-1. Migration of CT26 cells was also promoted only at a high concentration of Netrin-1 (500 ng/mL). Netrin-1 treatment was found to activate UNC5H2 and Neogenin receptors on CT26 cells and mediate pFAK/pMEK/pERK signalling pathways.

#### ***Colorectal cancer mice treated with Netrin-1***

In Chapter 5, the findings of the effect of Netrin-1 administration on the orthotopic CRC mice via i.p. injection are presented. The *in vivo* results indicated that a reduced number of tumour polyps were found in the CRC mice

treated with a high concentration of Netrin-1 (4 µg/mouse/day) in comparison to the CRC mice treated with saline. Furthermore, the CRC mice treated with a high concentration of Netrin-1 showed a limited proliferation of CT26 cells on the primary transplanted site, caecum, and less expression of the angiogenic marker, CD31, when compared to the saline-treated CRC mice. Overall, tumour progression in CRC mice was inhibited following a high concentration of Netrin-1 treatment when compared to CRC mice treated with saline. Further investigations will be required to validate this observation. For example, using luciferase-tagged CT26 cells could enable us to detect the progression of CT26 cells in the mice. Also, experiments with time-point tissue collection could enable us to assess the quantitative and comparable analysis on tumour regression in the presence of Netrin-1 treatment.

Our data show that the outcome observed in CT26 cells following Netrin-1 treatment was different to that seen for the CT26 cell-bearing mice after they received Netrin-1 treatment. This could be due to the presence of the immune system in the *in vivo* model. The orthotopic colorectal cancer model used in our study was not induced in immunodeficient mice. Therefore, Netrin-1 may have played a role in the immune response. This is supported by recent studies indicating that Netrin-1 is implicated in autoimmune and inflammatory responses [160]. The effect of Netrin-1 in the immune response is discussed further in section 6.6.3.

## **6.6 Limitations and future directions**

### **6.6.1 Primary enteric neuronal cell culture**

In contrast to primary neurons isolated from brain and spinal cord tissues, difficulties of isolating and culturing primary enteric neuronal cells from gut tissues have been previously described. Such difficulties include: 1) mixed cell types in the gut tissues; 2) a long neuronal network distribution from plexuses that are fused to the smooth muscle and mucosa layers and; 3) the presence of excretion, bacteria and fungi in the gut lumen [446]. In early studies, primary enteric neuronal cell cultures were mainly isolated from guinea-pigs, and that was thought to be relatively easy process at the time, since guinea-pigs have

anatomically larger and looser enteric neuronal plexuses than mice. However, in-bred mouse models have become preferable to many researchers since mice are versatile in breeding and it is relatively easy to produce genetically engineered strains. In recent years, researchers have demonstrated that primary enteric neurons can be successfully isolated from embryonic mice as well as post-natal mice and grown in culture. Still, obtaining a large number of neurons has been a major challenge [447], and further, growing neurons in *in vitro* system is limited because primary neurons are unable to propagate once they have terminally differentiated. In order to overcome those limitations, Professor Srinivasan's research group has recently generated immortalised fetal (IM-FEN) and post-natal (IM-PEN) enteric neuronal cell lines using immortal mice. Prior to the generation of those cell lines, studies concerning the ENS were mainly conducted by either using primary culture or transformed cell lines which resemble neuronal phenotypes. For example, the human neuroblastoma cell line (SH-SY5Y), which was originally derived from a subcloned population of the metastatic bone tumour biopsy, expresses immature neuronal markers and provides neuroblast-like morphology [448]. This cell line has been popularly used in *in vitro* systems for studying neuronal cell biology with respect to the CNS [449] as well as the ENS [450]. In addition, human teratocarcinoma cells (NT2 or also known as NTera 2) [451] and rat pheochromocytoma cells of the adrenal medulla (PC12) [452] have been used for neuronal differentiation studies of the ENS.

In this thesis, an IM-PEN cell line was used in *in vitro* settings and the effects of Netrin-1 treatment on IM-PEN cells were investigated with respect to the precursors and differentiated status. IM-FEN cell line was also given as a gift from Professor Srinivasan to compare the analysis between the fetal and post-natal enteric neurons. However, working with IM-FEN cell line was not successful due to the loss of adherent property of the cell line for unknown reasons.

Generally, the advantages of using immortalised cell lines are that a large number of cells are easily obtained and potential variability between cultures is minimised in comparison to using a primary cell culture. Despite this, the primary enteric neuronal cell cultures are still favourable to many

neuroscientists as they are more likely to recapitulate the neuronal cell properties as compared to the immortalised cells which integrated the oncogenic property [447].

Further investigations utilising primary enteric neurons in addition to IM-PEN cells would broaden our understanding of the effect of Netrin-1 in the ENS.

### **6.6.2 The ENS of CRC mice with Netrin-1 treatment**

In Chapter 5 of this thesis, no obvious neuronal damage or nerve atrophy of the colonic myenteric plexus was noted in CRC mice. This was assumed that there were no invasive tumours contained in the colon sections that were prepared for the wholemount immunofluorescence. Undamaged myenteric plexus in the prepared colon sections may be a partial reason why that Netrin-1 treatment was not noticeable in the ENS under CRC condition. Also, Netrin-1 expression already exists in almost all enteric ganglia and processes of the myenteric plexus, therefore Netrin-1 treatment may not have affected the ENS of those CRC mice.

Furthermore, this thesis demonstrated that DCC expression is found to remain intact in enteric neurons and processes of the colonic myenteric plexus during the course of CRC development. Hence, it is reasonable to hypothesise that if potential damage being induced in the myenteric plexus in the context of CRC condition, Netrin-1 treatment may have assisted in axonal regeneration.

However, even if nerve damage was found in the CRC mice, changes in the expression of DCC and Netrin-1 may not be evident in this experiment. This is because previous results from both adult CNS and PNS nerve injuries (discussed in section 1.11) indicated that changes in Netrin-1 and its receptors are noticeable several days or weeks after injury. Additional experiments employing time-point methods would clarify the changes in Netrin-1 and DCC expression during the course of CRC development.

In addition to DCC expression, UNC5B immunofluorescent labelling on the myenteric plexus of wholemount colon tissues was attempted but it was unsuccessful. Further investigations exploiting differential levels of DCC,

Neogenin and UNC5H1-4 expression in the mature ENS under CRC condition could provide a better understanding of the role of Netrin-1 in the ENS under CRC condition.

### **6.6.3 The effect of Netrin-1 in CRC immune response**

Accumulating evidence has revealed that the role of Netrin-1 is involved in immune response [252, 357, 415]. Recent studies have demonstrated that Netrin-1 serves as a guidance molecule for immune cell migration. For example, Netrin-1 is found to inhibit the recruitment of neutrophils, monocytes and macrophages during acute inflammation [415, 453]. Also, Netrin-1 is shown to suppress the leukocyte infiltration during an immune response to inflammatory bowel disease (IBD), and that results in attenuated inflammation [415]. Previously, *in vivo* studies using the acute colitis mouse model with knock-down of Netrin-1 (*Ntn-1<sup>-/-</sup>*) demonstrated that these mice exhibited histological tissue damages with infiltrating inflammatory cells. As a consequence, *Ntn-1<sup>-/-</sup>* mice displayed a markedly exacerbated course of an inflammatory condition in comparison to wild-type controls (*Ntn-1<sup>+/+</sup>*), suggesting that Netrin-1 plays a protective role in inflammation. Moreover, when DSS-colitis mice were subcutaneously treated with recombinant Netrin-1 (1 µg/mouse/day) using an osmotic pump for 6 days, neutrophil trafficking was preferentially suppressed among other immune cells following Netrin-1 treatment. Ultimately Netrin-1 treated DSS-colitis mice showed less severity of the disease compared to DSS-colitis mice treated with vehicle control (BSA) group [415].

Studies in animal models of pathological conditions including diabetes and chronic kidney disease have found that Netrin-1 modulates inflammation via NFκB and COX-2/PGE2 pathways in tissue injuries [327, 454]. Netrin-1 is shown to suppress NFκB activation which in turn inhibits COX-2 expression in epithelial cells as well as inhibiting PGE2 production in immune cells, such as neutrophils and monocytes [455].

Furthermore, a recent study has indicated that Netrin-1 promotes the migration of neogenin-expressing lymphocytes, especially CD4<sup>+</sup> T-helper cells [417]. The local injections of Netrin-1 into human skin engrafted severe combined immunodeficient mouse model exhibited an infiltration of T-lymphocytes [417]. The authors suggested that Netrin-1 induces migration of T-lymphocytes via

activation of the members of the RhoGTPase family including Rho, Rac and Cdc42. The Rho GTPase family are known for the important role they play in regulating actin cytoskeleton reorganisation, and the activation of this signalling pathway has been associated with changes in cellular motility [456].

In this thesis, Chapter 3 demonstrated *in vitro* experiments using CT26 cells that were used to generate the orthotopic CRC mouse model shown in Chapter 5. The results from *in vitro* studies indicated that addition of Netrin-1 enhanced the proliferation and migration of CT26 cells. However, it was noted that application of Netrin-1 did not contribute to invasive properties of CT26 cells. In Chapter 5, when a recombinant Netrin-1 protein was introduced to the orthotopic CRC mice via daily i.p injection for 6 days, the primary tumour growth and its progression were shown to be limited in the CRC mice treated with a high concentration of Netrin-1 (4 µg/mouse/day), in comparison to CRC mice treated with saline (vehicle control). Although it was hypothesised that Netrin-1 may play a role in immune response associated with CRC mice, this aspect has not been explored in this thesis due to the limited time and resources. Experiments involving the level of cytokines assessment and FACS analysis for the immune cell types recruited to the tumour site may be a useful examination. These additional investigations concerning immune responses in the CRC mice following Netrin-1 treatment will shed light on the better usage of Netrin-1 as a therapeutic agent in the CRC condition.

## 6.7 Conclusions

Studies in the past decade have demonstrated that Netrin-1 guidance is required for establishing submucosal plexus and vagal sensory afferent innervations in the developing gut. This thesis provides the first evidence that Netrin-1 and DCC are co-localised in almost all myenteric ganglia and processes in the mature ENS of mice colon tissues. Distribution of neurons expressing strong Netrin-1 was linked to certain neuronal subtypes. The guidance role of Netrin-1 was shown to be effective in the post-natal enteric neuronal precursors but not in differentiated neurons, suggesting that Netrin-1 can be a useful trophic factor for promoting adult enteroneurogenesis. Netrin-1 administration did not affect the enteric neurons under CRC condition in mice.

However, it limited CRC progression. Overall, this thesis provides groundwork for possible therapeutic targets where Netrin-1 can serve in the mature ENS in the context of CRC.

# References

1. Nagy, N. and A.M. Goldstein, *Enteric nervous system development: A crest cell's journey from neural tube to colon*. *Seminars in Cell & Developmental Biology*, 2017. **66**: p. 94-106.
2. Furness, J.B., *The enteric nervous system*. 2006: Malden, Mass. : Blackwell Pub., 2006.
3. Gabella, G., *Ultrastructure of the nerve plexuses of the mammalian intestine: the enteric glial cells*. *Neuroscience*, 1981. **6**(3): p. 425-436.
4. Fekete, É., M. Bagyánszki, and B.A. Resch, *Prenatal development of the myenteric plexus in the human fetal small intestine*. *Acta Biol Szeged*, 2000. **44**: p. 3-19.
5. Mittal, R., et al., *Neurotransmitters: The Critical Modulators Regulating Gut–Brain Axis*. *Journal of cellular physiology*, 2017. **232**(9): p. 2359-2372.
6. Gershon, M., *The second brain: The scientific basis of gut instinct*. 1998, New York: Harper Collins.
7. Furness, J.B., *The enteric nervous system: normal functions and enteric neuropathies*. *Neurogastroenterology & Motility*, 2008. **20**: p. 32-38.
8. Furness, J.B., *The enteric nervous system and neurogastroenterology*. *Nat Rev Gastroenterol Hepatol*, 2012. **9**(5): p. 286-294.
9. Wallace, A.S. and R.B. Anderson, *Genetic interactions and modifier genes in Hirschsprung's disease*. *World Journal of Gastroenterology*, 2011. **17**(45): p. 4937-4944.
10. Swenson, O. and J.H. Fisher, *Hirschsprung's Disease During Infancy*. *Surgical Clinics of North America*, 1956. **36**(6): p. 1511-1515.
11. Furness, J.B., et al., *The enteric nervous system and gastrointestinal innervation: integrated local and central control*, in *Microbial endocrinology: The microbiota-gut-brain axis in health and disease*. Springer, 2014. p. 39-71.
12. Kunze, W. and J. Furness, *The enteric nervous system and regulation of intestinal motility*. *Annual Review of Physiology*, 1999. **61**(1): p. 117-142.
13. Hansen, M.B., *The Enteric Nervous System I: Organisation and Classification*. *Pharmacology & Toxicology*, 2003. **92**(3): p. 105-113.
14. Ibba-Manneschi, L., et al., *Structural organization of enteric nervous system in human colon*. *Histology and Histopathology*, 1995. **10**: p. 17-17.
15. Timmermans, J.P., J. Hens, and D. Adriaensen, *Outer submucous plexus: an intrinsic nerve network involved in both secretory and motility processes in the intestine of large mammals and humans*. *The Anatomical Record*, 2001. **262**(1): p. 71-78.
16. Hansen, M.B., *The enteric nervous system I: organisation and classification*. *Basic & Clinical Pharmacology & Toxicology*, 2003. **92**(3): p. 105-113.
17. Furness, J.B., et al., *The Enteric Nervous System and Its Extrinsic Connections*. *Textbook of Gastroenterology*. 2009: Blackwell Publishing Ltd. 15-39.
18. Furness, J., *Enteric nervous system: neural circuits and chemical coding*. *Encyclopedia of neuroscience*. Academic Press, Oxford, 2009: p. 1089-1095.
19. Furness, J.B., *Types of neurons in the enteric nervous system*. *Journal of the Autonomic Nervous System*, 2000. **81**(1-3): p. 87-96.
20. Furness, J.B., *Types of neurons in the enteric nervous system*. *Journal of the Autonomic Nervous System*, 2000. **81**(1-3): p. 87-96.
21. Hao, M.M. and H.M. Young, *Development of enteric neuron diversity*. *Journal of Cellular and Molecular Medicine*, 2009. **13**(7): p. 1193-1210.

22. Hanani, M., et al., *Regeneration of myenteric plexus in the mouse colon after experimental denervation with benzalkonium chloride*. Journal of Comparative Neurology, 2003. **462**(3): p. 315-327.
23. Metzger, M., *Neurogenesis in the enteric nervous system*. Archives Italiennes De Biologie, 2010. **148**(2): p. 73-83.
24. Anderson, R.B., D.F. Newgreen, and H.M. Young, *Neural Crest and the Development of the Enteric Nervous System*, in *Neural Crest Induction and Differentiation*, J.-P. Saint-Jeannet, Editor. 2006, Springer US: Boston, MA. p. 181-196.
25. Anderson, R.B., A.L. Stewart, and H.M. Young, *Phenotypes of neural-crest-derived cells in vagal and sacral pathways*. Cell and Tissue Research, 2006. **323**(1): p. 11-25.
26. Le Douarin, N.M. and E. Dupin, *Multipotentiality of the neural crest*. Current Opinion in Genetics & Development, 2003. **13**(5): p. 529-536.
27. Saint-Jeannet, J.-P., *Neural crest induction and differentiation*. Vol. 589. 2007: Springer Science & Business Media.
28. Zorn, A.M. and J.M. Wells, *Vertebrate Endoderm Development and Organ Formation*. Annual Review of Cell and Developmental Biology, 2009. **25**: p. 221-251.
29. Obermayr, F., et al., *Development and developmental disorders of the enteric nervous system*. Nature Reviews Gastroenterology and Hepatology, 2013. **10**(1): p. 43-57.
30. Goldstein, A., R. Hofstra, and A. Burns, *Building a brain in the gut: development of the enteric nervous system*. Clinical Genetics, 2013. **83**(4): p. 307-316.
31. Paratore, C., et al., *Sox10 haploinsufficiency affects maintenance of progenitor cells in a mouse model of Hirschsprung disease*. Human Molecular Genetics, 2002. **11**(24): p. 3075-3085.
32. Young, H., et al., *Dynamics of neural crest-derived cell migration in the embryonic mouse gut*. Developmental Biology, 2004. **270**(2): p. 455-473.
33. Young, H.M., A.J. Bergner, and T. Müller, *Acquisition of neuronal and glial markers by neural crest-derived cells in the mouse intestine*. The Journal of Comparative Neurology, 2003. **456**(1): p. 1-11.
34. Young, H.M., et al., *Dynamics of neural crest-derived cell migration in the embryonic mouse gut*. Developmental Biology, 2004. **270**(2): p. 455-473.
35. Rühl, A., *Glial cells in the gut*. Neurogastroenterology & Motility, 2005. **17**(6): p. 777-790.
36. Laranjeira, C., et al., *Glial cells in the mouse enteric nervous system can undergo neurogenesis in response to injury*. The Journal of Clinical Investigation, 2011. **121**(9).
37. Pham, T.D., M.D. Gershon, and T.P. Rothman, *Time of origin of neurons in the murine enteric nervous system: sequence in relation to phenotype*. The Journal of Comparative Neurology, 1991. **314**(4): p. 789-798.
38. Rothman, T.P. and M.D. Gershon, *Phenotypic expression in the developing murine enteric nervous system*. Journal of Neuroscience, 1982. **2**(3): p. 381-393.
39. Schäfer, K.H., C.V. Ginneken, and S. Copray, *Plasticity and neural stem cells in the enteric nervous system*. The Anatomical Record, 2009. **292**(12): p. 1940-1952.
40. Dettmann, H.M., et al., *Isolation, expansion and transplantation of postnatal murine progenitor cells of the enteric nervous system*. PloS one, 2014. **9**(5): p. e97792.
41. Kim, H.J. and W. Sun, *Adult Neurogenesis in the Central and Peripheral Nervous Systems*. International Neurology Journal, 2012. **16**(2): p. 57-61.
42. Kruger, G.M., et al., *Neural Crest Stem Cells Persist in the Adult Gut but Undergo Changes in Self-Renewal, Neuronal Subtype Potential, and Factor Responsiveness*. Neuron, 2002. **35**(4): p. 657-669.
43. Almond, S., et al., *Characterisation and transplantation of enteric nervous system progenitor cells*. Gut, 2007. **56**(4): p. 489-496.
44. Estrada-Mondaca, S., A. Carreón-Rodríguez, and J. Belkind-Gerson, *Biology of the adult enteric neural stem cell*. Developmental Dynamics, 2007. **236**(1): p. 20-32.

45. Bixby, S., et al., *Cell-Intrinsic Differences between Stem Cells from Different Regions of the Peripheral Nervous System Regulate the Generation of Neural Diversity*. *Neuron*, 2002. **35**(4): p. 643-656.
46. Laranjeira, C., et al., *Glial cells in the mouse enteric nervous system can undergo neurogenesis in response to injury*. *The Journal of Clinical Investigation*, 2011. **121**(9): p. 3412.
47. Liu, M.-T., et al., *5-HT4 receptor-mediated neuroprotection and neurogenesis in the enteric nervous system of adult mice*. *Journal of Neuroscience*, 2009. **29**(31): p. 9683-9699.
48. Kulkarni, S., et al., *Adult enteric nervous system in health is maintained by a dynamic balance between neuronal apoptosis and neurogenesis*. *Proceedings of the National Academy of Sciences*, 2017: p. 201619406.
49. Tokui, K., M. Sakanaka, and S. Kimura, *Progressive reorganization of the myenteric plexus during one year following reanastomosis of the ileum of the guinea pig*. *Cell And Tissue Research*, 1994. **277**(2): p. 259-272.
50. Ramalho, F.S., et al., *Myenteric neuron number after acute and chronic denervation of the proximal jejunum induced by benzalkonium chloride*. *Neuroscience Letters*, 1993. **163**(1): p. 74-76.
51. Fox, D.A., M.L. Epstein, and P. Bass, *Surfactants selectively ablate enteric neurons of the rat jejunum*. *Journal of Pharmacology and Experimental Therapeutics*, 1983. **227**(2): p. 538-544.
52. Kulkarni, S., et al., *Adult enteric nervous system in health is maintained by a dynamic balance between neuronal apoptosis and neurogenesis*. *Proceedings of the National Academy of Sciences of the United States*, 2017(18): p. 3709.
53. Lu, R., et al., *Neurons generated from carcinoma stem cells support cancer progression*. *Signal Transduction and Targeted Therapy*, 2017. **2**: p. 16036.
54. Boilly, B., et al., *Nerve Dependence: From Regeneration to Cancer*. *Cancer Cell*. **31**(3): p. 342-354.
55. Schuller, H.M., *Neurotransmission and cancer: implications for prevention and therapy*. *Anti-Cancer Drugs*, 2008. **19**(7): p. 655-671.
56. Mancino, M., et al., *The neuronal influence on tumor progression*. *Biochimica et Biophysica Acta (BBA) - Reviews on Cancer*, 2011. **1816**(2): p. 105-118.
57. Li, H., X. Fan, and J. Houghton, *Tumor microenvironment: the role of the tumor stroma in cancer*. *Journal of Cellular Biochemistry*, 2007. **101**(4): p. 805-815.
58. Jobling, P., et al., *Nerve–Cancer Cell Cross-talk: A Novel Promoter of Tumor Progression*. *Cancer Research*, 2015. **75**(9): p. 1777-1781.
59. Ko, H.C., et al., *Original Report: A contouring guide for head and neck cancers with perineural invasion*. *Practical Radiation Oncology*, 2014. **4**: p. e247-e258.
60. Ozcan, F., *Correlation of perineural invasion on radical prostatectomy specimens with other pathologic prognostic factors and PSA failure*. *European Urology*, 2001. **40**(3): p. 308-312.
61. Takahashi, T., et al., *Perineural invasion by ductal adenocarcinoma of the pancreas*. *Journal Of Surgical Oncology*, 1997. **65**(3): p. 164-170.
62. Olar, A., et al., *Biologic correlates and significance of axonogenesis in prostate cancer*. *Human Pathology*, 2014(7): p. 1358.
63. Zhang, L., et al., *Parasympathetic neurogenesis is strongly associated with tumor budding and correlates with an adverse prognosis in pancreatic ductal adenocarcinoma*. *Chinese Journal of Cancer Research*, 2016. **28**(2): p. 180-186.
64. Zhao, C.-M., et al., *Denervation suppresses gastric tumorigenesis*. *Science Translational Medicine*, 2014. **6**(250): p. 250ra115-250ra115.
65. Rademakers, G., et al., *Review: The role of enteric neurons in the development and progression of colorectal cancer*. *BBA - Reviews on Cancer*, 2017. **1868**: p. 420-434.

66. Ferlay, J., et al., *Estimates of worldwide burden of cancer in 2008: GLOBOCAN 2008*. International Journal of Cancer, 2010. **127**(12): p. 2893-2917.
67. Center, M.M., A. Jemal, and E. Ward, *International Trends in Colorectal Cancer Incidence Rates*. Cancer Epidemiology Biomarkers & Prevention, 2009. **18**(6): p. 1688-1694.
68. Spano, D., et al., *Molecular networks that regulate cancer metastasis*. Seminars in Cancer Biology, 2012. **22**(3): p. 234-249.
69. Mendoza, M. and C. Khanna, *Revisiting the seed and soil in cancer metastasis*. The International Journal of Biochemistry & Cell Biology, 2009. **41**(7): p. 1452-1462.
70. Brooks, S.A., et al., *Molecular interactions in cancer cell metastasis*. Acta Histochemica, 2010. **112**(1): p. 3-25.
71. Fidler, I.J., *The pathogenesis of cancer metastasis: the 'seed and soil' hypothesis revisited*. Nature Reviews. Cancer, 2003. **3**(6): p. 453-458.
72. Oppenheimer, S.B., *Cellular basis of cancer metastasis: A review of fundamentals and new advances*. Acta Histochemica, 2006. **108**(5): p. 327-334.
73. Eccles, S.A. and D.R. Welch, *Metastasis: recent discoveries and novel treatment strategies*. The Lancet, 2007. **369**(9574): p. 1742-1757.
74. Hart, I.R. and I.J. Fidler, *The implications of tumor heterogeneity for studies on the biology and therapy of cancer metastasis*. Biochimica et Biophysica Acta (BBA) - Reviews on Cancer, 1981. **651**(1): p. 37-50.
75. Chambers, A.F., A.C. Groom, and I.C. MacDonald, *Dissemination and growth of cancer cells in metastatic sites*. Nature Reviews. Cancer, 2002. **2**(8): p. 563-572.
76. Langley, R.R. and I.J. Fidler, *The seed and soil hypothesis revisited—The role of tumor-stroma interactions in metastasis to different organs*. International Journal of Cancer, 2011. **128**(11): p. 2527-2535.
77. Kawaguchi, T. and K. Nakamura, *Analysis of the lodgement and extravasation of tumor cells in experimental models of hematogenous metastasis*. Cancer Metastasis Reviews, 1986. **5**(2): p. 77-94.
78. Honn, K.V., et al., *Tumor Cell-derived 12(S)-Hydroxyeicosatetraenoic Acid Induces Microvascular Endothelial Cell Retraction*. Cancer Research, 1994. **54**(2): p. 565-574.
79. Al-Mehdi, A.B., et al., *Intravascular origin of metastasis from the proliferation of endothelium-attached tumor cells: a new model for metastasis*. Nature Medicine, 2000. **6**(1): p. 100-102.
80. Sierra, A., *Metastases and their microenvironments: linking pathogenesis and therapy*. Drug Resistance Updates, 2005. **8**(4): p. 247-257.
81. Bergers, G. and L.E. Benjamin, *Tumorigenesis and the angiogenic switch*. Nature Reviews. Cancer, 2003. **3**(6): p. 401-410.
82. Dai, C.Y., C.M. Haqq, and J.E. Puzas, *Molecular Correlates of Site-Specific Metastasis*. Seminars in Radiation Oncology, 2006. **16**(2): p. 102-110.
83. Paget, S., *The distribution of secondary growth in cancer of breast*. Lancet, 1889. **1**: p. 571-573.
84. Ewing, J., *Neoplastic diseases : a treatise on tumors*. 1928: Philadelphia [u.a.] : Saunders, 1928.
85. Balkwill, F.R., M. Capasso, and T. Hagemann, *The tumor microenvironment at a glance*. Journal of Cell Science, 2012. **125**(23): p. 5591-5596.
86. Huszar, M., et al., *The tumor microenvironment: part 1*. Immunotherapy, 2011. **3**(11): p. 1367-84.
87. Bissell, M.J., P.A. Kenny, and D.C. Radisky, *Microenvironmental Regulators of Tissue Structure and Function Also Regulate Tumor Induction and Progression: The Role of Extracellular Matrix and Its Degrading Enzymes*. Cold Spring Harbor Symposia on Quantitative Biology, 2005. **70**: p. 343-356.

88. Weaver, V.M., et al., *Reversion of the Malignant Phenotype of Human Breast Cells in Three-Dimensional Culture and In Vivo by Integrin Blocking Antibodies*. The Journal of Cell Biology, 1997. **137**(1): p. 231-245.
89. Allinen, M., et al., *Molecular characterization of the tumor microenvironment in breast cancer*. Cancer Cell, 2004. **6**(1): p. 17-32.
90. Bissell, M.J. and D. Radisky, *Putting tumours in context*. Nature Reviews. Cancer, 2001. **1**(1): p. 46-54.
91. Kaplan, R.N., et al., *VEGFR1-positive haematopoietic bone marrow progenitors initiate the pre-metastatic niche*. Nature, 2005. **438**(7069): p. 820-827.
92. Rustgi, A.K., *The genetics of hereditary colon cancer*. Genes & development, 2007. **21**(20): p. 2525-2538.
93. Fearon, E., et al., *Identification of a chromosome 18q gene that is altered in colorectal cancers*. Science, 1990. **247**(4938): p. 49-56.
94. Taketo, M.M., *Roles of stromal microenvironment in colon cancer progression*. Journal of Biochemistry, 2012. **151**(5): p. 477-481.
95. Kitamura, T., et al., *SMAD4-deficient intestinal tumors recruit CCR1+ myeloid cells that promote invasion*. Nat Genet, 2007. **39**(4): p. 467-475.
96. Taketo, M.M., *Role of bone marrow-derived cells in colon cancer: lessons from mouse model studies*. Journal Of Gastroenterology, 2009. **44**(2): p. 93-102.
97. Kitamura, T., et al., *Inactivation of chemokine (C-C motif) receptor 1 (CCR1) suppresses colon cancer liver metastasis by blocking accumulation of immature myeloid cells in a mouse model*. Proceedings of the National Academy of Sciences, 2010. **107**(29): p. 13063-13068.
98. Coussens, L.M., B. Fingleton, and L.M. Matrisian, *Matrix metalloproteinase inhibitors and cancer: trials and tribulations*. Science (New York, N.Y.), 2002. **295**(5564): p. 2387-2392.
99. Overall, C.M. and O. Kleinfeld, *Tumour microenvironment - opinion: validating matrix metalloproteinases as drug targets and anti-targets for cancer therapy*. Nature Reviews. Cancer, 2006. **6**(3): p. 227-239.
100. Peterson, J.T., *The importance of estimating the therapeutic index in the development of matrix metalloproteinase inhibitors*. Cardiovascular Research, 2006. **69**(3): p. 677-687.
101. Murphy, G. and H. Nagase, *Progress in matrix metalloproteinase research*. Molecular Aspects of Medicine, 2008. **29**(5): p. 290-308.
102. Ferrara, N., et al., *Discovery and development of bevacizumab, an anti-VEGF antibody for treating cancer*. Nat Rev Drug Discov, 2004. **3**(5): p. 391-400.
103. Folkman, J., *Switch to the angiogenic phenotype during tumorigenesis Princess Takamatsu Symposia*. Princess Takamatsu Symposia, 1991. **22**: p. 339.
104. Gullino, P.M., *Angiogenesis and Oncogenesis*. Journal of the National Cancer Institute, 1978. **61**(3): p. 639.
105. Harris, A.L., *Hypoxia--a key regulatory factor in tumour growth*. Nature Reviews. Cancer, 2002. **2**(1): p. 38-47.
106. Weis, S.M. and D.A. Cheresh, *Tumor angiogenesis: molecular pathways and therapeutic targets*. Nature Medicine, 2011. **17**(11): p. 1359-1370.
107. Vartanian, A.A., *Signaling pathways in tumor vasculogenic mimicry*. Biochemistry (Moscow), 2012. **77**(9): p. 1044-1055.
108. Rmali, K.A., M.C.A. Puntis, and W.G. Jiang, *Tumour-associated angiogenesis in human colorectal cancer*. Colorectal Disease: The Official Journal of the Association of Coloproctology of Great Britain And Ireland, 2007. **9**(1): p. 3-14.
109. Ellis, L.M., et al., *Vascular Endothelial Growth Factor in Human Colon Cancer: Biology and Therapeutic Implications*. The Oncologist, 2000. **5**(suppl 1): p. 11-15.

110. Tokunaga, T., et al., *Vascular endothelial growth factor (VEGF) mRNA isoform expression pattern is correlated with liver metastasis and poor prognosis in colon cancer*. *British Journal of Cancer*, 1998. **77**(6): p. 998-1002.
111. Vaish, V. and S.N. Sanyal, *Role of Sulindac and Celecoxib in the regulation of angiogenesis during the early neoplasm of colon: Exploring PI3-K/PTEN/Akt pathway to the canonical Wnt/ $\beta$ -catenin signaling*. *Biomedicine & Pharmacotherapy*, 2012. **66**(5): p. 354-367.
112. Fukuda, R., B. Kelly, and G.L. Semenza, *Vascular Endothelial Growth Factor Gene Expression in Colon Cancer Cells Exposed to Prostaglandin E2 Is Mediated by Hypoxia-inducible Factor 1*. *Cancer Research*, 2003. **63**(9): p. 2330-2334.
113. Tsujii, M., et al., *Cyclooxygenase Regulates Angiogenesis Induced by Colon Cancer Cells*. *Cell*, 1998. **93**(5): p. 705-716.
114. Yoshida, S., et al., *COX-2//VEGF-Dependent Facilitation of Tumor-Associated Angiogenesis and Tumor Growth in vivo*. *Lab Invest*, 2003. **83**(10): p. 1385-1394.
115. Fukuda, R., et al., *Insulin-like Growth Factor 1 Induces Hypoxia-inducible Factor 1-mediated Vascular Endothelial Growth Factor Expression, Which is Dependent on MAP Kinase and Phosphatidylinositol 3-Kinase Signaling in Colon Cancer Cells*. *Journal of Biological Chemistry*, 2002. **277**(41): p. 38205-38211.
116. Subbaramaiah, K. and A.J. Dannenberg, *Cyclooxygenase 2: a molecular target for cancer prevention and treatment*. *Trends in Pharmacological Sciences*, 2003. **24**(2): p. 96-102.
117. McGettigan P, H.D., *Cardiovascular risk and inhibition of cyclooxygenase: A systematic review of the observational studies of selective and nonselective inhibitors of cyclooxygenase 2*. *JAMA*, 2006. **296**(13): p. 1633-1644.
118. Tol, J., et al., *Chemotherapy, Bevacizumab, and Cetuximab in Metastatic Colorectal Cancer*. *New England Journal of Medicine*, 2009. **360**(6): p. 563-572.
119. Carlo-Stella, C., et al., *Sorafenib Inhibits Lymphoma Xenografts by Targeting MAPK/ERK and AKT Pathways in Tumor and Vascular Cells*. *PLoS ONE*, 2013. **8**(4): p. e61603-e61603.
120. Guijarro-Muñoz, I., et al., *Gene expression profiling identifies EPHB4 as a potential predictive biomarker in colorectal cancer patients treated with bevacizumab*. *Medical Oncology*, 2013. **30**(2): p. 1-8.
121. Dorsam, R.T. and J.S. Gutkind, *G-protein-coupled receptors and cancer*. *Nature Reviews. Cancer*, 2007. **7**(2): p. 79-94.
122. George Paul, A., et al., *Piracy of Prostaglandin E2/EP Receptor-Mediated Signaling by Kaposi's Sarcoma-Associated Herpes Virus (HHV-8) for Latency Gene Expression: Strategy of a Successful Pathogen*. *Cancer Research*, 2010. **70**(9): p. 3697-3708.
123. Rajasekharan, S. and T. Kennedy, *The netrin protein family*. *Genome Biology*, 2009. **10**(9): p. 239.
124. Sun, K.L.W., J.P. Correia, and T.E. Kennedy, *Netrins: versatile extracellular cues with diverse functions*. *Development*, 2011. **138**(11): p. 2153-2169.
125. Culotti, J.G. and D.C. Merz, *DCC and netrins*. *Current Opinion in Cell Biology*, 1998. **10**(5): p. 609-613.
126. Mehlen, P. and C. Furne, *Netrin-1: when a neuronal guidance cue turns out to be a regulator of tumorigenesis*. *Cellular and Molecular Life Sciences*, 2005. **62**(22): p. 2599-2616.
127. Jiang, Y., M.-t. Liu, and M.D. Gershon, *Netrins and DCC in the guidance of migrating neural crest-derived cells in the developing bowel and pancreas*. *Developmental Biology*, 2003. **258**(2): p. 364-384.
128. Nakashiba, T., et al., *Netrin-G1: a Novel Glycosyl Phosphatidylinositol-Linked Mammalian Netrin That Is Functionally Divergent from Classical Netrins*. *The Journal of neuroscience*, 2000. **20**(17): p. 6540-6550.

129. Yurchenco, P.D. and W.G. Wadsworth, *Assembly and tissue functions of early embryonic laminins and netrins*. *Current Opinion in Cell Biology*, 2004. **16**(5): p. 572-579.
130. Cirulli, V. and M. Yebra, *Netrins: beyond the brain*. *Nat Rev Mol Cell Biol*, 2007. **8**(4): p. 296-306.
131. McKenna, W.L., et al., *Netrin-1-independent adenosine A2b receptor activation regulates the response of axons to netrin-1 by controlling cell surface levels of UNC5A receptors*. *Journal of Neurochemistry*, 2008. **104**(4): p. 1081-1090.
132. Bradford, D., S.J. Cole, and H.M. Cooper, *Netrin-1: Diversity in development*. *The International Journal of Biochemistry & Cell Biology*, 2009. **41**(3): p. 487-493.
133. Yee, K.T., et al., *Extension of Long Leading Processes and Neuronal Migration in the Mammalian Brain Directed by the Chemoattractant Netrin-1*. *Neuron*, 1999. **24**(3): p. 607-622.
134. Colamarino, S.A. and M. Tessier-Lavigne, *The axonal chemoattractant netrin-1 is also a chemorepellent for trochlear motor axons*. *Cell*, 1995. **81**(4): p. 621-629.
135. Hong, K., et al., *A Ligand-Gated Association between Cytoplasmic Domains of UNC5 and DCC Family Receptors Converts Netrin-Induced Growth Cone Attraction to Repulsion*. *Cell*, 1999. **97**(7): p. 927-941.
136. Keino-Masu, K., et al., *Deleted in Colorectal Cancer (DCC) Encodes a Netrin Receptor*. *Cell*, 1996. **87**(2): p. 175-185.
137. Mazelin, L., et al., *Netrin-1 controls colorectal tumorigenesis by regulating apoptosis*. *Nature*, 2004. **431**(7004): p. 80-84.
138. Grandin, M., et al., *Structural Decoding of the Netrin-1/UNC5 Interaction and its Therapeutical Implications in Cancers*. *Cancer Cell*. **29**(2): p. 173-185.
139. Kefeli, U., et al., *Netrin-1 in cancer: Potential biomarker and therapeutic target?* *Tumor Biology*, 2017. **39**(4): p. 1010428317698388.
140. Arakawa, H., *Netrin-1 and its receptors in tumorigenesis*. *Nature Reviews. Cancer*, 2004. **4**(12): p. 978-987.
141. Finci, L.I., et al., *The crystal structure of netrin-1 in complex with DCC reveals the bifunctionality of netrin-1 as a guidance cue*. *Neuron*, 2014. **83**(4): p. 839-849.
142. Xu, K., et al., *Structures of netrin-1 bound to two receptors provide insight into its axon guidance mechanism*. *Science*, 2014. **344**(6189): p. 1275-1279.
143. Tian, C. and J. Liu, *Repulsive Guidance Molecules (RGMs) and Neogenin in Bone Morphogenetic Protein (BMP) signaling*. *Molecular Reproduction and Development*, 2013. **80**(9): p. 700-717.
144. Meyerhardt, J.A., et al., *Identification and characterization of neogenin, a DCC-related gene*. *Oncogene*, 1997. **14**(10).
145. Bell, C.H., et al., *Structure of the Repulsive Guidance Molecule (RGM)—Neogenin Signaling Hub*. *Science (New York, N.Y.)*, 2013. **341**(6141): p. 77-80.
146. Bae, G.-U., et al., *Neogenin regulates skeletal myofiber size and focal adhesion kinase and extracellular signal-regulated kinase activities in vivo and in vitro*. *Molecular Biology Of The Cell*, 2009. **20**(23): p. 4920-4931.
147. Rajagopalan, S., et al., *Neogenin mediates the action of repulsive guidance molecule*. *Nature Cell Biology*, 2004. **6**(8): p. 756-762.
148. Siebold, C., et al., *RGMs: Structural Insights, Molecular Regulation, and Downstream Signaling*. *Trends in Cell Biology*, 2017. **27**(5): p. 365-378.
149. Wilson, N.H. and B. Key, *Neogenin interacts with RGMa and Netrin-1 to guide axons within the embryonic vertebrate forebrain*. *Developmental Biology*, 2006. **296**(2): p. 485-498.
150. Dun, X.-P. and D. Parkinson, *Role of Netrin-1 Signaling in Nerve Regeneration*. *International Journal of Molecular Sciences*, 2017. **18**(3): p. 491.
151. Wang, R., et al., *Autoinhibition of UNC5b Revealed by the Cytoplasmic Domain Structure of the Receptor*. *Molecular Cell*, 2009. **33**(6): p. 692-703.

152. Llambi, F., et al., *Netrin-1 acts as a survival factor via its receptors UNC5H and DCC*. EMBO J, 2001. **20**(11): p. 2715-2722.
153. Arakawa, H., *Netrin-1 and its receptors in tumorigenesis*. Nat Rev Cancer, 2004. **4**(12): p. 978-987.
154. Tanaka, K., et al., *Suppression of tumorigenicity in human colon carcinoma cells by introduction of normal chromosome 5 or 18*. Nature, 1991. **349**(6307): p. 340-342.
155. Velcich, A., *Altered phenotype of HT29 colonic adenocarcinoma cells following expression of the DCC gene*. Oncogene, 1999. **18**(16): p. 2599.
156. Thiagalingam, S., et al., *Evaluation of candidate tumour suppressor genes on chromosome 18 in colorectal cancers*. Nature Genetics, 1996. **13**(3): p. 343-346.
157. Fazeli, A., et al., *Phenotype of mice lacking functional Deleted in colorectal cancer (Dcc) gene*. Nature, 1997. **386**(6627): p. 796-804.
158. Mehlen, P., et al., *The DCC gene product induces apoptosis by a mechanism requiring receptor proteolysis*. Nature, 1998. **395**(6704): p. 801-804.
159. Mehlen, P. and D.E. Bredesen, *The dependence receptor hypothesis*. Apoptosis, 2004. **9**(1): p. 37-49.
160. Mehlen, P. and C. Guenebeaud, *Netrin-1 and its dependence receptors as original targets for cancer therapy*. Current Opinion in Oncology, 2010. **22**(1): p. 46-54, doi: 10.1097/CCO.0b013e3283333dcd1.
161. Bredesen, D.E., P. Mehlen, and S. Rabizadeh, *Receptors that mediate cellular dependence*. Cell Death Differ, 2005. **12**(8): p. 1031-1043.
162. Fitamant, J., et al., *Netrin-1 expression confers a selective advantage for tumor cell survival in metastatic breast cancer*. Proceedings of the National Academy of Sciences, 2008. **105**(12): p. 4850-4855.
163. Stein, E., et al., *Binding of DCC by Netrin-1 to Mediate Axon Guidance Independent of Adenosine A2B Receptor Activation*. Science, 2001. **291**(5510): p. 1976-1982.
164. Ren, X.-r., et al., *Focal adhesion kinase in netrin-1 signaling*. Nat Neurosci, 2004. **7**(11): p. 1204-1212.
165. Li, W., et al., *FAK and Src kinases are required for netrin-induced tyrosine phosphorylation of UNC5*. Journal of Cell Science, 2006. **119**(1): p. 47-55.
166. Round, J. and E. Stein, *Netrin signaling leading to directed growth cone steering*. Current Opinion in Neurobiology, 2007. **17**(1): p. 15-21.
167. Ma, W., et al., *Phosphorylation of DCC by ERK2 Is Facilitated by Direct Docking of the Receptor P1 Domain to the Kinase*. Structure (London, England : 1993), 2010. **18**(11): p. 1502-1511.
168. Luo, L., *Rho GTPases in neuronal morphogenesis*. Nature Reviews. Neuroscience, 2000. **1**(3): p. 173-180.
169. Buck, K.B. and J.Q. Zheng, *Growth Cone Turning Induced by Direct Local Modification of Microtubule Dynamics*. The Journal of Neuroscience, 2002. **22**(21): p. 9358-9367.
170. Ming, G.-l., et al., *Phospholipase C- $\beta$  and Phosphoinositide 3-Kinase Mediate Cytoplasmic Signaling in Nerve Growth Cone Guidance*. Neuron, 1999. **23**(1): p. 139-148.
171. Gomez, T.M. and J.Q. Zheng, *The molecular basis for calcium-dependent axon pathfinding*. Nat Rev Neurosci, 2006. **7**(2): p. 115-125.
172. Nishiyama, M., et al., *Cyclic AMP/GMP-dependent modulation of Ca<sup>2+</sup> channels sets the polarity of nerve growth-cone turning*. Nature, 2003. **423**(6943): p. 990-995.
173. Corset, V., et al., *Netrin-1-mediated axon outgrowth and cAMP production requires interaction with adenosine A2b receptor*. Nature, 2000. **407**(6805): p. 747-750.
174. Manitt, C., *Peri-Pubertal Emergence of UNC-5 Homologue Expression by Dopamine Neurons in Rodents*. PLoS ONE, 2010. **5**(7): p. e11463.
175. Tong, J., et al., *Netrin Stimulates Tyrosine Phosphorylation of the UNC-5 Family of Netrin Receptors and Induces Shp2 Binding to the RCM Cytodomain*. Journal of Biological Chemistry, 2001. **276**(44): p. 40917-40925.

176. Mehlen, P. and L. Mazelin, *The dependence receptors DCC and UNC5H as a link between neuronal guidance and survival*. *Biology of the Cell*, 2003. **95**(7): p. 425-436.
177. Goldschneider, D. and P. Mehlen, *Dependence receptors: a new paradigm in cell signaling and cancer therapy*. *Oncogene*, 2010. **29**(13): p. 1865-1882.
178. Mehlen, P. and C. Thibert, *Dependence receptors: between life and death*. *Cellular and Molecular Life Sciences*, 2004. **61**(15): p. 1854-1866.
179. Llambi, F., et al., *The dependence receptor UNC5H2 mediates apoptosis through DAP-kinase*. *EMBO J*, 2005. **24**(6): p. 1192-1201.
180. Williams, M.E., et al., *UNC5H1 induces apoptosis via its juxtamembrane domain through an interaction with NRAGE*. *J. Biol. Chem.*, 2003: p. M300415200.
181. Forcet, C., et al., *The Dependence Receptor DCC (Deleted in Colorectal Cancer) Defines an Alternative Mechanism for Caspase Activation*. *Proceedings of the National Academy of Sciences of the United States of America*, 2001. **98**(6): p. 3416-3421.
182. Erhardt, P., E.J. Schremser, and G.M. Cooper, *B-Raf Inhibits Programmed Cell Death Downstream of Cytochrome c Release from Mitochondria by Activating the MEK/Erk Pathway*. *Molecular and Cellular Biology*, 1999. **19**(8): p. 5308-5315.
183. Seaman, C., et al., *Localization of the netrin guidance receptor, DCC, in the developing peripheral and enteric nervous systems*. *Mechanisms of Development*, 2001. **103**(1-2): p. 173-175.
184. Newgreen, D. and H.M. Young, *Enteric Nervous System: Development and Developmental Disturbances—Part 1*. *Pediatric and Developmental Pathology*, 2002. **5**(3): p. 224-247.
185. Burns, A.J. and N.M. Le Douarin, *Enteric nervous system development: Analysis of the selective developmental potentialities of vagal and sacral neural crest cells using quail-chick chimeras*. *The Anatomical Record*, 2001. **262**(1): p. 16-28.
186. Young, H.M., R.B. Anderson, and C.R. Anderson, *Guidance cues involved in the development of the peripheral autonomic nervous system*. *Autonomic Neuroscience*, 2004. **112**(1-2): p. 1-14.
187. Ming, G.-l., et al., *cAMP-Dependent Growth Cone Guidance by Netrin-1*. *Neuron*, 1997. **19**(6): p. 1225-1235.
188. Ratcliffe, E.M., et al., *Netrin/DCC-mediated attraction of vagal sensory axons to the fetal mouse gut*. *The Journal of Comparative Neurology*, 2006. **498**(5): p. 567-580.
189. Ratcliffe, E.M., et al., *Enteric neurons synthesize netrins and are essential for the development of the vagal sensory innervation of the fetal gut*. *Developmental Neurobiology*, 2011. **71**(5): p. 362-373.
190. Murase, S.-i. and A.F. Horwitz, *Deleted in Colorectal Carcinoma and Differentially Expressed Integrins Mediate the Directional Migration of Neural Precursors in the Rostral Migratory Stream*. *The Journal of Neuroscience*, 2002. **22**(9): p. 3568-3579.
191. Astic, L., et al., *Expression of netrin-1 and netrin-1 receptor, DCC, in the rat olfactory nerve pathway during development and axonal regeneration*. *Neuroscience*, 2002. **109**(4): p. 643-656.
192. Lin, L., Y. Rao, and O. Isacson, *Netrin-1 and slit-2 regulate and direct neurite growth of ventral midbrain dopaminergic neurons*. *Molecular and Cellular Neuroscience*, 2005. **28**(3): p. 547-555.
193. Burgess, R.W., T.J. Jucius, and S.L. Ackerman, *Motor Axon Guidance of the Mammalian Trochlear and Phrenic Nerves: Dependence on the Netrin Receptor Unc5c and Modifier Loci*. *The Journal of Neuroscience*, 2006. **26**(21): p. 5756-5766.
194. Jarjour, A.A., et al., *Netrin-1 Is a Chemorepellent for Oligodendrocyte Precursor Cells in the Embryonic Spinal Cord*. *The Journal of Neuroscience*, 2003. **23**(9): p. 3735-3744.
195. Masuda, T., *Netrin-1 signaling for sensory axons: Involvement in sensory axonal development and regeneration*. *Cell Adhesion & Migration*, 2009. **3**(2): p. 171.
196. Deiner, M.S., et al., *Netrin-1 and DCC Mediate Axon Guidance Locally at the Optic Disc: Loss of Function Leads to Optic Nerve Hypoplasia*. *Neuron*, 1997. **19**(3): p. 575-589.

197. Kennedy, T.E., et al., *Netrins are diffusible chemotropic factors for commissural axons in the embryonic spinal cord*. Cell, 1994(3): p. 425.
198. Manitt, C., et al., *Widespread expression of netrin-1 by neurons and oligodendrocytes in the adult mammalian spinal cord*. The Journal Of Neuroscience: The Official Journal of The Society For Neuroscience, 2001. **21**(11): p. 3911-3922.
199. Manitt, C., et al., *Positioned to inhibit: netrin-1 and netrin receptor expression after spinal cord injury*. Journal of Neuroscience Research, 2006. **84**(8): p. 1808-1820.
200. Manitt, C., K.M. Thompson, and T.E. Kennedy, *Developmental shift in expression of netrin receptors in the rat spinal cord: predominance of UNC-5 homologues in adulthood*. Journal of Neuroscience Research, 2004. **77**(5): p. 690-700.
201. Löw, K., et al., *Netrin-1 is a novel myelin-associated inhibitor to axon growth*. The Journal Of Neuroscience: The Official Journal of The Society For Neuroscience, 2008. **28**(5): p. 1099-1108.
202. Madison, R.D., A. Zomorodi, and G.A. Robinson, *Regular Article: Netrin-1 and Peripheral Nerve Regeneration in the Adult Rat*. Experimental Neurology, 2000. **161**: p. 563-570.
203. Madison, R.D., A. Zomorodi, and G.A. Robinson, *Netrin-1 and Peripheral Nerve Regeneration in the Adult Rat*. Experimental Neurology, 2000. **161**(2): p. 563-570.
204. Buskbjerg Jager, S., et al., *The Mouse Median Nerve Experimental Model in Regenerative Research*. BioMed Research International, 2014. **2014**: p. 701682.
205. Masuda, T., et al., *Netrin-1 acts as a repulsive guidance cue for sensory axonal projections toward the spinal cord*. The Journal of Neuroscience: The Official Journal of The Society for Neuroscience, 2008. **28**(41): p. 10380-10385.
206. Webber, C.A., et al., *Schwann cells direct peripheral nerve regeneration through the Netrin-1 receptors, DCC and Unc5H2*. Glia, 2011. **59**(10): p. 1503-1517.
207. Bin, Jenea M., et al., *Complete Loss of Netrin-1 Results in Embryonic Lethality and Severe Axon Guidance Defects without Increased Neural Cell Death*. Cell Reports, 2015. **12**(7): p. 1099-1106.
208. Jaminet, P., et al., *Evaluating the role of Netrin-1 during the early phase of peripheral nerve regeneration using the mouse median nerve model*. Restorative Neurology And Neuroscience, 2013. **31**(3): p. 337-345.
209. Mehlen, P. and F. Llambi, *Role of netrin-1 and netrin-1 dependence receptors in colorectal cancers*. Br J Cancer, 2005. **93**(1): p. 1-6.
210. Thiébault, K., et al., *The netrin-1 receptors UNC5H are putative tumor suppressors controlling cell death commitment*. Proceedings of the National Academy of Sciences, 2003. **100**(7): p. 4173-4178.
211. Bernet, A., et al., *Inactivation of the UNC5C Netrin-1 Receptor Is Associated With Tumor Progression in Colorectal Malignancies*. Gastroenterology, 2007. **133**(6): p. 1840-1848.
212. Taniguchi, Y., S.-H. Kim, and S.S. Sisodia, *Presenilin-dependent "γ-Secretase" Processing of Deleted in Colorectal Cancer (DCC)*. Journal of Biological Chemistry, 2003. **278**(33): p. 30425-30428.
213. Friedl, P. and K. Wolf, *Tumour-cell invasion and migration: diversity and escape mechanisms*. Nature Reviews. Cancer, 2003. **3**(5): p. 362-374.
214. Friedl, P. and E.B. Bröcker, *The biology of cell locomotion within three-dimensional extracellular matrix*. Cellular and Molecular Life Sciences CMLS, 2000. **57**(1): p. 41-64.
215. Rodrigues, S., et al., *Opposing roles of netrin-1 and the dependence receptor DCC in cancer cell invasion, tumor growth and metastasis*. Oncogene, 2007. **26**(38): p. 5615-5625.
216. Nguyen, Q.-D., et al., *Commutators of PAR-1 signaling in cancer cell invasion reveal an essential role of the Rho-Rho kinase axis and tumor microenvironment*. Oncogene, 2005. **24**(56): p. 8240-8251.

217. Forcet, C., et al., *The dependence receptor DCC (deleted in colorectal cancer) defines an alternative mechanism for caspase activation*. PNAS, 2001. **98**(6): p. 3416-3421.
218. Carmeliet, P. and M. Tessier-Lavigne, *Common mechanisms of nerve and blood vessel wiring*. Nature, 2005. **436**(7048): p. 193-200.
219. Lu, X., et al., *The netrin receptor UNC5B mediates guidance events controlling morphogenesis of the vascular system*. Nature, 2004. **432**(7014): p. 179-186.
220. Park, K.W., et al., *The axonal attractant Netrin-1 is an angiogenic factor*. Proceedings of the National Academy of Sciences of the United States of America, 2004. **101**(46): p. 16210-16215.
221. Larrivée, B., et al., *Activation of the UNC5B receptor by Netrin-1 inhibits sprouting angiogenesis*. Genes & Development, 2007. **21**(19): p. 2433-2447.
222. Dakouane-Giudicelli, M., et al., *Hypoxia-inducible factor 1 controls the expression of the uncoordinated-5-B receptor, but not of netrin-1, in first trimester human placenta*. The International Journal of Developmental Biology, 2011. **55**(10-12): p. 981-987.
223. Wilson, B.D., et al., *Netrins Promote Developmental and Therapeutic Angiogenesis*. Science, 2006. **313**(5787): p. 640-644.
224. Castets, M., et al., *Inhibition of Endothelial Cell Apoptosis by Netrin-1 during Angiogenesis*. Developmental Cell, 2009. **16**(4): p. 614-620.
225. Lu, H., et al., *Netrin-1 hyperexpression in mouse brain promotes angiogenesis and long-term neurological recovery after transient focal ischemia*. Stroke (00392499), 2012. **43**(3): p. 838-843.
226. Li, Q., et al., *Transplantation of MSCs in Combination with Netrin-1 Improves Neoangiogenesis in a Rat Model of Hind Limb Ischemia*. Journal of Surgical Research, 2011. **166**(1): p. 162-169.
227. Tsuchiya, A., et al., *Expression of netrin-1 and its receptors DCC and neogenin in rat brain after ischemia*. Brain Research, 2007. **1159**: p. 1-7.
228. Dumartin, L., et al., *Netrin-1 Mediates Early Events in Pancreatic Adenocarcinoma Progression, Acting on Tumor and Endothelial Cells*. Gastroenterology, 2010. **138**(4): p. 1595-1606.e8.
229. Shimizu, A., et al., *Netrin-1 Promotes Glioblastoma Cell Invasiveness and Angiogenesis by Multiple Pathways Including Activation of RhoA, Cathepsin B, and cAMP-response Element-binding Protein*. Journal of Biological Chemistry, 2013. **288**(4): p. 2210-2222.
230. Wang, Q.H., et al., *Role of Axonal Guidance Factor Netrin-1 in Human Placental Vascular Growth*. Journal of Huazhong University of Science and Technology-Medical Sciences, 2011. **31**(2): p. 246-250.
231. Xie, H., et al., *Effects of netrin-1 and netrin-1 knockdown on human umbilical vein endothelial cells and angiogenesis of rat placenta*. Placenta, 2011. **32**(8): p. 546-553.
232. Lu, H., et al., *Netrin-1 Hyperexpression in Mouse Brain Promotes Angiogenesis and Long-Term Neurological Recovery After Transient Focal Ischemia*. Stroke, 2012. **43**(3): p. 838-843.
233. Bouvrée, K., et al., *Netrin-1 inhibits sprouting angiogenesis in developing avian embryos*. Developmental Biology, 2008. **318**(1): p. 172-183.
234. Paradisi, A., *Netrin-1, a missing link between chronic inflammation and tumor progression*. Cell Cycle, 2010. **9**(7): p. 1253.
235. Paradisi, A., et al., *Netrin-1 up-regulation in inflammatory bowel diseases is required for colorectal cancer progression*. Proceedings of the National Academy of Sciences, 2009. **106**(40): p. 17146-17151.
236. Paradisi, A., et al., *NF- $\kappa$ B Regulates Netrin-1 Expression and Affects the Conditional Tumor Suppressive Activity of the Netrin-1 Receptors*. Gastroenterology, 2008. **135**(4): p. 1248-1257.
237. Yang, Y., et al., *TNF- $\alpha$  Mediates Macrophage-Induced Bystander Effects through Netrin-1*. Cancer Research, 2012. **72**(20): p. 5219-5229.

238. Ramesh, G., A. Berg, and C. Jayakumar, *Plasma netrin-1 is a diagnostic biomarker of human cancers*. *Biomarkers*, 2011. **16**(2): p. 172-180.
239. Son, T.W., et al., *Netrin-1 protects hypoxia-induced mitochondrial apoptosis through HSP27 expression via DCC- and integrin [alpha]6[beta]4-dependent Akt, GSK-3[beta], and HSF-1 in mesenchymal stem cells*. *Cell Death Dis*, 2013. **4**: p. e563.
240. Uccelli, A., L. Moretta, and V. Pistoia, *Mesenchymal stem cells in health and disease*. *Nature Reviews. Immunology*, 2008. **8**(9): p. 726-736.
241. Pandey, P., et al., *Hsp27 functions as a negative regulator of cytochrome c-dependent activation of procaspase-3*. *Oncogene*, 2000. **19**(16): p. 1975-1981.
242. Serafini, T., et al., *The netrins define a family of axon outgrowth-promoting proteins homologous to C. elegans UNC-6*. *Cell*, 1994. **78**(3): p. 409-424.
243. Ming, G.-l. and H. Song, *Adult Neurogenesis in the Mammalian Brain: Significant Answers and Significant Questions*. *Neuron*, 2011. **70**(4): p. 687-702.
244. Czaja, K., M. Fornaro, and S. Geuna, *Neurogenesis in the adult peripheral nervous system*. *Neural Regeneration Research*, 2012. **7**(14): p. 1047-1054.
245. Krzysztof Czaja, W.E.C., Maria G. Giacobini-Robecchi, Stefano Geuna and Michele Fornaro, *Injury-Induced DNA Replication and Neural Proliferation in the Adult Mammalian Nervous System, DNA Replication and Related Cellular Processes*. InTech, 2011.
246. Hatai, S., *Number and size of the spinal ganglion cells and dorsal root fibers in the white rat at different ages*. *Journal of Comparative Neurology*, 1902. **12**(2): p. 107-124.
247. Becker, L., et al., *Ex Vivo Neurogenesis within Enteric Ganglia Occurs in a PTEN Dependent Manner*. *PLoS ONE*, 2013. **8**(3): p. 1-10.
248. Liu, M.-T., et al., *5-HT Receptor-Mediated Neuroprotection and Neurogenesis in the Enteric Nervous System of Adult Mice*. *The Journal of Neuroscience*, 2009. **29**(31): p. 9683-9699.
249. Tamada, H. and H. Kiyama, *Suppression of c-Kit signaling induces adult neurogenesis in the mouse intestine after myenteric plexus ablation with benzalkonium chloride*. *Scientific Reports*, 2016. **6**: p. 32100.
250. Raghavan, S., R.R. Gilmont, and K.N. Bitar, *Neuroglial differentiation of adult enteric neuronal progenitor cells as a function of extracellular matrix composition*. *Biomaterials*, 2013. **34**(28): p. 6649-6658.
251. Ko, S.Y., C.R. Dass, and K. Nurgali, *Netrin-1 in the developing enteric nervous system and colorectal cancer*. *Trends in Molecular Medicine*, 2012. **18**(9): p. 544-554.
252. Aherne, C.M., C.B. Collins, and H.K. Eltzschig, *Netrin-1 guides inflammatory cell migration to control mucosal immune responses during intestinal inflammation*. *Tissue Barriers*, 2013. **1**(2): p. e24957-e24957.
253. Lv, J., et al., *Netrin-1 induces the migration of Schwann cells via p38 MAPK and PI3K-Akt signaling pathway mediated by the UNC5B receptor*. *Biochemical and Biophysical Research Communications*, 2015. **464**(1): p. 263-268.
254. Mancino, M., et al., *Neuronal Guidance Protein Netrin-1 Induces Differentiation in Human Embryonal Carcinoma Cells*. *Cancer Research*, 2009. **69**(5): p. 1717-1721.
255. Nguyen, A. and H. Cai, *Netrin-1 induces angiogenesis via a DCC-dependent ERK1/2-eNOS feed-forward mechanism*. *Proceedings of the National Academy of Sciences*, 2006. **103**(17): p. 6530-6535.
256. Ahmed, R.P.H., et al., *Sonic Hedgehog Gene Delivery to the Rodent Heart Promotes Angiogenesis via iNOS/Netrin-1/PKC Pathway*. *PLoS ONE*, 2010. **5**(1).
257. Liu, L., et al., *Netrin-1 Pretreatment Protects Rat Kidney against Ischemia/Reperfusion Injury via Suppression of Oxidative Stress and Neuropeptide Y Expression*. *Journal of Biochemical and Molecular Toxicology*, 2013: p. n/a-n/a.
258. Bouhidel, J.O., et al., *Netrin-1 improves post-injury cardiac function in vivo via DCC/NO-dependent preservation of mitochondrial integrity, while attenuating autophagy*.

- Biochimica et Biophysica Acta (BBA) - Molecular Basis of Disease, 2015. **1852**(2): p. 277-289.
259. Paradisi, A., et al., *Combining chemotherapeutic agents and netrin-1 interference potentiates cancer cell death*. EMBO Molecular Medicine, 2013. **5**(12): p. 1821-1834.
260. Anitha, M., et al., *Characterization of Fetal and Postnatal Enteric Neuronal Cell Lines With Improvement in Intestinal Neural Function*. Gastroenterology, 2008. **134**(5): p. 1424-1435.
261. Jat, P.S., et al., *Direct derivation of conditionally immortal cell lines from an H-2Kb-tsA58 transgenic mouse*. Proceedings of the National Academy of Sciences of the United States of America, 1991. **88**(12): p. 5096-5100.
262. Mayor, R. and E. Theveneau, *The neural crest*. Development, 2013. **140**(11): p. 2247-2251.
263. Rollo, B.N., et al., *Enteric Neural Cells From Hirschsprung Disease Patients Form Ganglia in Autologous Aneuronal Colon*. Cellular and Molecular Gastroenterology and Hepatology. **2**(1): p. 92-109.
264. Sundberg, M., et al., *CD marker expression profiles of human embryonic stem cells and their neural derivatives, determined using flow-cytometric analysis, reveal a novel CD marker for exclusion of pluripotent stem cells*. Stem Cell Research, 2009. **2**(2): p. 113-124.
265. Pruszek, J., et al., *CD15, CD24, and CD29 Define a Surface Biomarker Code for Neural Lineage Differentiation of Stem Cells*. Stem Cells, 2009. **27**(12): p. 2928-2940.
266. Joseph, N.M., et al., *Enteric glia are multipotent in culture but primarily form glia in the adult rodent gut*. The Journal Of Clinical Investigation, 2011. **121**(9): p. 3398-3411.
267. Kemshead, J.T., et al., *Human Thy-1: expression on the cell surface of neuronal and glial cells*. Brain Research, 1982. **236**(2): p. 451-461.
268. Singhal, P.K., et al., *Mouse embryonic fibroblasts exhibit extensive developmental and phenotypic diversity*. Proceedings of the National Academy of Sciences, 2016. **113**(1): p. 122-127.
269. Trzpis, M., et al., *Epithelial Cell Adhesion Molecule: More than a Carcinoma Marker and Adhesion Molecule*. The American Journal of Pathology, 2007. **171**(2): p. 386-395.
270. Mirantes, C., et al., *Deletion of Pten in CD45-expressing cells leads to development of T-cell lymphoblastic lymphoma but not myeloid malignancies*. Blood, 2016. **127**(15): p. 1907-1911.
271. Hedlund, E., et al., *Embryonic stem cell-derived Pitx3-enhanced green fluorescent protein midbrain dopamine neurons survive enrichment by fluorescence-activated cell sorting and function in an animal model of Parkinson's disease*. Stem Cells (Dayton, Ohio), 2008. **26**(6): p. 1526-1536.
272. Lee, H.K., et al., *Netrin-1 induces proliferation of Schwann cells through Unc5b receptor*. Biochemical and Biophysical Research Communications, 2007. **362**(4): p. 1057-1062.
273. He, X., et al., *Netrin-1 overexpression promotes white matter repairing and remodeling after focal cerebral ischemia in mice*. Journal of Cerebral Blood Flow & Metabolism, 2013. **33**(12): p. 1921-1927.
274. Delloye-Bourgeois, C., et al., *Netrin-1 acts as a survival factor for aggressive neuroblastoma*. The Journal of Experimental Medicine, 2009. **206**(4): p. 833-847.
275. O'Leary, C.J., et al., *The Netrin/RGM Receptor, Neogenin, Controls Adult Neurogenesis by Promoting Neuroblast Migration and Cell Cycle Exit*. Stem Cells, 2015(2): p. 503.
276. Khodosevich, K. and H. Monyer, *Signaling involved in neurite outgrowth of postnatally born subventricular zone neurons in vitro*. BMC Neuroscience, 2010. **11**(1): p. 18.
277. Hisaoka, M., et al., *Microtubule-Associated Protein-2 and Class III [bgr]-Tubulin Are Expressed in Extraskelatal Myxoid Chondrosarcoma*. Mod Pathol, 0000. **16**(5): p. 453-459.

278. Constantinescu, R., et al., *Neuronal differentiation and long-term culture of the human neuroblastoma line SH-SY5Y*. Journal Of Neural Transmission. Supplementum, 2007(72): p. 17-28.
279. Achilleos, A. and P.A. Trainor, *Neural crest stem cells: discovery, properties and potential for therapy*. Cell Res, 2012. **22**(2): p. 288-304.
280. Vannucchi, M.G. and M.S. Faussone-Pellegrini, *Synapse formation during neuron differentiation: an in situ study of the myenteric plexus during murine embryonic life*. The Journal Of Comparative Neurology, 2000. **425**(3): p. 369-381.
281. Vannucchi, M.G., et al., *Neurofilament formation and synaptic activity are delayed in the myenteric neurons of the rat fetus with gastroschisis*. Neuroscience Letters, 2004. **364**(2): p. 81-85.
282. Hao, M.M., et al., *Early Development of Electrical Excitability in the Mouse Enteric Nervous System*. The Journal of Neuroscience, 2012. **32**(32): p. 10949-10960.
283. Hao, M.M., et al., *The emergence of neural activity and its role in the development of the enteric nervous system*. Developmental Biology, 2013. **382**(1): p. 365-374.
284. Böttner, M., et al., *GDNF induces synaptic vesicle markers in enteric neurons*. Neuroscience Research, 2013. **77**(3): p. 128-136.
285. Xiaoling, T., et al., *Netrin-1 mediates neuronal survival through PIKE-L interaction with the dependence receptor UNC5B*. Nature Cell Biology, 2008. **10**(6): p. 698-706.
286. Wilson, N.H. and B. Key, *Neogenin: One receptor, many functions*. The International Journal of Biochemistry & Cell Biology, 2007. **39**(5): p. 874-878.
287. Mediero, A., et al., *Netrin-1 Is a Critical Autocrine/Paracrine Factor for Osteoclast Differentiation*. Journal of bone and mineral research : the official journal of the American Society for Bone and Mineral Research, 2015. **30**(5): p. 837-854.
288. Strizzi, L., et al., *Netrin-1 Can Affect Morphogenesis and Differentiation of the Mouse Mammary Gland*. Journal of Cellular Physiology, 2008. **216**(3): p. 824-834.
289. Galderisi, U., F.P. Jori, and A. Giordano, *Cell cycle regulation and neural differentiation*. Oncogene, 2003. **22**(33): p. 5208-5219.
290. Besson, A., S.F. Dowdy, and J.M. Roberts, *CDK Inhibitors: Cell Cycle Regulators and Beyond*. Developmental Cell. **14**(2): p. 159-169.
291. Coqueret, O., *New roles for p21 and p27 cell-cycle inhibitors: a function for each cell compartment?* Trends in Cell Biology, 2003. **13**(2): p. 65-70.
292. Nguyen, L., et al., *p27(kip1) independently promotes neuronal differentiation and migration in the cerebral cortex*. Genes & Development, 2006. **20**(11): p. 1511-1524.
293. Suzuki, A., et al., *Resistance to Fas-mediated apoptosis: activation of Caspase 3 is regulated by cell cycle regulator p21WAF1 and IAP gene family ILP*. Oncogene, 1998. **17**(8): p. 931-939.
294. Lee, S. and D.M. Helfman, *Cytoplasmic p21Cip1 is involved in Ras-induced inhibition of the ROCK/LIMK/cofilin pathway*. The Journal Of Biological Chemistry, 2004. **279**(3): p. 1885-1891.
295. Strizzi, L., et al., *Netrin-1 regulates invasion and migration of mouse mammary epithelial cells overexpressing Cripto-1 in vitro and in vivo*. Journal of Cell Science, 2005. **118**(20): p. 4633-4643.
296. Andrusiak, M.G., et al., *Rb/E2F Regulates Expression of Neogenin during Neuronal Migration*. Molecular and Cellular Biology, 2011. **31**(2): p. 238-247.
297. Wang, W., W.B. Reeves, and G. Ramesh, *Netrin-1 increases proliferation and migration of renal proximal tubular epithelial cells via the UNC5B receptor*. American Journal of Physiology - Renal Physiology, 2009. **296**(4): p. F723-F729.
298. Castets, M., *Netrin-1 role in angiogenesis: to be or not to be a pro-angiogenic factor?* Cell Cycle, 2010. **9**(8): p. 1466.
299. Tu, T., et al., *CD146 acts as a novel receptor for netrin-1 in promoting angiogenesis and vascular development*. Cell Research, 2015. **25**(3): p. 275-287.

300. O'Donnell, M., R.K. Chance, and G.J. Bashaw, *Axon Growth and Guidance: Receptor Regulation and Signal Transduction*. Annual Review of Neuroscience, 2009. **32**(1): p. 383-412.
301. van den Heuvel, D.M.A., A.J.C.G.M. Hellemons, and R.J. Pasterkamp, *Spatiotemporal expression of repulsive guidance molecules (RGMs) and their receptor neogenin in the mouse brain*. Plos One, 2013. **8**(2): p. e55828-e55828.
302. Hata, K., et al., *RGMa inhibition promotes axonal growth and recovery after spinal cord injury*. The Journal of Cell Biology, 2006. **173**(1): p. 47-58.
303. Yamashita, T., B.K. Mueller, and K. Hata, *Neogenin and repulsive guidance molecule signaling in the central nervous system*. Current Opinion in Neurobiology, 2007. **17**: p. 29-34.
304. Hata, K., et al., *Unc5B Associates with LARG to Mediate the Action of Repulsive Guidance Molecule*. 2009, Rockefeller University Press. p. 737.
305. Metzger, M., et al., *RGMa inhibits neurite outgrowth of neuronal progenitors from murine enteric nervous system via the neogenin receptor in vitro*. Journal of Neurochemistry, 2007. **103**(6): p. 2665-2678.
306. De Vries, M. and H.M. Cooper, *Emerging roles for neogenin and its ligands in CNS development*. Journal of Neurochemistry, 2008. **106**(4): p. 1483-1492.
307. Mediero, A., et al., *Netrin-1 Is a Critical Autocrine/Paracrine Factor for Osteoclast Differentiation*. Journal of Bone & Mineral Research, 2015. **30**(5): p. 837-854.
308. Löw, K., et al., *Netrin-1 Is a Novel Myelin-Associated Inhibitor to Axon Growth*. The Journal of Neuroscience, 2008. **28**(5): p. 1099-1108.
309. Jenea, M.B., et al., *Complete Loss of Netrin-1 Results in Embryonic Lethality and Severe Axon Guidance Defects without Increased Neural Cell Death*. Cell Reports, Vol 12, Iss 7, Pp 1099-1106 (2015), 2015(7): p. 1099.
310. Cirulli, V. and M. Yebra, *Netrins: beyond the brain*. Nature Reviews Molecular Cell Biology, 2007(4): p. 296.
311. Srinivasan, K., et al., *Netrin-1/Neogenin Interaction Stabilizes Multipotent Progenitor Cap Cells during Mammary Gland Morphogenesis*. Developmental Cell, 2003. **4**(3): p. 371-382.
312. Ylivinkka, I., et al., *Motility of glioblastoma cells is driven by netrin-1 induced gain of stemness*. Journal of Experimental & Clinical Cancer Research, 2017. **36**(1): p. 9.
313. Yin, K., et al., *Netrin-1 promotes gastric cancer cell proliferation and invasion via the receptor neogenin through PI3K/AKT signaling pathway*. Oncotarget, 2017. **8**(31): p. 51177-51189.
314. Castets, M., et al., *DCC constrains tumour progression via its dependence receptor activity*. Nature, 2011. **482**(7386): p. 534-537.
315. Fitamant, J., et al., *Netrin-1 expression confers a selective advantage for tumor cell survival in metastatic breast cancer*. PNAS, 2008. **105**.
316. Fitamant, J., et al., *Netrin-1: a promising therapeutic target in metastatic breast cancer. Expression analysis in localized and metastatic breast tumors and preclinical validation*. Cancer Research, 2009. **69**(2 Supplement): p. 3075.
317. Papanastasiou, A.D., et al., *Netrin-1 overexpression is predictive of ovarian malignancies*. Oncotarget, 2011. **2**(5): p. 363-367.
318. Andrea, P., et al., *Netrin-1 Up-Regulation in Inflammatory Bowel Diseases Is Required for Colorectal Cancer Progression*. Proceedings of the National Academy of Sciences of the United States of America, 2009(40): p. 17146.
319. Sturlan, S., et al., *Loss of heterozygosity of APC and DCC tumor suppressor genes in human sporadic colon cancer*. Journal of Molecular Medicine, 1999(3): p. 316.
320. Kong, C.-z., et al., *Interactional expression of netrin-1 and its dependence receptor UNC5B in prostate carcinoma*. Tumour Biology: The Journal Of The International Society For Oncodevelopmental Biology And Medicine, 2013. **34**(5): p. 2765-2772.

321. Toda, K., et al., *Genetic and epigenetic alterations of netrin-1 receptors in gastric cancer with chromosomal instability*. *Clinical Epigenetics*, 2015.
322. Larrivée, B., et al., *Activation of the UNC5B receptor by Netrin-1 inhibits sprouting angiogenesis*. *Genes Dev*, 2007. **21**.
323. Tadagavadi, R.K., W. Wang, and G. Ramesh, *Netrin-1 Regulates Th1/Th2/Th17 Cytokine Production and Inflammation through UNC5B Receptor and Protects Kidney against Ischemia–Reperfusion Injury*. *The Journal of Immunology*, 2010. **185**(6): p. 3750-3758.
324. Fitamant, J., et al., *Netrin-1 expression confers a selective advantage for tumor cell survival in metastatic breast cancer*. *Proceedings of the National Academy of Sciences of The United States of America*, 2008. **105**(12): p. 4850-4855.
325. Harter, P.N., et al., *Netrin-1 Expression Is an Independent Prognostic Factor for Poor Patient Survival in Brain Metastases*. *PLOS ONE*, 2014. **9**(3): p. e92311.
326. An, X.-Z., et al., *Netrin-1 suppresses the MEK/ERK pathway and ITGB4 in pancreatic cancer*. *Oncotarget*, 2016. **7**(17): p. 24719-24733.
327. Mohamed, R., et al., *Kidney Proximal Tubular Epithelial-Specific Overexpression of Netrin-1 Suppresses Inflammation and Albuminuria through Suppression of COX-2-Mediated PGE2 Production in Streptozotocin-Induced Diabetic Mice*. *The American Journal of Pathology*, 2012. **181**(6): p. 1991-2002.
328. Mediero, A., et al., *Netrin-1 is highly expressed and required in inflammatory infiltrates in wear particle-induced osteolysis*. *Annals of the Rheumatic Diseases*, 2016. **75**(9): p. 1706-1713.
329. Mirakaj, V., et al., *Netrin-1 Signaling Dampens Inflammatory Peritonitis*. *Journal of Immunology*, 2011. **186**(1): p. 549-555.
330. Terranova, V.P., et al., *Role of Laminin in the Attachment and Metastasis of Murine Tumor Cells*. *Cancer Research*, 1982. **42**(6): p. 2265-2269.
331. Geng, L., et al., *Fibronectin is chemotactic for CT 26 colon carcinoma cells: sub-lines selected for increased chemotaxis to fibronectin display decreased tumorigenicity and lung colonization*. *Clinical & Experimental Metastasis*, 1998. **16**(8): p. 683-691.
332. Liang, C.-C., A.Y. Park, and J.-L. Guan, *In vitro scratch assay: a convenient and inexpensive method for analysis of cell migration in vitro*. *Nat. Protocols*, 2007. **2**(2): p. 329-333.
333. Forcet, C., et al., *The dependence receptor DCC (deleted in colorectal cancer) defines an alternative mechanism for caspase activation*. *Proceedings of the National Academy of Sciences*, 2001. **98**(6): p. 3416-3421.
334. Luck, R. and M.H.H. Schmidt, *Axon Guidance Factors in Developmental and Pathological Angiogenesis*. *Endothelial Signaling in Development and Disease*, 2015. p. 259-291.
335. Ahmad Khalili, A. and M.R. Ahmad, *A Review of Cell Adhesion Studies for Biomedical and Biological Applications*. *International Journal of Molecular Sciences*, 2015. **16**(8): p. 18149-18184.
336. Humphries, M.J., *Cell Adhesion Assays*, in *Extracellular Matrix Protocols: Second Edition*, S. Even-Ram and V. Artym, Editors. 2009, Humana Press: Totowa, NJ. p. 203-210.
337. Liotta, L.A., *Tumor Invasion and Metastases—Role of the Extracellular Matrix: Rhoads Memorial Award Lecture*. *Cancer Research*, 1986. **46**(1): p. 1-7.
338. Cavallaro, U. and G. Christofori, *Cell adhesion in tumor invasion and metastasis: loss of the glue is not enough*. *Biochimica Et Biophysica Acta*, 2001. **1552**(1): p. 39-45.
339. Shimizu, A., et al., *Netrin-1 Promotes Glioblastoma Cell Invasiveness and Angiogenesis by Multiple Pathways Including Activation of RhoA, Cathepsin B, and cAMP-response Element-binding Protein*. *The Journal of Biological Chemistry*, 2013. **288**(4): p. 2210-2222.

340. Yebra, M., et al., *Recognition of the Neural Chemoattractant Netrin-1 by Integrins  $\alpha 6\beta 4$  and  $\alpha 3\beta 1$  Regulates Epithelial Cell Adhesion and Migration*. *Developmental Cell*, 2003. **5**(5): p. 695-707.
341. Stanley Borowicz, a., et al., *The Soft Agar Colony Formation Assay*. *Journal of Visualized Experiments*, 2014(92).
342. Li, L., et al., *Collective cell migration: Implications for wound healing and cancer invasion*. *Burns & Trauma*, 2013. **1**(1): p. 21-26.
343. Entschladen, F., et al., *Tumour-cell migration, invasion, and metastasis: navigation by neurotransmitters*. *The Lancet Oncology*, 2004. **5**(4): p. 254-258.
344. Ylivinkka, I., J. Keski-Oja, and M. Hyytiäinen, *Netrin-1: A regulator of cancer cell motility?* *European Journal of Cell Biology*, 2016. **95**(11): p. 513-520.
345. Zuo, Y., et al., *An Uncoordinated-5 Homolog B Receptor Monoclonal Antibody Regulates A375 Melanoma Cell Migration*. *Monoclonal Antibodies in Immunodiagnosis and Immunotherapy*, 2014. **33**(4): p. 280-286.
346. Durko, M., et al., *Rat C6 glioma cell motility and glioma growth are regulated by netrin and netrin receptors *unc5B* and *DCC**. *Journal of Cancer Therapeutics and Research*, 2013. **2**(1).
347. Jarjour, A.A., et al., *Autocrine Netrin Function Inhibits Glioma Cell Motility and Promotes Focal Adhesion Formation*. *PLoS ONE*, 2011. **6**(9): p. 1-11.
348. Han, P., et al., *Netrin-1 promotes cell migration and invasion by down-regulation of *BVES* expression in human hepatocellular carcinoma*. *American Journal of Cancer Research*, 2015. **5**(4): p. 1396-1409.
349. Larrivee, B., et al., *Activation of the *UNC5B* receptor by Netrin-1 inhibits sprouting angiogenesis*. *Genes & Development*, 2007(19): p. 2433.
350. Navankasattusas, S., et al., *The netrin receptor *UNC5B* promotes angiogenesis in specific vascular beds*. *Development (Cambridge, England)*, 2008. **135**(4): p. 659-667.
351. Ly, N.P., et al., *Netrin-1 inhibits leukocyte migration in vitro and in vivo*. *Proceedings of the National Academy of Sciences of the United States of America*, 2005. **102**(41): p. 14729-14734.
352. Taylor, L., et al., *Netrin-1 Reduces Monocyte and Macrophage Chemotaxis towards the Complement Component *C5a**. *PLoS ONE*, 2016. **11**(8): p. 1-22.
353. Kong, C., et al., *Overexpression of *UNC5B* in bladder cancer cells inhibits proliferation and reduces the volume of transplantation tumors in nude mice*. *BMC Cancer*, 2016. **16**(1): p. 892.
354. Yebra, M., et al., *Recognition of the neural chemoattractant Netrin-1 by integrins  $\alpha 6\beta 4$  and  $\alpha 3\beta 1$  regulates epithelial cell adhesion and migration*. *Developmental Cell*, 2003. **5**(5): p. 695-707.
355. Nikolopoulos, S.N. and F.G. Giancotti, *Netrin-integrin signaling in epithelial morphogenesis, axon guidance and vascular patterning*. *Cell Cycle (Georgetown, Tex.)*, 2005. **4**(3): p. e131-e135.
356. Stanco, A., et al., *Netrin-1- $\alpha 3\beta 1$  integrin interactions regulate the migration of interneurons through the cortical marginal zone*. *Proceedings of the National Academy of Sciences*, 2009. **106**(18): p. 7595-7600.
357. Han, Y., et al., *Netrin-1 simultaneously suppresses corneal inflammation and neovascularization*. *Investigative Ophthalmology & Visual Science*, 2012. **53**(3): p. 1285-1295.
358. Barallobre, M.J., et al., *The Netrin family of guidance factors: emphasis on Netrin-1 signalling*. *Brain Research Reviews*, 2005. **49**(1): p. 22-47.
359. Cristóbal, I., et al., *PP2A inhibition is a common event in colorectal cancer and its restoration using FTY720 shows promising therapeutic potential*. *Molecular Cancer Therapeutics*, 2014. **13**(4): p. 938-947.

360. Guenebeaud, C., et al., *The Dependence Receptor UNC5H2/B Triggers Apoptosis via PP2A-Mediated Dephosphorylation of DAP Kinase*. *Molecular Cell*, 2010. **40**(6): p. 863-876.
361. Hata, K., et al., *Unc5B associates with LARG to mediate the action of repulsive guidance molecule*. *The Journal of Cell Biology*, 2009. **184**(5): p. 737-750.
362. Staff, N.P., et al., *Chemotherapy-induced peripheral neuropathy: A current review*. *Annals of Neurology*, 2017. **81**(6): p. 772-781.
363. Haryani, H., et al. *Chemotherapy-Induced Peripheral Neuropathy Assessment Tools: A Systematic Review*. in *Oncology nursing forum*. 2017.
364. Alberti, P., *Chemotherapy-induced peripheral neurotoxicity – outcome measures: the issue*. *Expert Opinion on Drug Metabolism & Toxicology*, 2017. **13**(3): p. 241-243.
365. Zhang, X., W.W. Chen, and W.J. Huang, *Chemotherapy-induced peripheral neuropathy*. *Biomedical Reports*, 2017. **6**(3): p. 267-271.
366. Chua, K.C. and D.L. Kroetz, *Genetic advances uncover mechanisms of chemotherapy-induced peripheral neuropathy*. *Clinical Pharmacology & Therapeutics*, 2017. **101**(4): p. 450-452.
367. Boyette-Davis, J.A., et al., *Subclinical peripheral neuropathy is a common finding in colorectal cancer patients prior to chemotherapy*. *Clinical cancer research : an official journal of the American Association for Cancer Research*, 2012. **18**(11): p. 3180-3187.
368. Godlewski, J., *Morphological changes in the enteric nervous system caused by carcinoma of the human large intestine*. *Folia Histochemica Et Cytobiologica / Polish Academy Of Sciences, Polish Histochemical And Cytochemical Society*, 2010. **48**(1): p. 157-162.
369. Kozłowska, A., et al., *Myenteric plexuses atrophy in the vicinity of colorectal cancer tissue is not caused by apoptosis or necrosis*. *Folia Histochemica et Cytobiologica*, 2016. **54**(2): p. 99-107.
370. Thorsell, A., et al., *Proteome analysis of serum-containing conditioned medium from primary astrocyte cultures*. *J Proteomics Bioinformatics*, 2011. **2008**: p. 128-142.
371. Kaneko, Y., et al., *Neuronal Differentiation of Hippocampus-Derived Neural Stem Cells Cultured in Conditioned Medium of Embryonic Rat Retina*. *Ophthalmic Research*, 2003. **35**(5): p. 268-275.
372. Faijerson, J., et al., *Reactive astrogliosis induces astrocytic differentiation of adult neural stem/progenitor cells in vitro*. *Journal of Neuroscience Research*, 2006. **84**(7): p. 1415-1424.
373. D'amelio, M., V. Cavallucci, and F. Cecconi, *Neuronal caspase-3 signaling: not only cell death*. *Cell Death and Differentiation*, 2010. **17**(7): p. 1104.
374. Fernando, P., S. Brunette, and L.A. Megeney, *Neural stem cell differentiation is dependent upon endogenous caspase 3 activity*. *The FASEB journal*, 2005. **19**(12): p. 1671-1673.
375. Williams, D.W., et al., *Local caspase activity directs engulfment of dendrites during pruning*. *Nature Neuroscience*, 2006. **9**(10): p. 1234.
376. Rotschafer, S.E., M.R. Allen-Sharpley, and K.S. Cramer, *Axonal Cleaved Caspase-3 Regulates Axon Targeting and Morphogenesis in the Developing Auditory Brainstem*. *Frontiers in Neural Circuits*, 2016. **10**: p. 84.
377. Wang, W., et al., *Netrin-1 Overexpression Protects Kidney from Ischemia Reperfusion Injury by Suppressing Apoptosis*. *The American Journal of Pathology*, 2009. **175**(3): p. 1010-1018.
378. Strizzi, L., et al., *Netrin-1 can affect morphogenesis and differentiation of the mouse mammary gland*. *Journal of Cellular Physiology*, 2008. **216**(3): p. 824-834.
379. Hakanen, J., S. Duprat, and M. Salminen, *Netrin1 is required for neural and glial precursor migrations into the olfactory bulb*. *Developmental Biology*, 2011. **355**(1): p. 101-114.

380. Trupp, M., et al., *Ret-dependent and -independent Mechanisms of Glial Cell Line-derived Neurotrophic Factor Signaling in Neuronal Cells*. Journal of Biological Chemistry, 1999. **274**(30): p. 20885-20894.
381. Wang, N., et al., *Gastric electrical stimulation improves enteric neuronal survival*. International Journal of Molecular Medicine, 2017. **40**(2): p. 438-446.
382. Burke, R.E., M. Antonelli, and D. Sulzer, *Glial cell line-derived neurotrophic growth factor inhibits apoptotic death of postnatal substantia nigra dopamine neurons in primary culture*. Journal of Neurochemistry, 1998. **71**(2): p. 517-525.
383. Noda, M., et al., *Role of immune cells in brain metastasis of lung cancer cells and neuron-tumor cell interaction*. Neuroscience and Behavioral Physiology, 2011. **41**(3): p. 243-251.
384. De Giorgio, R., et al., *Enteric glia and neuroprotection: basic and clinical aspects*. American Journal of Physiology - Gastrointestinal and Liver Physiology, 2012. **303**(8): p. G887-G893.
385. Abdo, H., et al., *Enteric glial cells protect neurons from oxidative stress in part via reduced glutathione*. The FASEB Journal, 2010. **24**(4): p. 1082-1094.
386. Wright, P.S. and S.L. Thomas, *Constipation and diarrhea: The neglected symptoms*. Seminars in Oncology Nursing, 1995. **11**(4): p. 289-297.
387. Lee, C.S., E.J. Ryan, and G.A. Doherty, *Gastro-intestinal toxicity of chemotherapeutics in colorectal cancer: The role of inflammation*. World Journal of Gastroenterology : WJG, 2014. **20**(14): p. 3751-3761.
388. Escalante, J., et al., *Impact of chemotherapy on gastrointestinal functions and the enteric nervous system*. Maturitas, 2017.
389. Stojanovska, V., S. Sakkal, and K. Nurgali, *Platinum-based chemotherapy: gastrointestinal immunomodulation and enteric nervous system toxicity*. American Journal of Physiology-Gastrointestinal and Liver Physiology, 2015. **308**(4): p. G223-G232.
390. Benarroch, E.E., *Enteric nervous system*. Neurology, 2007. **69**(20): p. 1953.
391. Costa, M., *Anatomy and physiology of the enteric nervous system*. Gut, 2000. **47**(suppl 4): p. iv15.
392. Carelle, N., et al., *Changing patient perceptions of the side effects of cancer chemotherapy*. Cancer, 2002. **95**(1): p. 155-163.
393. Wafai, L., et al., *Effects of oxaliplatin on mouse myenteric neurons and colonic motility*. Frontiers in Neuroscience, 2013. **7**.
394. McQuade, R.M., et al., *Role of oxidative stress in oxaliplatin-induced enteric neuropathy and colonic dysmotility in mice*. British Journal of Pharmacology, 2016. **173**(24): p. 3502-3521.
395. Quasthoff, S. and H.P. Hartung, *Chemotherapy-induced peripheral neuropathy*. Journal of Neurology, 2002. **249**(1): p. 9-17.
396. James, S.E., et al., *Anti-cancer drug induced neurotoxicity and identification of Rho pathway signaling modulators as potential neuroprotectants*. NeuroToxicology, 2008. **29**(4): p. 605-612.
397. Forcet, C., *Netrin-1-mediated axon outgrowth requires deleted in colorectal cancer-dependent MAPK activation*. Nature, 2002. **417**(6887): p. 443.
398. Osborne, P.B., *Localization of immunoreactivity for deleted in colorectal cancer (DCC), the receptor for the guidance factor netrin-1, in ventral tier dopamine projection pathways in adult rodents*. Neuroscience, 2005. **131**(3): p. 671.
399. Barberá, V.M., et al., *The 18q21 region in colorectal and pancreatic cancer: independent loss of DCC and DPC4 expression*. Biochimica et Biophysica Acta (BBA) - Molecular Basis of Disease, 2000. **1502**(2): p. 283-296.
400. Castets, M., et al., *DCC constrains tumour progression via its dependence receptor activity*. Nature, 2011. **482**(7386): p. 534-537.

401. Robinson, A.M., et al., *Effects of Oxaliplatin Treatment on the Enteric Glial Cells and Neurons in the Mouse Ileum*. Journal of Histochemistry and Cytochemistry, 2016. **64**(9): p. 530.
402. Flatmark, K., et al., *Twelve colorectal cancer cell lines exhibit highly variable growth and metastatic capacities in an orthotopic model in nude mice*. European Journal of Cancer, 2004. **40**: p. 1593-1598.
403. William Tseng, a., a. Xianne Leong, and a. Edgar Engleman, *Orthotopic Mouse Model of Colorectal Cancer*. Journal of Visualized Experiments, 2007(10).
404. Castle, J.C., et al., *Immunomic, genomic and transcriptomic characterization of CT26 colorectal carcinoma*. BMC Genomics, 2014. **15**(1): p. 190.
405. Coria-Avila, G.A., et al., *Cecum location in rats and the implications for intraperitoneal injections*. Lab Animal, 2007(7): p. 25.
406. Schlegel, M., et al., *The neuroimmune guidance cue netrin-1 controls resolution programs and promotes liver regeneration*. Hepatology (Baltimore, Md.), 2016. **63**(5): p. 1689-1705.
407. Boesmans, W., et al., *Imaging neuron-glia interactions in the enteric nervous system*. Frontiers in Cellular Neuroscience, 2013. **7**(183).
408. Sharrad, D.F., B.N. Chen, and S.J.H. Brookes, *Neurochemical coding compared between varicose axons and cell bodies of myenteric neurons in the guinea-pig ileum*. Neuroscience Letters, 2013. **534**: p. 171-176.
409. Mille, F., et al., *Interfering with multimerization of netrin-1 receptors triggers tumor cell death*. Cell Death & Differentiation, 2009. **16**(10): p. 1344-1351.
410. Krimpenfort, P., et al., *Deleted in colorectal carcinoma suppresses metastasis in p53-deficient mammary tumours*. Nature, 2012. **482**(7386): p. 538-541.
411. Shin, S.K., et al., *Epigenetic and Genetic Alterations in Netrin-1 Receptors UNC5C and DCC in Human Colon Cancer*. Gastroenterology, 2007. **133**(6): p. 1849-1857.
412. Ngoc, P.L., et al., *Netrin-1 Inhibits Leukocyte Migration in vitro and in vivo*. National Academy of Sciences, 2005 p. 14729.
413. Chen, J., et al., *Netrin-1 protects against L-Arginine-induced acute pancreatitis in mice*. 2012.
414. Mirakaj, V., et al., *Netrin-1 signaling dampens inflammatory peritonitis*. The Journal of Immunology, 2011. **186**(1): p. 549-555.
415. Aherne, C.M., et al., *Neuronal guidance molecule netrin-1 attenuates inflammatory cell trafficking during acute experimental colitis*. Gut, 2012. **61**(5): p. 695-705.
416. Aherne, C.M., C.B. Collins, and H.K. Eltzschig, *Netrin-1 guides inflammatory cell migration to control mucosal immune responses during intestinal inflammation*. Tissue Barriers, 2013. **1**(2): p. e24957.
417. Boneschansker, L., et al., *Netrin-1 augments chemokinesis in CD4(+) T cells in vitro and elicits a proinflammatory response in vivo*. Journal of immunology (Baltimore, Md. : 1950), 2016. **197**(4): p. 1389-1398.
418. Shepherd, G.M.G., M. Raastad, and P. Andersen, *General and variable features of varicosity spacing along unmyelinated axons in the hippocampus and cerebellum*. Proceedings of the National Academy of Sciences of the United States of America, 2002. **99**(9): p. 6340-6345.
419. Gabella, G., *Fine structure of the myenteric plexus in the guinea-pig ileum*. Journal of Anatomy, 1972. **111**(Pt 1): p. 69-97.
420. Böttner, M., et al., *GDNF induces synaptic vesicle markers in enteric neurons*. Neuroscience Research, 2013. **77**: p. 128-136.
421. Sugita, S., et al., *VACHT overexpression increases acetylcholine at the synaptic cleft and accelerates aging of neuromuscular junctions*. Skeletal Muscle, 2016. **6**: p. 1-17.
422. Tong, Q. and A.L. Kirchgessner, *Localization and function of metabotropic glutamate receptor 8 in the enteric nervous system*. American Journal of Physiology - Gastrointestinal and Liver Physiology, 2003. **285**(5): p. G992-G1003.

423. Jessen, K.R. and R. Mirsky, *Glial cells in the enteric nervous system contain glial fibrillary acidic protein*. *Nature*, 1980. **286**(5774): p. 736-737.
424. Hao, M.M., et al., *Arundic Acid Prevents Developmental Upregulation of S100B Expression and Inhibits Enteric Glial Development*. *Frontiers in Cellular Neuroscience*, 2017. **11**(42).
425. Hibi, K., et al., *Aberrant methylation of the netrin-1 receptor genes UNC5C and DCC detected in advanced colorectal cancer*. *World Journal of Surgery*, 2009. **33**(5): p. 1053-1057.
426. Sang, Q. and H.M. Young, *Chemical coding of neurons in the myenteric plexus and external muscle of the small and large intestine of the mouse*. *Cell And Tissue Research*, 1996. **284**(1): p. 39-53.
427. Nurgali, K., M.J. Stebbing, and J.B. Furness, *Correlation of electrophysiological and morphological characteristics of enteric neurons in the mouse colon*. *The Journal Of Comparative Neurology*, 2004. **468**(1): p. 112-124.
428. Tricoire, L. and T. Vitalis, *Neuronal nitric oxide synthase expressing neurons: a journey from birth to neuronal circuits*. *Frontiers in Neural Circuits*, 2012. **6**: p. 82.
429. Porter, A.J., et al., *Cholinergic and nitrergic interneurons in the myenteric plexus of the human colon*. *Gut*, 2002. **51**(1): p. 70-75.
430. Vicentini, G.E., et al., *Experimental Cancer Cachexia Changes Neuron Numbers and Peptide Levels in the Intestine: Partial Protective Effects after Dietary Supplementation with L-Glutamine*. *PLoS ONE*, 2016. **11**(9): p. 1-23.
431. Jiang, Y., et al., *Visualizing the enteric nervous system using genetically engineered double reporter mice: Comparison with immunofluorescence*. *PLoS ONE*, 2017. **12**(2): p. e0171239.
432. Murphy, E.M.A., et al., *Quantification of subclasses of human colonic myenteric neurons by immunoreactivity to Hu, choline acetyltransferase and nitric oxide synthase*. *Neurogastroenterology And Motility: The Official Journal Of The European Gastrointestinal Motility Society*, 2007. **19**(2): p. 126-134.
433. Wattchow, D., et al., *Regional variation in the neurochemical coding of the myenteric plexus of the human colon and changes in patients with slow transit constipation*. *Neurogastroenterology And Motility: The Official Journal Of The European Gastrointestinal Motility Society*, 2008. **20**(12): p. 1298-1305.
434. Chandrasekharan, B., et al., *Colonic motor dysfunction in human diabetes is associated with enteric neuronal loss and increased oxidative stress*. *Neurogastroenterology and motility : the official journal of the European Gastrointestinal Motility Society*, 2011. **23**(2): p. 131-e26.
435. Furness, J.B., *Enteric Nervous System*. *Scholarpedia*, 2007. **2**(10): p. 4064.
436. Bergeron, K.F., D.W. Silversides, and N. Pilon, *The developmental genetics of Hirschsprung's disease*. *Clinical Genetics*, 2013. **83**(1): p. 15-22.
437. Casella, G., et al., *Neurological disorders and inflammatory bowel diseases*. *World Journal of Gastroenterology : WJG*, 2014. **20**(27): p. 8764-8782.
438. Oliveira, E.C., et al., *Neuropathy of gastrointestinal Chagas' disease: immune response to myelin antigens*. *Neuroimmunomodulation*, 2009. **16**(1): p. 54-62.
439. Ratcliffe, E.M., et al., *Netrin/DCC-mediated attraction of vagal sensory axons to the fetal mouse gut*. *Journal of Comparative Neurology*, 2006. **498**(5): p. 567-580.
440. Seaman, C., et al., *Localization of the netrin guidance receptor, DCC, in the developing peripheral and enteric nervous systems*. *Mechanisms of Development*, 2001. **103**(1): p. 173-175.
441. Aherne, C.M., et al., *Neuronal guidance molecule netrin-1 attenuates inflammatory cell trafficking during acute experimental colitis*. *Gut*, 2012(5): p. 695.
442. Rangiah, K., et al., *Differential secreted proteome approach in murine model for candidate biomarker discovery in colon cancer*. *Journal of Proteome Research*, 2009. **8**(11): p. 5153-5164.

443. Wang, Y.-R., et al., *Cathepsin L Plays a Role in Quinolinic Acid-Induced NF-Kb Activation and Excitotoxicity in Rat Striatal Neurons*. PLoS ONE, 2013. **8**(9): p. e75702.
444. Xiang, B., et al., *Cathepsin L is involved in 6-hydroxydopamine induced apoptosis of SH-SY5Y neuroblastoma cells*. Brain Research, 2011. **1387**(Supplement C): p. 29-38.
445. Julien, F., et al., *Netrin-1 Expression Confers a Selective Advantage for Tumor Cell Survival in Metastatic Breast Cancer*. Proceedings of the National Academy of Sciences of the United States of America, 2008(12): p. 4850.
446. Zhang, Y. and W. Hu, *Mouse Enteric Neuronal Cell Culture*. Methods in Molecular Biology (Clifton, N.J.), 2013. **1078**: p. 55-63.
447. Gordon, J., S. Amini, and M.K. White, *General overview of neuronal cell culture*. Methods in Molecular Biology (Clifton, N.J.), 2013. **1078**: p. 1-8.
448. Kovalevich, J., et al., *Considerations for the Use of SH-SY5Y Neuroblastoma Cells in Neurobiology*. Humana Press: Totowa, 2013. NJ. p. 9.
449. Xicoy, H., B. Wieringa, and G.J.M. Martens, *The SH-SY5Y cell line in Parkinson's disease research: a systematic review*. Molecular Neurodegeneration, 2017. **12**(1): p. 10.
450. Moriez, R., et al., *Neuroplasticity and neuroprotection in enteric neurons: Role of epithelial cells*. Biochemical and Biophysical Research Communications, 2009. **382**(3): p. 577-582.
451. Langlois, A. and D. Duval, *Differentiation of the human NT2 cells into neurons and glia*. Methods in Cell Science, 1997. **19**(3): p. 213-219.
452. Melo, C.G.d.S., et al., *Enteric innervation combined with proteomics for the evaluation of the effects of chronic fluoride exposure on the duodenum of rats*. Scientific Reports, 2017. **7**(1): p. 1070-1070.
453. Ranganathan, P.V., et al., *Basic Research: Netrin-1 regulates the inflammatory response of neutrophils and macrophages, and suppresses ischemic acute kidney injury by inhibiting COX-2-mediated PGE2 production*. Kidney International, 2013. **83**: p. 1087-1098.
454. Ranganathan, P.V., et al., *Netrin-1 regulates the inflammatory response of neutrophils and macrophages, and suppresses ischemic acute kidney injury by inhibiting COX-2 mediated PGE2 production*. Kidney International, 2013. **83**(6): p. 1087-1098.
455. Ranganathan, P., et al., *Guidance Cue Netrin-1 and the Regulation of Inflammation in Acute and Chronic Kidney Disease*. Mediators of Inflammation, 2014. **2014**: p. 13.
456. Ridley, A.J., *Rho GTPase signalling in cell migration*. Current Opinion in Cell Biology, 2015. **36**: p. 103-112.

# Appendices

---

# Appendix A

## Western blot replicates

**Figure 2.1 D**

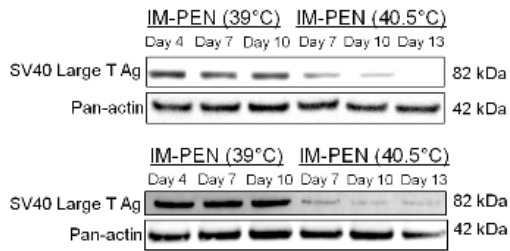


**Figure 3.2 B**

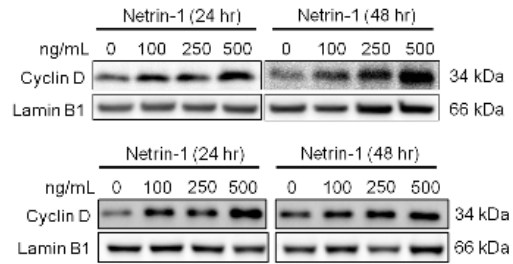


**Figure 3.2 D**

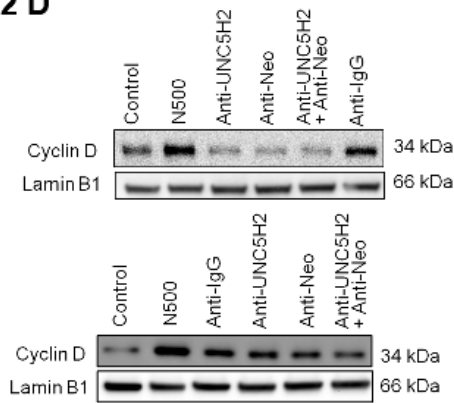
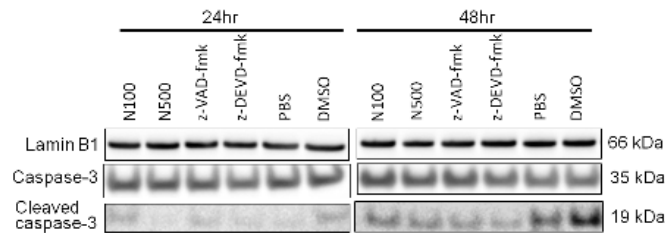


**Figure 3.2 E**



## Appendix B

### Western blot replicates

Figure 3.6 A

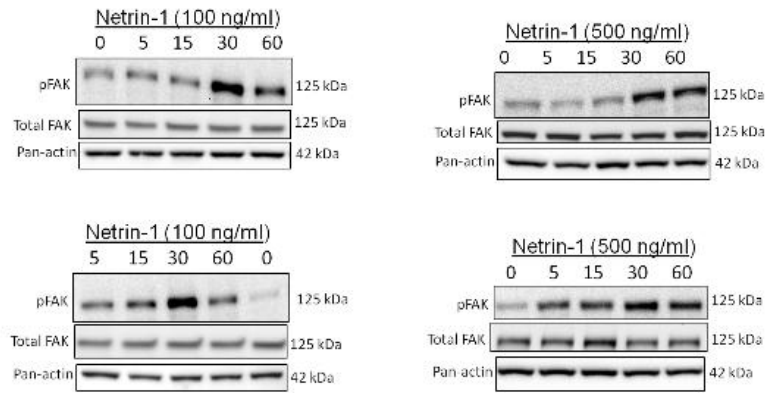
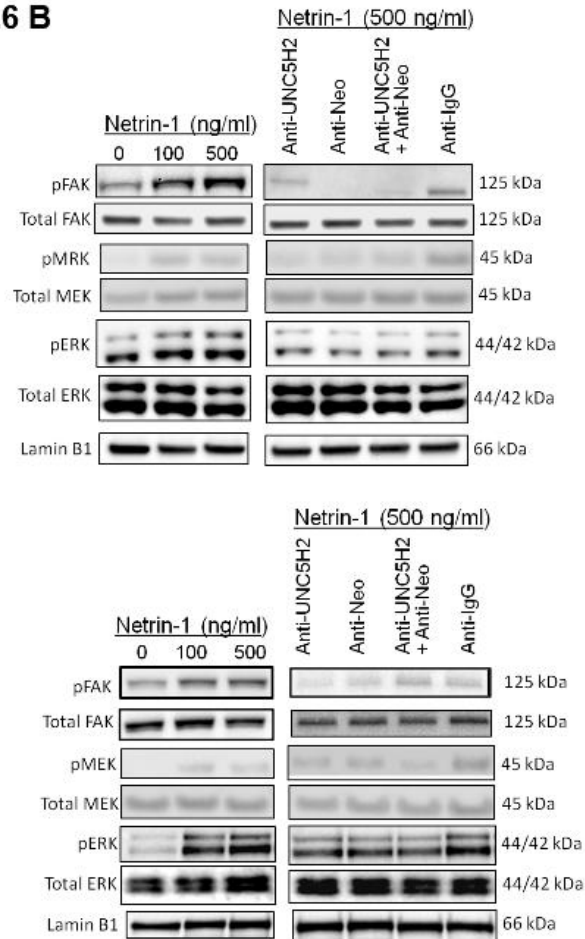


Figure 3.6 B



# Publications

---

The full-text of these articles are subject to copyright restrictions, and cannot be included in the online version of the thesis.

Ko, S.Y., CDass, C.R., Nurgali, K. Netrin-1 in the developing enteric nervous system and colorectal cancer. *Trends in Molecular Medicine*, 18(9), 544- 554 (2012). <https://doi.org/10.1016/j.molmed.2012.07.001>.

Ko, S.Y., Blatch, G.L. & Dass, C.R. Netrin-1 as a potential target for metastatic cancer: focus on colorectal cancer. *Cancer Metastasis Rev* 33, 101–113 (2014). <https://doi.org/10.1007/s10555-013-9459-z>